Université de Montréal

DÉVELOPPEMENT ET UTILISATION DE SOURCES DE PLASMA POUR STÉRILISER DES INSTRUMENTS MÉDICAUX

par

Jérôme Pollak

Département de physique

Faculté des Arts et des Sciences

Thèse présentée à la Faculté des Études Supérieures

en vue de l'obtention du grade de

Philosophiæ Doctor (Ph.D.)

(Physique)

Université de Montréal

Université de Montréal

Faculté des études supérieures

Cette thèse intitulée :

DÉVELOPPEMENT ET UTILISATION DE SOURCES DE PLASMA POUR STÉRILISER DES INSTRUMENTS MÉDICAUX

par

Jérôme Pollak

a été évaluée par le jury des personnes suivantes :

Joëlle Margot	Présidente du jury
Michel Moisan	Directeur de recherche
Jean Barbeau	Membre du jury
Michel Wertheimer	Membre du jury
Mounir Laroussi	Examinateur externe

Sommaire

Les avancées en stérilisation par plasma de dispositifs médicaux (DM) sont tributaires à la fois du développement de sources de plasma adaptées au traitement de ces DM et de la compréhension des mécanismes d'inactivation des micro-organismes. Les principaux objectifs poursuivis au cours de cette thèse étaient, d'une part, le développement de sources de plasma à la fois spatialement uniformes et de faible température du gaz (< 50 °C) et, d'autre part, l'identification et l'optimisation des agents biocides de ces plasmas (e.g. le rayonnement UV).

Au cours de ce travail, nous avons conçu et mis au point trois types d'applicateurs de champ électromagnétique pouvant entretenir un plasma. Tout d'abord, un réseau de sources de plasma, de type antenne, distribuées autour de l'enceinte à décharge de nature diélectrique ; chacune des sources de ce réseau est alimentée individuellement en puissance haute-fréquence (HF), ce qui a nécessité la mise au point d'un diviseur de puissance en technologie guide d'onde. Ce concept de sources distribuées a rapidement été abandonné au profit de deux autres sources de plasma, car ces dernières offraient des avantages immédiats pour la stérilisation biomédicale ainsi qu'en termes d'efficacité énergétique et de largeur de bande en fréquence (impédance d'entrée quasi constante). Ces deux sources de plasma sont basées sur des lignes de transmission planes où le plasma fait partie intégrante de la ligne de transmission, l'une étant destinée à stériliser l'intérieur de tubes diélectriques thermosensibles (e.g. cathéters cardiaques) et l'autre permettant l'immersion d'objets tridimensionnels dans le plasma (e.g. forceps).

Deux types de micro-organismes ont été utilisés pour tester les performances, identifier et optimiser les agents biocides des sources de plasma que nous avons développées: des spores bactériennes sédimentées à partir d'une suspension de *Bacillus atrophaeus* et des bactéries végétatives de type *Staphylococcus aureus* intégrées dans une matrice de biofilms. L'inactivation de ces micro-organismes placés dans nos stérilisateurs plasma est obtenue grâce au rayonnement UV. Ce procédé de stérilisation est rapide (quelques minutes), non toxique (pas d'aération subséquente nécessaire) et dégrade relativement peu les polymères thermosensibles (érosion non détectée).

Mots-clés: source de plasma haute-fréquence (HF), impédance d'entrée, lignes de transmission planes, stérilisation, spores bactériennes, biofilm, dispositifs médicaux (DM) thermosensibles.

Abstract

Advances in plasma sterilization of medical devices (MDs) are dependent upon both the development of plasma sources adapted to the processing of these MDs, and upon the understanding of the inactivation mechanisms of microorganisms. The main objectives of this thesis were, on the one hand, to develop plasma sources that are spatially uniform and that have a low gas temperature (< 50 °C) and, on the other hand, the identification and optimization of biocidal agents (e.g. UV radiation) in their plasmas.

In the course of this work, we have designed and developed three types of electromagnetic field applicators to sustain plasma. The first was a network of distributed antennas on the outside of the dielectric discharge-vessel, which possessed multiple high-frequency (HF) input ports fed by a waveguide-based power divider. This distributed source concept was soon abandoned in favour of two other plasma source designs, since the latter ones provided immediate advantages for biomedical sterilization, and also in terms of energy efficiency and frequency bandwidth (e.g. near-constant input impedance). These two plasma sources are based on planar transmission line designs where the plasma is part of the transmission line: the first allows one to sterilize the inner surfaces (lumen) of thermally sensitive dielectric tubes (e.g. cardiac catheters), while the other enables one to immerse three-dimensional objects within the plasma (e.g. forceps).

Two types of microorganisms were used to test the performances to identify and to optimise the biocidal agents of the plasma sources that we have developed namely, sedimented bacterial spores from a suspension of *Bacillus atrophaeus* and vegetative *Staphylococcus aureus* bacteria embedded in a biofilm matrix. Inactivation of these microorganisms in our plasma sterilizers results through irradiation. This sterilization process is rapid (a few minutes), non-toxic (it does not require venting), and it affects thermally sensitive polymers relatively little (no erosion was detected).

Keywords: high-frequency (HF) plasma sources, input impedance, planar transmission lines, sterilization, bacterial spores, biofilm, thermally sensitive medical devices (MDs).

Table des matières

Liste des figures et tableaux (hors publications)

Listes des notations et symboles

Acronymes

ATCC	American type culture collection
DOS	Décharge d'onde de surface
EM	Electromagnétique
HF	Haute fréquence
LSPQ	Laboratoire de santé publique du Québec
PA	Pression atmosphérique
PE	Polyéthylène
PTFE	Polytétrafluoroéthylène
RF	Radio fréquence
TEM	Transverse electric and magnetic
TOS	Taux d'onde stationnaire
UV	Ultraviolet
UVV	Ultraviolet du vide (de 100 à 200 nm)

Abréviations

B. subtilis	*Bacillus subtilis*
°C	Degré Celsius
mLsm	Millilitre standard par minute

Symboles latins

A	Aire d'une section transversale d'un tube
A_L	Coefficient d'absorption totale d'une raie
D	Diamètre interne d'un tube
e	Charge de l'électron
f_{max}	Fréquence maximale d'utilisation d'une ligne triplaque sur le mode purement TEM
h	Distance entre les plans de masse d'une ligne triplaque
m_e	Masse de l'électron
n_c	Densité critique
P_A	Puissance absorbée par le plasma
P_I	Puissance incidente

P_R	Puissance réfléchie
P_S'	Puissance rayonnée à l'extérieur de la ligne triplaque
P_S''	Puissance dissipée dans les conducteurs et le diélectrique d'une ligne triplaque
P_T	Puissance transmise
Q	Débit
t	Epaisseur de la bande conductrice centrale d'une ligne triplaque
w	Largeur de la bande conductrice centrale d'une ligne triplaque
Z_{IN}	Impédance d'entrée
Z_0	Impédance caractéristique d'une ligne de transmission
Z_L	Impédance caractéristique d'une charge
Z_P	Impédance caractéristique de la ligne triplaque contenant les tubes diélectriques et le plasma

Symboles grecs

ε_0	Permittivité diélectrique du vide
ε_{eff}	Permittivité relative effective
ε_r	Permittivité relative
λ_0	Longueur d'onde du champ électromagnétique dans le vide
λ_g	Longueur d'onde du champ électromagnétique guidée
ω	Pulsation du champ électromagnétique

Remerciements

Les travaux de recherche présentés dans cette thèse de doctorat sont le fruit d'un travail d'équipe auquel je suis fier d'avoir participé. Ces trois années de recherche m'ont apporté beaucoup de plaisir et je tiens à exprimer ma profonde reconnaissance à tous ceux qui y ont contribué.

Tout d'abord, j'aimerais remercier mon directeur de recherche, le professeur Michel Moisan, qui m'a offert tous les moyens pour mener à bien ce projet de recherche dans les meilleures conditions. De plus, grâce à la confiance qu'il m'a témoignée, j'ai eu l'opportunité d'évoluer dans un climat de recherche stimulant et agréable. Je tiens tout particulièrement à le remercier pour m'avoir permis de participer à des conférences internationales et pour m'avoir communiqué le plaisir d'écrire des demandes de brevet et des articles scientifiques. Les moments les plus intéressants de mon doctorat resteront la réécriture en commun de passages de futures publications où j'ai pu admirer toutes ses qualités scientifiques.

Toute ma gratitude va également au professeur Jean Barbeau pour son constant soutien et ses encouragements ainsi que pour tous les conseils microbiologiques qu'il m'a prodigués.

Jacynthe Séguin, une microbiologiste d'une grande compétence, enthousiaste et pleine d'énergie, a joué un rôle crucial dans les recherches présentées dans cette thèse: elle a non seulement effectué l'essentiel du travail de préparation et de récupération des échantillons microbiologiques, mais elle a de plus participé à la conception de nombreuses expériences.

Les sources de plasma développées au cours de cette thèse ont été construites par Jean-Sébastien Mayer, notre chef d'atelier de mécanique. En fait son apport se situe bien au-delà de ses seules attributions de technicien: en plus de construire des pièces, il a activement participé à la conception des structures mises au point en proposant plusieurs solutions techniques avantageuses. Par ailleurs, il m'a patiemment enseigné les règles du dessin technique et l'utilisation du logiciel Autocad, ce que j'ai grandement mis à profit au cours de ma thèse.

Depuis son arrivée dans le Groupe il y a un an, Pierre Levif et moi avons travaillé en équipe sur l'optimisation de certaines sources de plasma ce qui donnera lieu, je l'espère, à de nouvelles publications. Ce fut un plaisir de travailler avec lui.

Mes remerciements vont également à Danielle Kéroack pour son aide en informatique ainsi qu'au laboratoire. Par exemple, l'un des résultats les plus importants de ma thèse fut

l'identification des rayons UV situés en-dessous de 180 nm (qui sont des agents très efficaces d'inactivation des micro-organismes) et j'ai pu le faire grâce à l'utilisation d'un spectromètre sous vide que Danielle avait préalablement remis en état de marche, aligné et configuré de manière précise.

J'aimerais également remercier Thomas Fleisch et Yassine Kabouzi pour notre belle collaboration sur l'optimisation d'une source de plasma de type Surfaguide, collaboration ayant d'ailleurs résulté en un article en commun.

Ma reconnaissance se porte également sur Karim Boudam pour sa participation à l'identification des agents biocides du plasma et à la mise au point d'un dispositif de spectroscopie d'absorption optique.

Tous mes remerciements vont à Didier Leconte de la société Univalor pour ses encouragements, ses judicieux conseils et sa gentillesse à mon égard.

Je souhaite souligner la participation de l'agent de brevet David Saint-Martin à la réécriture des revendications et à la version finale des deux demandes de brevets figurant dans cette thèse.

Mes remerciements vont également aux étudiants de l'Université de Montréal à qui j'ai eu la chance d'enseigner en tant qu'auxiliaire d'enseignement puis chargé de cours.

Je tiens à exprimer mes plus vifs remerciements aux professeurs Jean-Jacques Laurin, Jacques Pelletier, Ke Wu, L'Hocine Yahia et Zenon Zakrzewski pour leurs nombreux conseils scientifiques. Par exemple, ce dernier m'a transmis dans le passé des connaissances sur les techniques micro-ondes qui furent amplement mises à profit durant mon doctorat.

Plusieurs membres ou anciens membres du Groupe de physique des plasmas et du Groupe de contrôle des infections m'ont apporté leur aide au cours de mon doctorat. C'est le cas d'Annie Leduc, Ahlem Mahfoudh, Eduardo Castaños Martínez, Bachir Saoudi et Jérôme Saussac ainsi que les stagiaires David Chiasson, Rosalie Plantefève et Paul Gavra. Ma gratitude va également aux autres membres de ces deux groupes pour leur sympathie à mon égard.

Je tiens à remercier les membres de mon jury de thèse, les professeurs Margot, Barbeau, Laroussi et Wertheimer d'avoir accepté d'y participer.

Finalement, je remercie infiniment Natacha (ma douce moitié), mon petit frère Sébastien, Janine et Noël, mes parents Martine et Pierre, ainsi que mes amis de Montréal et d'Europe pour leur appui au cours de ces trois années remplies de défis.

Chapitre 1

Introduction

La stérilisation par plasma se veut une alternative aux méthodes de stérilisation conventionnelles basées sur la chaleur et/ou sur l'utilisation de composés chimiques biocides. Au sens strict du terme, cette méthode n'est pas encore utilisée en milieu hospitalier, bien que certains manufacturiers de systèmes de stérilisation prétendent y avoir déjà recours [1]. Parmi les avantages de cette technique en voie de développement, citons la possibilité de stériliser à moins de 50 °C, en utilisant un plasma froid, et sans avoir à respecter un temps d'aération après traitement [2]. Ainsi, il est possible de stériliser, avec peu d'endommagement des polymères thermo-sensibles (à la différence de l'autoclave ou du four à chaleur sèche). De plus, contrairement au traitement par l'oxyde d'éthylène et autres composés chimiques biocides, les objets sont immédiatement disponibles une fois terminé le processus de stérilisation. Enfin, la stérilisation par plasma, lorsqu'elle utilise des gaz comme l'argon ou un mélange comme N_2-O_2 à faible teneur en O_2, apparaît comme moins oxydante pour les objets à traiter que la stérilisation par ozone, également un procédé à basse température.

Dans le cadre de cette thèse, nous avons conçu et mis au point des sources de plasma que nous avons par la suite utilisées pour la stérilisation, ce travail de recherche sur les structures électromagnétiques constituant d'ailleurs une part importante des travaux regroupés dans ce document. Généralement, un plasma de laboratoire peut s'obtenir en utilisant de l'énergie électromagnétique. La décharge gazeuse peut s'obtenir par un champ électrique continu ou par un champ électrique alternatif de haute fréquence (fréquences radio, le plus souvent 13.56 ou 27.12 MHz, ou micro-ondes, le plus souvent 915 ou 2450 MHz, ces fréquences étant autorisées à des fins industrielles, scientifiques et médicales (fréquences ISM)). Le Groupe de physique des plasmas de l'Université de Montréal possède une longue tradition quant au développement de sources de plasma alimentées par des champs de haute-fréquence (HF). Plusieurs des dispositifs mis au point dans ce groupe sont d'ailleurs utilisés par différents groupes de recherche à travers le monde. Certains sont produits en série, et nous pouvons citer en exemple un lanceur d'onde de surface compact, le Surfatron, commercialisé par la compagnie française Sairem. Ce savoir-faire

s'est forgé au fil des années grâce à l'inventivité de Michel Moisan et des autres membres du groupe, souvent avec l'apport scientifique de chercheurs invités, tel le professeur Zenon Zakrzewski, et parfois au contact d'entreprises privées, telle Air Liquide, manifestant des besoins industriels particuliers.

Parallèlement à ces travaux, depuis une dizaine d'année, le Groupe de physique des plasmas de l'Université de Montréal s'est donné un nouveau défi à relever: la stérilisation de dispositifs médicaux (DM) par plasma. De nombreuses études sont menées internationalement sur ce sujet, qui connaît un essor impressionnant parmi le champ des applications plasmas.

La présente thèse de doctorat s'inscrit dans la continuité des recherches déjà entreprises, car elle représente le mariage entre l'activité historique du groupe (le développement de sources de plasma), et sa principale activité actuelle de recherche, la stérilisation par plasma. Nous avons ainsi pu profiter au maximum des connaissances déjà acquises et des outils en place pour structurer nos travaux de recherche.

Avant d'aborder la présentation des objectifs de la thèse, nous allons tout d'abord effectuer un historique des travaux antérieurs en stérilisation par plasma, ce qui nous permettra par la suite de mieux situer notre activité de recherche.

1.1 Historique des travaux antérieurs en stérilisation par plasma

Les premiers pas en stérilisation par plasma ont été rappelés par différents auteurs (e.g. [3-6]). La mise au point du premier stérilisateur par plasma se situe, chronologiquement, bien après le développement du premier stérilisateur à vapeur d'eau (autoclave) par Chamberland (1880) et du premier stérilisateur à air chaud par Poupinel (1884) [6]. De fait, les premiers travaux remontent à un brevet de Menashi [7] en 1968 qui utilisait un champ RF pulsé pour entretenir un plasma d'argon à la pression atmosphérique et stériliser l'intérieur d'un récipient, par exemple une bouteille. Une électrode linéaire était insérée dans le récipient, tandis qu'un autre conducteur enroulé autour du récipient servait d'électrode de masse. Ce système permettait de stériliser des bouteilles contenants des dépôts de 10^6 spores en moins d'une seconde. L'action biocide résidait selon Menashi en un chauffage intense des spores en un temps suffisamment court pour ne pas endommager le récipient. Ce mécanisme fut plus tard appelé micro-incinération par Peeples et Anderson [8].

Les premières expériences en stérilisation par plasma utilisaient pour la plupart des gaz rares tels l'argon ou l'hélium seuls [2] ou, comme Jacobs and Lin [9], de façon additionnelle du peroxyde d'hydrogène (H_2O_2) en plus dans un procédé, dans ce dernier cas, en deux étapes: (1) injection et contact du H_2O_2 avec les objets à stériliser et (2) utilisation d'une décharge RF de gaz rare pour éliminer les résidus toxiques de la surface des objets stérilisés. En fait, certains des systèmes développés dans les années 70 et 80 n'utilisaient pas les agents biocides propres à la phase plasma [10], mais plutôt des espèces possédant directement des propriétés biocides (comme H_2O_2 ou des aldéhydes).

Au milieu des années 90, Laroussi utilisa une décharge à barrière diélectrique (DBD) en mode diffus à la pression atmosphérique pour décontaminer des surfaces [11]. Parallèlement, de nombreux dispositifs de stérilisation par plasma ont été mis au point avec différentes configurations géométriques et modes d'action, à la fois à pression réduite et à la pression atmosphérique. L'un des travaux majeurs pendant cette période fut celui de Lerouge *et al* [12], qui ont notamment démontré que la composition du gaz est un facteur déterminant de l'efficacité biocide d'un plasma.

Il est à mentionner qu'obtenir la stérilité ne garantit pas nécessairement l'élimination de la masse physique des microorganismes et, souvent, des résidus bactériens sont encore présents après la phase de stérilisation, substances éventuellement pyrogènes, c'est-à-dire pouvant provoquer, entre autres, de la fièvre chez l'homme. Ce problème connexe, potentiellement présent dans toutes les techniques de stérilisation, connaît un intérêt particulier dans le cadre de la stérilisation par plasma (voir e.g. certains des articles publiés par le groupe de F. Rossi [13, 14]).

La stérilisation par plasma peut s'effectuer selon deux régimes assez distincts de pression de gaz : à pression réduite (0.1-15 mbar) et à la pression atmosphérique [2]. La pression atmosphérique a l'avantage sur la pression réduite d'offrir une plus grande densité d'espèces chimiquement actives, de l'ordre de cent fois. Par contre, les photons UV à la pression atmosphérique ont un plus faible parcours avant d'être absorbés par le gaz ambiant du fait d'une plus grande densité d'atomes et de molécules d'où, probablement, une contribution moins importante à l'inactivation des micro-organismes par ces photons. De plus, autres inconvénients, les plasmas à la pression atmosphérique sont généralement de plus petit volume et de température plus élevée.

À l'heure actuelle, plusieurs équipes de chercheurs en stérilisation par plasma produisent des résultats innovants et structurés dont les ramifications sont multiples, allant de la détermination des agents biocides (voir e.g. les travaux des groupes d'Awakowicz [15] et de Laroussi [16]) à l'interaction d'un plasma avec des tissus vivants (e.g. groupe de Fridman [17] et de Stoffels [18]), en passant par la destruction protéique (groupes de Kong [19] et de Rossi [13]), pour ne citer que quelques-unes de ces équipes.

Une revue de la stérilisation par plasma peut se diviser selon au moins deux axes: par exemple on peut effectuer la distinction entre (i) les procédés de décharge et de post-décharge ou (ii) le mode d'action des espèces biocides, les rayons UV ou les espèces chimiquement réactives provoquant l'érosion des micro-organismes. Nous allons brièvement résumer ces différentes approches.

1.1.1 Exposition directe et indirecte d'objets à stériliser au plasma

On peut envisager deux types de stérilisateur par plasma [2]: ceux où les micro-organismes sont soumis à la décharge électrique elle-même (stérilisation directe) et ceux où les micro-organismes reçoivent les effluents de la décharge (stérilisation en post-décharge).

La post-décharge en flux de gaz s'obtient en faisant en sorte que le gaz ionisé et excité soit entraîné, très rapidement, dans l'enceinte de stérilisation: à cette fin, en amont, on introduit le gaz sous un grand débit et, en aval, on le "tire" au moyen d'une pompe à vide, comme le montre la figure 1.1 [2]. Les espèces ainsi transportées sont majoritairement électriquement neutres, car les particules chargées se "recombinent" (un ion positif s'alliant à un électron pour former une particule neutre) dès qu'elles quittent la zone de décharge. Les atomes, comme O et N, et les molécules excitées comme N_2, pouvant aussi bien servir à former des molécules émettrices de photons UV que d'avoir une forte réactivité chimique, sont à durée plus grande mais limitée ($\approx$ milliseconde), d'où la nécessité de les amener rapidement en leur point d'utilisation, c'est-à-dire à l'endroit où se trouvent les micro-organismes à inactiver. Ceci peut être obtenu en agissant sur leur vitesse d'écoulement qui dépend de la pression et du débit de gaz. Il faut également veiller à ce que ces espèces soient distribuées de manière uniforme dans la chambre de traitement afin que la stérilité y soit atteinte de façon simultanée partout. Moisan *et al.* [20] ont présenté les avantages et les inconvénients de ces deux techniques. Nous les avons résumés dans le tableau 1.

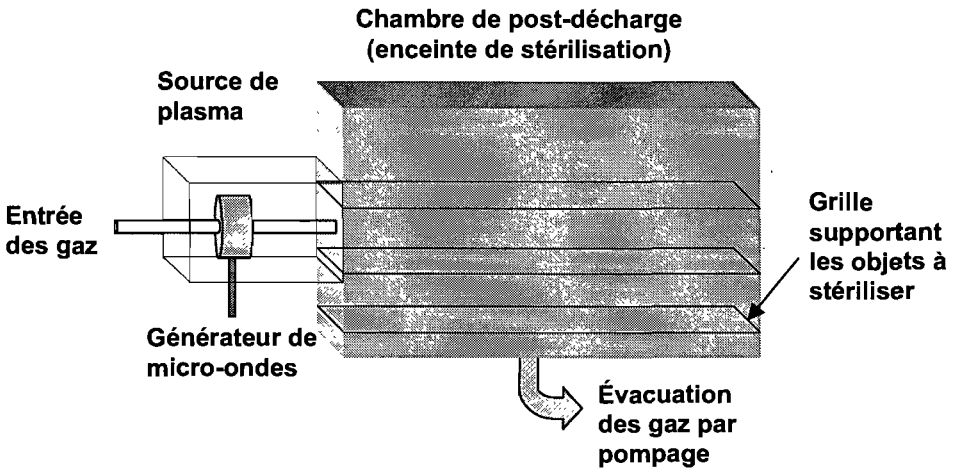

Figure 1.1 Schéma de principe d'un stérilisateur à plasma froid de type post-décharge en flux (prototype 50 L, Université de Montréal) [2].

Tableau 1.1 Comparaison des principales caractéristiques des systèmes de stérilisation par plasma fonctionnant en décharge et en post-décharge, (adapté de Moisan *et al.* [20]).

Caractéristiques	Décharge	Post-décharge
Temps nécessaire à l'obtention de la stérilité	Généralement inférieur à 10 minutes	Généralement supérieur à 10 minutes
Espèces présentes à proximité des surfaces à traiter	Ions, molécules, électrons, radicaux, atomes et molécules neutres ou excités, UV	Radicaux, atomes et molécules neutres ou excités, UV Faible densité d'espèces chargées
Présence d'un champ électrique à proximité des surfaces à traiter	OUI	Généralement NON
Température du gaz près des surfaces à traiter	Généralement élevée (> 50 °C)	Généralement faible (< 50 °C)

Il est possible d'obtenir plus rapidement (quelques minutes) qu'en post-décharge la stérilité en décharge, ce qui représente l'avantage essentiel de ce type de système. Par ailleurs, la post-décharge permet généralement de remplir des chambres de stérilisation de plus grand volume (e.g. 50 L). De plus, placer des objets dans une enceinte de post-décharge permet généralement de mieux les préserver en raison de la plus faible densité d'espèces chargées, d'une plus faible température du gaz et de l'absence de champ électrique HF à l'emplacement des objets à stériliser, évitant ainsi l'échauffement des pièces conductrices [20]. Par ailleurs, les stérilisateurs utilisant une post-décharge d'ondes de surface ont permis une remarquable compréhension des mécanismes de stérilisation ([21]).

Les systèmes fonctionnant en décharge et en post-décharge nous apparaissent complémentaires : c'est pourquoi l'approche choisie par plusieurs Groupes dont le nôtre consiste à développer chacune de ces deux techniques pour bien en évaluer les avantages et inconvénients, lesquels peuvent d'ailleurs dépendre de l'application considérée.

1.1.2 Mode d'action des espèces biocides

Une espèce biocide est un agent capable de tuer des micro-organismes. Un plasma peut contenir plusieurs types d'espèces biocides. Étudier les mécanismes de stérilisation par plasma consiste principalement à déterminer l'efficacité biocide de chacune de ces espèces. Ce point n'est pas trivial car il est parfois difficile de trouver des conditions opératoires permettant d'isoler certaines espèces uniquement. Par exemple, il est particulièrement ardu de s'affranchir de toute émission UV. Ce point a donc fait l'objet de très nombreuses études (e.g. [22, 23]) dont nous allons résumer les résultats les plus significatifs.

Les espèces biocides d'un plasma sont principalement les rayons ultra-violets (UV) et les radicaux. Dans le spectre du rayonnement électromagnétique (EM), la plage de longueur d'onde couverte par les UV s'étend de 10 à 400 nm. Elle peut être grossièrement divisée en deux parties: les UV qui sont absorbés par l'air ($\lambda < 200$ nm), qui portent le nom d'UV du vide (UVV), et ceux qui ne le sont pas, appelés UV proches ($200\text{ nm} < \lambda < 400\text{ nm}$). Une partie seulement de la gamme de longueur d'onde couverte par les UV possède des effets biocides (c'est-à-dire permettant de tuer efficacement des micro-organismes): ce sont les UV dont la longueur d'onde

est inférieure à 300 nm [24]. Un élément important à mentionner est le fait qu'une endospore bactérienne inactivée par des UV apparaît similaire au microscope électronique à balayage (MEB) à une spore non exposée aux UV (voir la figure 1.2, d'après Crevier [25]).

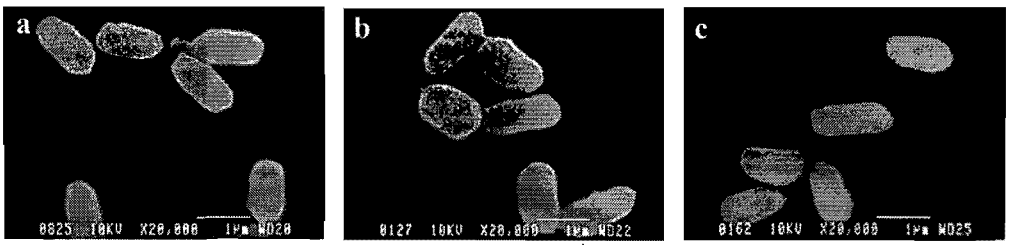

Figure 1.2 Micrographies par MEB de a) spores non traitées; b) spores traitées avec une post-décharge d'argon (40 minutes); c) spores traitées avec une lampe Hg (40 minutes), d'après Crevier [25].

Les radicaux libres (atomes (e.g. O) ou molécules (e.g. OH)) amènent une érosion des micro-organismes. Par exemple, Lerouge *et al* [12] ont démontré l'importance de l'effet de la volatilisation de la matière organique en décharge en utilisant un plasma réactif. Ces auteurs ont utilisé un mélange O_2/CF_4 connu pour son efficacité à éroder les polymères. Une réduction de 5 log de la viabilité des spores a été obtenu en 5 min d'exposition par une importante érosion des spores (figure 1.3).

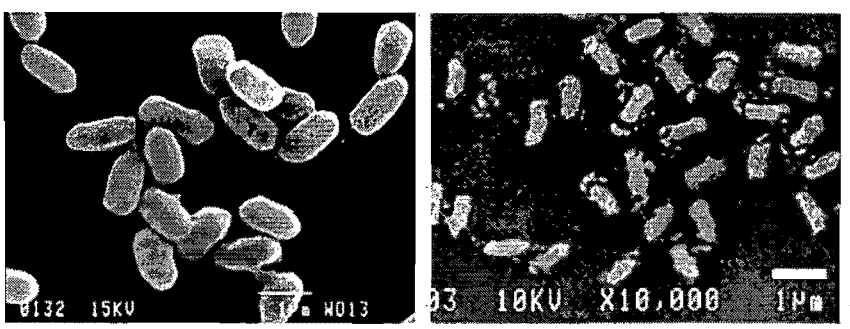

Figure 1.3 Micrographies de spores (Lerouge *et al* [12]): (gauche) spores de contrôle non traitées; (droite) spores après 30 min d'exposition à un plasma d'un mélange O_2/CF_4.

Lors de la détermination des espèces biocides d'un plasma, l'observation de l'érosion des spores au MEB constitue un premier indice à prendre en compte pour suggérer l'implication des des radicaux libres dans le processus d'inactivation de spores. Dans les faits, à basse pression, c'est principalement par le choix initial du gaz plasmagène qu'est prédéterminé le mode d'action

biocide: les plasmas de gaz inertes comme l'argon entraînent relativement peu d'érosion des micro-organismes (du moins pas détectable au MEB!) comparé aux plasmas réactifs comme les plasmas d'oxygène ou de CF_4 (comparaison des figures 1.2 et 1.3).

Pour terminer, il est à mentionner que d'autres explications aux propriétés biocides des plasmas ont été proposées. Par exemple, Mendis *et al.* [26] ont suggéré que les particules chargées jouent un rôle significatif à la pression atmosphérique dans la rupture de la membrane externe de cellules bactériennes. Selon ces auteurs, ce mécanisme physique s'applique uniquement aux bactéries à Gram négatif comme *E. coli*, qui possèdent de fines membranes externes.

1.2 Science de surface de polymères traités par plasma

La science de surface des polymères est l'une des facettes importantes de la stérilisation par plasma, car pour des raisons économiques un objet traité doit pouvoir être réutilisé plusieurs fois, donc avec une détérioration limitée de sa surface. C'est un très vaste sujet de recherche dont les ramifications sont multiples et nous allons seulement ici en rappeler quelques aspects importants, tout d'abord en nous intéressant à l'effet des UV/VUV sur les polymères, puis à l'effet des espèces chimiquement actives (e.g. O, OH) sur ceux-ci.

1.2.1 Photo-dégradation des polymères

L'irradiation d'un polymère par des photons peut mener à toute une série de phénomènes allant de la modification chimique de la surface jusqu'à la décomposition du polymère [27]. Le tableau 1.2 rappelle les longueurs d'ondes pour la dissociation des liaisons chimiques typiques dans les polymères (tableau adapté de Rabek [28]).

Tableau 1.2 Longueur d'onde pour la dissociation des liaisons chimiques typiques dans les polymers par ordre croissant de longueur d'onde d'absorption (tableau adapté de Rabek [28]).

Liaison	λ (nm)
O-O	35
C-Br	45-70
C-Cl	60-86
C = C	179
O-H	249-336
C-H	286-301

L'intensité du rayonnement absorbé (dI) est proportionnelle au nombre de collisions entre les photons et les molécules [28, 29]:

$$\frac{dI}{I} = -N\delta_a dx \tag{1.1}$$

où I est l'intensité du rayonnement incident (photons / cm^2), N est le nombre de molécules absorbantes par centimètre cube, δ_a est l'aire de la section transversale d'interaction (cm^2) représentant la probabilité qu'un photon soit absorbé par une molécule et dx est l'épaisseur de l'échantillon. Cette équation peut être intégrée directement quand la concentration des molécules absorbantes est uniforme dans la direction du flux et est indépendante de l'intensité du rayonnement (cette dernière condition est valide lorsque le nombre de photons absorbés est une très faible fraction des molécules absorbantes). On en déduit l'équation intégrée:

$$I_a = I_0 \exp(-\delta_a NI) \tag{1.2}$$

Truica-Marasescu et Wertheimer [30] ont regroupé sur une unique figure la distribution spectrale, mesurée expérimentalement, des densités optiques dans le VUV de 4 différents polymères: polyéthylène (PE), polypropylène (PP), polystyrène (PS) et polyméthacrylate de méthyle (PMMA) (figure 1.4). Ces quatre spectres montrent une augmentation subite de l'absorption des polymères pour des longueurs d'ondes inférieures à 160 nm, due à l'absorption des chaînes alkyles et/ou à la photoionisation.

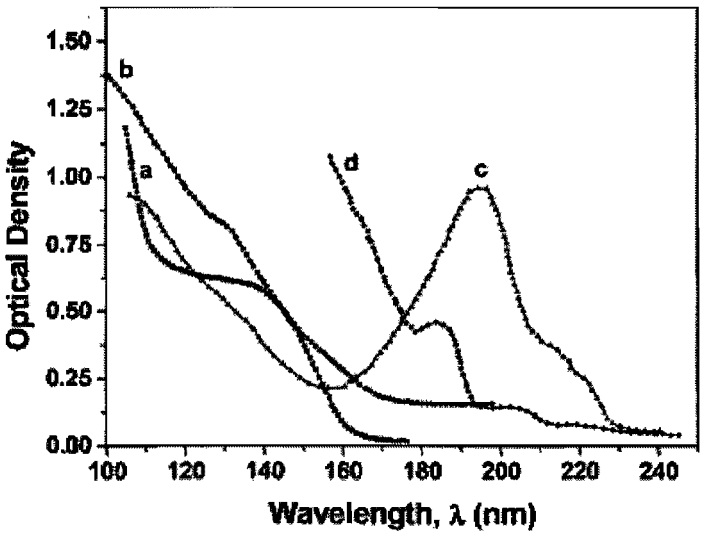

Figure 1.4 Spectre d'absorption VUV d'un film de a) 70 nm d'épaisseur de polyéthylène (PE), b) 29 nm polypropylène (PP), c) 33-nm de polystyrène (PS) et d) polyméthacrylate de méthyle (PMMA), (d'après Truica-Marasescu et Wertheimer [30]).

On observe sur la figure 1.4 que les quatre spectres montrent une densité optique importante en-dessous de 160 nm due à l'absorption des chaînes alkyles et/ou à la photoionisation. De ce fait, la profondeur de pénétration des VUV est limitée à quelques dizaines de nanomètres, contrairement à la pénétration des UV qui est de l'ordre de quelques micromètres dans les polymères hydrocarbonés communs [30].

1.2.2 Érosion des polymères par des espèces réactives

Un exemple d'érosion de polymères par des espèces réactives d'un plasma est donné à la figure 1.4 [31]. Ces deux micrographies obtenues au microscope électronique à balayage montrent l'érosion de microsphères de polystyrène par un plasma O_2/CF_4 (15 minutes de traitement).

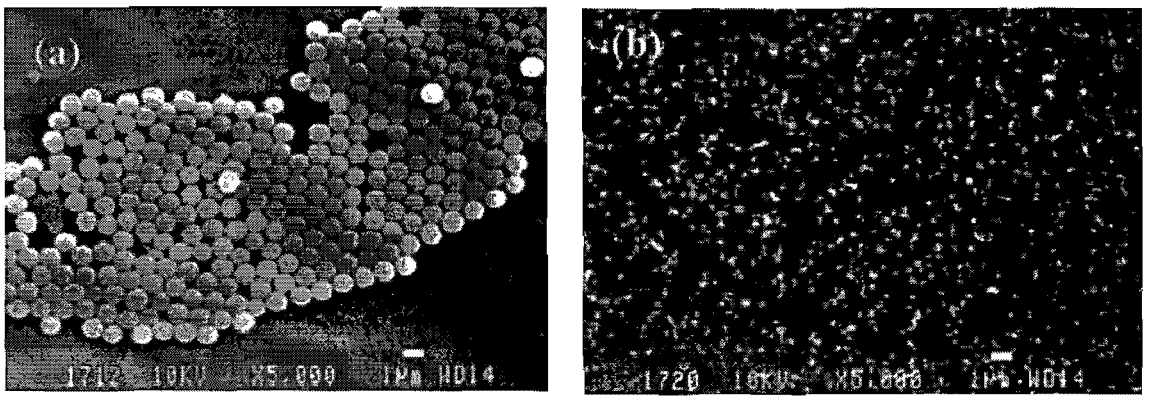

Figure 1.5 Micrographies obtenues au microscope électronique à balayage de particules de polystyrene : (a) contrôle non exposé ; (b) après 15 minutes d'exposition à un plasma de O_2/CF_4 (p = 100 mbar; P = 200 W; F = 50 sccm; [CF4] = 15%), d'après Lerouge *et al.* [31].

Les travaux de Crevier [19] ont, quant à eux, mis en évidence l'érosion de microsphères de polystyrène, cette fois dans une post-décharge de N_2-O_2 : il a été montré que l'érosion de ces microsphères est proportionnelle, entre 0.2 et 2 % O_2, au pourcentage d'O_2 injecté dans la décharge.

Finalement, il est à noter qu'il est possible de se représenter les interactions plasma/micro-organismes, tel que montré par Pelletier [32], comme l'interaction d'un plasma avec un polymère. Cette approche se justifie du fait que les micro-organismes sont formés de chaînes carbonées, d'azote, d'oxygène et de phosphore, et peuvent donc en première approximation être considérés comme des polymères dans le domaine de la stérilisation par plasma [33]. De fait, l'inactivation de micro-organismes par l'érosion due aux espèces chimiques réactives s'accompagne généralement de l'érosion des polymères sur lesquels reposent ces micro-organismes.

En somme, quel que soit le type mode d'action des agents biocides, il existe toujours des dommages aux matériaux. Ces effets sont cependant présents à divers degrés: par exemple, l'érosion due aux UV n'est généralement pas décelable sur des micrographies de polymères obtenues au microscope électronique à balayage. Toutefois, il est possible de mettre en lumière ces dommages en utilisant des techniques de diagnostics plus poussées comme une microbalance

à cristal de quartz, la spectroscopie de photoélectrons X [30], la goniométrie de surface [34] ou la microscopie à force atomique [35].

1.3 Notions microbiologiques pour physiciens

Cette thèse rassemble des travaux de recherches multidisciplinaires touchant à de nombreux thèmes tels l'électromagnétisme, la microbiologie et la physique des plasmas. Une partie non négligeable des travaux de cette thèse ayant trait à l'étude des effets d'un plasma sur des micro-organismes, il nous apparaît utile, à ce stade introductif, de rappeler quelques notions micro-biologiques pertinentes pour la compréhension de cette thèse.

1.3.1 Bactéries végétatives, endospores bactériennes et biofilms

Les bactéries sont des organismes vivants unicellulaires dépourvus de noyau: l'ADN est libre dans la cellule. Elles ont des dimensions de quelques micromètres de longueur, variables d'un genre à un autre, et peuvent présenter différentes morphologies: sphériques (coques), allongées ou en bâtonnets (bacilles), plus ou moins spiralées [36]. Deux types de micro-organismes ont été utilisés pour tester l'efficacité des stérilisateurs que nous avons développés: des endospores et des biofilms. L'origine historique de la découverte des endospores remonte à la deuxième moitié du 19ème siècle où Tyndall, Cohn et Koch ont indépendamment découverts que certaines espèces de bactéries passaient au moins une partie de leur vie sous la forme de structures cellulaires dormantes [37]. Certaines bactéries ont la capacité de former des endospores à partir de la forme végétative lorsque les conditions extérieures ne sont pas propices à leur croissance [25]. Elles protègent ainsi leur matériel génétique en formant une "coquille" tout autour de l'ADN. En fait, la spore n'a aucune activité métabolique; elle est en état de dormance [37]. Cependant, lorsque les conditions externes redeviennent favorables, la spore germe et forme de nouveau une bactérie métaboliquement active.

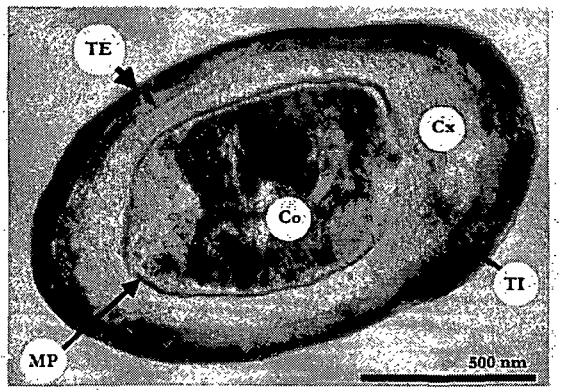

Figure 1.6 Micrographie par microscope à transmission d'une spore de *B. atrophaeus* sur laquelle les différentes tuniques protectrices du matériel génétique contenu dans le coeur sont identifiées. TE: Tunique Externe; TI: Tunique Interne; MP: Membrane Plasmatique; Cx: Cortex; Co: Coeur [38].

En raison de leurs résistances à des conditions extrêmes, les spores bactériennes de *Bacillus. subtilis* (bactérie récemment renommées *B. atrophaeus* [39]) ont été très étudiées. Selon Setlow [40], elles résistent particulièrement bien aux traitements chimiques, à la chaleur et aux UV.

En dépit de leur apparente simplicité, les bactéries peuvent aussi former des associations complexes [41]. Les bactéries présentes dans un biofilm présentent un arrangement particulièrement bien structuré de cellules et de composants extra-cellulaires (majoritairement des polymères de sucres), donnant lieu à des structures secondaires appelées microcolonies, dans lesquelles peut se former un réseau de canaux facilitant la diffusion des nutriments et l'élimination des produits du métabolisme. Dans son livre, « The biofilm primer » [42], Costerton a décrit les modes de développement des bactéries dans un biofilm. Ceux-ci sont complexes, car un biofilm possède une structure sociale. Selon Barbeau [43], "les premiers colonisateurs des surfaces changent inévitablement leur microenvironnement et le prépare à l'érection d'une communauté. L'organisation spatiale des différentes espèces suit des schèmes particuliers, dictés par les besoins de chacune d'elles: nécessité nutritionnelle et besoins respiratoires. Ainsi, comme dans les sociétés plus évoluées, les différentes diasporas microbiennes se regroupent souvent en micro-colonies. Le mode de vie sessile (attaché aux surfaces) favorise aussi la production et la sécrétion, par certaines espèces, de polymères de sucres qui serviront, entre autres, à enchâsser les individus dans le biofilm". Dans le cas de la stérilisation par plasma la matrice de sucre

entourant les bactéries leur permet de mieux résister aux attaques des agents biocides comme les UV et les espèces chimiquement actives, comme nous le verrons au cours de cette thèse.

1.3.2 Niveau d'assurance de stérilité (NAS)

La stérilité absolue d'un échantillon n'est pas vérifiable de façon pratique avec des tests microbiologiques [25]. On se sert plutôt de la notion de probabilité pour évaluer si une technique de stérilisation est fiable ou non. On utilise, en particulier, le niveau d'assurance de stérilité (NAS). Ainsi, le NAS d'un procédé est exprimé comme la probabilité d'occurrence d'un article non stérile dans une population d'articles donnée. Un NAS de 10^{-6} correspond à la probabilité d'au plus un micro-organisme survivant sur une population initiale de 10^{6} spores. Les spores bactériennes étant des micro-organismes beaucoup plus résistants que leur forme végétative, celles-ci sont utilisées comme indicateur biologique. Il est à noter que le NAS est un critère selon nous ambigu dans la mesure où il ne précise en rien la densité surfacique de spores devant être inactivées, un paramètre essentiel dans l'efficacité de la stérilisation par plasma, comme nous allons le voir dans la prochaine section.

1.3.3 Courbes de survie

Une courbe de survie représente le nombre (sous forme logarithmique) de micro-organismes survivants après traitement en fonction du temps ou de la dose d'agents actifs. Nous avons décrit une procédure très détaillée pour l'obtention d'une courbe de survie (voir page 75). Une version simplifiée d'un protocole standard utilisé pour l'obtention d'une courbe de survie a été présentée par Boudam [33]. "Afin de construire cette courbe, on a recours à deux méthodes: i) la méthode de numération directe, utilisée lorsque le nombre de survivants est assez élevé (supérieur à 100) et qui consiste à étaler, par dilutions successives, sur un milieu de culture solide la charge microbienne récupérée après traitement, et d'en effectuer le décompte après incubation; ii) la méthode de filtration sur membrane utilisée (avantageusement, parce que beaucoup plus précise) lorsque la population de survivants est inférieure à 100, et qui consiste à filtrer la totalité de la suspension de récupération à travers une membrane dont la porosité retient les microorganismes.

La membrane est ensuite déposée sur un milieu de culture solide et un décompte est effectué après incubation."

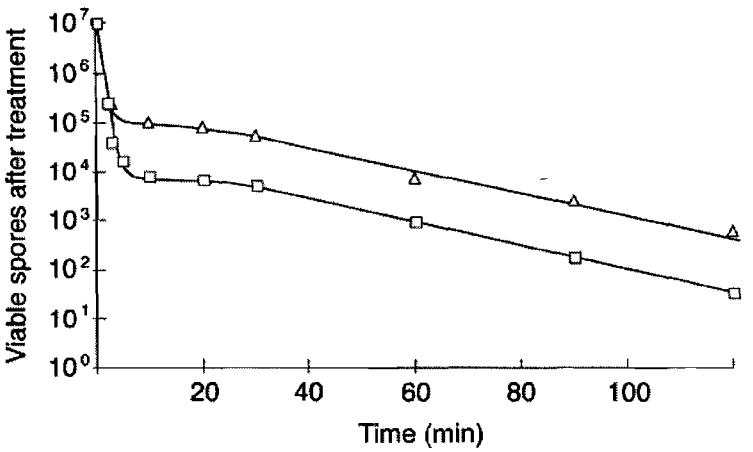

Figure 1.7 Exemple de courbe de survie, d'après Hury *et al.* [44]: influence de la densité surfacique de spore sur l'inactivation de *B. atrophaeus* après exposition à un plasma de CO_2. Haute densité surfacique de spores (Δ) obtenue avec 50 µl d'une suspension de 2.10^8 spores.ml^{-1}; faible densité surfacique de spores (□) obtenue avec 500 µl d'une suspension de 2.10^7 spores.ml^{-1}.

Deux exemples de courbe de survie sont représentés sur la figure 1.7 (d'après Hury *et al.* [44]). Ces courbes de survie ont été obtenues dans les mêmes conditions plasma, avec le même nombre initial de spores (10^7), mais avec deux densités surfaciques de spores différentes, ce qui permet d'obtenir des empilements de spores plus ou moins importants. L'explication donnée par ces auteurs (et qui constitue l'hypothèse généralement acceptée en stérilisation par plasma à pression réduite) est que les agents biocides du plasma inactivent d'abord les spores isolées et celles à la surface d'empilements, tandis que la ou les couches de spores plus profondes sont principalement inactivées, plus tardivement, dans ce qu'on appelle la deuxième phase. Ceci constitue une ambigüité dans le niveau d'assurance de stérilité (NAS), qui ne précise pas la densité surfacique de spores à inactiver.

1.4 Contribution de l'auteur, démarche de recherche et objectifs de la thèse

Cette thèse rassemble les brevets et les articles scientifiques pour lesquels notre contribution est majeure, tel qu'attestée par le fait d'en être premier auteur. Il s'agit de 2 demandes de brevets (la version américaine de chacune y est reportée pour l'essentiel) et de 5 articles (dont 4 déjà publiés). Pour chacune de ces publications, nous avons contribué à la conception des expériences, à la prise de mesures ainsi qu'à l'écriture et la mise en forme du manuscrit soumis à publication. Notre contribution ainsi que celles des co-auteurs est précisée pour chacun de ces 7 documents dans l'annexe 4, tel que demandé dans le guide de présentation des thèses de doctorat de l'Université de Montréal. Afin de mieux visualiser l'organisation de la présente thèse par article, l'annexe 4 contient également une figure montrant la localisation de ces publications dans la thèse.

Pour faire ressortir la cohérence de cet ensemble de travaux, nous avons inséré, en amont de chacune de ces publications, une section introductive expliquant l'enchaînement des idées directrices, c'est-à-dire la logique et les motivations qui ont structuré notre démarche de recherche. De surcroît, pour mieux équilibrer notre présentation et gagner en clarté, chaque chapitre comporte une section de discussion et sa propre conclusion.

La finalité de la thèse est de produire des sources plasma pour la stérilisation d'objets médicaux. L'originalité de la démarche de recherche adoptée est décrite à la figure 1.8. Ce diagramme montre l'enchainement des étapes qui ont guidé notre démarche de recherche. Nous avons tout d'abord identifié certains besoins industriels qui pouvaient potentiellement être comblés en stérilisation par plasma, comme par exemple le retraitement de cathéters cardiaques. Ensuite, nous avons inventé des applicateurs de champs électromagnétiques permettant de créer des sources de plasma adaptées *a priori* à ces objets en tenant compte de leur géométrie et de leur nature (e.g. polymères thermosensibles). Une fois ces sources de plasma mises au point, nous avons travaillé dans plusieurs directions tels (i) l'uniformité du plasma en modifiant les paramètres géométriques de la source de plasma, (ii) les performances électrodynamiques de l'applicateur de champ HF où nous avons optimisé le transfert énergétique du générateur vers le plasma, (iii) l'efficacité biocide du plasma en utilisant des indicateurs biologiques particulièrement résistant au plasma (des spores et des biofilms) ainsi que des méthodes de

caractérisation des agents biocides (e.g. spectroscopie d'émission optique) et (iv) la minimisation des dommages aux matériaux contenus dans l'objet médical à traiter (e.g. le Téflon) et des matériaux connus pour être particulièrement dégradés par un plasma (e.g. des microsphères de polystyrène).

Pour chacune de ses quatre étapes, nous avons évalué les limites de l'efficacité du procédé (symbole ✧ sur le diagramme) et avons donc parfois remis en question la capacité des systèmes que nous avions développés à stériliser l'instrument médical en question. Ceci nous a poussés, entre autres, à arrêter le développement d'une source de plasma utilisant des antennes distribuées autour d'un tube diélectrique (voir section 2.2) et à abandonner nos tentatives de mises au point d'un stérilisateur pour endoscopes souples (voir section 2.6). Nous avons souhaité discuter de ces systèmes qui n'ont pas fonctionné, car ce sont, d'une part, ces informations qui ont orienté notre démarche de recherche en nous offrant une meilleure connaissance des problèmes rencontrés et, d'autre part, afin de faciliter les recherches qui se poursuivent dans notre Groupe et dans le monde sur le développement de sources de plasma et sur le retraitement des endoscopes souples.

Par ailleurs, au cours de ces travaux, certaines questions de science fondamentale ont été soulevées et sont discutées dans nos articles ainsi qu'à la section 3.3 où nous avons apporté certains éléments de réflexion supplémentaires.

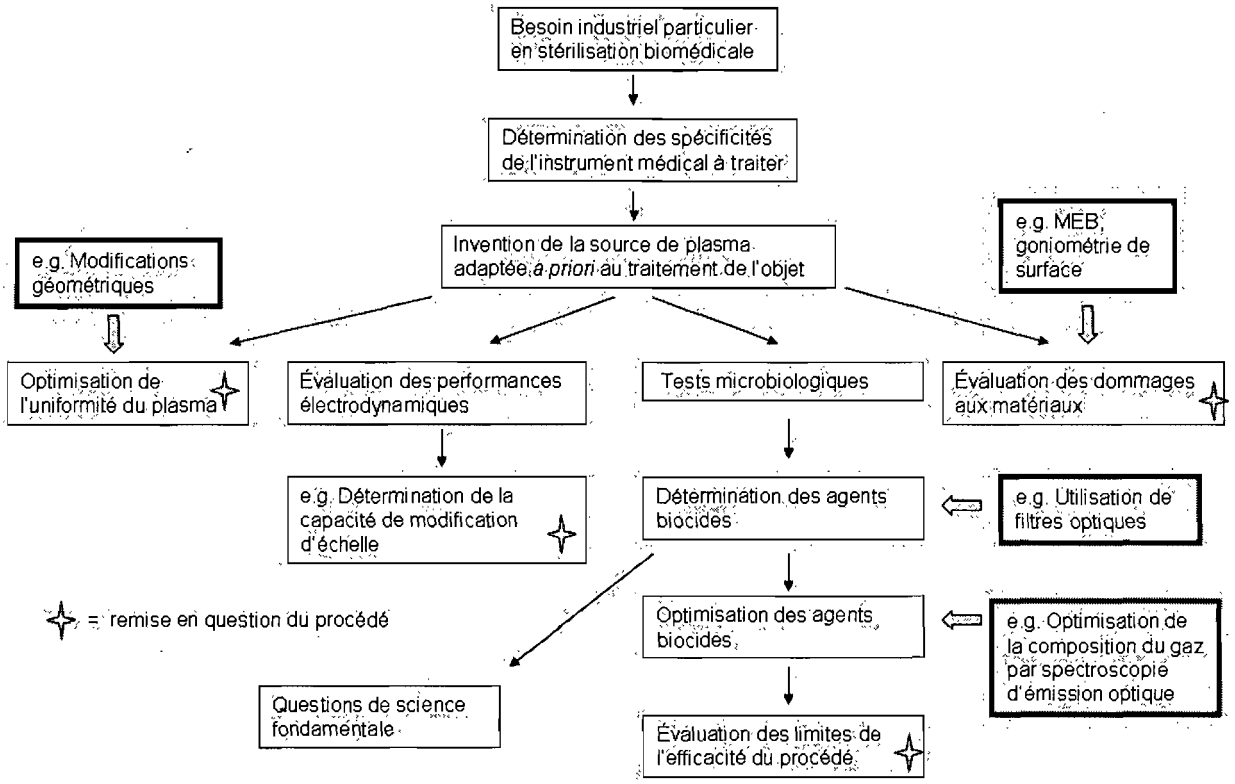

Figure 1.8 Diagramme de la structure des travaux effectués et des idées maîtresses de la thèse.

D'un point de vue plus concret, la structure des travaux effectués reflète également les objectifs précis que nous nous étions fixés en débutant nos travaux:

1) Caractériser un applicateur de champ électromagnétique, conçu pendant notre travail de maîtrise mais demeuré jusque là à l'état brut, permettant de créer un plasma dans des tubes diélectriques possédant un faible diamètre interne (< 4 mm) et une grande longueur (> 50 cm).

2) Stériliser par plasma en quelques minutes l'intérieur de tubes diélectriques formés de polymères thermosensibles (tel le Téflon) couramment utilisés dans la fabrication des cathéters cardiaques (actuellement, la plupart de ces dispositifs médicaux sont à usage unique).

3) Déterminer et optimiser les agents biocides (e.g. photons UV, espèces chimiquement actives) participant à l'inactivation par plasma dans la décharge.

4) Évaluer puis minimiser les dommages causés par le traitement plasma aux polymères afin que les tubes puissent subir plusieurs cycles de stérilisation sans dommages structurels empêchant leur réutilisation.

5) Développer, tester et optimiser un système de stérilisation en décharge permettant un traitement rapide (< 3 minutes) de surfaces dans une source de plasma d'environ 5 litres.

Pour bâtir cette thèse, nous l'avons logiquement divisée en deux chapitres de résultats et de discussions, avec pour guide l'enchaînement des idées de la figure 1.8: au chapitre 2, nous présenterons une structure pouvant stériliser l'intérieur de tubes diélectriques thermosensibles (e.g. des cathéters cardiaques) et au chapitre 3, un dispositif permettant la stérilisation, par immersion dans le plasma, d'objets tridimensionnels (e.g. des forceps). Pour chacune de ces deux sources de plasma, nous avons également déterminé puis optimisé les agents biocides permettant d'inactiver des micro-organismes. Dans notre cas, il s'agit principalement de la gamme de rayons ultra-violets (UV) de longueur d'onde inférieure à 300 nm, qu'il convient donc d'enrichir si on veut accroître la vitesse d'inactivation, en photons d'où l'intérêt des études spectroscopiques présentées au cours de cette thèse.

Chapitre 2

Stérilisation de la surface interne de tubes diélectriques

Certains dispositifs médicaux (DM) tels les cathéters cardiaques et les endoscopes souples sont constitués de polymères thermosensibles comme le polyuréthane et le Téflon. Ces instruments ne peuvent donc pas être stérilisés par les méthodes à haute température sans qu'il y ait endommagement de leurs propriétés. De plus, la particularité géométrique de ces structures qui comprennent un ou plusieurs canaux longs (souvent de plus d'un mètre) et étroits (parfois de diamètre aussi faible que 1.5 mm) ajoute à la difficulté de la méthode même de stérilisation. Dans les faits, ces dispositifs sont soit à usage unique, ce qui est majoritairement le cas des cathéters, soit seulement hautement désinfectés, et non stérilisés, dans le cas des endoscopes souples. Des recherches universitaires et industrielles sont activement menées à l'échelle internationale pour proposer des solutions efficaces permettant de réaliser la stérilisation de ces dispositifs.

L'obstacle scientifique principal du retraitement d'instruments médicaux comportant de longues parties creuses est la capacité de pénétration des agents biocides à l'intérieur des canaux, la stérilisation de leur surface externe ne posant que peu de problèmes techniques. En ce qui concerne les méthodes plasma, les dispositifs de post-décharge, bien qu'efficaces sur des objets comportant des parties creuses de faible profondeur, sont mal adaptés à la stérilisation de la surface interne de tubes de petit diamètre et de grande longueur. En effet, dans le cas de la post-décharge, il est nécessaire d'imposer une importante vitesse d'écoulement au gaz afin d'utiliser les espèces actives (émetteurs de photons UV, radicaux) créées en décharge, espèces d'une durée de vie limitée ($\leq$ 500 ms). Les tubes de petit diamètre possédant une faible conductance hydrodynamique, il est difficile d'exploiter les espèces actives, car il se forme à leur entrée une importante élévation de pression qui ralentit la progression des espèces biocides au point où celles-ci se désactivent avant qu'elles n'aient pu jouer leur rôle sur la totalité de la longueur du DM [3].

Il restait donc à mettre au point une méthode de stérilisation par plasma adaptée au traitement de l'intérieur de ces tubes qui ont la propriété d'être de nature diélectrique (transparents aux champs électromagnétiques (EM)), où le plasma serait créé directement à l'intérieur des tubes,

sur toute leur longueur, à partir d'un applicateur de champ haute-fréquence (HF) situé extérieurement. Pour mettre au point cette méthode de stérilisation, plusieurs stratégies ont été envisagées. Avant de les présenter, nous allons tout d'abord rappeler, en guise d'introduction, les principaux types d'applicateurs de champ EM HF, ce qui nous servira par la suite à mieux caractériser et situer les sources de plasma développées.

2.1 Introduction

Il existe de nombreux types d'applicateur de champ haute-fréquence (HF) permettant de créer et d'entretenir une décharge. Nous pouvons citer en exemple les bobines conductrices entourant un tube diélectrique donnant lieu aux décharges dites inductives et les lanceurs d'ondes de surface qui, au contraire d'une bobine HF, peuvent être localisés sur quelques cm de longueur du tube à décharge et donner naissance à un plasma s'étendant sur une beaucoup plus grande distance. Chaque type de plasma possède ses propres caractéristiques opérationnelles, offrant un large éventail de possibilité pour l'utilisateur. Cependant, malgré le grand nombre de sources de plasma HF déjà disponibles, pour certaines applications et pour des besoins industriels particuliers, le développement de nouvelles sources de plasma peut s'avérer nécessaire.

Le schéma de la figure 2.1 propose une classification des principaux applicateurs de champs électrique HF. Cette classification est largement inspirée des travaux de Zakrzewski et Moisan publiés en 1995 [45]. Initialement, les sources de plasma micro-ondes étaient surtout créées à l'intérieur de cavités résonnantes avec pour conséquence que leurs dimensions et leur volume étaient très limités. Par la suite, pour obtenir un plasma micro-ondes de grande longueur par rapport à la longueur d'onde du champ EM (avant l'introduction des plasmas d'onde de surface), le champ électrique qui entretient la décharge devait provenir d'une onde, progressive ou stationnaire, qui est portée par un applicateur de champ s'étendant tout le long de l'enceinte à décharge. Souvent ce type d'applicateur possède une dimension beaucoup plus grande que les deux autres et est, pour cette raison, dénommée « applicateur linéaire ». Dans ce cas, on fait souvent appel, comme applicateur de champ, à une ligne de transmission : par exemple, un guide d'onde rectangulaire enserrant le tube à décharge ou un guide d'onde à fente irradiant vers le tube à décharge situé à l'extérieur. Pour les mêmes fins, il est également possible de disposer une ou plusieurs antennes le long du réacteur. En fait, le plasma est soit créé à l'intérieur de la structure

de propagation (applicateur de type « ligne de transmission » tel que désigné dans l'article de Zakrzewski et Moisan [45]) ou extérieurement à celle-ci (applicateur dit de type « antennes »). Les sources de plasma constituant le cœur de notre thèse sont des applicateurs linéaires de type ligne de transmission et fonctionnant en mode d'onde progressive.

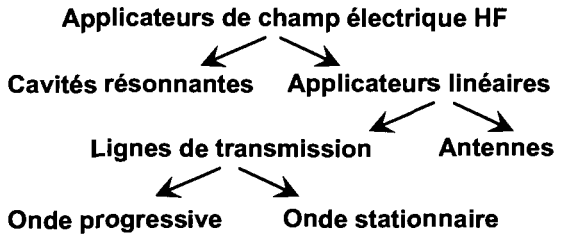

Figure 2.1 Classification des différents types d'applicateurs de champ électromagnétique permettant l'entretien de décharges HF, d'après Zakrzewski et Moisan [45].

Dans le cadre de notre recherche axée sur le thème de la stérilisation médicale, nous nous sommes intéressé à créer des sources de plasma offrant plusieurs caractéristiques spécifiques: (i) une faible température du gaz (< 50 °C) pour ne pas endommager les dispositifs médicaux (DM) formés de polymères dits thermosensibles ; (ii) une bonne uniformité spatiale du plasma pour traiter simultanément un ensemble de DM ; (iii) une technologie suffisamment adaptable géométriquement pour traiter des objets de forme complexe tel, par exemple, l'intérieur de longs tubes creux.

Étant donné que les deux problèmes majeurs auxquels nous faisons face quant aux sources de plasma déjà existantes étaient leur trop forte température du gaz en décharge pour pouvoir y introduire des objets médicaux et/ou la non-uniformité spatiale du plasma sur une longueur de plusieurs dizaines de cm, voire du mètre, nous avons tout d'abord pensé à recourir à un réseau de sources de plasma distribuées, tel que présenté à la prochaine section.

2.2 Développement d'une source de plasma utilisant des antennes distribuées autour d'une enceinte cylindrique à décharge

Nous avons tenté d'assembler le rayonnement de différentes antennes pour créer un plasma de quelques litres. Le schéma de principe de cette structure est présenté à la figure 2.2. Ce dispositif possède quatre arrivées de puissances micro-ondes coaxiales (en connecteurs N), chacune

alimentant deux antennes de type « patch » micro-ruban (donc 8 antennes en tout) rayonnant vers l'intérieur du système, là où est placé le tube à décharge. La fréquence d'opération choisie était de 2450 MHz, ce qui imposait des dimensions précises aux antennes (une demi-longueur d'onde guidée à la résonance).

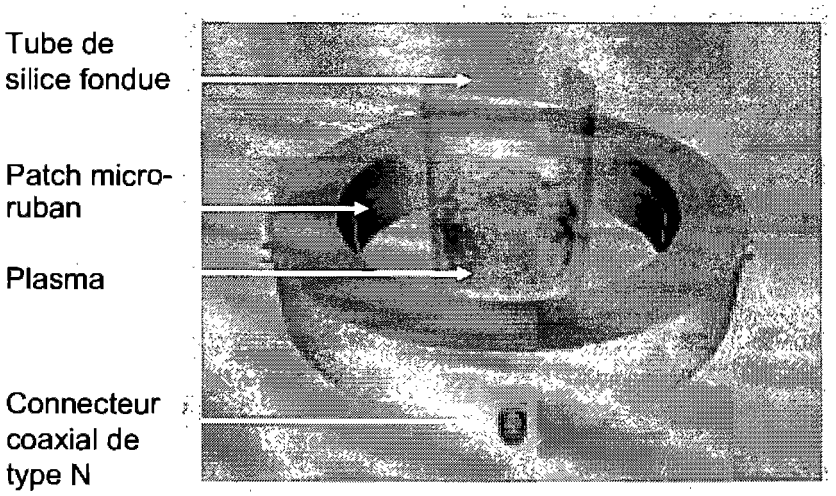

Figure 2.2 Schéma de principe d'une source de plasma à éléments distribués.

Malheureusement, nous avons rapidement réalisé que cette source de plasma ne permettait pas d'atteindre nos objectifs (en particulier, le plasma était fortement non uniforme, même à pression réduite), ce qui nous a poussés à arrêter son développement et à nous tourner vers d'autres types de sources de plasma telles que présentées à la section suivante.

Par ailleurs, l'alimentation en puissance micro-ondes (2450 MHz) des nombreuses antennes de la source de plasma nécessitait de scinder l'arrivée de puissance HF en plusieurs portions égales pour chaque groupe d'antennes, préférablement sans qu'il y ait interférence de leur part sur la distribution de puissance. Ceci a pu être assuré au moyen d'un dispositif en guide d'ondes rectangulaire que nous avons perfectionné à partir des travaux initiaux de Pelletier *et al* [46]. Nous avons résumé brièvement les recherches que nous avons effectuées sur ce dispositif dans le paragraphe ci-dessous (les détails de ce dispositif sont disponibles dans un article situé à l'annexe 1).

Diviseur de puissance

Nous avons caractérisé une structure micro-ondes permettant, à partir du flux de puissance circulant dans un guide d'onde rectangulaire, de réaliser sur ce flux un nombre arbitraire de prise

de puissance de valeur égale (ou non selon les besoins), chacune renvoyée sur autant de sorties coaxiales (figure 2.3). Concrètement, le flux de puissance micro-ondes provenant du générateur se propage initialement le long d'une section de guide d'onde rectangulaire puis est réfléchi en raison d'une plaque conductrice placée à son extrémité, créant ainsi une onde stationnaire le long du guide d'onde. La division de puissance s'obtient en introduisant dans le grand côté du guide d'onde des antennes de type champ électrique placées aux positions de maximums d'intensité du champ électrique stationnaire. En utilisant la méthode des circuits équivalents, nous avons élaboré les expressions analytiques donnant l'admittance d'entrée de ce dispositif en fonction du nombre de sorties coaxiales. Nous avons raffiné ce circuit équivalent en considérant de surcroît l'influence mutuelle entre antennes. En somme, ce diviseur de puissance pouvant fonctionner sur un flux micro-ondes de haute puissance (≥ kW) apparaît à la fois compact et efficace en termes de caractéristiques électrodynamiques, ce qui en fait un dispositif de choix pour alimenter simultanément et de façon non interactive plusieurs sources de plasmas.

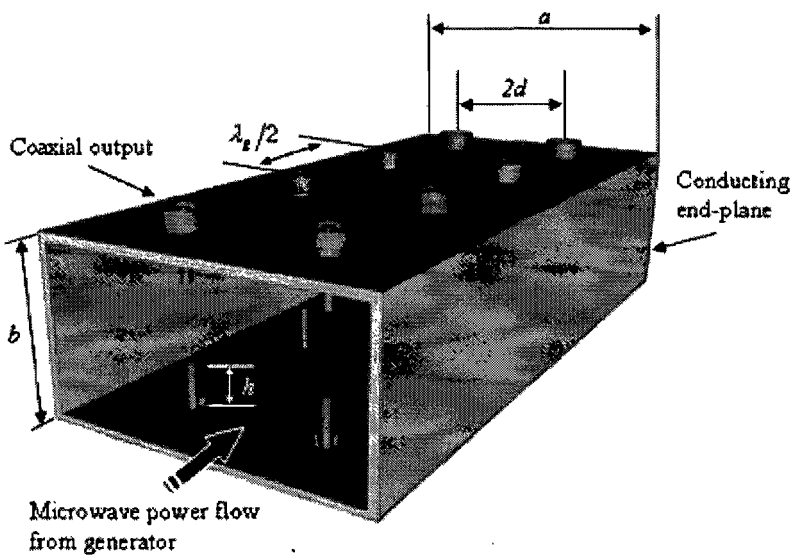

Figure 2.3 Représentation simplifiée en trois dimensions du diviseur de puissance que nous avons caractérisé et optimisé (voir l'article reproduit à l'annexe 1 pour plus de détails).

En somme, ces travaux initiaux, bien que peu encourageant dans l'optique d'atteindre nos objectifs fixés en introduction, nous ont apporté plusieurs enseignements dans notre quête du développement d'une source de plasma permettant de traiter efficacement des objets médicaux.

Tout d'abord, les applicateurs de champs électromagnétiques à développer doivent posséder une configuration suffisamment simple pour pouvoir facilement en réaliser une réduction ou extension d'échelle (e.g. pour traiter des tubes diélectriques d'un diamètre interne allant de 1.5 à 8 mm). C'est pourquoi nous avons cherché d'autres alternatives et nous sommes tournés vers le développement de structures utilisant une ligne de transmission plane, telle que celle présentée dans la prochaine section pour le traitement de l'intérieur de tubes médicaux.

2.3 Développement d'une source de plasma linéaire pour tubes diélectriques

Les lignes de transmission planes possédant au moins deux conducteurs parallèles l'un à l'autre présentent un intérêt certain, peu encore exploité, pour créer et entretenir un plasma. Le récent engouement qu'elles ont suscité résulte principalement du fait qu'elles propagent un mode Transverse Électrique et Magnétique (TEM) ou quasi-TEM, ce qui offre la possibilité de les exploiter dans une large bande de fréquence (typiquement 27-2450 MHz), à la différence des guides d'onde classique (rectangulaires ou cylindriques). De plus, elles peuvent être facilement adaptées à différentes configurations d'enceintes à décharge. En outre, les caractéristiques électrodynamiques de ces structures sont peu affectées par la présence du plasma créé à l'intérieur de celle-ci (bien adaptée du point de vue impédance sans plasma, il n'apparaît aucune puissance réfléchie avec plasma). De ce fait, l'optimisation de ses performances en absence de plasma est une démarche suffisante, qui s'effectue en considérant l'impédance caractéristique de la ligne de transmission, la fréquence maximale d'opération de celle-ci et les possibilités de réduction ou d'extension d'échelle requises. Finalement, comme ce sont des structures ouvertes qui ne rayonnent pas moyennant le respect de certaines contraintes géométriques, il est possible d'évaluer l'uniformité axiale des plasmas ainsi entretenus par des mesures optiques, comme nous allons également le voir dans l'article qui suit. Le lecteur intéressé pourra également trouver des informations d'ordre plus techniques sur le concept de cette source de plasma dans la demande de brevet située à l'annexe 2.

Long and uniform plasma columns generated by linear field-applicators based on stripline technology

(article publié dans Plasma sources science and technology 2007 **16** 310-323)

J. Pollak, M. Moisan, Z. Zakrzewski

Abstract

Long plasma columns generated by high-frequency (HF) fields and extending over distances longer than the free-space wavelength of the applied electromagnetic (EM) field are of interest in various applications. A commonly used method to achieve such long plasma columns calls for the propagation of EM surface waves that use the plasma as their propagating medium. In such a case, the HF field applicator, called a wave-launcher, is much shorter than the actual length of the plasma column. Long plasma columns can also be sustained by using field applicators that run along the full length of the discharge tube. Most such linear applicators rely on waveguide components. However, it is possible to use TEM (transverse electric magnetic) planar transmission lines based on stripline technology to design efficient linear field-applicators. Using such an approach, we have developed a new type of HF linear field applicator that operates on a relatively wide frequency range (typically, 200-2450 MHz). Comparison of the discharge that it generates with a surface-wave discharge (SWD) sustained under similar operating conditions shows that the discharge volume is larger than that obtained with a SWD at the same power level, hence a lower gas temperature and a plasma column more axially uniform, two valuable features for some applications. The contraction of these plasma columns is shown to occur at higher gas pressures than with SWDs. All these measurements are carried out in argon as the discharge gas.

2.3.1 Introduction

There are many ways of applying a high frequency (HF: this term designates jointly radio and microwave frequencies) field to generate, within dielectric tubes, plasma columns that are long compared to the free-space wavelength of the applied electromagnetic (EM) field. Nowadays, most of these discharges are sustained through the propagation of EM surface waves where the field applicator, in this case called a wave launcher, needs to extend only over a short segment of the plasma column created (see, e.g. [1]). Long HF plasma columns can also be sustained by field applicators that run along the full intended discharge length. These elongated structures with one dimension much larger than the others, termed linear applicators, are mainly based on waveguide technology. A review and a classification of such applicators have been presented in [2].

The current article reports a new type of linear field applicator that provides long, uniform and low-gas-temperature plasma columns, which could be used, for instance, to sterilize heat-sensitive, long and small-diameter hollow tubes such as endoscopes [3]. This novel plasma source is based on the stripline, a transmission line of planar configuration well known in microwave engineering [4]. The concept and features of this plasma source will be examined in the case of a low-pressure discharge (0.1 - 20 torr; 13 – 2600 Pa).

This work is not the first attempt at utilizing planar transmission lines in the design of plasma sources. In recent years, microstrip structures have been employed to generate micro-plasmas. A microstrip is comprised of a conducting strip "deposited" on a dielectric substrate resting on a conducting surface, but it should not be understood as necessarily meaning a microstructure. Micro-plasmas are of a very limited spatial extent as implied by their designation, and are supplied at very low HF power levels that, in some cases, nonetheless correspond to high-density values of absorbed HF power [5-10]. The motivations driving research on these microsystems are discussed by Broekaert [11]: these microstrip structures are mainly used to generate plasma at atmospheric pressure for spectrochemical analysis. In contrast, our novel system aims at producing large volume plasmas, actually plasma columns that are much longer than the free-space wavelength of the EM field, and at power levels (10 to 500 W) much higher than for micro-plasmas.

The paper is organized as follows. Section 2.3.2 introduces the concept of long plasma-column generation with stripline field applicators. The electrodynamic properties of such structures

without plasma and with plasma are examined in sections 2.3.3 and 2.3.4, respectively. A comparison, under similar experimental conditions, between the plasma column generated by a stripline field applicator and that sustained by a surface wave is presented in section 2.3.5. Section 2.3.6 suggests a classification of planar transmission lines when utilized as field applicators to sustain plasma. Section 2.3.7 is the conclusion.

2.3.2 Using striplines to generate plasma columns

2.3.2.1 The stripline configuration used

Microwave guiding structures can be divided into two broad categories: those that propagate TEM or quasi TEM modes, and those that support the other modes [12]. The stripline belongs to the first category. The stripline is a planar transmission line (also called triplate line), as shown in figure 1. It consists of a conducting strip (which can be cylindrical or planar: here it is planar) of width w and thickness t centred between two wide, parallel, conducting (ground) plates of width L separated by a distance h. A homogeneous dielectric of relative permittivity ε_r fills the entire region comprised between the parallel ground-plates and the conducting strip. The HF power is generally applied at one end of the conducting strip.

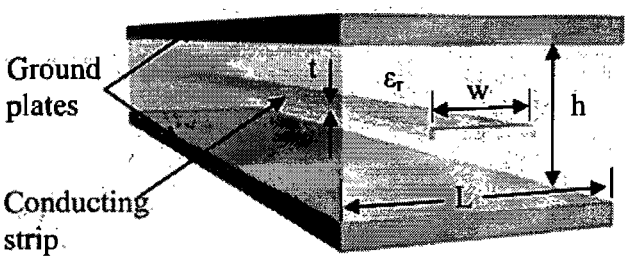

Figure 1. Configuration and characteristic dimensions of our stripline transmission-line.

An approximate sketch of the electric field lines within this planar transmission line is shown in figure 2, which corresponds to a cross-sectional view of figure 1. The direction of propagation of the electromagnetic TEM wave is along z and its field components are E_y and H_x, except at the lateral edges of the conducting strip where some E_x-field component is generated.

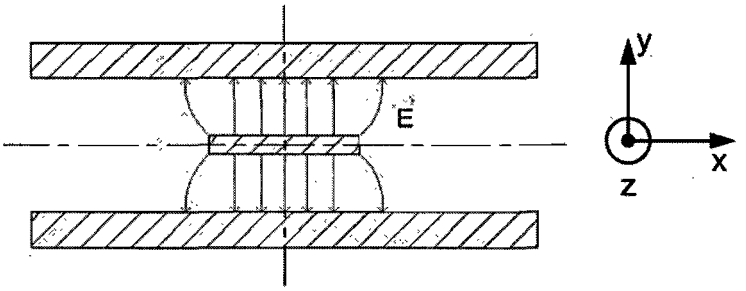

Figure 2. Approximate representation of the electric field lines within the stripline transmission-line of figure 1.

Intuitively, one can think of the present stripline as a sort of "flattened out" coaxial line. The conceptual evolution, shown in figure 3, from a coaxial line to this stripline supports this view.

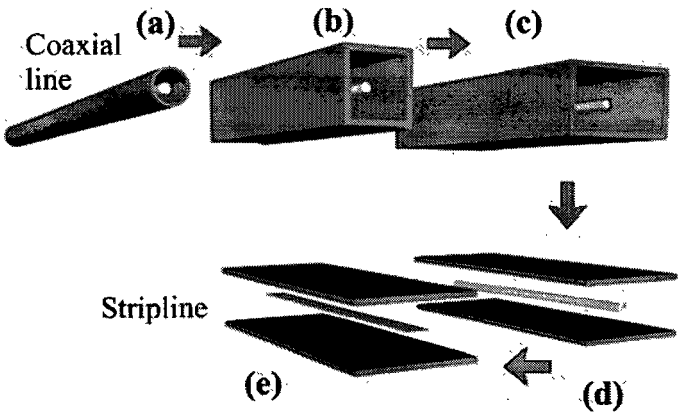

Figure 3. Conceptual evolution from the coaxial line to the stripline, a partially open flat-transmission-line (after [13]).

The coaxial line and the stripline transmission-line can both propagate the fundamental TEM mode. Since the coaxial line (figure 3(a)) is a closed structure, no electromagnetic energy can flow out of it. In contrast, the stripline (figure 3(e)) is a partially open structure from which, provided some dimensional restrictions are obeyed, no microwave energy leaks out: specifically, it requires the width L of the conducting ground-plates to be large enough compared to the distance h between these plates and to the width w of the conducting strip (figure 1). Then, the lateral closing plates can be removed (figure 3(d)) without fearing microwave leakage, as we now show experimentally.

2.3.2.2 Dimensional conditions for the stripline transmission-line to be a non-radiating open structure

The fact that a stripline transmission-line, under appropriate dimensional conditions, is non-radiating is known from the literature, but it has not been demonstrated experimentally in the way that we are going to do it. This is because, as rule, for compactness reasons, classical striplines are imbedded in a dielectric substrate (of a high ε_r value), whereas in our case the stripline lies in air, allowing the introduction of a probing antenna within it. The variation of the electric field component E_x (clearly E_y cannot exit the stripline), detected with an electric-field antenna (see inset in figure 4), is plotted in figure 4 as the antenna is withdrawn by 1 mm steps along the x-axis, starting at 1 mm from the conducting strip (y = 0). The observed decrease of $E_x(x)$ is so fast that, at x = 25 mm (compared to L = 200 mm), its intensity is already less than 10 % of its value at the origin. We further note that the degree of confinement of the electric field is almost independent of the actual frequency of the electromagnetic field, at least between 200 MHz and 800 MHz. The HF electric field is confined within the stripline because: i) its main component is directed along the y axis and its presence essentially limited to the width of the conducting strip (supplied with HF power) and its immediate vicinity (see the approximate E-field sketch in figure 2): no leakage is expected provided $L \gg w$; ii) the E_x component is generated on the lateral edges of the conducting strip (since an E field needs to be perpendicular to any conducting surface) and its intensity decreases as |x| increases because the E field, as we move away from the lateral edge of the conducting strip, rapidly tends to align in the y direction to become perpendicular to the surrounding conducting (ground) plates (see figure 2 again): no leakage is expected provided $L \gg h$. Figure 5 compares the relative variation of the E_x-field intensity of our striplines with h = 24.0 mm and h = 71.8 mm, at approximately the same width values w. It is clear that field confinement is better when the distance h between the ground plates is smaller, even though L is smaller in the present case (90 mm instead of 200 mm): as a matter of fact, h/L = 0.27 for the small h case and h/L = 0.35 for the large h case.

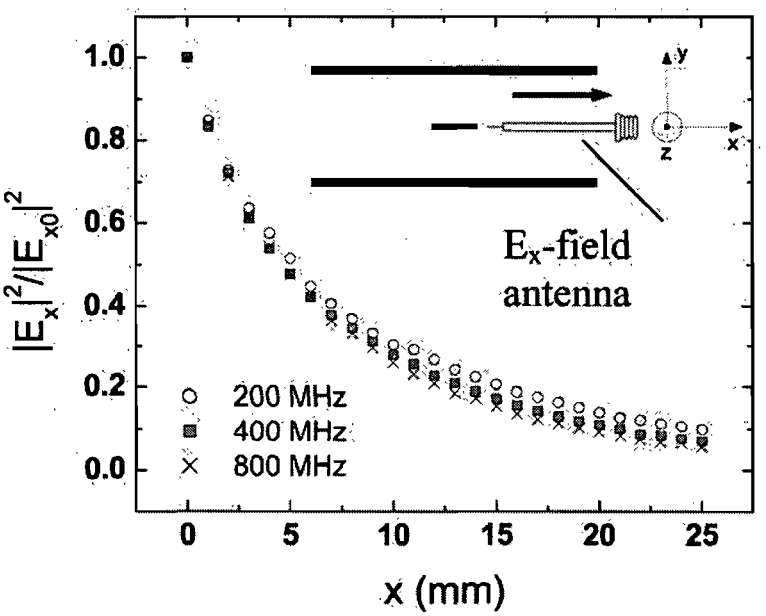

Figure 4. Variation of the intensity of the E_x component of the electric field, relatively to its value at x = 0, as a function of x for the stripline of figure 1, in air, where w = 31.0 mm, h = 71.8 mm and L = 200 mm, at three different frequencies of the electromagnetic field. The origin of the x-axis corresponds to the tip (5 mm long) of the antenna (0.6 mm/2 mm i.d./o.d.) positioned at 1 mm from the conducting strip.

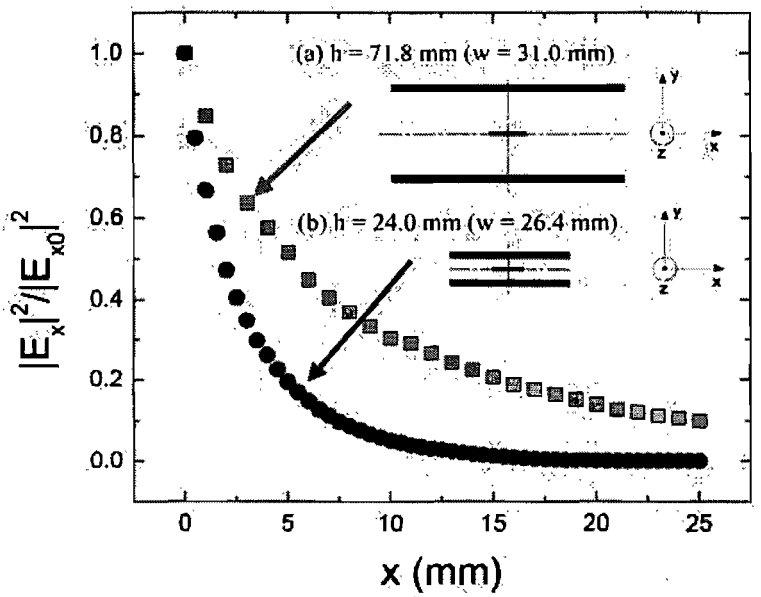

Figure 5. Relative variation along x of the E_x-field intensity showing that the E-field confinement depends mainly on the stripline height h: (a) h = 71.8 mm (w = 31.0 mm and L = 200 mm); (b) h = 24.0 mm (w = 26.4 mm and L = 90 mm). Applied field frequency is 200 MHz.

2.3.2.3. The stripline as a field applicator sustaining plasma columns

Figure 6 shows the design of the stripline plasma source that we are proposing: one or more dielectric tubes can be placed on both sides of the strip conductor within an air-dielectric environment.

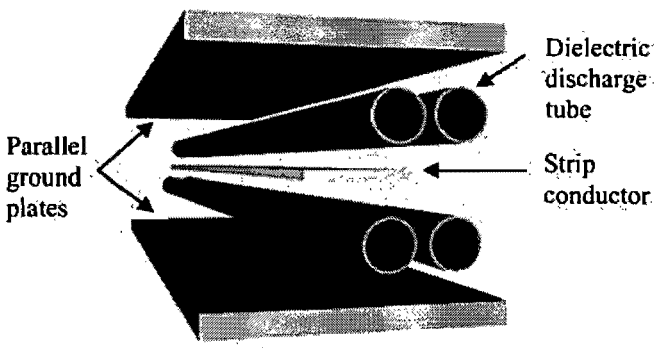

Figure 6. Schematic representation of a stripline field applicator showing, as an example, how four plasma columns can be sustained at the same time. The system can also be operated with less discharge tubes, even just one.

In the case of a pure TEM mode, the electric field is perpendicular to the direction of wave propagation (figure 2) and, therefore, there is no electric field component directed axially within the dielectric discharge tubes ($E_z = 0$). This prevents the launching of a surface wave that would, otherwise, generate a plasma column[3] with properties independent of those of the stripline field applicator (see section 2.3.5.3).

In what follows, we examine the electrodynamical properties of our striplines as field applicators, in the absence (section 2.3.3) and in the presence (section 2.3.4) of a discharge.

2.3.3 Electrodynamic properties of the stripline field applicator in the absence of plasma

An important feature of our stripline system is that its properties (including E-field profile, line characteristic impedance, ultimately input-power reflection coefficient) are very little affected, as will be shown, by the presence of plasma. As a result, the plasma source can be optimised, in particular in terms of power efficiency, by working on the dimensions of the stripline field applicator itself, a task that can be achieved with a network analyser since, in absence of plasma, HF powers as low as a few mW can be used. The following points need to be considered for ease of design and proper operation: i) HF power should preferably be supplied to the plasma source using conventional 50 Ω coaxial lines, which implies setting the values of the w and h parameters such that they yield 50 Ω for the applicator characteristic impedance; ii) the position and structure of the input and output HF power connectors to and from this new type of field applicator have to be examined. In particular, the fact that the discharge tubes are set parallel to the stripline axis requires the connectors to be implemented sideways (see appendix A1); iii) proper operation of the stripline applicator requires the EM power to flow in the TEM mode, which imposes some constraints on the scaling-up of this system.

2.3.3.1. Characteristic impedance of our stripline field applicator

[3] It has been shown by Sauvé *et al.* [14] with a waveguide-type field applicator that an electric field directed perpendicularly to the discharge tube does not excite a surface wave plasma whereas a slightly tilted EM beam does.

The value of the characteristic impedance Z_0 of our stripline was determined, first, experimentally, employing a method proposed by Yue *et al.*[15]. For that purpose, a network analyzer is utilized for recording the magnitude of the stripline input voltage-reflection coefficient, $|\Gamma_{in}|$, as a function of frequency, the stripline being terminated here by a load impedance Z_L (equal to 50 Ω). Classically, it leads to the voltage standing-wave ratio (VSWR) since VSWR = $(1 + |\Gamma_{in}|)/ (1 - |\Gamma_{in}|)$, as illustrated in figure 7. The value of Z_0 is then obtained from the following expression [16] :

$$\left(\frac{Z_0}{Z_L}\right)^{\pm 1} = \sqrt{(\mathrm{VSWR})_{max}(\mathrm{VSWR})_{min}} \qquad (1)$$

where the exponent +1 is used when $Z_0 > Z_L$ and −1 when $Z_0 < Z_L$. The ambiguity related to the ± sign in equation (1) can, in practice, be readily removed as we know that Z_0 decreases monotonously with increasing w/h.

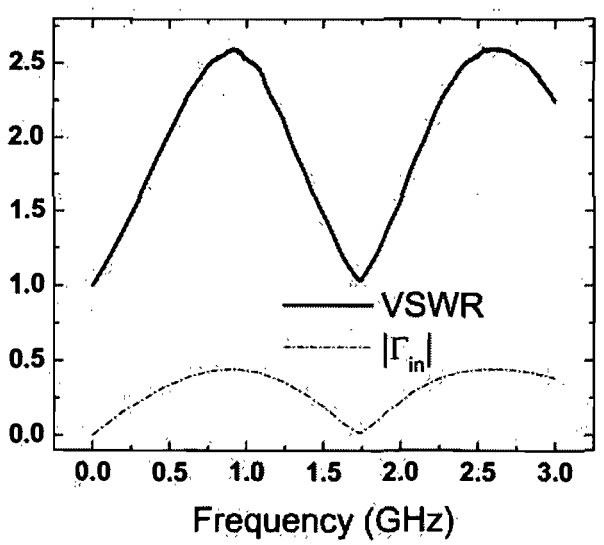

Figure 7. Example of a VSWR pattern determined experimentally from the magnitude of the recorded input voltage-reflection coefficient, $|\Gamma_{in}|$, as a function of frequency for a stripline of characteristic dimensions h = 24.0 mm, t = 3.2 mm and w = 48.0 mm and terminated by a 50-ohm load.

The measurements shown in figure 8 for Z_0 were carried out by varying the conducting strip width w. The domain of w/h values investigated was such that the measured Z_0 values were close

to the impedance of the feeding line. The Z_0 values are plotted in figure 8 as a function of the w/h ratio, the height h being kept constant (h = 24.0 mm).

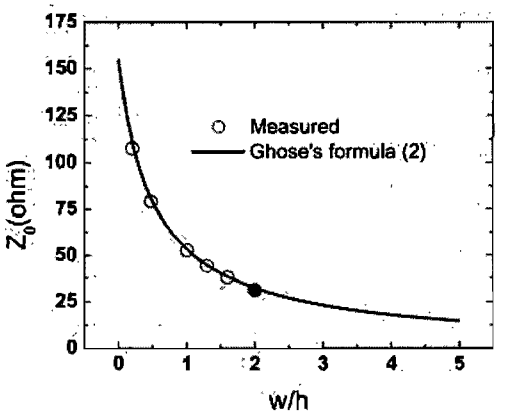

Figure 8. Measured characteristic impedance of the stripline as a function of the conducting strip width (open circle); the full circle data point at w/h = 2.0 is inferred from figure 7. The theoretical curve is obtained from relation (2).

Various expressions for the characteristic impedance of a stripline can be found in the literature (e.g. [4, 17, 18]). Here, we use a simple empirical formula provided by Ghose [19] :

$$Z_0\sqrt{\varepsilon_r}=94.15\left(\frac{w}{(h-t)}+1.18\frac{t}{h}+0.45\right)^{-1}, \qquad (2)$$

where the characteristic impedance Z_0 is expressed in ohm. The rest of the notation is as defined in figure 1. As both the distance h separating the ground plates and the thickness t of the six conducting strips considered (varying w) in establishing figure 8 remained the same, the value of the t/h parameter in (2) was actually constant and, in the present case, equal to 3.2 mm/24.0 mm = 0.133. Figure 8 shows a remarkable agreement between our measurements and the values of Z_0 calculated from Ghose's formula [19], underlining the dominant role of the w/h parameter in determining the value of Z_0.

2.3.3.2. Limitations in the scaling-up of our stripline applicator

Our way of utilizing a stripline as a field applicator for plasma column generation is not classical since the distance h separating the parallel ground plates is much larger (typically by a

factor 10) than what is commonly employed in microwave engineering. Therefore, we need to look for possible limitations when scaling-up this field applicator.

In that respect, we already know that in order to avoid energy leakage to the outside of the structure, whenever increasing h, L has to be widen (see figure 5). As for the stripline characteristic impedance, it can be set at 50 Ω by turning to realistic values of *w* and *h* in relation (2) (generally $t \ll h$ and t can thus be neglected in (2)). Finally, the domain of validity for operating in the TEM mode, in particular for expression (2) to be applicable, has to be ascertained. Formula (2) ceases to be valid whenever increasing w or h makes any of them becoming equal to a certain fraction of the EM wavelength. As a matter of fact, the maximum frequency for TEM mode operation of a stripline of given dimensions can be expressed as [20]:

$$f_{max}\,(\mathrm{GHz}) = \frac{15}{h\sqrt{\varepsilon_r}} \frac{1}{\left(\frac{w}{h} + \frac{\pi}{4}\right)} \tag{3}$$

where w and h are in cm. This maximum frequency corresponds to the cutoff frequency of the first TE mode since this mode, when increasing frequency, is the next one after the (fundamental) TEM mode to be excited within a stripline. The variation of this cutoff frequency as a function of h for two different characteristic impedances, 50 ohms and 100 ohms, is plotted in figure 9 (recall that the Z_0 value chosen sets the value of the w/h ratio through relation (2), assuming t can be neglected as compared to h).

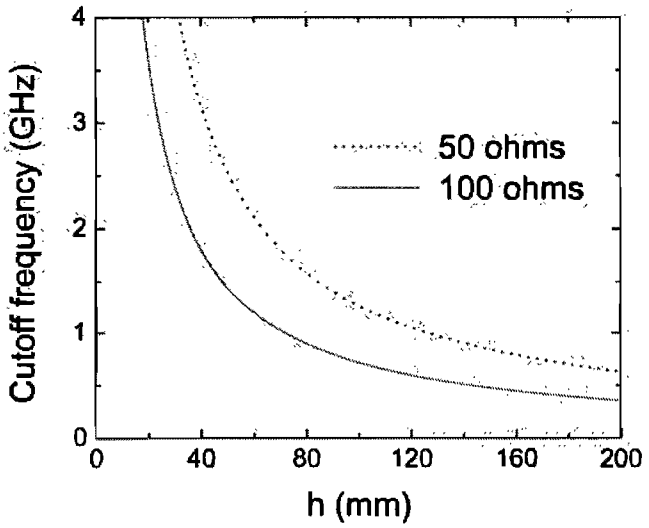

Figure 9. Maximum frequency of operation of the stripline field applicator under a pure TEM mode as a function of the distance h separating the parallel ground plates, as calculated from relation (3) for characteristic impedances of 50 ohms and 100 ohms.

The physical meaning of formula (3) can be illustrated by considering the following example. When h is larger than 30 mm, figure 9 indicates that the stripline applicator at 2.45 GHz with a 50-ohm line would no longer operate in the TEM mode and, as a result, it would not be power efficient. The fact that the free-space EM wavelength at 2.45 GHz is 122 mm implies that the height h should not be typically higher than a quarter of a wavelength.

2.3.3.3 Practical realization of our stripline field applicator

We have designed, built and experimentally characterized several field applicators in two geometries: linear and circular. Only the linear one is described in this paper. Its structure is sketched according to cross-sectional, top and side views in figures 10(a), (b) and (c), respectively. The thickness of the two ground plates is 6.4 mm and that of the strip is 3.2 mm. Dielectric supports are used to hold both the discharge tubes and the conducting strip; conducting spacers are used to connect electrically the two ground plates and ensure a constant distance h between them. Greater design detail is given in the appendix.

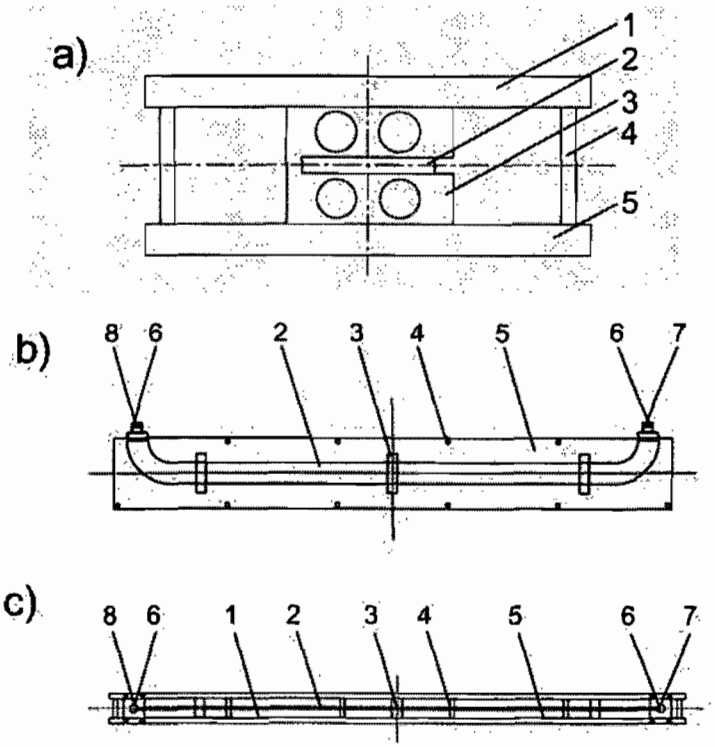

Figure 10. (a) Schematic cross-sectional view of a linear stripline field-applicator (flat conducting strip) designed to sustain simultaneously four plasma columns (or less). (b) Schematic top view of the applicator in figure 10(a), with the upper plate (1) removed. (c) Schematic side view of the applicator shown in figure 10(a).

Number designation

1. Upper conducting plate
2. Centred conducting strip
3. Dielectric support for the conducting strip and discharge tubes
4. Conducting post (spacer)
5. Lower conducting plate
6. N-type coaxial connector
7. Incoming HF power from generator through coaxial cable
8. Matched load at the stripline output for dissipating the HF power not absorbed by plasma

2.3.4 Electrodynamic properties of our stripline field applicator in the presence of plasma

2.3.4.1 Experimental arrangement for plasma generation and HF-power measurements

The experimental arrangement for generating plasma with our stripline applicator is shown in figure 11. We have worked at powers from a few watts up to a few hundred watts with applied field frequencies varying from 50 to 2450 MHz (data reported only in the 200 - 2450 MHz range).

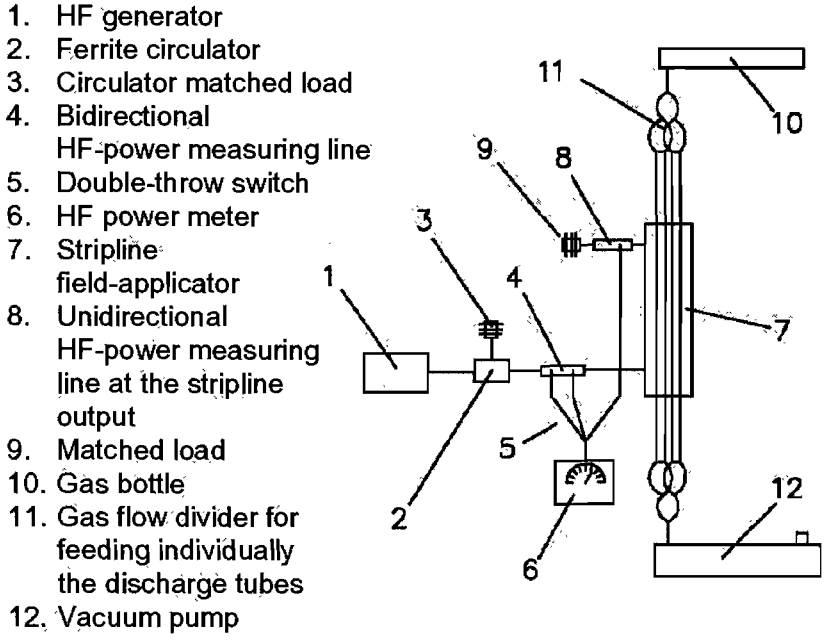

Figure 11. Schematic representation of the experimental arrangement showing the components related to feeding and measuring microwave power as well as those required for gas feeding and flow control.

Measurements of the incident power P_I and of the reflected power P_R at the stripline input are made using a calibrated bidirectional power-measuring-line (4) (together with a thermistor power meter (6)) located between the output port of the circulator and the stripline applicator input. Measurements of the transmitted power P_T exiting from the applicator are made using a directional power coupler (8) (together with a thermistor power meter (6)) located between the stripline end (output) and a matched load (9). The terminating matched load (9) prevents HF power to be reflected at the end of the stripline, which would affect the HF field intensity distribution along the stripline field applicator. This is the only matching means of this plasma source, which is frequency independent!

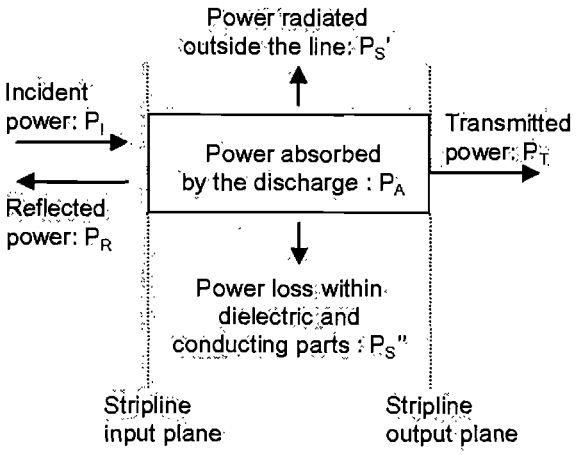

Figure 12. Schematic representation of the power flows to, in, and out of the stripline field applicator in the presence of plasma, with indications of the various loss mechanisms.

Figure 12 is a schematic representation of the HF power flows within the stripline field applicator with indications of the loss mechanisms. Using energy conservation (and the notation in figure 12), the power P_A absorbed by the plasma can be written as:

$$P_A = P_I - P_R - P_T - P_S' - P_S''. \quad (4)$$

By using wide enough parallel ground plates, we ensure that there is no radiated power outside the applicator (see figure 5)[4], and thus $P_S' = 0$. Utilizing a network analyser in the transmission mode (see appendix), we can check that the power lost within the stripline structure (air environment) in the absence of plasma is negligible compared to the incident power. Therefore, relation (4) reduces to:

$$P_A = P_I - P_R - P_T \quad (5)$$

which allows a fast determination of the power absorbed in the discharge, P_A. Comparing P_A with P_I amounts to determining the power efficiency of the stripline plasma-source, the ratio value $P_A/P_I = 1$ implying a 100% efficiency.

2.3.4.2 HF-power efficiency of the stripline plasma source

To characterize the power efficiency of our plasma source, we have used a single (fused silica) discharge tube of 6 mm inner diameter (i.d.), centred with respect to the conducting strip. The argon flow was set to 10 sccm (standard cubic centimetre/min) at a pressure of 100 mtorr (13 Pa) and a field frequency of 2.45 GHz. The stripline dimensions are those of figure 5(b). Figure 13 examines the power absorbed by the plasma as a function of the incident power under these operating conditions. The percentage of reflected power at the stripline input remains zero over the whole range of incident HF power examined (10-110 W). As the HF power is raised from 10 to 20 W, the plasma column length increases (not shown in the figure); at 20 W, the whole tube length located within the field applicator (620 mm) is filled with plasma; at higher incident HF powers, part of the incoming power flow going across the field applicator is not absorbed in the plasma and is, in fact, sent to the matched load located at the output of the applicator (see figure 11) to prevent reflection at the applicator end. Because of this, above 20 W, there is a decrease of the percentage of absorbed power by the plasma, as shown in the figure.

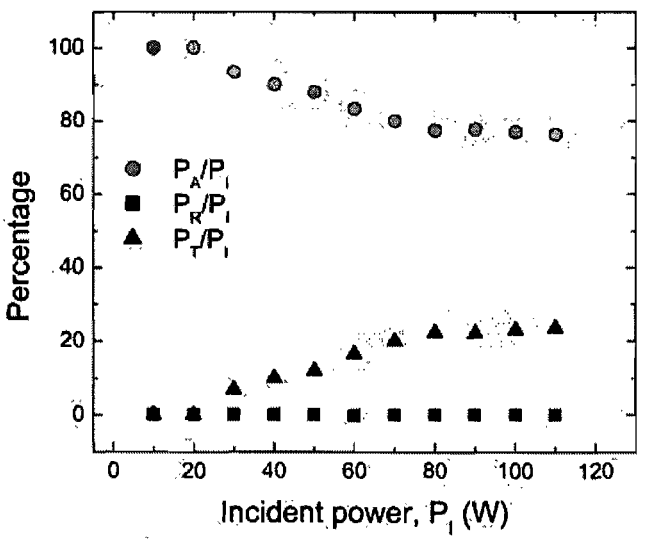

Figure 13. Percentage of the reflected power, P_R, of the transmitted power, P_T and of the absorbed power, P_A, normalized to the incident power, P_I, as functions of P_I, at 2.45 GHz. The discharge tube, 6 mm i.d., is made from fused silica, and argon gas is used at a 10 sccm flow and a 100 mtorr pressure. Stripline dimensions as in figure 5, case (b).

---

[4] This can also be shown by fully closing the stripline structure by adding lateral conducting walls and observing then that there is no change in the measured power flows P_I, P_R and P_T.

The same type of power measurements as in figure 13 was carried out also at 200 MHz and 600 MHz in addition to 2.45 GHz, as shown in figure 14. Altogether, less than 3 % of the incident power is reflected at the applicator input plane (not shown). It means that no impedance matching system is, practically speaking, needed at the applicator input to achieve an efficient power transfer from the HF generator to the plasma source over the 200-2450 MHz frequency range. However, we observe in figure 14 that the applied frequency has a significant impact over the percentage of absorbed power by the plasma: it increases with frequency. This is due to the fact that the electron density increases as the frequency of the field applied to the discharge is raised, as supported experimentally by the increase in the emitted light intensity (not shown) and by calculations presented in the section that follows.

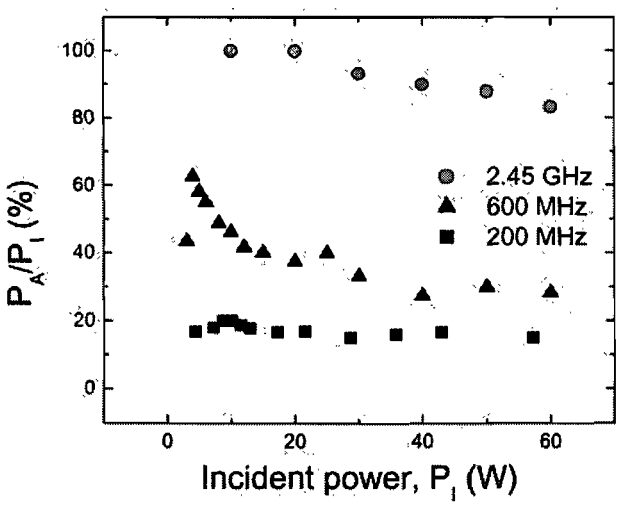

Figure 14. Percentage of power absorbed by the plasma with respect to incident power as a function of the incident power at three field frequencies, namely 200 MHz, 600 MHz and 2.45 GHz (stripline dimensions as in figure 5, case (b)).

2.3.4.3 Influence of the electron density regime on the electrodynamical properties

This section is devoted to determining whether and to what extent the plasma is overdense, having in mind possible effects on, for example, the distribution of the electric field intensity existing in absence of plasma. An HF discharge is overdense when its electron plasma (angular) frequency, $\omega_{pe} = (n_e e^2/m_e \varepsilon_0)^{1/2}$, exceeds the applied (angular) field frequency, ω, where n_e, is the

electron density, e and m_e the electron charge and mass respectively, and ε_0 the permittivity of free space. The value of electron density obtained when $\omega_{pe} = \omega$ is termed the critical density, n_c, and an overdense plasma can also be defined by $n_e > n_c$.

2.3.4.3.1 Density of the plasma and minimum field frequency of operation as functions of the tube diameter. Most standard diagnostic techniques for measuring the electron density could not be utilized with our stripline plasma. Such is the case with, for example, double Langmuir probes (HF field perturbation), resonant cavities (no accessibility), Stark broadening (too low an electron density). We therefore turned to the estimation of the electron density of the stripline plasma on the basis of the absorbed power per unit length [1]:

$$L(n_e) \equiv \pi R^2 n_e \theta \tag{6}$$

where θ is the power lost (and absorbed) per electron, R, the inner radius of the discharge tube. Values of θ have been obtained experimentally by Moisan *et al.* [21] from the absorbed power in surface-wave discharges, and these values confirmed by theoretical calculations [22]. As shown in [23], the value of θ deduced from a given kind of discharge is, in fact, applicable to all kinds of electrical discharges sustained under the same operating conditions. Using such published values of θ and our experimentally observed L values averaged over the stripline plasma column, one can infer the electron density from relation (6). It is plotted in figure 15. We observe that n_e is larger than n_c suggesting that the discharge is (slightly) overdense over the 200 to 2450 MHz domain investigated.

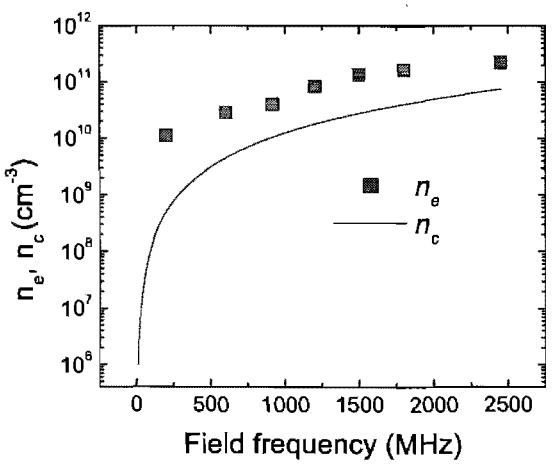

Figure 15. Comparison between the critical density, n_c, and the estimated value of the electron density, n_e, using equation (6). Experimental conditions: 0.1 torr of argon, 6 mm/8 mm i.d./o.d. tube to which there corresponds $\theta \approx 10^{-11}$ W as reported in [23].

A further argument supporting the electron density values displayed in figure 15 is related to the fact that a discharge can be achieved only provided the plasma sheath width is not larger than the radius of the discharge tube. Following Lieberman and Lichtenberg [24], we take the sheath width s as a few times the Debye length λ_{De}, say 3 times its value:

$$s \approx 3\,\lambda_{De} = 3\left(\frac{\varepsilon_0 T_e}{e n_e}\right)^{1/2}, \tag{7}$$

where T_e is the electron temperature in eV. Estimation of the electron temperature using, for example, calculations by Steenbeck and Von Engel [25] yields $T_e \approx 2$ eV as a reasonable numerical value. Figure 16 shows the sheath width calculated from expression (7) as a function of field frequency, assuming that the electron density is either the critical one or ten times this value, and adding the electron density value as plotted from experiments in figure 15.

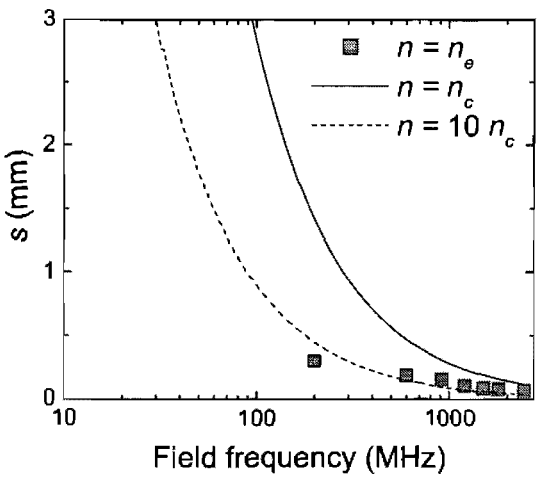

Figure 16. Estimated sheath width calculated using relation (7) as a function of field frequency, assuming that the electron density is either n_c, the critical one, or ten times this value (dotted and full lines, respectively). The sheath thickness corresponding to the n_e values inferred from equation (6) for a 6 mm i.d. tube are also shown (full squares).

Figure 16 shows a relative good agreement between the sheath width stemming from the estimated n_e values (figure 15) and that when assuming $n_e = 10\ n_c$. Considering that a discharge cannot be achieved when s exceeds half the tube diameter, figure 16 implies that the discharge could not be sustained below 30 MHz in the case $n_e = 10\ n_c$, while assuming $n_e = n_c$ would raise the cut-off to 100 MHz.

Figure 17 plots the minimum power, P_{min}, required to sustain a discharge as a function of the field frequency. The results for the 6 mm i.d. tube shows that the stripline discharge can be sustained at least down to 27 MHz, a fact consistent with considering $n_e \approx 10\ n_c$ in figure 16. As expected, the smaller the tube diameter, the higher the minimum frequency at which a discharge can be sustained: a practical cut-off frequency can be considered to be reached when P_{min} exceeds 200 W in the case where the discharge can be sustained at higher frequencies with only 10 to 20 W (actually, a 2 cm long discharge is taken as a reference).

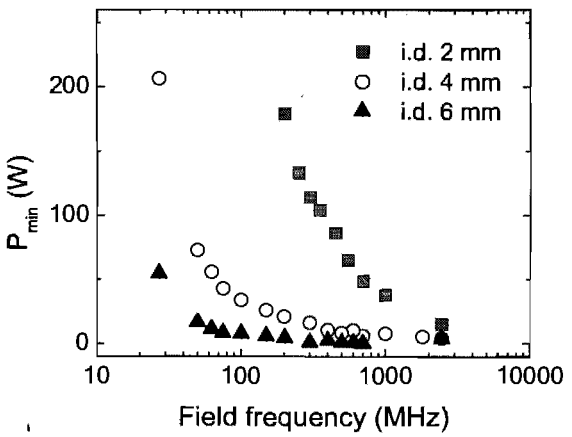

Figure 17. Measured minimum power value required to sustain a 2 cm-long (reference) stripline discharge as a function of the applied field frequency, for three discharge tube diameters.

2.3.4.3.2. Influence of the overdense plasma on the stripline impedance matching and on the electric field intensity profile. The arguments suggesting that the stripline plasma is overdense are not in contradiction with the fact that the power reflected at the stripline input, over the whole frequency range tested (27-2450 MHz), is not modified ($P_R/P_I \leq 3$ %) when the discharge is sustained (see section 2.3.4.2). This is because the characteristic impedance of the stripline is the same, whether the plasma is on or off: in other words, the stripline does not "see" the plasma. It

comes from the fact that the power transferred per unit length from the stripline to the discharge is small compared to the power flow (see also sections 2.3.5.1 and 2.3.5.2).

When a plasma is overdense, as a rule, the distribution of the electric field imposed by the EM field applicator in absence of plasma is modified when the plasma is switched on. This is not the case here, essentially because the plasma is only slightly overdense. This can be seen from figure 18 that compares the lateral decrease of the (normalized) intensity of the x-component of the electric field as measured with an x-oriented electric-field antenna (see figure 4), with and without the discharge: both profiles of the electric field intensity are similar. This behaviour can be explained by considering the penetration depth, δ, that expresses the evanescence (non-collisional "skin effect") of the EM field in an overdense plasma. It can be written as:

$$\delta \simeq \frac{c}{\sqrt{\omega_{pe}^2 - \omega^2}} = \frac{c}{\sqrt{\frac{e^2}{m\varepsilon_0}(n_e - n_c)}}. \qquad (8)$$

We find here that the tube radius is much smaller than the skin depth ($\delta / R \approx 4-20$) at any frequency between 27 and 2450 MHz and therefore, although the plasma is overdense but only slightly, its presence should not affect the profile of the electric field intensity as the discharge is switched on, shown in figure 18.

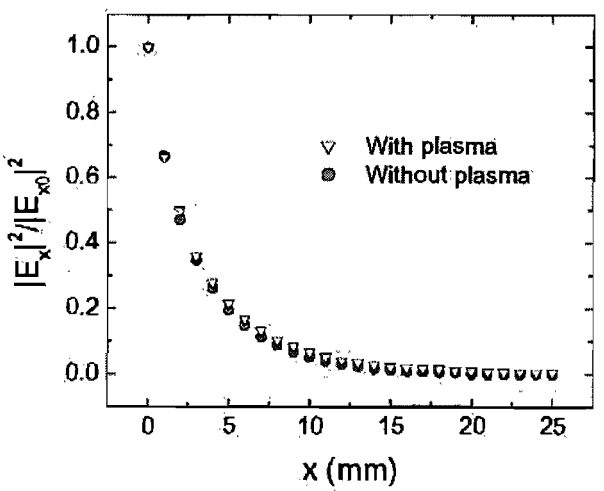

Figure 18. Profile (normalized distribution) of the intensity of the E_x component of the electric field, relatively to its value at x = 0, as a function of x, with and without the discharge. The intensity of these two recordings is normalized at unity for x = 0 (in presence of plasma, the

measured field intensity at mid-axial position decreases to 0.8 times its value without plasma). Experimental conditions: f = 600 MHz, 1 torr of argon, 6 mm/8 mm i.d./o.d. discharge tube.

2.3.5 Comparison between the discharge from a stripline field applicator and that from an EM surface wave

2.3.5.1 Power density absorbed in the discharge

For given discharge conditions, the HF power absorbed per unit plasma volume is much less in the stripline discharge than in the surface-wave discharge (SWD) as we show. Consider the inset in figure 19 where two stripline discharge configurations are depicted: a single discharge tube in one case and two discharge tubes in the second case. Since the length of the central conducting strip is 62 cm, this is the maximum plasma column length that the present prototype of stripline applicator can yield when using a single discharge tube. To have more power fully absorbed into plasma, we subjected two discharge tubes to the field applicator; in such a case, the plasma volume created is obtained by adding up these two plasma columns. Figure 19 shows the length of the single plasma column and that of the double plasma column as obtained with the same stripline applicator as well as the length of the plasma column from the surface-wave discharge as functions of absorbed microwave power, under the same operating conditions, namely argon gas at 1 torr, 6 mm i.d. discharge tube and 915 MHz applied-field frequency; stripline dimensions as in figure 5 case (b) and the wave launcher is a surfatron [26]. The observed threshold length of the SWD as a function of absorbed power comes from the fact that a minimum electron density (absorbed power) is required for the surface wave to propagate [1].

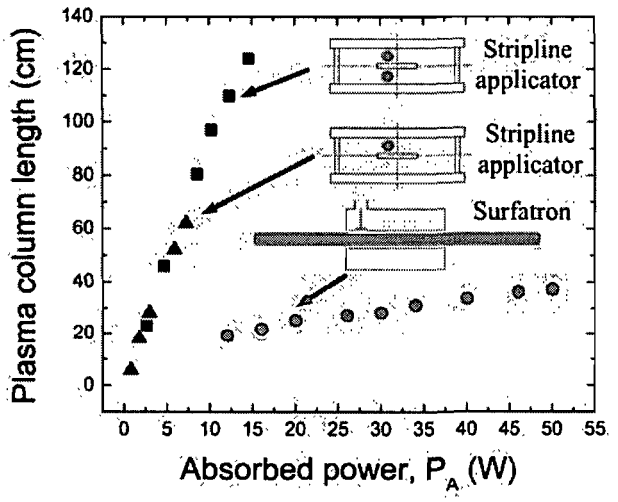

Figure 19. Length of the plasma column sustained by a stripline field applicator in the case of a single discharge tube (▲) and total length of the plasma columns in the case of two discharge tubes (■), compared with the length of the plasma column sustained by a surface wave (●) as functions of absorbed power (stripline dimensions as in figure 5 case (b), field frequency 915 MHz).

We observe that, for a given absorbed power, the stripline discharges are five times longer than the SWD. It implies that the absorbed power per unit plasma volume is five times lower in the stripline discharges than in the SWD. This result is consistent with a qualitative observation of the discharge tube temperature after a few minutes of operation: the stripline discharge tube is almost at ambient temperature, while the SWD tube is too hot to be touched (over 50 °C).

2.3.5.2. Measured axial distribution of emitted light intensity

Figure 20 shows the emitted light intensity recorded with a photodiode (and a collimator: see section 2.3.5.3) over the 330-800 nm range along the SWD and along the stripline discharge, in both cases at a field frequency of 915 MHz. The emitted light intensity is more uniform axially in the case of the stripline discharge, implying that its plasma density is also more uniform. This can be explained by considering that, although these two kinds of discharges are sustained by a travelling wave, the wave power absorbed by the stripline discharge per unit length, dP_A/dz, is much smaller and related to a lower electron density in the discharge (see section 2.3.5.4).

Because the power deposited locally is much smaller than the power flow, the wave power decreases only slightly along the field applicator, leading to an electron density, on the average, that decreases only slightly axially.

At any rate, in both cases, the electron density tends to decrease with increasing z, as can be seen in figure 20, as a result of the power flow of the propagating wave being expended in sustaining the discharge. The overall decrease of the electron density along the stripline is more pronounced the longer the stripline applicator, the larger the tube diameter or the higher the field frequency. Such a nonuniformity of the plasma could have undesirable effects for some applications. A possible solution to compensate for the electron density decrease is to switch the HF power feeding port with that of the matched load at half process time. A second solution would be to reduce gradually the cross-sectional dimensions of the applicator structure when going from the power input side to the matched load side, as already proposed by Zakrzewski and Moisan [2] in the general case of a long linear field applicator and by Slinko et al. [27] in the specific case of a plasma column laying longitudinally within a rectangular waveguide, the height of which is gradually decreased in the power flow direction. A third possibility is to remove the matched load and use its port to actually feed the stripline from a second microwave generator (not phase related with the first one to avoid standing waves along the stripline).

The integration as a function of z of the light intensity axial profiles recorded in figure 20 shows that the total intensity of the stripline discharge is approximately 10 times less than that of the SWD while its power density (related to plasma column length), in figure 19, is only 5 times less than that of the SWD. A factor of 2 higher for the light intensity compared to plasma column length (absorbed power) for the stripline discharge could result from various factors that include the difference in pressure between figure 19 (1 torr) and figure 20 (100 mtorr) as well as a difference in radial distribution of the emitted light intensity in these two types of discharge, as discussed in the next section.

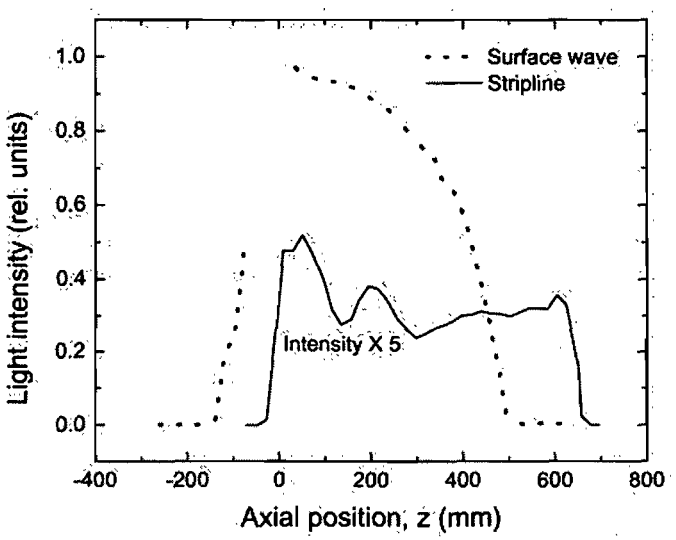

Figure 20. Recorded axial distribution of emitted light intensity along the plasma columns sustained by a stripline field applicator and a surface wave (surfatron wave-launcher) at 915 MHz in argon gas at 100 mtorr in a 6 mm i.d. tube. The surfatron launching gap is located at z = 0 where a front (z > 0) and a back surface wave (z < 0) are excited. The surfatron body extends from z = - 80 mm to z = 0, preventing light collection over that z interval. The light collimator was aiming at the diameter chord of each discharge tube.

2.3.5.3. Light intensity recorded transversally to the discharge tube axis as an indication of the discharge radial uniformity

The intensity of the emitted light, in this section, is recorded transversally, i.e. as a function of lateral position y (see figure 4), at z = 310 mm, under the following operating conditions: argon gas at 20 torr, an applied field frequency of 600 MHz, a 26 mm i.d. discharge tube. To ensure some spatial resolution to these lateral measurements, a 1 mm-diameter light collimator, 30 mm long, connecting to an optical fibre, was used. Figure 21 shows that the lateral profile of the stripline discharge and that of the SWD do not have the same symmetry. The lateral profile of the SWD is symmetric with respect to the discharge tube axis, while the profile of the stripline discharge is clearly asymmetric with the maximum of intensity off-axis (preventing us from performing Abel inversion to obtain the radial profile of light intensity from the stripline discharge). In fact, the lateral profile of the stripline discharge is wider than that of the SWD, suggesting a radially more uniform plasma than with a SWD. The lateral decrease of the light

intensity of the stripline discharge with increasing y is consistent with the continuous decrease of the electric field intensity from the central strip (y = 0) to the ground plate. By comparison with measurements made at one torr (not reported), the lateral profile of the light intensity of the SWD at 20 torr is slimmer, i.e. the plasma glow no longer fully fills the discharge tube radial cross-section. This is known as discharge contraction [28].

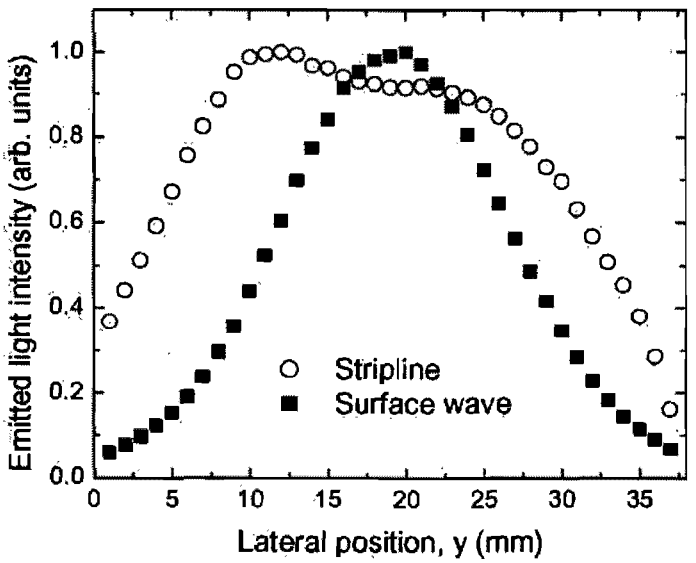

Figure 21. Recorded lateral profile of the intensity of emitted light from a tubular discharge sustained by a stripline field applicator compared to that obtained from a SWD under the same operating conditions: argon gas at 20 torr, an applied field frequency of 600 MHz and 26 mm i.d. discharge tubes. A 1 mm-diameter light collimator, 30 mm long with its tip located at 100 mm from the tube and connecting to an optical fibre, was used to provide some spatial resolution to these lateral measurements.

2.3.5.4 Avoiding the launching of surface waves along a plasma column

As a rule, surface-wave discharges are azimuthally symmetric and, therefore, the wave propagates in the TM (transverse magnetic) mode, i.e. the field components in the discharge tube (cylindrical coordinates) are E_z, E_r and H_ϕ; the wave main electric field component within the plasma is the axial component E_z [1]. This field component, required to excite the wave, is present at the launching gap due to fringe-field effects there. In contrast, as already mentioned, the stripline being a TEM structure, its electric field lines are truly perpendicular to the discharge

tube axis, in particular, there is no E_z component. However, when the discharge tubes are longer than the stripline structure, SWD can be excited at the two extremities of the stripline because of fringe-field effects occurring where the conducting strip ends (figure 22). This is supported by the following facts: i) at a sufficiently high HF power level, the discharge starts to extend outwardly from the conducting strip end in a region where the E-field cannot be that of the TEM mode; ii) the intensity of the emitted light in the outward segment (and in the corresponding inward segment with respect to the conducting-strip end) is higher than that measured along the stripline discharge itself, indicating a higher electron density there; this is consistent with a higher coefficient of wave power absorption whenever the plasma is sustained by a surface wave, as already discussed in relation with figures 19 and 20; iii) the length of the higher-density discharge segment located on both sides of the surface-wave launching region (i.e. the conducting-strip end) increases with increasing HF power, an intrinsic property of surface-wave discharges (the existence of a front and a back surface wave has already been mentioned in relation with figure 20).

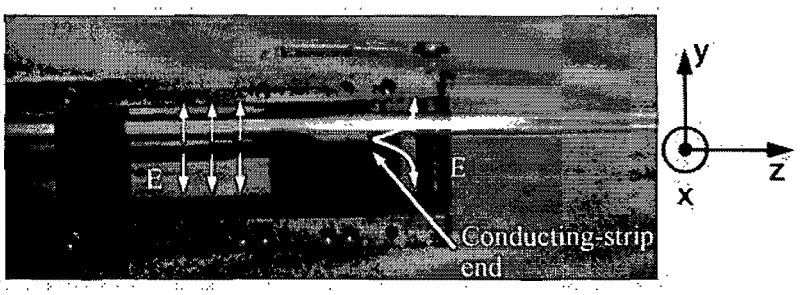

Figure 22. The brighter segment of the discharge is sustained by surface waves excited (in both directions) at the end of the stripline field applicator due to fringe-field effects resulting from the abrupt ending of the conducting strip. The arrows represent approximately the direction of the electric field in that region, suggesting the possibility of an E_z component there. Operating conditions: argon gas at 1 torr, 6 mm i.d. discharge tube, field frequency of 600 MHz.

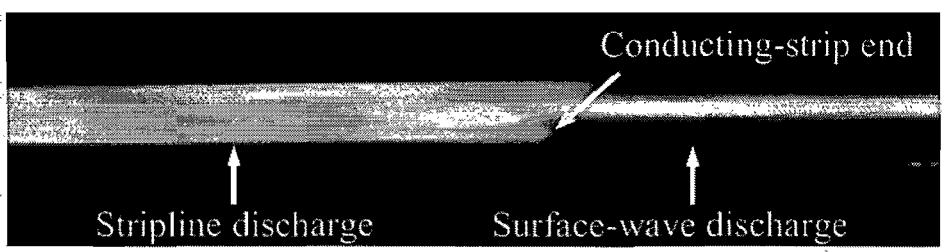

Figure 23. Discharge close-up view near an extremity of the stripline applicator. A surface wave discharge is excited outwardly past the end of the conducting strip in a 26 mm i.d. discharge tube (argon gas at 20 torr, field frequency of 600 MHz).

The launching of surface waves at the extremity of the conducting strip of the stripline field applicator is also observed along a larger diameter tube (26 mm i.d. compared to 6 mm i.d. in figure 22) as microwave power is increased above the power level required to make the discharge occupy the full length of the field applicator (see section 2.3.4.2). Figure 23 shows that the SWD actually excited at the end of the stripline structure is radially contracted at 20 torr in contrast to the stripline discharge that fills the entire radial cross-section of the tube. The fact that the stripline discharge is not contracted is consistent with a flatter lateral profile of the emitted light intensity than with a SWD, as already discussed in relation with figure 21.

In closing, let us mention that Schermer *et al.*, in presenting a new compact open-ended microstrip field applicator to generate plasma [8], noticed that the discharge extended outside the applicator as microwave power was increased sufficiently. They, however, did not identify this additional plasma segment as resulting from a SWD.

2.3.6 The stripline field applicator as part of the family of planar transmission lines used for generating plasma

The stripline field applicator described in the present article is a new concept within the family of planar transmission lines used to sustain plasma columns. A distinguishing feature of our system is its use to achieve plasma columns that are long compared to the HF wavelength in contrast to the plasma length of the other members of the family of planar transmission lines (meter range compared to cm range). Situating our field applicator within the family of planar transmission lines sustaining plasma is helpful in extending the understanding of the present stripline system.

Most HF field applicators used to sustain plasma are essentially based on two types of transmission lines, namely waveguide and coaxial lines. Planar transmission lines were utilized to sustain microwave discharges starting only at the end of the 1990's [9]. This fact is quite surprising for many reasons:

- Plasma processing of planar surfaces is of importance for industrial applications that could be efficiently dealt with planar HF field applicators.
- Microwave engineering R&D has been developing planar transmission lines for more than three decades, essentially for communication purposes, and aiming at their miniaturization and circuit integration. As a result, the modelling of these lines is well-advanced, which should facilitate their design and modelling as EM-field applicators for plasma generation.
- Planar transmission lines are TEM (Transverse Electric Magnetic) or quasi-TEM structures [17]. This property leads to two beneficial characteristics when designing HF sustained plasma sources: 1) these transmission lines can be operated over a broad frequency range, as shown in this paper; 2) they can satisfy industrial requirements as to compactness and miniaturization of microwave plasma sources. In that respect, note that rectangular waveguides are really cumbersome at low microwave frequencies (≤ 915 MHz). In contrast, as shown by Broekaert [11], planar transmission lines are well-suited for the miniaturization of plasma sources (more easily achieved when high-permittivity dielectrics are used within them).
- Due to their intrinsic properties, microwave-field applicators using planar transmission lines can be readily arranged in arrays (eventually fed from a unique HF source) to provide large plasma volumes.

Such a limited use of planar transmission lines to sustain microwave discharges can probably be attributed to a widespread misconception that considers microstrip lines and striplines only suitable for low power applications. In fact, their microwave-power handling capacity is simply limited, as in the case of other transmission lines, by Joule losses in conductors and dielectrics and by electrical breakdown [18]. By applying the usual microwave design rules for high power operation (large enough thickness of the current carrier, water cooling, minimum distance between conductors to avoid arcing), one could most probably extend their power range to a few kWs.

We distinguish three categories of HF field applicators based on planar transmission lines, as shown in figure 24: a) the EM-field applicator is supplied by the planar transmission line, possible field applicators being microstrip split-ring resonators (see figure 24 (a)) [6, 7], plasma-

torch systems [10], etc. In this case, the planar transmission line merely serves as an impedance matching unit; b) the field applicator is provided by a portion of the planar transmission line, which terminates on two open-circuits [5, 8, 9]. Impedance matching is achieved with at least one tuning means (e.g. an open-circuit of a given length) and it is located at an appropriate position along the transmission line (e.g. close to the power input); c) the whole length of the transmission line can serve as the field applicator. Impedance matching is realized by terminating the planar transmission line with a matched load. The impedance matching means of structures (a) and (b) critically depend on the frequency of operation in contrast to systems terminated with a matched load (case (c) as described in this paper). In fact, system (a) is resonant owing to the split-ring circumference that must be an integer number of half-wavelengths (the feeding conducting-strip is generally a quarter of wavelength long); as for system (b), the frequency dependence comes from the length of the open-circuit segments at the transmission line extremities and from the use of an impedance matching length (open-circuit).

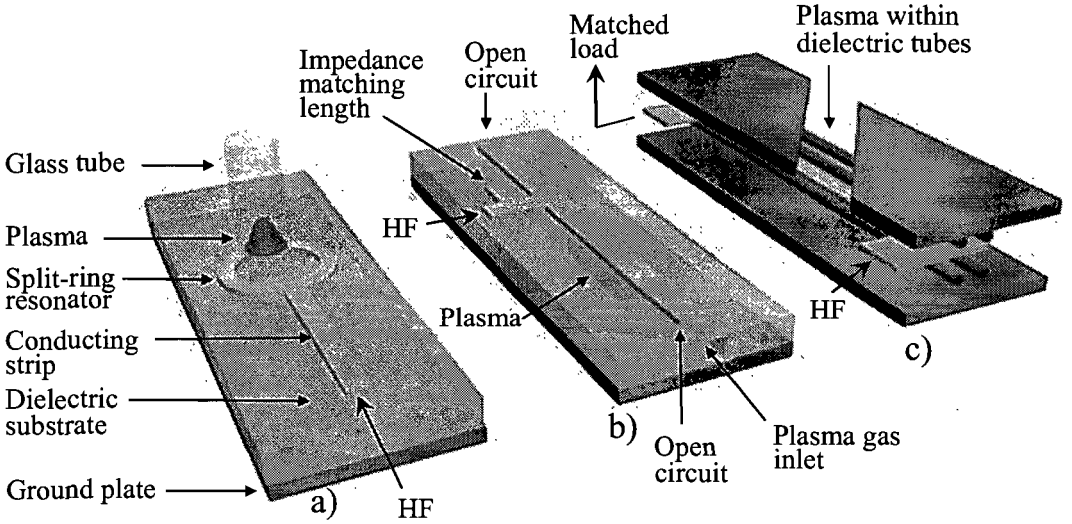

Figure 24. Suggested classification of planar transmission lines when utilized as field applicators to sustain plasma. Case a): the EM-field applicator is supplied by the planar transmission line, where the split-ring resonator is an example of a possible field applicator [6, 7]. Impedance matching is achieved at a fixed frequency only; b) the field applicator is provided by a portion of the planar transmission line, which terminates on two open-circuits [5, 8, 9]. Impedance matching is also dependent on frequency; c) the whole length of the transmission line can serve as the field applicator. Since impedance matching is realized by terminating the planar transmission line with a matched load, the system is frequency independent in absence of plasma. Because the plasma produced is of sufficiently low density, the power reflection coefficient at the power input is frequency independent.

The use of a stripline (triplate line) instead of a microstrip line as a field applicator to sustain plasma offers two main advantages; 1) the stripline is radiation-free whereas the microstrip line looses a fraction of its energy to the outside (the higher the frequency, the more important is this loss). This a remarkable feature of the stripline, both in terms of efficiency and hazard protection, when used as a long linear field applicator at high HF power levels; 2) the possibility of sustaining many discharge tubes at the same time and in a compact system is of possible interest for industrial applications.

2.3.7 Conclusion

We have designed and tested a new type of plasma source, where the discharge is generated by a linear HF field applicator based on the stripline technology. The obtained discharges have been analyzed by comparison with surface-wave discharges sustained under similar operating conditions. For instance, for a given HF power, the stripline plasma columns are observed to be five times longer than SWDs at 915 MHz. This implies a lower density of absorbed power in such a discharge, hence a lower discharge gas-temperature. The following features were found to be characteristic of our stripline discharges:

- The stripline field applicator presented can, in fact, be designed in the absence of plasma and, nonetheless, requires no tuning system to obtain, in the presence of plasma, a perfect impedance match at the applicator input from 27 MHz to 2450 MHz. This is related to the fact that the HF power expended to the discharge per unit axial length (dP/dz) by the TEM-mode wave is small compared to the power flow. The field applicator behaves, to some extent, like an antenna [2], meaning that it is essentially the stripline structure that determines the wave-field characteristics, and not the discharge.
- The main disadvantage of all traveling-wave discharges is, by essence, the axial decrease of the electron density since the wave power decreases as it is expended in the discharge as it propagates. This non uniformity effect is, however, much less important in the case of a stripline plasma source because of a lower coefficient of power absorption by the plasma. It, therefore, leads to a plasma column that is much more uniform axially than with a SWD.
- The gas temperature being lower than in SWDs, the onset of plasma contraction occurs at higher gas pressure than for SWDs.

The stripline discharge appears complementary to the SWD as far as achieving long plasma columns is concerned. Its specific features could help widening the applications of long HF-sustained plasma columns. For instance, its lower gas temperature allows to subject thermosensitive polymers directly to plasma to sterilize polymer-based tubes, eventually such parts of medical devices (e.g. endoscopes, catheters) [3].

2.3.8 Acknowledgments

The authors would like to thank L. Goyet, T. Arial and J. S. Mayer for technical assistance, Dr D. Kéroack, Dr Y. Kabouzi and Dr. B. Saoudi for comments. Financial support for this work was provided by the Fond Québécois pour la Recherche sur la Nature et la Technologie (FQRNT) and the Conseil de Recherches en Sciences Naturelles et Génie du Canada (CRSNG).

Appendix. Design details

A1. Transitions from coaxial lines to stripline applicators

The junctions between the coaxial (input and output) ports and the stripline need to be carefully designed to avoid possible reflections. Typically, the input and output junctions to a stripline are implemented at its extremities, either along the axis of the stripline or perpendicularly to it [29]. As we already mentioned, the fact that the discharge tubes are set parallel to the stripline axis and extend past the conducting strip (together with their input and output gas connections) requires the connectors to be implemented sideways, as shown in figure A1.

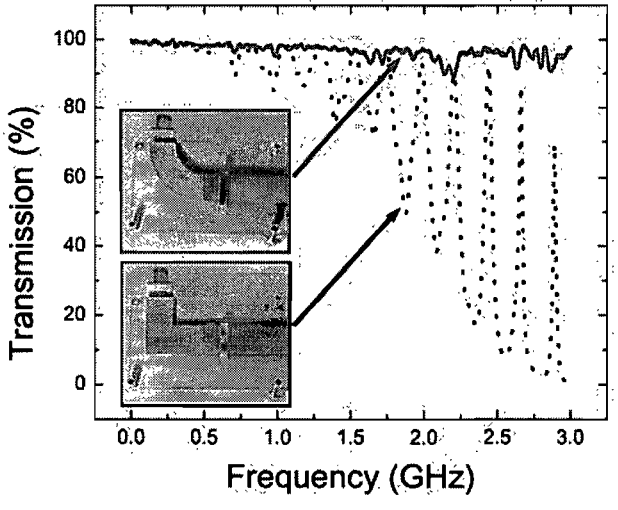

Figure A1. Percentage of a (low-power) input signal transmitted across the stripline and observed at its output port in absence of plasma, in cases where the input and output ports are either right-angle bends or circular bends.

The transmission response with frequency reported in figure A1 has been obtained with a network analyzer in the transmission mode. Figure A1 shows that using a circular bend instead of a right-angle bend significantly improves signal transmission as a function of frequency across the stripline.

A2. Perturbations introduced by the dielectric supports designed to hold the discharge tubes and the central conducting strip

Dielectric holders were designed to mechanically support both the discharge tubes and the conducting strip. These spacers are particularly necessary when flexible polymers are employed as discharge tubes. Because the holders have a higher permittivity than that of air, they introduce impedance changes along the stripline, which amounts to considering them as obstacles as far as the propagation of the electromagnetic waves along the stripline is concerned.

To reduce the influence of these supports, one can use very low permittivity material such as low-density polystyrene (ε_r=1.1), which however is not mechanically strong. To ensure a better mechanical behaviour, an interesting compromise is to use Teflon since the relative permittivity (2.1) of this material is not too high while it is much more sturdy. Still, the influence of these Teflon supports can be reduced provided their axial length T remains small with respect to the wavelength, actually the shortest wavelength used (122 mm for 2.45 GHz). This is illustrated in figure A2 which clearly shows that the smaller the axial extent of the support, the better the signal transmission across the field applicator. It also indicates that the transmission tends to degrade as the wave frequency becomes high enough, say above 1.5 GHz for T = 12.7 mm.

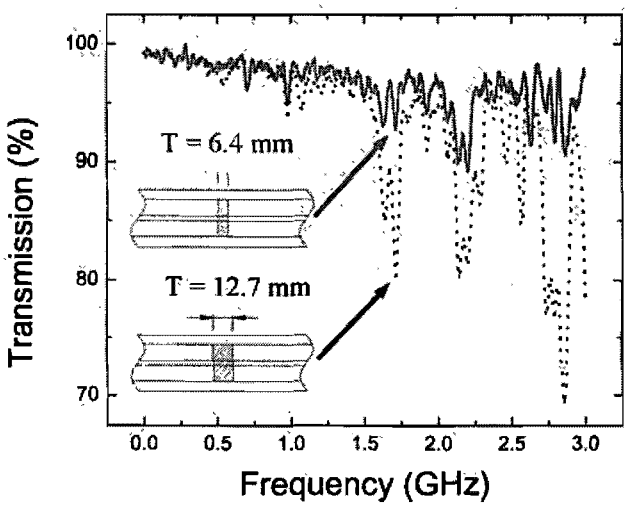

Figure A2. Percentage of a low-power input signal transmitted across the stripline and observed at its output port in absence of plasma, when utilizing Teflon dielectric supports (see figure 10(a) for their shape and figure 10(b) for their axial positioning) of axial length T = 12.7 mm and T = 6.4 mm.

References

1. Moisan M and Zakrzewski Z 1991 Plasma sources based on the propagation of electromagnetic surface waves *J. Phys. D: Appl. Phys.* **24** 1025-1048.
2. Zakrzewski Z and Moisan M 1995 Plasma sources using long linear microwave field applicators: main features, classification and modelling *Plasma Sources Sci. Technol.* **4** 379-397.
3. Pollak J, Moisan M, Saoudi B and Zakrzewski Z, *Process for the plasma sterilization of dielectric objects comprising a hollow part.* 2005, Patent application US2005/0269199, (PCT) WO2004/050128.
4. Howe KC (1979) *Stripline Circuit Design,* Artech House.
5. Bass A, Chevalier C and Blades MW 2001 A capacitively coupled microplasma formed in a quartz wafer *J. Anal. At. Spectrom.* **16** 919-921.
6. Iza F and Hopwood JA 2003 Low-power microwave plasma source based on a microstrip split resonator *IEEE transactions on plasma science* **31** 782-787.

7. Iza F and Hopwood JA 2005 Split-ring resonator microlasma: microwave model, plasma impedance and power efficiency *Plasma Sources Sci. Technol.* **14** 397-406.
8. Schermer S, Bings NH, Bilgic AM, Stonies R, Voges E and Broekaert JAC 2003 An improved microstrip plasma for optical emission spectrometry of gaseous species *Spectrochimica Acta A Part B* **58** 1585-1596.
9. Bilgic AM, Engel U, Voges E, Kückelheim M and Broekaert JAC 2000 A new low-power microwave plasma source using microstrip technology for atomic emission spectrometry *Plasma Sources Sci. Technol.* **9** 1-4.
10. Stonies R, Schermer S, Voges E and Broekaert JAC 2004 A new small microwave plasma torch *Plasma Sources Sci. Technol.* **13** 604-611.
11. Broekaert JAC 2002 The development of microplasmas for spectrochimical analysis *Anal. Bioanal. Chem.* 182-187.
12. Pozar DM (1998) *Microwave Engineering,* Wiley.
13. Harvey AF (1963) *Microwave Engineering,* Academic Press.
14. Sauvé G, Moisan M, Zakrzewski Z and Bishop CA 1995 Sustaining long linear uniform plasmas with microwaves using a leaky-wave (throughguide) field applicator *IEEE Trans. on antennas and propagation* **43** 248-256.
15. Yue H, Virga KL and Leprince JL 1998 Dielectric constant and loss tangent measurement using a stripline fixture *IEEE Electronic Components and Technology conference*
16. Caulton M. JJH, H. Sobol 1966 Measurements on the properties of microstrip transmission lines for microwave integrated circuits *RCA Review*
17. Shih YC and Itoh T (1993) *Antenna Handbook,* Y.T. Lo and S.W. Lee.
18. Gupta KC, Garg R, Bahl I and Bhartia P (1996) *Microstrip lines and slotlines,* Artech.
19. Ghose RN (1963) *Microwave circuit theory and analysis,* McGraw-Hill.
20. Bahl I and Garg R (1978) *A designer's guide to stripline circuits,* Artech.
21. Moisan M, Barbeau C, Claude R, Ferreira CM, Margot J, Paraszczak J, Sá AB, Sauvé G and Wertheimer MR 1990 Radio frequency or microwave plasma reactors? Factors determining the optimum frequency of operation *Journal of Vacuum Science & Technology B: Microelectronics and Nanometer Structures* **9** 8-25.
22. Ferreira CM and Loureiro J 1984 Characteristics of high-frequency and direct-current argon discharges at low pressures: a comparative analysis *J. Phys. D: Appl. Phys.* **17** 1175-1188.

23. Moisan M and Pelletier J (1992) *Microwave excited plasmas,* Elsevier.

24. Lieberman A and Lichtenberg AJ (1994) *Principles of plasma discharges and materials processing,* Wiley-Interscience.

25. Von Engel A (1955) *Ionized gases,* Oxford Univerity Press.

26. Moisan M, Zakrzewski Z and Pantel R 1979 The theory and characteristics of an efficient surface wave launcher (surfatron) producing long plasma columns *J. Phys. D:Appl. Phys.* **12** 219-237.

27. Slinko VN, Sulakshin SS and Sulakshina LV 1988 On producing an extended microwave discharge at high pressure *Sov. Phy. Tech. Phys.* **33** 363-365.

28. Kabouzi Y, Calzada MD, Moisan M, Tran KC and Trassy C 2002 Radial contraction of microwave-sustained plasma columns at atmospheric pressure *Journal of applied physics* **91** 1008-1019.

29. Rizzi PA (1988) *Microwave engineering Passive circuits,* Prentice-Hall.

2.4 Inactivation de spores empilées dans des tubes diélectriques

Stériliser un objet signifie en termes pratiques la réduction d'au moins 6 log d'une population de spores bactériennes initialement déposées à sa surface. Tel que mentionné dans la section 1.3.2 portant sur le NAS, cette définition à ceci d'ambigu qu'elle ne précise pas la manière de déposer les bactéries et la forme des types de dépôt qui en découle. Or, il est connu que la répartition des micro-organismes, notamment leur agrégation et empilement, a un impact critique sur les résultats d'inactivation obtenus: dans le cas d'une inactivation par photons UV, plus l'empilement est important, plus il faudra de photons pour arriver à traverser les spores du dessus et atteindre la spore la plus cachée. Dans l'article qui suit, nous avons tout d'abord effectué une revue bibliographique des méthodes permettant de tester l'efficacité d'un procédé de stérilisation dans un tube. Nous avons ensuite proposé une nouvelle méthode qui permet, entre autres, d'obtenir des dépôts de spores bactériennes empilées. Notre méthode de stérilisation par plasma a alors été mise à l'épreuve pour inactiver ces spores empilées. La figure 2.4, qui a fait la couverture du numéro de janvier 2008 de la revue *Plasma Processes and Polymers*, illustre le type d'empilement important que notre procédé plasma a permis d'inactiver.

Cover: The cover presents two SEM micrographs showing stacks of bacterial spores on the inner surface of a Teflon tube (i.d./o.d. 4/6 mm). Low-damage sterilization is achieved using a glow-discharge in flowing argon at reduced pressure, directly within the thermally-sensitive dielectric tube. Further details can be found in the article by J. Pollak, M. Moisan,* D. Kéroack, J. Séguin, and J. Barbeau on page 14.

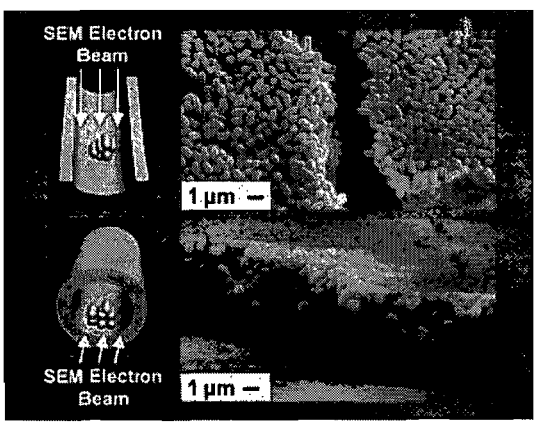

Figure 2.4 Page de couverture du numéro de janvier 2008 de la revue *Plasma Processes and Polymers*. Ces micrographies illustrent le type d'empilement que notre procédé plasma a permis d'inactiver.

Plasma sterilization within long and narrow bore dielectric tubes contaminated with stacked bacterial spores

(article publié dans Plasma processes and polymers **5** 2008 14-25)

J. Pollak, M. Moisan, D. Kéroack, J. Séguin, J. Barbeau

Abstract

Catheters, which comprise small diameter (≤ 4 mm), long (typically more than a meter), thermosensitive polymer tubings, are generally used only once. This is because conventional low temperature sterilisation techniques are considered inadequate for used catheters. The plasma sterilisation method proposed in the current paper should allow for the achievement of re-sterilisation of catheters according to accepted regulations. The plasma process described enables one to sterilise, in less than 10 min, the inner part of a long 4 mm i.d. Teflon tube contaminated initially with 10^6 *Bacillus atrophaeus* spores. This result was obtained by achieving an argon discharge at reduced pressure (750 mTorr) within the hollow (dielectric) tube itself. The discharge was sustained using a microwave field-applicator called a stripline, fully enclosing the tube to be treated. This linear field-applicator yields a uniform plasma all along the tube, hence the uniform biocide action. The biocide agents are the vacuum ultra-violet (VUV) photons, which include oxygen and nitrogen atomic lines, the N_2 Lyman-Birge-Hopfield (LBH) bands, the UV photons emitted by the NO_β and NO_γ molecular systems resulting from the contamination, even though at a very low-level, of the argon gas (high purity argon is used) by air. Scanning electron microscopy (SEM) revealed no apparent damage to the external structure of the spores and to polystyrene microspheres exposed to plasma during the time required for reaching sterility.

To check for sterility in such narrow bore tubes without having to cut them into two pieces, a procedure was developed to introduce and afterwards collect the bacterial spores used as bio-indicators. This diagnostic procedure allowed, at the same time, the imaging of the microorganisms relatively efficiently with SEM, showing the eventual stacking of bacterial spores, a possible source of sterilisation failure.

2.4.1 Introduction

For practical and economical reasons, re-sterilisation of costly medical devices (MDs) is clearly desirable. However, this is not always possible. For instance, MDs comprising one or many hollow parts, such as catheters and flexible endoscopes, are hard to sterilise, essentially for the following reasons: (i) since these MDs include thermosensitive components, they cannot be processed by dry or moist heat, implying that chemical sterilants need to be used. Contact time with these chemicals can be as long as 10 h and, because of their toxicity, they further require a long venting time (typically 10 h), besides being generally harmful to the environment (this approach is far from satisfactory); (ii) the devices (also called lumens) are characterised by a small inner diameter (typically 1.5–6 mm) and a comparatively long length (0.5–2 m). Such a high aspect ratio makes it more difficult for biocide species to reach all parts of the MD, preventing the process from being fully safe. As a matter of fact, treated re-used endoscopes are, to date, deemed highly disinfected, but not sterilised, while catheters are simply disposed of after one use.

Among the various medical devices comprising hollow parts, the single lumen catheter is the one with the simplest configuration. This paper deals with the plasma sterilisation of an idealised catheter, i.e., one having the following characteristics: (i) a constant inner and outer diameter (i.d./o.d.: 4/6 mm) along its full length (62 cm) with no bypass or derivation; (ii) made from a low loss dielectric material (mostly Teflon), excluding any conducting part.

The sterilisation of catheters requires treating both their external and internal surfaces. In 2005, Pollak et al.[1] filed a patent for a two step process ensuring the sterilisation of small diameter long length tubes: sterilisation of the outer part of the tube was performed by means of a plasma flowing afterglow, while its inner part was processed with a plasma achieved within it by a so-called stripline discharge.[2] The current paper focuses on the sterilisation of the inner part of a lumen using such a discharge.

There have been previously many attempts at sterilising long, small diameter tubes by plasma. When it is necessary to achieve sterilisation of thermosensitive polymers, one possible attractive way is to use a spatial flowing afterglow (post-discharge), as it is generally of a lower gas temperature than the discharge from which it originates.[3] Such an afterglow, when dealing with bacterial spores deposited on planar surfaces (e.g., polystyrene Petri dishes), leads to sterilisation within less than 45 min.[4] However, this method was found not to be applicable to lumens because of their too low hydrodynamic conductance, which prevents circulating a gas within them at high speed (high flow rate), an essential condition

when relying on the biocide action of the short-lived species associated with the discharge afterglow. In addition, because of the low hydrodynamic conductance, the gas pressure rises at the tube entrance with respect to its exit value, the ensuing axial density gradient of species leading to non-uniform inactivation kinetics along the tube; eventually for a long enough tube, inactivation ceases past a certain distance from the entrance because of the limited lifetime of the transiting active species. Under these conditions, one has to contemplate achieving a discharge within the lumen itself.

A first arrangement in that direction was suggested by Bousquet et al. in a patent application[5] where, throughout the lumen, a central conducting wire was introduced, coaxially enclosed within a meshed cylinder resting on the lumen inner wall. A high voltage (HV) was applied between these two dielectric coated conductors to achieve a discharge in a N_2/O_2 gas mixture. Note that, after completion of plasma processing this method implies removing, under sterile conditions, the HV line from the inside of the lumen. Another method is that proposed by Helhel et al.[6] where the hollow tube tested was located within an electron cyclotron resonant discharge: the authors employed only 2 cm long tubes (inner diameter not specified), which is not really convincing. A further method of achieving a discharge within the lumen was considered in our laboratory, which involved making use of a plasma sustained by an electromagnetic surface wave, where there is no limitation as far as the tube length and diameter are concerned. However, this technique yields too high a gas temperature for polymer tubes[a] and, because the wave power is expended as it propagates along the tube, it is also associated with an important (decreasing) axial gradient of electron density (hence of active species, implying a non-uniform inactivation rate).[b] Finally, we recently designed a new kind of high frequency (HF) field-applicator of the linear type that provides an axially uniform and low temperature discharge, as we will show. A linear field-applicator has one of its structure dimensions much larger than the others; it is therefore particularly suited for processing long tubes. It is the purpose of the present article to evaluate the biocide efficiency of this new plasma source on the inner part of lumens.

The paper is organised as follows. We first describe the plasma source that we have used to sterilise dielectric lumens. Then we review the available methods for testing the biocide efficiency when dealing with lumens and afterwards introduce our new diagnostic technique. Next, the inactivation of reference bacterial spores, as obtained with our stripline plasma

[a] It could possibly be used at frequencies lower than 100 MHz since the electron density is much lower then (hence gas temperature), but impedance matching then depends on LC matching systems, which are less reliable than microwave ones.

[b] Modulating the high frequency field does not lessen the axial gradient of electron density.

source, is examined. The level of damage induced by the plasma on the spore and polymer surfaces is then considered, before a discussion on further work, a summary of the paper and a general conclusion in the final section.

2.4.2 The stripline, a linear HF field-applicator for sustaining a low-temperature axially uniform plasma within long dielectric tubes

The electrodynamic characteristics and peculiar features of the present field applicator are described in detail in Pollak et al.[2] In what follows, we limit ourselves to recalling its design and some operating results. Figure 1(a) is a schematic representation of this HF field-applicator. It is essentially a transmission line, actually an open planar variant of the classical coaxial line since the wave propagates on a transverse electric magnetic (TEM) mode. HF power is applied at one extremity of the conducting strip [Figure 1(b)]; the terminating matched load on the other extremity of the strip prevents residual HF power from being reflected at this end of the stripline, which would inhibit the uniformity of the HF field intensity along the field applicator. This 50 Ω load is the only matching means of the HF plasma source, and impedance matching of this system is frequency independent (200-2450 MHz range tested). Figure 1(c) is a photograph of an HF argon discharge sustained with the field applicator within Teflon tubes, one being located above and the other below the conducting strip as schematised in Figure 1(b). Provided the ratios w/L and h/L are small, this structure does not radiate to the outside.

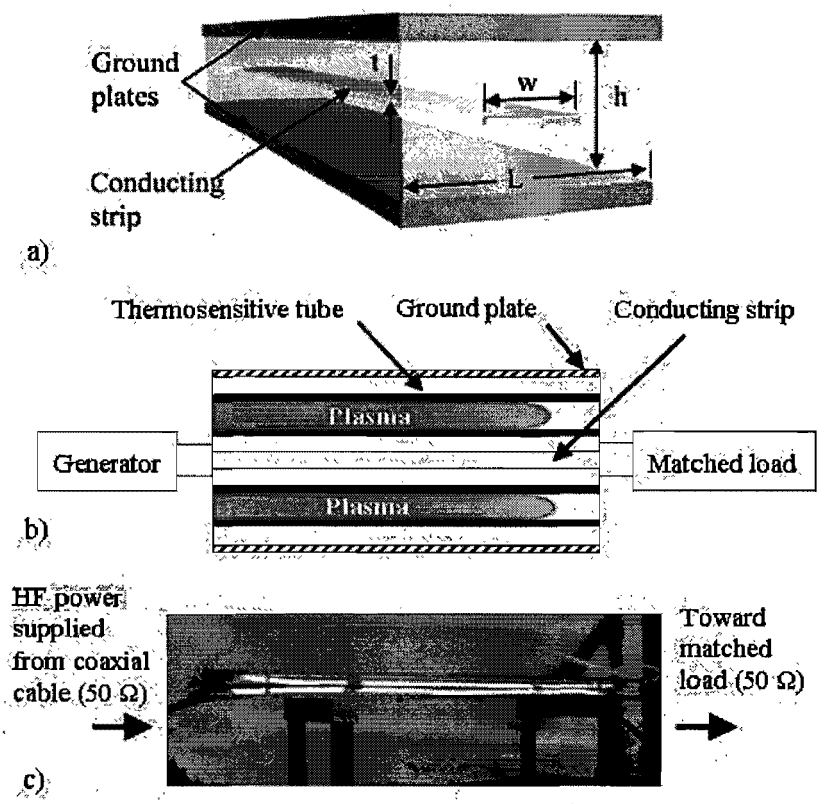

Figure 1. (a) Schematic representation of the bare stripline HF field-applicator, a waveguiding structure operating on the TEM mode. (b) Cross-sectional schematic representation of the field applicator, with a discharge tube positioned above and another one below the conducting strip, showing that HF power was supplied to the conducting strip from an extremity of the line while the other side was terminated with a matched load. (c) Actual photograph of two discharge tubes (uniformly) illuminated by an HF argon discharge sustained within them (the sterilisation experiments were performed in such tubes). The 4/6 mm i.d./o.d. tubes were made from Teflon. The field applicator was 62 cm long with the following characteristic dimensions: w = 26.4 mm, t = 3.2 mm, h = 24 mm, L = 90 mm. This plasma source can also be operated with up to four discharge tubes (i.d./o.d. 4/6 mm tested) per conducting strip, and with eventually many conducting strips, but in the current paper we considered the simpler case of a single discharge tube.

Figure 2(a) shows the emitted light intensity recorded with a photodiode (330–800 nm range) along the stripline discharge, at three field frequencies: 200, 700 and 2450 MHz. A 1 mm inner diameter light collimator, 30 mm long, directed transversally to the tube axis with its tip at 50 mm from it, and linked to an optical fibre, was used to provide axial resolution of the light intensity along it. The corresponding profile of this intensity, as can be seen from

Figure 2(a), is relatively uniform, for at least two reasons:[2] (i) only a small fraction of the HF power flow is diverted, as a function of axial position z, to sustain plasma, in contrast to most other types of travelling wave sustained discharges such as, for example, the surface-wave discharge (SWD); wave power expenditure of SWDs at a given z position is a significant portion of the power flow at z, hence the decreasing value of the cross-sectional average value of electron density (and therefore of emitted light intensity).[7] Phrased differently, this is because the axial wave attenuation coefficient of the stripline is much smaller than that of a surface wave discharge at the same frequency; (ii) the terminating matched load implemented at the stripline end minimises possible reflections due to the residual (unabsorbed) power flow of the travelling wave at that point. Figure 2(b) shows that the emitted light intensity is more uniform axially in the 2 and 4 mm i.d. tubes than in the 7 mm i.d. tube, which suits our needs best since the i.d. of most catheters ranges from 1.5 to 4 mm.

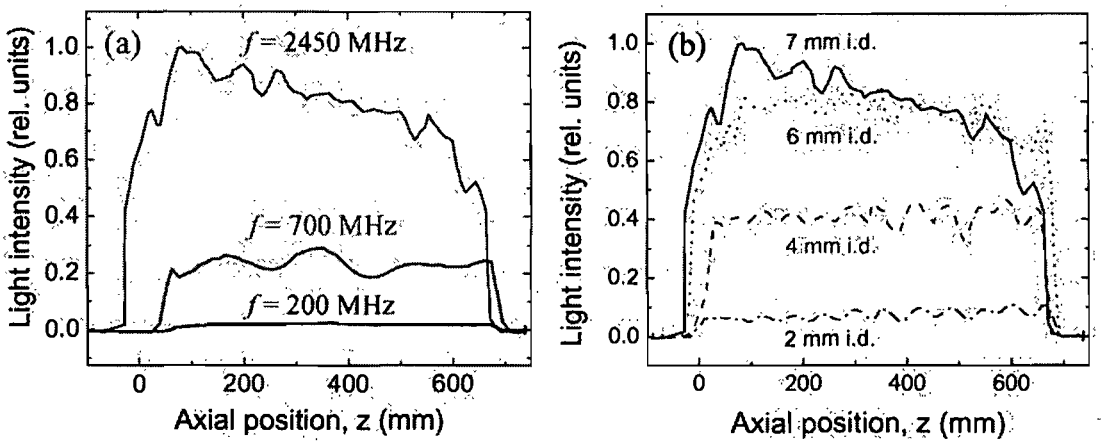

Figure 2. Axial profile of the emitted light intensity as recorded with a photodiode (330–800 nm range) along the plasma column sustained by a stripline field applicator. The conducting strip extended from z = 36 mm to z = 664 mm. The light collimator (1 mm i.d., 30 mm long) was directed at the diameter chord of the discharge tube. Experimental conditions: 100 sccm of argon at 750 mTorr. (a) The discharge was sustained in a 7 mm i.d. fused silica tube at three operating frequencies f. (b) The discharge was sustained at f = 2450 MHz within four different i.d. tubes.

In closing this section, let us mention that the stripline field applicator used in this paper for the sterilisation of Teflon tubing is 62 cm long while cardiac catheters are more than twice that length. Further studies are therefore necessary to develop a field applicator that could deal with such extended lengths, in particular to ensure an axially uniform electron density. A

possible way of achieving this would be to compensate for the significant decrease of power flow from the power input side to the matched load side that shows up with increased applicator lengths by gradually reducing the cross-sectional dimensions of the applicator structure, as already proposed by Zakrzewski and Moisan[8] in the general case of a long linear fieldapplicator. In the specific case of a plasma column lying longitudinally within a rectangular waveguide, Slinko et al.[9] suggested gradually reducing the waveguide height in the power flow direction. A second possible solution would be to switch the HF power feeding port with that of the matched load at half process time. A third possibility would be to remove the matched load and use its port to simultaneously feed the stripline from a second microwave generator (not phase related to the first one to avoid standing waves along the stripline), therefore compensating for the power flow decrease as power is expended to sustain the discharge. For compactness reasons, instead of a straight linear field-applicator, it could be more interesting to consider circular field applicators, with a sufficiently large angle of curvature of the conducting strip not to overbend the catheters and affect their physical characteristics.[10]

2.4.3 Currently used methods for testing the biocide efficiency of various sterilization techniques on lumens and a proposed new method

A standard reprocessing protocol for lumens comprises 3 sequential steps: decontamination, cleaning and sterilisation.[11] In this section, we focus on the testing methods for assessing the efficiency of the sterilisation process itself, and more specifically its action on the inner part of lumens.

2.4.3.1 A review of the published methods for appraising the efficiency of a sterilization process on the inner wall of lumens

Such testing methods essentially involve a two step procedure: the insertion of the microorganisms in the long small bore tubes and their subsequent removal for enumeration.

Ethylene Oxide Sterilisation

The German company gke has developed the Steri-Record® system,[12] an indicator made of a long (1.5 m) small diameter Teflon tube (2 mm i.d.) open at one end and closed at the other end by a metallic holder containing a (renewable) chemical or biological indicator [see Figure

3(a)], the tube laying freely among MDs of various kinds within the steriliser vessel. This system is, in fact, not designed specifically for testing lumen sterilisation. The company claims that its system simulates the toughest penetration case for the sterilant as encountered in bulk processing.

Ozone Sterilisation of Stainless Steel Tubes

For validating its technique on lumens, TSO3®[13] inserts paper strips containing 10^6 spores of *Geobacillus stearothermophilus* at the mid-axial position in the case of a 4 mm i.d. tube (indicated length of 0.6 m) [see Figure 3(b)]. For tubes with smaller inner diameters (e.g., 2 mm), paper strips are inserted by cutting the tube at a mid-axial position and afterwards closing it using hermetic junctions.

Steam-in-Place Sterilisation

In this case steam is forced into the tubes. Young[14] used biological indicators consisting of filter paper disks contaminated with 1.3×10^6 spores of *G. stearothermophilus* that can be inserted at different axial positions within (stainless steel) dead ended tubes [see Figure 3(c)]. Tubes of various inner diameters are mentioned (4, 10 and 17 mm).

Hydrogen Peroxide Plasma Sterilisation

Penna et al.[15] introduce a 28 mL suspension of *Bacillus subtilis* spores (bacteria recently reclassified as *Bacillus atrophaeus*[16]) that deposit along the whole length of stainless steel needles (100×0.6 mm) [see Figure 3(d)]. Then, the items are kept horizontal at 45 °C for 72 h in a mechanical aerator oven to dry residual water, causing the spores to adhere along the edge of the inner wall. Spore recovery is achieved by rinsing 10 times the inner wall of each needle with 5 mL of Trypticase Soy Broth (TSB) culture medium.

A Method Applicable to Different Sterilisation Techniques

Alfa et al.[17] developed a lumen carrier assembly, which is made of a central 2 cm piece of tubing inoculated with bacteria and dried, connected afterwards on each side to two 61.5 cm long tubings of the same diameter, using a 2 cm long ''linker'' section ensuring a gas-tight fit [see Figure 3(e)].

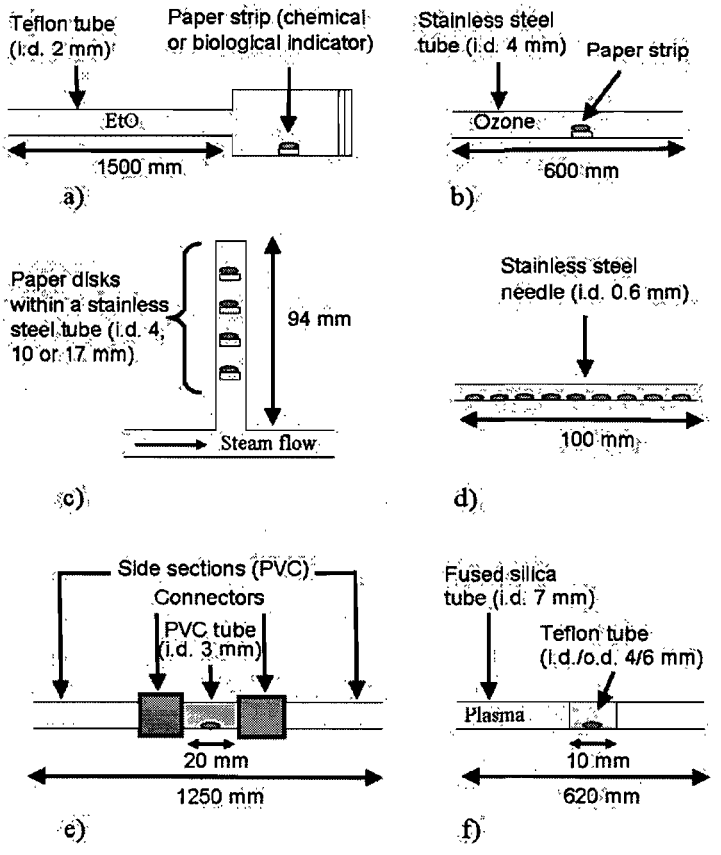

Figure 3. Schematic representation of the techniques used to check sterility within long narrow-bore tubes. (a) Ethylene oxide sterilisation (gke-Steri-Record® [12]): the tube is open at one end and closed at the other end by a metallic holder containing an indicator (chemical or biological). (b) Ozone sterilisation (TSO3® [13]): a paper strip containing 10^6 spores of *Geobacillus stearothermophilus* is introduced at a mid-axial position within a stainless steel tube. (c) Steam-in-place sterilisation (Young[14]): biological indicators each containing 1.3×10^6 spores of *G. stearothermophilus* are displayed at different axial positions within a stainless steel dead-ended tube. (d) Hydrogen peroxide plasma sterilisation of stainless steel needles: Penna et al.[15] introduce a 28 mL suspension of *Bacillus atrophaeus* spores that deposit along the whole length of stainless steel needles.[16] (e) No specific sterilisation method (Alfa et al.[17]): A lumen testing assembly is made of a central 2 cm piece of tubing inoculated with bacteria and dried, and is afterwards connected to two 61.5 cm long outer pieces of tubing, using 2 cm''linker'' lengths of tubing on each side to ensure a gas-tight fit. (f) Our plasma sterilisation method: a short segment (typically 10 mm long) of a Teflon tube, seeded with 10^6 *B. atrophaeus* spores, and having the same i.d. as that of the small bore lumen to be tested, is introduced into a larger diameter (fused silica) supporting tube, the length of which is considered representative of that of the small bore lumen under investigation.

2.4.3.2 Introducing a new method for checking the biocide efficiency of sterilization techniques within lumens

Before dwelling on the interest and features of our own method for assessing sterilisation in long, small bore tubes, we describe here the practical procedure that it involves.

We used 10 mm long segments of Teflon tubings (i.d./o.d. 4/6 mm), open at both ends, within which spores of *Bacillus atrophaeus* ATCC® 9372 were deposited and dried (see Figure 3(f)). The inoculated Teflon segment was then pushed, for example, into a mid-axial position within a fused silica tube of a slightly larger diameter (i.d./o.d. 7/9 mm), thereby assuming that if sterility was obtained at the mid-position, we can imply that it was also achieved everywhere along the tube. Our reasoning is supported by the fact that the axial distribution of the emitted light intensity was relatively uniform along the plasma column (Figure 2). Fused silica was employed as a support for the Teflon tubing because of its relatively low cut-off optical wavelength value (180 mm), which enabled us to record UV emission above 180 nm (see above section) during plasma exposure.

We developed a method of our own for testing lumens in order to deal with the following problems: (i) a planar surface biological indicator introduced within a cylindrical low bore duct could lead to gas flow modifications affecting the inactivation process; as a rule, bio-indicators for lumens should preferably follow their inner shape as much as possible; (ii) connecting together 2 (or 3) tube sections, even using hermetic junctions, can lead to small gas leaks at these locations, eventually modifying the sterilisation capabilities of the system; (iii) another point, very seldom considered when comparing the efficiency of sterilising methods, is the surface density of the deposited test spores. In fact, when microorganisms are stacked onto many layers, the biocide species (in the gaseous state for most sterilisation techniques) have to diffuse through the stack, layer after layer, to reach the last one underneath. This situation, which could occur with even thoroughly decontaminated and cleaned lumens, is not clearly accounted for in the pre-existing testing methods. We will expand on this stacking issue a little further below.

We now consider in more detail our experimental procedure for assessing the inactivation of bacterial spores within the tube segments already described. A spore suspension was first prepared in a classical way [schematically summarised in Figure 4(a)]. Then, 10^6 spores diluted in 50 mL of sterilised water were deposited within 10 mm Teflon tube segments; these deposits were allowed to dry out over 48 h, in the dark at ambient temperature, while the

tubes were resting steadily on a rack [Figure 4(b)]. Due to gravity, the sedimented microorganisms were located on the lower half of the tubing segments. This is clearly illustrated with photographs in Figure 4(b), where India ink particulates (of approximately the same size as the spores) have been used to mimic the sedimentation mechanism. Spore collection was achieved as follows [Figure 4(c)]. The tube segment, containing plasma-exposed spores of *Bacillus atrophaeus*, was transferred into a culture test tube containing 10 mL of recovery solution (0.5% Tween 80 in saline). The tube was then vigorously vortexed for 2 min, 10-fold dilutions were prepared with recovery solution and 50 to 200 mL volumes were plated, in triplicate, onto Trypticase Soy Agar (TSA). After a 24 h incubation at 37 °C, Colony-forming units (CFU) were enumerated, and values were corrected for dilution and volume, thus allowing estimation of survival spore numbers. Recovery of all spores by membrane filtration was carried when low numbers of CFU were expected.

In case sterility was observed by the above method, to make sure that no microorganisms were left sticking to the original Teflon segment, the latter was incubated in a test tube with Trypticase Soy Broth (TSB) at 37 °C. The incubation of such, a priori, negative cultures was actually prolonged for 7 d. Spore counting on non-exposed samples demonstrated that our recoverymethodwas really efficient and reproducible. For example, an expected 1×10^{6} spore deposit yielded a mean recovery (triplicate) of $1.28\times10^{6}\pm7.2\times10^{5}$ spores.

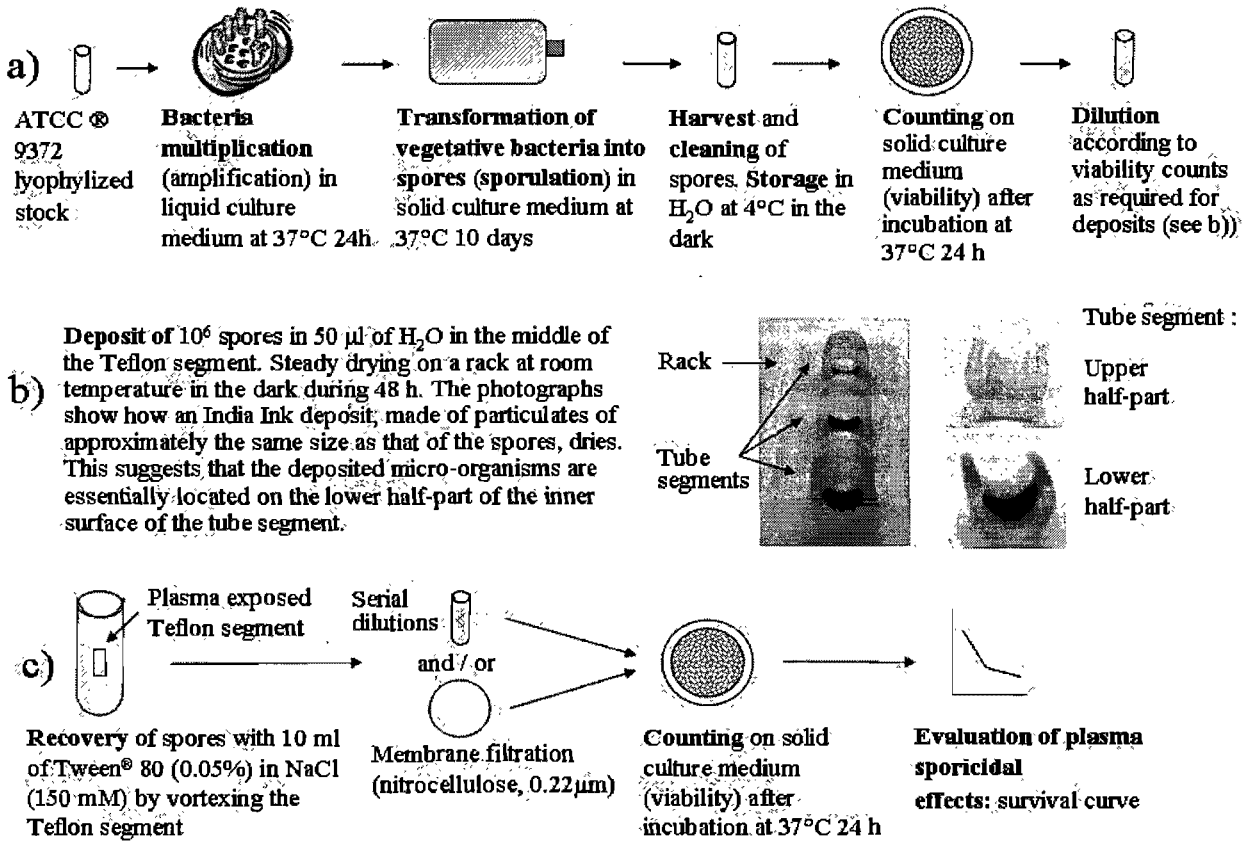

Figure 4. (a) Schematic representation of the various steps involved in the preparation of Bacillus atrophaeus spore suspensions. (b) Photographs taken after deposition and drying of India ink particulates on the Teflon tube segments (i.d./o.d. 4/6 mm, 10 mm long). (c) Recovery and counting procedure of the viable spores after exposure to the stripline plasma.

For scanning electron microscope (SEM) viewing purposes, the tube segments were cut into two halves along their length. The spores were found on the lower half of the inner surface of the Teflon tube segment (i.d./o.d. 4/6 mm, 10 mm long). Figure 5 shows SEM micrographs, with successively increasing magnification, of dried suspensions of 10^6 *Bacillus atrophaeus* spores where the lower half of the Teflon segment was aligned to face the SEM beam, as shown in the inset. As can be observed in Figure 5(b), the deposit was not uniform and continuous. In addition, multi-layered structures of spores can clearly be seen in Figure 5(c). Estimation of the number of stacked layers of bacterial spores using Figure 5(c) was hard. Therefore, the Teflon tube segment was cut, this time along a cross-section, the electron beam directed as shown in the inset of Figure 6. Figure 6 shows that the Teflon segment inner wall was coated with approximately 8 layers of stacked spores.

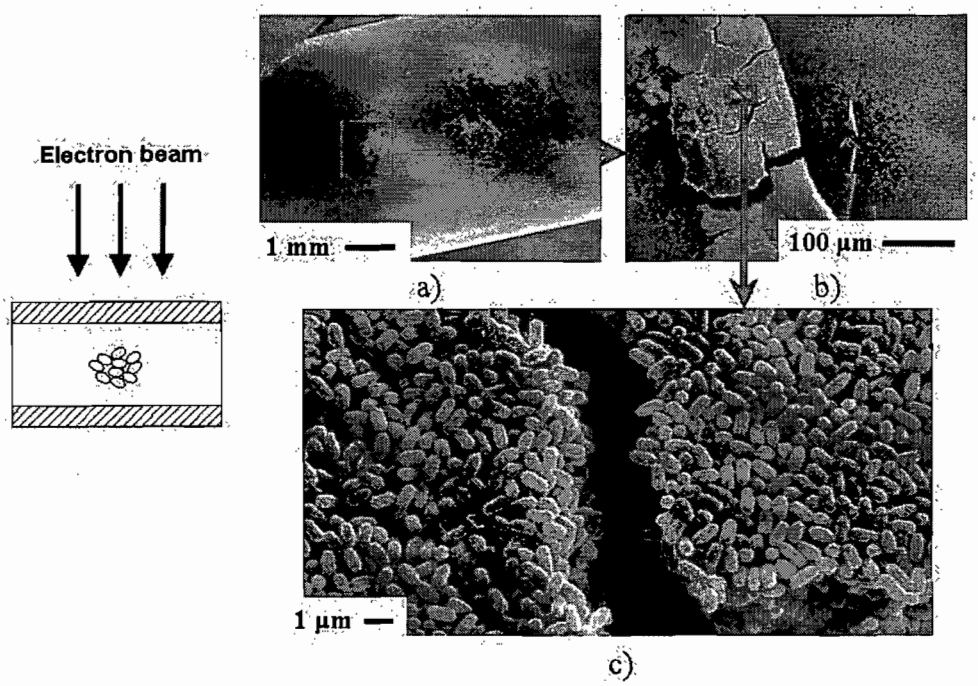

Figure 5. Increasingly enlarged [from (a) to (c)] SEM micrographs of 10^6 dried *B. atrophaeus* spores deposited on the inner surface of a Teflon tube segment (i.d./o.d. 4/6 mm). To obtain these micrographs, the Teflon tube segment was cut into two halves along its axis. The spores were found on the lower half of the segment [see Figure 4(b)]. This lower half was aligned to face the SEM beam, as shown in the inset.

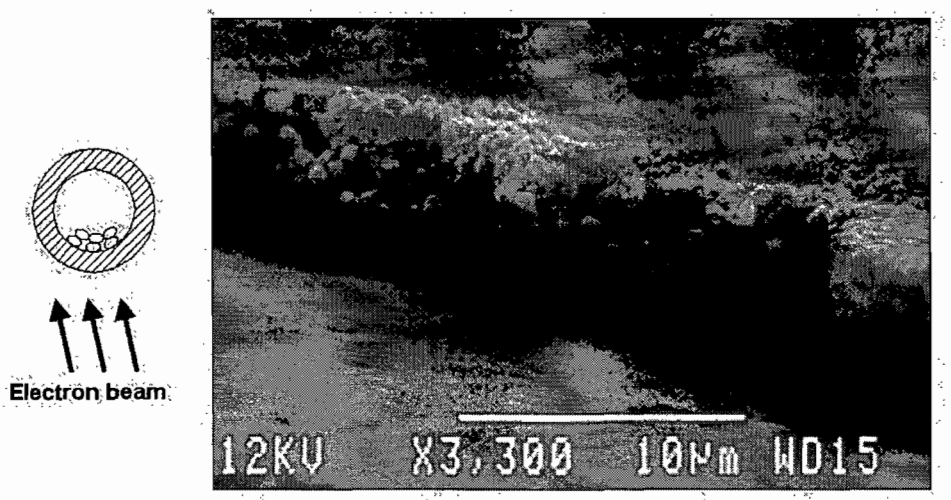

Figure 6. SEM micrograph of dried B. atrophaeus spores deposited on the inner surface of a Teflon tube segment (i.d./o.d. 4/6 mm). The tube segment was cut along a cross section (at approximately the mid length of the segment) and the SEM beam directed as shown in the inset.

In summary, in this section we have described a general procedure that enables one to achieve, in a reproducible way, the stacking of many layers of spores within narrow bore tubes. The method proposed has the further advantage of lending itself easily to making SEM micrographs of the spore deposit (before and after exposure to biocide species). This testing method is of interest to determine the ability of any given sterilisation process to deal with microorganism stacking. Stacking of microorganisms is a possible situation that needs to be considered when re-sterilising MDs, even though these have been thoroughly cleaned (brushed out) and disinfected before being subjected to the sterilisation process itself. The present sterilisation testing method is used in the coming section to assess the sporicide efficiency of our stripline plasma source.

2.4.4. Plasma inactivation of *B. atrophaeus* spores using the stripline discharge: an experimental study

Figure 7 shows the survival curves obtained when subjecting the contaminated Teflon tube segments (see above section) to an argon stripline discharge at two operating frequencies, namely 700 and 2450 MHz. In both cases, the argon pressure was fixed at 750 mTorr (100 Pa), with a gas flow of 100 standard cubic $cm.min^{-1}$ (sccm). At 700 MHz, the incident power was set to 20 W to fill the whole tube length, the HF power absorbed by the plasma being 14 W. A 1 log reduction in the number of viable spores was observed after 10 min of exposure to plasma. In contrast, at 2450 MHz, the corresponding incident power was 51 W and it was fully absorbed by the discharge. Sterility of the Teflon segment, as attested from 3 independent experiments, was reached in 9 min (and confirmed at 10 min). By convention (related to statistical considerations), no count on 3 independent experiments is plotted as 1/3 on the log scale.

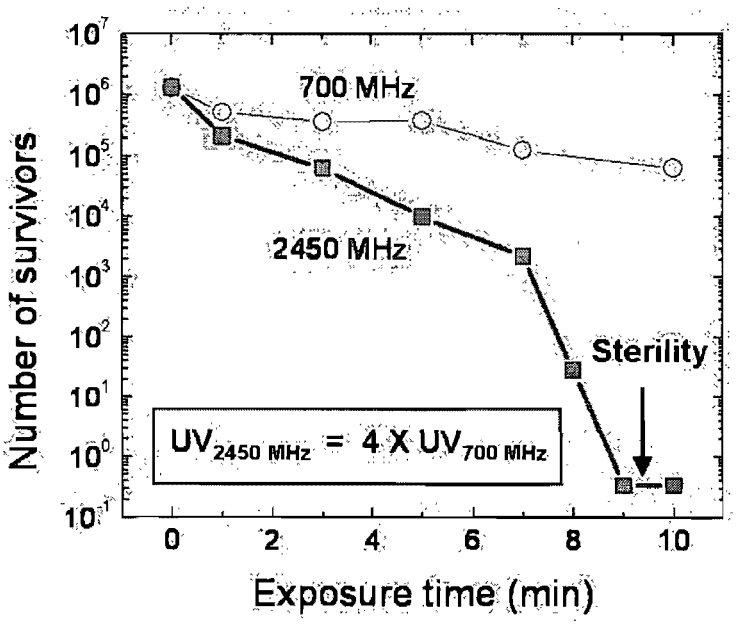

Figure 7. Survival curves of B. atrophaeus spores, deposited in Teflon tubings and subjected to a stripline argon plasma operated at field frequencies of 700 and 2 450 MHz. Argon gas flow was 100 sccm at 750 mTorr (100 Pa). The total UV emission intensity in the 180–300 nm range (recorded with a photomultiplier located perpendicularly to the discharge tube) was 4 times larger at 2450 MHz than at 700 MHz, as indicated in the inset.

The emission intensity from the stripline argon plasma was recorded between 112 and 300 nm using a 1 m focal length VUV spectrometer (McPherson 225). UV photons at wavelengths larger than 300 nm are known not to have significant sporicide effects on *B. atrophaeus* spores.[18] This recording was made with the extremity of the discharge tube (pumping outlet side, past the stripline applicator) introduced into the monochromator entrance port and directed along its optical axis. The monochromator was isolated from the discharge tube by a MgF_2 window (cutoff wavelength at 112 nm) and it was pumped down independently of the discharge tube to less than 100 mTorr. Figure 8 shows the observed emission spectra (from 112 nm to 200 nm in Figure 8(a) and from 200 to 300 nm in Figure 8(b)) with identification of the characteristic atomic lines and molecular band heads. The fact that oxygen and nitrogen atomic lines, the N_2 Lyman-Birge-Hopfield (LBH) bands as well as the NO_β and NO_γ systems are present in this supposedly pure argon dis-charge is indicative of impurities coming from air.[c] The 112–300 nm spectrum is dominated by the nitrogen atomic lines and by

[c] Although the air impurity level is extremely low in the argon gas bottle used, argon discharges are known to be very efficient in exciting air impurities, as shown by Masoud et al.[19] These authors "used research grade argon and nitrogen gas with a stated purity of 99.999% in conjunction with stainless-steel gas lines. However,

the LBH bands. The wavelength extension of the LBH system, according to Massoud et al.[19], is indicated by the arrow in Figure 8.

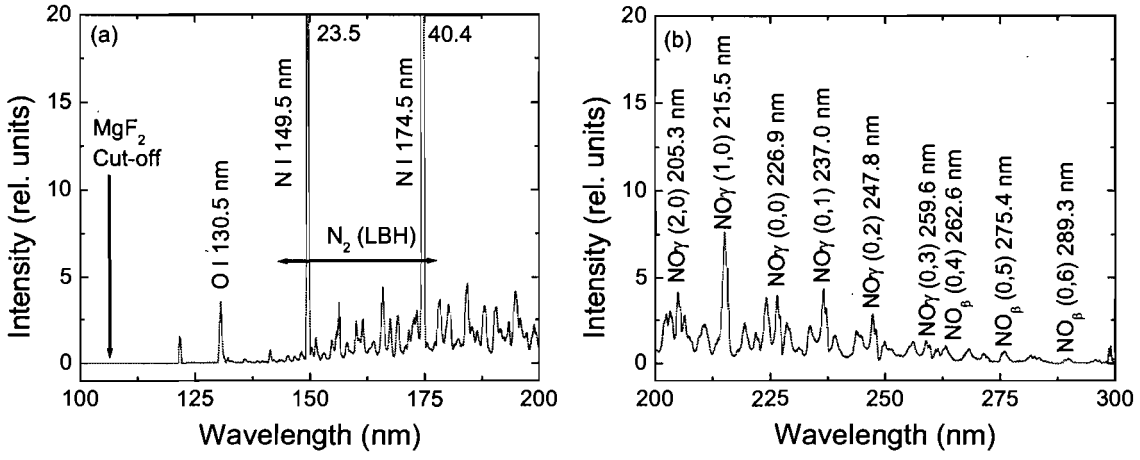

Figure 8. UV emission spectrum from the stripline argon plasma with identification of the main atomic lines and characteristic molecular band heads (a) between 112 and 200 nm and (b) between 200 and 300 nm. The oxygen and nitrogen atomic lines, the N_2 Lyman-Birge-Hopfield (LBH) bands as well as the NO_β and NO_γ systems, are indicative of the presence of impurities in the argon gas. The intensity of the N I 149.5 and 174.5 nm atomic lines are off-scale with peak values of 23.5 and 40.4, respectively. Operating conditions: 2450 MHz, 100 sccm of argon at 750 mTorr. Note that this UV emission spectrum is not corrected for intensity variations with wavelength.

The total UV emission intensity in the 180–300 nm range (recorded with a photomultiplier located perpendicularly to the discharge tube) was 4 times larger at 2450 MHz than at 700 MHz, as indicated in the inset in Figure 7. Recording the UV intensity in this way was also used to ensure that the discharge was operating in a reproducible mode, i.e., for a given set of experimental conditions, the UV intensity obtained remained the same. In fact, increasing the field frequency of the stripline naturally provides a higher electron density,[2] hence a higher electron excitation rate, which in the present case is actually close to the ratio of absorbed microwave power at these two frequencies.

---

measurements of the emissions from pure argon, after evacuating the discharge chamber to a base pressure in the 10^{-7} Torr range for at least 24 h before backfilling the source, revealed that even in this case emissions from impurities were found in the wavelength range from 115 to 180 nm''. Also, one cannot exclude the possibility of very small air leaks into the gas circuit.

To make sure that the inactivation rate observed on the survival curves in Figure 7 does not result from eventual effluents released by the Teflon tubing under argon plasma exposure, we subjected inoculated tubing segments of fused silica to the argon discharge in the same way as for the Teflon ones. Then, instead of working out a full survival curve to solve this matter, we decided to check simply whether sterility was achieved or not within the same time interval as with Teflon tubings by performing +/- tests. These tests were conducted immediately after plasma exposure, by incubating at 37 °C each fused silica segment in a test tube containing nutrients [Trypticase Soy Broth (TSB)] with phenol red as pH indicator. Provided not even a single spore is still alive, the TSB remains the same colour (a colour change being indicative of growth). The incubation of such tubes is actually prolonged for 7 d before looking for a colour change. The results obtained using the +/- tests with the fused silica tubing finally showed that the Teflon tubing has no significant influence on the processing time, sterility also being attained in less than 10 min.[d]

As mentioned previously, the inoculated Teflon tubing segments were placed at a mid-axial position (z = 31 cm) within the fused silica tube. To ensure that the observed inactivation rate was approximately the same at other axial positions, we subjected inoculated Teflon segments at both extremities of the plasma column (z = 5 and 57 cm). In both cases, sterility was achieved within 10 min of plasma exposure (in each case, 3 independent experiments), as would be expected, since the axial distribution of the emitted light intensity was relatively uniform along the plasma column (Figure 2).

To look for an eventual influence of the temperature of the discharge gas on the spore inactivation process, we first needed to measure, as a function of exposure time to the discharge, the temperature of the Teflon tube (outer surface) segments (see above section). This was done some 10 s after turning off the discharge (Figure 9). The temperature increased initially with time and saturates after approximately 3 min, going from 23 (ambient temperature) to 31 °C at 700 MHz, reaching 48 °C at 2450 MHz; the substrate temperature was therefore higher at 2450 MHz.[e] As shown, for instance by Petin et al.,[20] heating the microorganisms can synergistically enhance their inactivation by UV photons. In the present case, we are nonetheless unable to sort out the respective influence, on the survival curve, of

[d] Although the nature of the dielectric tubing presumably influences the configuration of the spore deposit through its hydrophobicity degree.

[e] Since the temperature measurements are achieved using a surface thermocouple applied to the outer surface of the tube, the temperature of the spores (located on the inner surface of the tube and in direct contact with the argon discharge) should be higher, at least for the first few minutes of plasma exposure.

an increased VUV/UV emission intensity and of a larger gas temperature at 2450 MHz. Further studies are needed to resolve this.

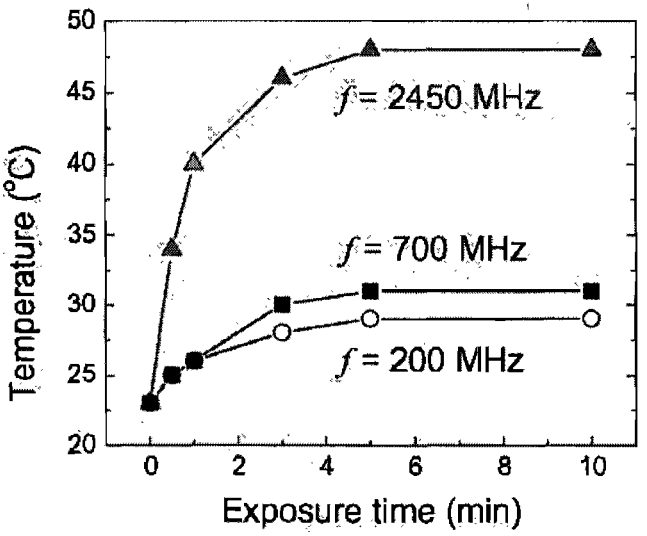

Figure 9. Recorded temperature of the Teflon segment surface, as measured with a thermocouple, as a function of plasma exposure time at three different field frequencies *f*. Operating conditions: 100 sccm of argon at 750 mTorr.

2.4.5 Damage to spores and polymer surfaces exposed to the stripline argon discharge

This section focuses on eventual erosion and, more generally, damage of any kind caused by the stripline argon plasma to the microorganisms and to their polymer substrates during processing time. This is an important issue since: (i) a sterilisation process, to be acceptable, must not affect the physicochemical and mechanical properties of MDs, including those comprising polymeric parts; (ii) examining eventual damage to spores and to their polymer substrate can provide information on the species responsible for it and it can also help in identifying (or confirming the identification of) the biocide species produced by our stripline plasma. Recall that UV photons generally induce very little damage compared to radicals as shown by Crevier et al.[21]

2.4.5.1 Damage to spores

Figure 10 shows SEM micrographs of *B. atrophaeus* spores which have been (a) unexposed or (b) exposed for 10 min to the argon plasma at 2450MHz. Recall, from Figure 7, that 10 min are more than enough to inactivate the totality of the 10^6 exposed spores under our standard

conditions. Nonetheless, no significant erosion of the exposed spores was observed, as can be seen by comparing Figure 10(a) and 10(b), and there is absolutely no sign of lysis. This fact is an additional argument supporting our basic assumption that, in the frame of our work on plasma sterilisation, spore inactivation results from lesions to the deoxyribonucleic acid (DNA) through UV radiation alone. The fact that the *B. atrophaeus* spores exhibit no visible morphological damage (as observed with SEM micrographs) on exposure to the plasma rules out any electrostatic disruption or even damage, such as that described by Laroussi et al.[22] on vegetative cells like *E. coli*.

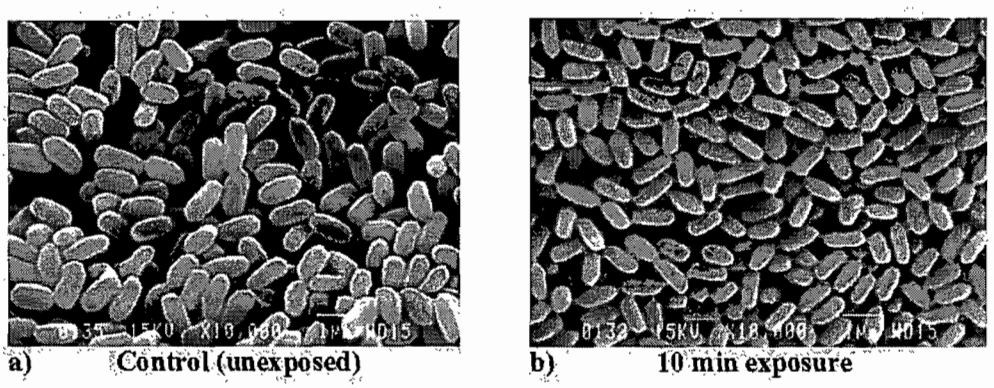

Figure 10. SEM micrographs of B. atrophaeus spores deposited within Teflon tube segments: (a) unexposed spores; (b) spores subjected to an argon plasma for 10 min at mid-axial position of the stripline system (and all inactivated [see Figure 7)]. Argon gas pressure was 750 mTorr at a flow rate of 100 sccm.

2.4.5.2 Damage to polymers

No damage was observed with SEM on the Teflon segments used throughout the sterilisation experiments, but uniform erosion could not be a priori ruled out. To look more closely in that direction, we turned to polystyrene, a less sturdy polymer than Teflon, and subjected microspheres of this material (approximately 1 mm in diameter, i.e., similar in size to the tested spores) to the stripline argon plasma. Such microspheres have already been employed (Boudam et al.[23]) to compare damage induced by the early and the late N_2/O_2 afterglows (in the context of plasma sterilisation). On that occasion, these polystyrene microspheres[f] were shown to be quite responsive to the various plasma species present in the N_2/O_2 afterglows. For instance, the observed off-axis erosion rate was correlated with the increase of the density

[f] In the elaboration process of microspheres, to avoid their coagulation and aggregation a tensoactive solution is added to the polymer: when exposed to plasma, the properties of these spheres could be different from those of the conventional polystyrene (F. Poncin-E´paillard, private communication).

of O atom density as the O_2 percentage in the N_2/O_2 mixture was increased, whereas the on-axis erosion observed at 0% O_2.

A suspension of 10^6 polystyrene microspheres diluted within 50 mL of water was therefore prepared. The microspheres were then deposited within Teflon segments using the same procedure as that used for spores. Because the polystyrene microspheres were approximately the same size as the spores, the configuration and distribution of the deposited microspheres were similar to those of the spores. The totality of the polystyrene microspheres was located on the lower half of the Teflon tube segment, and multi-layered structures could also be seen. Figure 11 shows SEM micrographs of the polystyrene microspheres: (a) unexposed; (b) subjected for 10 min to the stripline discharge using the same operating conditions that ensured sterility in 10 min (field frequency was 2450 MHz, argon gas pressurewas 750 mTorr with a gas flow rate of 100 sccm). No noticeable differences between the exposed and unexposed microspheres were observed using SEM micrographs. Statistics on 100 microspheres showed that the average diameter of the unexposed microspheres was 0.99 +/- 0.04 mm, while that for the exposed microspheres was 0.99 +/- 0.03 mm.

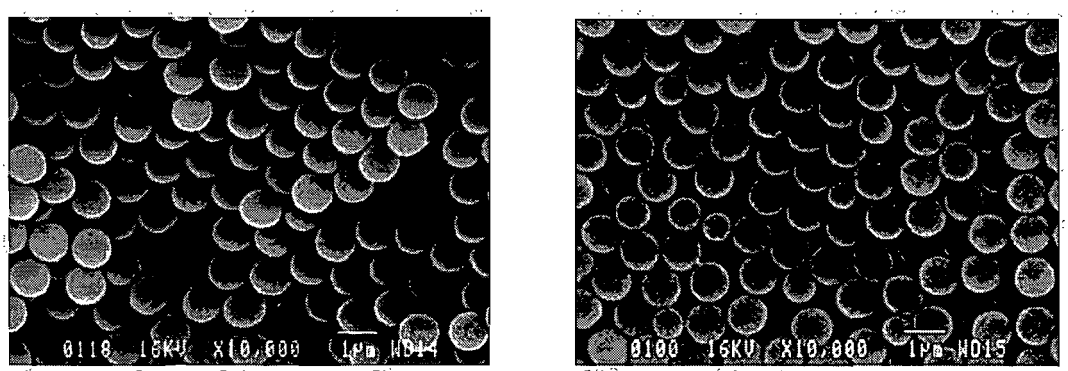

Figure 11. SEM micrographs of polystyrene microspheres deposited within a Teflon tube segment (section 2.3.3.2): (a) unexposed microspheres, (b) microspheres subjected for 10 minutes to the stripline argon discharge using the same operating conditions that led to spore sterility in 10 minutes (field frequency is 2450 MHz, argon gas pressure is 750 mTorr with a gas flow rate of 100 sccm).

In conclusion, damage to Teflon tubings and even to polystyrene microspheres cannot be detected with SEM, tending to prove that the stripline argon discharge, when operated under conditions that yield sterility in 10 min, induces relatively little damage to these polymers. In

contrast, erosion damage on polystyrene microspheres, although mild, is nevertheless observable in the flowing afterglow of a N_2/O_2 discharge under conditions for maximum UV radiation (shortest sterilisation time).[23]

2.4.6 Discussion

Since narrow bore tubes are difficult to clean, there is always some possibility, even after a thorough cleaning procedure, that bio-burdens, originating mostly from blood products in the case of catheters, be present as the tube is subjected to plasma sterilisation. This could lead to sterilisation failure depending on the thickness of the remaining (unclean) deposit since the action of UV photons is limited by the thickness of the material that they have to go through. We know from experiments that a 10 mm deposit (as is the case for Figure 7) can readily be taken care of, while we have observed that this is not so with a sedimented whole blood stain[g] of 300 mm thickness containing 10^6 *B. atrophaeus* spores. More work in this area is needed, a major difficulty being control of the thickness of the sedimented blood stain. It is worth noting that this problem (that is to say a reduction of the inactivation efficiency due to bio-burden) was reported by Alfa et al.[17] to occur with other sterilisation processes (ion plasma, vaporised hydrogen peroxide and ethylene oxide sterilisers) when bacteria were inoculated within lumens with salt or serum. Actually, as stressed by Penna et al.[15], ''to achieve an acceptable sterility assurance level through a terminal sterilisation process, the critical medical device must be freed from all adherent materials that interfere with the sterilising agent''.

In summary, we have presented a plasma system allowing sterilisation (in less than 10 min) of the inner part of long, narrow bore dielectric tubes contaminated with 10^6 *B. atrophaeus* spores by exposing them directly to a low temperature argon discharge. Such an arrangement appears to be adequate for re-sterilising thermosensitive catheters, at least the simplest ones, while preserving their integrity. Damage to polystyrene, a ''fragile'' polymer, was not detected by SEM after it had been exposed to plasma for the period of time needed for sterilisation. The required low temperature and axially uniform discharge was obtained with a linear field-applicator of our own design, called a stripline.[2]

---

[g] Ethylenediaminetetraacetic acid (EDTA) was added to the human blood prior to the inoculation of the Teflon pieces to prevent coagulation. The deposit was then dried up in the same way as that of spores diluted in a water suspension.

The sterilisation process was achieved by the VUV/UV photons that were provided by the oxygen and nitrogen atomic lines, the N_2 Lyman-Birge-Hopfield (LBH) bands, the NO_β and $NO\gamma$ molecular systems. The presence of oxygen and nitrogen in the discharge was attributed to residual air impurities present in the argon gas of the discharge. The level of these impurities, although high enough to provide a fast UV inactivation, was still sufficiently low not to create apparent damage to the spores and to polymers such as Teflon and polystyrene.

Finally, to check that sterility was effectively achieved within narrow bore tubes, we developed a procedure to introduce and remove bacterial spores used as bioindicators, which also allows imaging of these microorganisms relatively efficiently with an SEM. This approach further provides a way of controlling, in a reproducible way, the influence of (and the eventual limit imposed by) the stacking of bacterial spores forming multilayered structures, a problem that could be encountered on some occasions even after the standard decontaminating and cleaning procedure previous to the sterilisation step.

2.4.7 Conclusion

In conclusion, the sterilisation method that we have developed for catheters is of much interest but further investigations are needed to take into account the eventual presence of bio-burdens or to make sure that they are absent. In the first case, this implies considering the cases where (i) the microorganisms are partially embedded in human blood and (ii) the microorganisms are partially embedded ''in an amorphous extracellular material composed of exopolysaccharides of bacterial origin that cement the cells firmly to the surface and to each other'',[24] better known as a biofilm.

2.4.8 Acknowledgments

The authors are grateful to J. S. Mayer for skilful technical assistance, to Pr. J. Margot and Pr. J. J. Laurin for valuable comments on the plasma physics and microwave aspects of this work, respectively. Thanks are also due to Mrs. A. Pelletier and D. Turnblom from Sainte-Justine Hospital (Montréal) for highly pertinent comments on hospital regulations concerning cardiac catheters. Financial support for this work was provided by the Fonds Québécois pour la Recherche sur la Nature et la Technologie (FQRNT) and the Conseil de Recherches en Sciences Naturelles et Génie du Canada (CRSNG).

2.4.9 References

[1] Patent application US 0269199 (2005), WO 050128 (2004), Université de Montréal, invs.: J. Pollak, M. Moisan, B. Saoudi, Z. Zakrzewski.

[2] J. Pollak, M. Moisan, Z. Zakrzewski, Plasma Sources Sci. Technol. **2007**, 16, 310.

[3] M. Moisan, J. Barbeau, M. C. Crevier, J. Pelletier, N. Philip, B. Saoudi, Pure Appl. Chem. **2002**, 74, 349.

[4] N. Philip, B. Saoudi, M. C. Crevier, M. Moisan, J. Barbeau, J. Pelletier, IEEE Trans. Plasma Sci. **2002**, 30, 1429.

[5] WO0054819 (2000), invs.: S. Bousquet, P. Destrez, M. Jaffrezic, F. Perruchot.

[6] S. Helhel, L. Oksuz, A. Yousefi Rad, Int. J. Infrared Millimeter Waves **2005**, 26, 1613.

[7] M. Moisan, J. Pelletier, "Physique des plasmas collisionnels", EDP Sciences, Grenoble 2006.

[8] Z. Zakrzewski,M. Moisan, Plasma Sources Sci. Technol. **1995**, 4, 379.

[9] V. N. Slinko, S. S. Sulakshin, L. V. Sulakshina, Sov. Phys. Tech. Phys. **1988**, 33, 363.

[10] US patent provisional application 60/884,344 (2007), Université de Montréal, invs.: J. Pollak, M. Moisan.

[11] F. Tessarolo, I. Caola, P. Caciagli, G. M. Guarrera, G. Nollo, Infect. Control Hosp. Epidemiol. **2006**, 27, 1385.

[12] http://www.gkeaustralia.com/products.htm, July 20, 2007.

[13] http://www.tso3.com/fr/pdf/WhitePaper125L_r0404_fr.pdf, July 20, 2007.

[14] J. H. Young, Biotechnol. Bioeng. **1993**, 42, 125.

[15] T. C. V. Penna, C. M. F. Ferraz, M. A. Cassola, Infect. Control Hosp. Epidemiol. **1999**, 20, 465.

[16] D. Fritze, R. Pukall, Int. J. Syst. Evolut. Microbiol. 2001, 51, 35.

[17] M. J. Alfa, R. T. Degagne, N. Olson, T. Puchalski, Infect. Control Hosp. Epidemiol. **1996**, 17, 92.

[18] A. Cabaj, R. Sommer, W. Pribil, T. Haider, Water Sci. Technol.: Water Supply **2002**, 12, 175.

[19] N. Masoud, K. Martus, K. Becker, J. Phys. D: Appl. Phys. **2005**, 38, 1674.

[20] V. G. Petin, G. P. Zhurakovskaya, L. N. Komarova, J. Photochem. Photobiol. B: Biol. **1997**, 38, 123.

[21] M. C. Crevier, Masters thesis, Université de Montréal 2003.

[22] M. Laroussi, D. A. Mendis, M. Rosenberg, New J. Phys. **2003**, 5, 1.

[23] M. K. Boudam, B. Saoudi, M. Moisan, A. Ricard, J. Phys. D: Appl. Phys. **2007**, 40, 1694.

[24] A. Pajkos, K. Vickery, Y. Cossart, J. Hosp. Infect. **2004**, 58, 224.

2.5 Inactivation de biofilms dans des tubes diélectriques

La conformation la plus naturellement répandue de micro-organismes sur une surface est leur réunion en colonie "ordonnée" par elles-mêmes pour former ce que l'on appelle un biofilm. Il s'agit d'une configuration de microbes qui a développé, à partir de nutriments fournis par l'environnement, une matrice de sucre leur permettant, en plus des fonctions métaboliques essentielles, un très solide ancrage à la surface. De plus, lorsque cette matrice est suffisamment épaisse (plusieurs microns), elle les aide à parer les attaques extérieures par des espèces chimiquement actives et les UV. Pour illustrer notre propos, nous avons rassemblé sur la figure 2.5 quelques exemples de biofilms répertoriés après l'usage d'instruments médicaux contenant des parties creuses: un tube (a) endotrachéal [47], (b) d'endoscope souple [48], (c) de dialyse [49] et (d) d'une unité de médecine dentaire (prélevé à l'Université de Montréal par J. Barbeau).

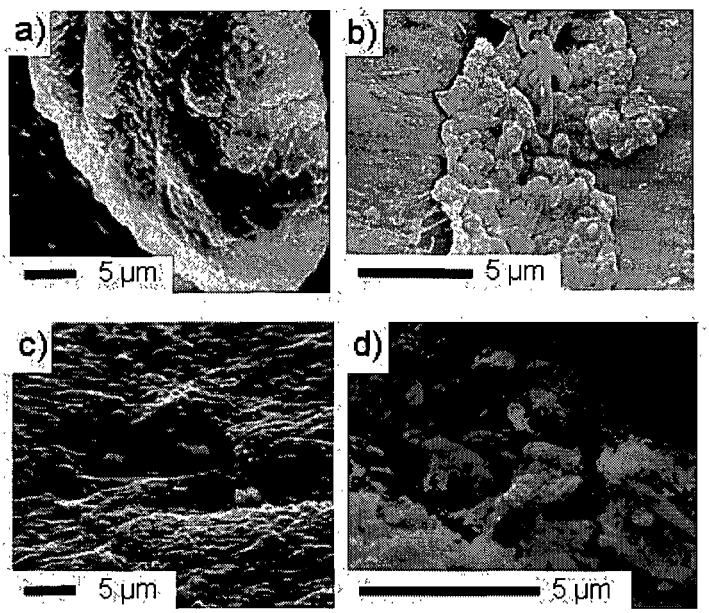

Figure 2.5 Exemples de biofilms rencontrés dans des tubes à usage médicale: surface d'un tube (a) endotrachéal Costerton [47], (b) d'endoscope souple [48], (c) de dialyse [49] et (d) de médecine dentaire (prélevé dans l'unité étudiante de médecine dentaire de l'Université de Montréal par J. Barbeau).

Dans chaque cas, les biofilms présentent un danger pour les patients, ce qui explique l'intérêt du monde médical envers ces communautés de micro-organismes extrêmement répandues, tenaces et particulièrement résistantes aux antibiotiques. Dans l'article suivant, nous avons tout

d'abord mis au point une méthode *in vitro* permettant d'obtenir des biofilms dans des tubes, puis nous l'avons utilisé pour évaluer les performances de notre stérilisateur pour tubes diélectriques creux.

Biofilm sterilization within polymer tubings by a low temperature gaseous plasma (ionized gas)

(article soumis à International journal of pharmaceutics)

J. Pollak, J. Séguin, J. Barbeau, M. Moisan

Abstract

There is a growing interest in the development of sterilizers for processing long and narrow-bore tubes such as cardiac catheters and flexible endoscopes. These medical devices are hard to sterilize due to their thermosensitive nature and geometrical configuration. Various pathogens can be found within the lumens of these devices, mostly as biofilms which are resistant to disinfectants and conventional sterilization techniques. The current paper deals with the use of gaseous plasmas (ionized gases) to inactivate bacterial cells in thin biofilms (few μm). *Staphylococcus aureus* biofilms were grown for that purpose in long narrow-bore Teflon tubes that mimic catheters. A novel low-temperature and spatially uniform plasma source was used to inactivate such biofilms. Cells were recovered on a time course after plasma exposure. Full inactivation was achieved within 5 minutes in argon gas ionised by a high-frequency (HF) electric field (700-2450 MHz) under reduced pressure conditions (100 Pa).

2.5.1 Introduction

At present time, most flexible endoscopes are not sterilized but highly disinfected, while cardiac catheters are disposed of after single use. Among the various reasons associated with sterilization failure of these devices, is the presence of biofilms. Biofilms are complex structures that grow at a solid–liquid or solid–air interface and are composed of bacteria organized in an extracellular matrix. Biofilm communities can easily develop within medical devices (MDs) comprising long and narrow-bore tubes such as catheters (Macleod et al., 2007) and endoscopes (Pajkos et al., 2004): biofilms are known to be more resistant to disinfectants and sterilization agents than free-living bacteria (Kim et al., 2007). Nonetheless, for practical, economical and ecological concerns, it is worth developing a sterilization

method that could allow reutilization of these devices according to validated and controlled regulations.

The introduction into various organs and tissues of artificial devices, often made of synthetic material such as implants and prostheses, is somehow hindered by the ability of microorganisms to adhere to these devices and develop thereon biofilms, which protect them from the activity of antimicrobial agents and from host defence mechanisms (Khardori et al., 1995): bacterial cells are embedded in exopolysaccharides and soil, which permit strong adherence to surfaces (Ahimou et. al., 2007; Sutherland, 2001) and shield them from the damaging effect of disinfectants. In that respect, unequivocal direct observations have established that bacteria causing device-related and other chronic infections often grow in matrix-enclosed biofilms. Actually, while mechanical brushing generally removes a great deal of biofilm on MDs, it is hardly applicable to narrow-bore channels while cleaning them by detergent alone appears ineffective (Kim et al., 2007). Obviously there is a need for methods that could, at best, prevent biofilm formation or, at least, inactivate them when present on MDs, in particular on those presenting complex geometrical configurations. For instance, *in vivo* aggregates can form on the lumenal surface of endotracheal tubes (Costerton et al., 2003). These aggregates routinely break off of these surfaces and can then be aspirated into patients' lungs. Biofilms can also be present in endoscope channels after a routine cleaning procedure conducted according to infection control guidelines (Pajkos et al., 2004). As far as dialysis apparatus are concerned (Man et al., 1998), scanning electron microscopy (SEM) of the inner surface of fresh silicon tubings and of tubing samples drawn from the various fluid paths demonstrated the significance of biofilm development on the various surfaces of the hydraulic circuits. Bacteria are not expected to cross the dialysis membrane, but it is possible for endotoxins to do so and this is why pyrogenic reactions have been associated with the practice of dialyser re-use (Roth et al., 2000). Evacuation systems used in dentistry can also be a source of contamination between patients through the backflow of bacteria dislodged from the saliva ejector tubings (Barbeau et al., 1998). Clearly, there is a need for sterilization techniques that could deal with biofilms formed on the inner wall of long narrow-bore tubes.

Applying gaseous plasmas to the field of sterilization offers tremendous opportunities in solving various problems related to MD sterilization. The main features of this sterilization technique are its rapidity, efficiency and the absence of vent time. Various stable and efficient plasma sources have been developed and characterized for that application in recent years. For instance, atmospheric pressure cold plasma jets/plumes (mini plasma-torches) (Laroussi et al., 2007) are useful for localised inactivation treatments. Low-temperature plasmas operated

in closed chambers at reduced pressure (i.e. below atmospheric pressure) can be the basis of efficient sterilization systems ensuring low damage to MDs, either when these are exposed to the plasma itself (Pollak et al., 2008b) or located in the flowing effluents from the plasma source (flowing afterglow scheme) (Moisan et al., 2001). However, only few trials to inactivate biofilms by plasma have been attempted. For one, it was shown that inactivation, although partial, of bacterial biofilms developed in polystyrene microplates, can be obtained by using an atmospheric-pressure He-N_2 plasma jet (Becker et al., 2005): the number of cells was reduced by more than two orders of magnitude after a 5 min plasma exposure and by 3.5 orders of magnitude after 60 min. In 2006, re-using the same experimental design, partial biofilm inactivation by an atmospheric-pressure cold plasma jet was confirmed (Abramzon et al., 2006). The results, reported in the form of survival curves (logarithm of the number of viable micro-organisms as a function of exposure time to the biocide agent), show an initial rapid linear decrease (so-called first inactivation phase), followed by a much slower subsequent decrease (second phase), a usual form of survival curves when inactivating microorganisms with plasma (Moisan et al., 2001). More recently, it was shown that atmospheric-pressure low-temperature He-O_2 plasmas can inactivate, but again only partially, *Pantoea agglomerans* biofilms (Vleugels et al, 2007). Also using an atmospheric-pressure low-temperature plasma, this time in the form of a needle plasma-torch, growth inhibition of *Streptococcus mutans* biofilms (Sladek et al, 2007) was observed after a single 1 min plasma exposure when the biofilms were cultured without sucrose (post-incubation observation periods up to 12 h). However, on biofilms cultured with up to 15% sucrose, growth was only reduced, not inhibited, by even repeated plasma treatments of 1 min.

We recently presented a new plasma source designed to sustain a low gas-temperature plasma within thermally-sensitive dielectric tubings (Pollak et al., 2005). Its design, electrodynamic characteristics and axial uniformity are discussed elsewhere (Pollak et al., 2007). This plasma source was subsequently used to completely inactivate stacked bacterial spores (up to 8 layers of them) within long and narrow-bore dielectric tubings (Pollak et al., 2008a). It is the purpose of the present paper to evaluate its efficiency when dealing with thin biofilms grown within these tubings.

2.5.2 Materials and methods

2.5.2.1 In vitro biofilm formation method

A clinical strain of *Staphylococcus aureus* (Laboratoire de Santé Publique du Québec (LSPQ 2520)), reported capable of biofilm formation (Bendouah et al., 2006), was grown overnight in Trypticase Soy Broth (TSB) medium at 37 °C. The bacterial suspension was washed with sterile water and the pellet was re-suspended to obtain an optical density of 0.100 at 620 nm. This suspension was diluted and plated on Trypticase Soy Agar (TSA) medium to evaluate the number of colony forming units (CFUs). A 10^{-6} dilution in TSB was used as inoculum. Results based on 6 independent similar cultures showed that the inoculum was equivalent to $5.5 \cdot 10^3 \pm 1.6 \cdot 10^3$ bacteria /ml.

Strict sterile conditions were observed throughout the protocol procedure. A 90 mm Teflon tube (i.d./o.d 4 mm/6 mm, Johnston Industrial Plastics) and two tight-fitting closures of this tube (custom-made Teflon caps) were washed and autoclaved. The Teflon tube was capped at one end and inserted into a 15 ml sterile centrifuge tube (of slightly larger diameter and length allowing ease of manipulation). The bacterial suspension (1.0 ml) was introduced into the Teflon tube using a 3 ml syringe and a hypodermic needle and the other end of the tubing was capped. The centrifuge tube was closed and positioned onto a turn table rotating at 10 turns / minute. This assembly was kept at 37 °C in an incubator destined to biofilm formation.

2.5.2.2 Biofilm recovery method

After 24 h of incubation, the Teflon tube was uncapped and the broth containing the non-adherent cells and spent medium was drained. Subsequently, the tubing was rinsed twice with 10 ml of Tween saline (0.5 % Tween 80™ in 0.85 % NaCl). Care was taken not to contaminate the external surface of the Teflon tube during the procedure. This tube was placed in a sterile Petri dish where it was cut in 8 segments of approximately 11 mm length each, using a sterile blade. These segments were individually placed in wells culture plate and kept at 4 °C until plasma exposure. The biofilm from the various segments was dislodged using a pre-wetted cotton swab and transferred to a 5.0 ml Tween saline solution for evaluation of the number of CFUs. This suspension was diluted and aliquots were incubated on TSA plates. Counts were evaluated after 24 h at 37 °C. Efficiency of our recuperation method was verified by examination of the Teflon tubings with an SEM, which shows that

most of the biofilm incorporating the microorganisms has been removed (SEM micrographs not shown). Recovery of all bacteria from the biofilm by filtration of the whole 5 ml on 0.22μm membrane (Millipore) was carried out when low numbers of CFUs were expected. Membranes were then placed on TSA plates. The original Teflon segment and the swab used for recovery were also incubated in a test tube with TSB at 37 °C for 7 days.

2.5.2.3 Plasma source and experimental arrangement

The electrodynamic characteristics and features of the present high-frequency (HF) field applicator are described in detail elsewhere (Pollak et al., 2007). A schematic representation of this field applicator is shown in Fig. 1(a). It is essentially a transmission line, actually an open planar variant of the classical coaxial line since the wave propagates on a transverse electric magnetic (TEM) mode. HF power is applied at one extremity of the conducting strip (Fig. 1(b)); the terminating matched load at the other extremity of the strip prevents any residual HF power from being reflected at its end, which would hinder uniformity of the HF field intensity, hence of the plasma, along the field applicator. This 50 Ω load is the only impedance matching means of the HF plasma source to the HF power generator, this matching being frequency independent (200–2450 MHz range tested). Figure 1(c) is a photograph of an HF argon gas-discharge sustained with this field applicator within Teflon tubes, one being located above and the other below the conducting strip as schematised in Fig. 1(b). Provided the ratios w/L and h/L are small, this structure does not radiate to the outside, which ensures security to the operator. The main biocide agents in the present argon discharge are believed to be ultraviolet (UV) and vacuum UV (VUV: ≤ 180 nm) photons (Pollak et al., 2008a).

2.5.2.4 Checking the efficiency of the sterilization technique within lumens

Plasma was created here within a single discharge tube made of fused silica. The inoculated Teflon segment was pushed at mid-axial position within the fused silica tube (of a slightly larger diameter: i.d./o.d. 7/9 mm), thereby assuming that if sterility was obtained at mid-position, it would also be achieved everywhere along the tube. Such a reasoning is supported by the fact that the axial distribution of the emitted light intensity is relatively uniform along the plasma column. Fused silica was employed as a support for the Teflon

tubing because it enabled us to record UV emission at optical wavelength as low as 180 nm during plasma exposure.

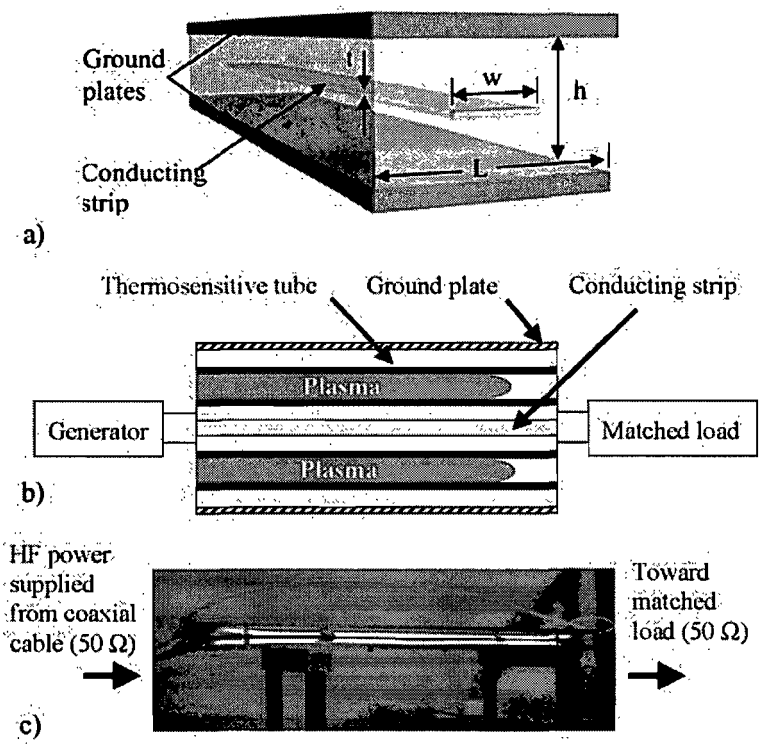

Fig. 1. (a) Schematic representation of the bare HF field-applicator, a stripline structure operating on the transverse electric magnetic (TEM) mode of wave propagation; (b) Schematic representation of the field applicator, with a discharge tube positioned above the conducting strip and a second one below it; (c) Photograph of two Teflon tubes fed with argon gas and uniformly illuminated by the HF discharge sustained within them. Sterilization experiments were conducted in such tubes made of Teflon with 4/6 mm i.d./o.d. The field applicator was 62 cm long with the following characteristic dimensions: w = 26.4, t = 3.2, h = 24 and L = 90 mm. An interesting feature of this plasma source, economically speaking, is that it can also be operated with up to four discharge tubes (i.d./o.d. 4/6 mm tested) per conducting strip, and with eventually more conducting strips, but in the current paper we considered the simpler case of a single discharge tube.

2.5.3 Results

2.5.3.1. Characterization of the biofilms using an SEM

Figure 2 presents SEM micrographs of a *Staphylococcus aureus* biofilm formed with our scheme onto the inner surface of the Teflon tubing. Figure 2 shows that *S. aureus* bacteria are embedded in an extracellular matrix, that the biofilm is not uniform and that its thickness is approximately 2 µm. We checked that immersing the Teflon tube into a detergent and vortexing it for 2 minutes does not dislodge the biofilm from its surface, in contrast to the situation observed with sedimented bacteria (this was done by measuring CFUs and comparing SEM micrographs pre- and post-vortexing in both cases on 8 replicas).

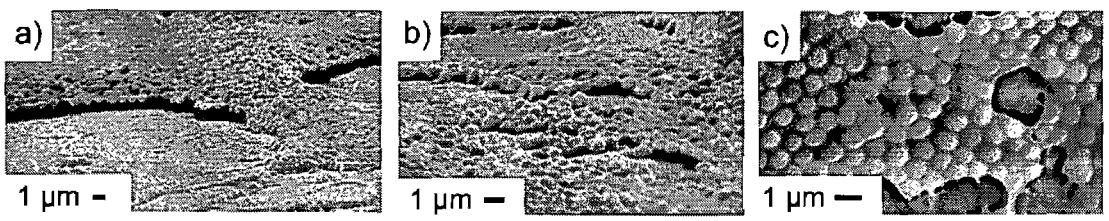

Fig. 2. Scanning electron microscope (SEM) micrographs of a 24 hour growth-time *S. aureus* biofilm formed onto the inner surface of a Teflon tube (i.d./o.d. 4/6 mm).

2.5.3.2. Number of CFUs recovered from the biofilm

Figure 3 shows the recovery of viable *S. aureus* bacteria from biofilms formed over a 24 h period in the eight 11 mm long Teflon segments as a function of their position in the original 90 mm tube under different drying time and storage conditions before recovery. The distribution of CFUs along the 90 mm Teflon tube is fairly uniform when the biofilm is still fresh (~ 10^8 bacteria are recovered within each of the 8 segments), as it varies by approximately only one log. However, after a drying period of 7 days at 22 °C, there is an important quantitative decrease in the number of viable bacteria with, in this case, important variations (up to 3 log) between the different segments. We observed that this decline was steady over the 7 day period (data not shown). In contrast, keeping the segments during 7 days at a lower temperature (4 °C) increases by far the survival rate and also decreases the differences in the number of viable bacteria recovered from the different segments. In view of

those results, the inactivation experiments by plasma were all conducted using segments containing biofilms kept at 4 °C for less than 7 days.

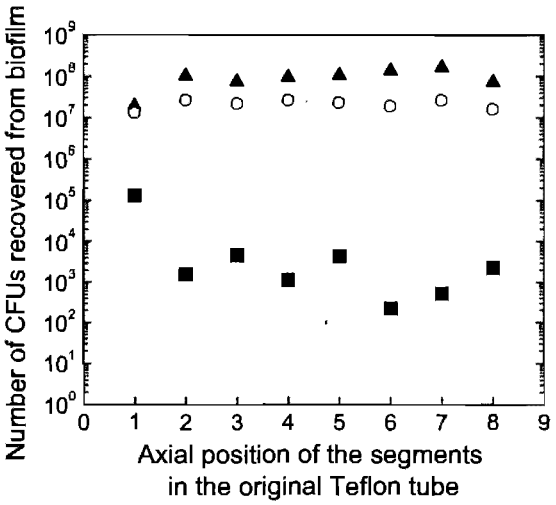

Fig. 3. Recovered CFUs of *S. aureus* 24 h biofilm, formed onto the inner surface of a 90 mm long Teflon tube (i.d./o.d. 4/6 mm). The CFU number is plotted as a function of axial position along the original Teflon tube, considering various drying periods and storage conditions: ▲, fresh biofilm (recovered immediately after rinsing the tube); ○, segment kept for 7 days at 4 °C; ■, segment kept for 7 days at room temperature (22 °C).

2.5.3.3. Survival curves of S. aureus biofilm obtained under different operating conditions

We have previously reported that the UV photons are the dominant biocide agents of the present argon plasma source (Pollak et al., 2008a). Figure 5 shows survival curves from 24 h biofilms of *S. aureus* when exposed to the plasma source. Two different sets of operating conditions were examined: an applied field frequency of 700 MHz with a plasma absorbed power of 14 W or at 2450 MHz with 51 W of absorbed power. Four times more UV photons are obtained with the higher density of absorbed power. Two independent experiments were made at each exposure time. During the first minutes of plasma exposure, a rapid decline of viability is observed, followed by a much slower decrease between 2 and 10 minutes (two-phase survival curves).

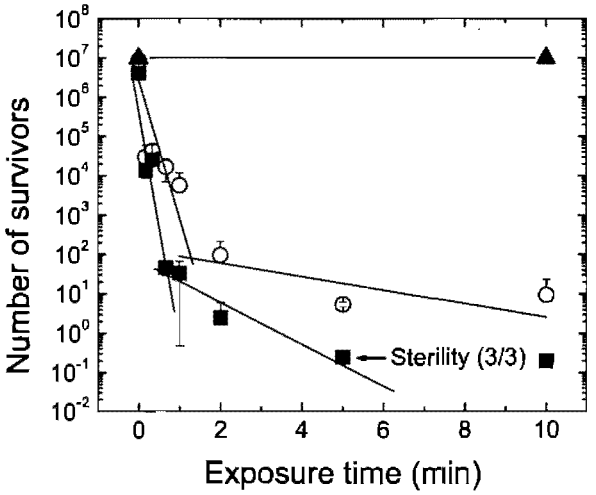

Fig. 4. Survival curves of 24 h biofilms of *S. aureus* as a function of plasma exposure time under two different operating conditions: field frequencies set at 700 MHz with a plasma absorbed power of 14 W (○) and at 2450 MHz with 51 W (■); all operating conditions but plasma not ignited (▲).

2.5.3.4. Validation of our sterilization method

As shown in Fig. 4, complete inactivation of the biofilm is obtained after 5 minutes of exposure at 2450 MHz, which is not the case at 700 MHz. To strive recuperating all the bacteria from the biofilm, we not only used both plate and filtration recovery methods for all samples, but we also incubated, in TSB culture medium over a week the membranes, the used swabs and the swab-treated segments. The corresponding results are shown in Table 1.

Table 1

Sterility check after filtration of recovery fluid and incubation of swabs and tubing segments in culture medium.

700 MHz	Exposure time	Filtration membrane		Swab used for recovery		Post-recovery Teflon segment	
		Exp. 1	Exp. 2	Exp. 1	Exp. 2	Exp. 1	Exp. 2
	10 s	C*	C	+	+	+	+
	20 s	C	C	+	+	+	+
	40 s	C	C	+	+	+	+
	1 min	>1000	>1000	+	+	+	-
	2 min	176	7	+	-	-	-
	5 min	6	5	+	+	-	-
	10 min	19	0	-	-	-	-
2450 MHz	Exposure time	Filtration membrane		Swab used for recovery		Post-recovery Teflon segment	
		Exp. 1	Exp. 2	Exp. 1	Exp. 2	Exp. 1	Exp. 2
	10 s	C	C	+	+	+	+
	20 s	>500	C	+	+	+	+
	40 s	31	58	-	-	-	-
	1 min	55	10	+	-	-	-
	2 min	5	0	-	-	-	-
	5 min	0	0	-	-	-	-
	10 min	2	0	-	-	-	-

*C = confluent growth, + : growth, - : no growth

Table 1 shows and confirms that operating at 2450 MHz rather than 700 MHz is more efficient to inactivate the biofilms, and to reach sterility. To further check for sterility at both operating frequencies (700 and 2450 MHz), we exposed additional Teflon segments for 10 minutes to plasma. These segments were then immediately and individually incubated, directly, in TSB at 37 °C. After a one week incubation period, +/- tests showed that at 700 MHz, only 1/3 segment was sterile, while at 2450 MHz, 3/3 segments were sterile. These

results are consistent with those presented in Fig. 4 and Table 1: operating at 2450 MHz rather than 700 MHz is more efficient to inactivate the biofilms due to the fact that four times more UV photons are obtained with the higher frequency.

2.5.4. Discussion

It can be argued that some of the different steps involved in the plasma exposure protocol itself could have *a priori* biocidal properties: 1) The Teflon segments with their biofilms are still hydrated when introduced into the fused silica tube for plasma exposure. As a result, this residual water could absorb the applied microwave power and thus inactivate the bacteria through heating. 2) Vacuum-induced dehydration could reduce the viability of the biofilm. 3) Pressure variations inflicted to the biofilm can cause stresses (e.g. osmotic) to the bacteria. 4) The argon flow, although it is an inert gas, could affect the biofilm. To check these hypotheses, we subjected the Teflon segments to the inactivation process, respecting all the protocol steps but one: the plasma was not ignited. The unexposed biofilms and the biofilms subjected to all the conditions of the plasma exposure protocol but without igniting plasma showed the same number of viable bacteria (see Fig. 4). We can therefore conclude that the different steps involved in the plasma exposure protocol listed above do not have biocidal effects on *S. aureus* biofilm, unless the plasma is ignited.

When operating at 2450 MHz, complete inactivation of the *S. aureus* biofilm (7 log) was achieved in 5 minutes and was confirmed by membrane filtration and +/- tests. As shown elsewhere (Pollak et al., 2008a), the biocide agents of the present plasma source are the vacuum ultra-violet (VUV) photons, which include oxygen and nitrogen atomic lines, the N_2 Lyman-Birge-Hopfield (LBH) bands, the UV photons emitted by the NO_β and NO_γ molecular systems resulting from the contamination, even though at a very low-level, of the argon gas (high purity argon is used) by air. The biocidal wavelength range of the present plasma source extends from 105 up to 300 nm due to the emission of these various atomic and molecular lines.

Two-phase survival curves were obtained when the biofilms are subjected to the present plasma source: during the first minutes of plasma exposure, a rapid decline of viability was observed, followed by a much slower decrease. Survival curves of bacterial spores subjected to plasma inactivation usually show two kinetic phases (Moisan et al., 2001), a quick first reduction in viability followed by a slow reduction phase generally 10 to 20 times longer, which is attributed to the stacking of microorganisms, resulting in a shielding effect affecting

the underlying spores. This is supported by the fact that when the initial (deposit) density is reduced, the second phase involves fewer spores (Pollak et al, 2008b). In the present case, the assumed shielding effect might not only be due to the stacking of the bacteria, but also to variations in the presence of the biofilm matrix. This assumption is supported by observations made with UV lamps (Elasri et al., 1999) showing that the UV intensity is significantly reduced by the presence of the biofilm matrix. This suggests that the thicker the matrix the longer is the UV irradiation time required to inactivate the embedded bacteria.

Care must be taken, at this stage, not to conclude to the capacity of the glow plasma to inactivate any kind of biofilm. Since a major limitation of the plasma-sterilization techniques, especially when relying on UV irradiation, is the maximum thickness of the bioburden that can be inactivated, one has to assess the efficiency of our plasma process when dealing with various types and thicknesses of microorganisms eventually recovered with soil (e.g. blood and food products). Using flow cell systems (Khaled et al., 2001; Marion-Ferey et al., 2003) or our *in vitro* method to grow biofilm, this could be studied by i) varying the composition of the culture medium and the incubation time to increase the biofilm thickness; ii) varying the initial number of bacteria in the inoculum of a given strain; iii) using of pure vs. mixed biofilms (Rickard et al., 2003). These studies are presently under investigation in our laboratories.

In summary, we have developed an efficient protocol for growing reproducible bioflms within tubes and for testing the inactivation effect of plasma on them. Sterility of biofilms of approximately 2 μm subjected to our low temperature glow plasma operated at 2450 MHz was achieved in less than 5 minutes. To our knowledge, this is the first report of complete inactivation of biofilm in tubes by plasma. Besides being of much interest for the development of sterilization methods of medical devices comprising long narrow-bore tubes such as cardiac catheters, we believe that our plasma sterilization process could be extended to inactivate biofilm present on dielectric pipeworks used in the food industry. For instance, it could be scaled down as a movable table-top apparatus to sterilize the inner surface of polymer tubings without disassembling or removing the pipe installation.

2.5.5 Acknowledgments

The authors are grateful to R. Plantefève and P. Gavra for valuable microbiological assistance. Thanks are also due to J.S. Mayer for skilful technical expertise in building the plasma source prototypes. The authors are also grateful to Pr. M. Lavoie for helpful

comments. Financial support of this work was provided by the Fonds Québécois pour la Recherche sur la Nature et la Technologie (FQRNT) and the Conseil de Recherches en Sciences Naturelles et Génie du Canada (CRSNG).

2.5.6 References

Abramzon, N., et al., 2006. Biofilm destruction by RF high-pressure cold plasma jet. IEEE Trans. Plasma Science. 34, 1304-1309.

Ahimou, F., et al., 2007. Effect of Protein, polysaccharide, and oxygen concentration profiles on biofilm cohesiveness. Appl. Environ. Microbiol. 73, 2905–2910.

Barbeau, J., et al., 1998. Cross-contamination potential of saliva ejectors in dentistry. J. Hosp. Infection. 40, 303-311.

Becker, K., et al. 2005. Environmental and biological applications of microplasmas. Plasma Phys. Control. Fus. 47, 513–523.

Bendouah, Z., et al., 2006. Biofilm formation by Staphylococcus aureus and Pseudomonas aeruginosa is associated with an unfavorable evolution after surgery for chronic sinusitis and nasal polyposis. Otolaryngology–Head and Neck Surgery. 134, 991-996.

Costerton, W., et al., 2003. The application of biofilm science to the study and control of chronic bacterial infections. J. Clin. Invest. 112, 1466-1477.

Elasri, M. O., et al., 1999. Study of the response of a biofilm bacterial community to UV radiation. Appl. Environ. Microbiol. 65, 2025-2031.

Khaled, G. H., et al., 2001. Method for studying development of colonization and infection of dialysis catheters. Adv. Perit. Dial. 17, 163-171.

Khardori, N., Yassien, M., 1995. Biofilms in device-related infections. J. industrial Microbiol. Biotechnol. 15, 141-147.

Kim, H., et al., 2007. Effectiveness of disinfectants in killing enterobacter sakazakii in suspension, dried on the surface of stainless steel, and in a biofilm. Appl. Environ. Microbiol. 73, 1256-1265.

Laroussi, M., Akan., T., 2007. Arc-free atmospheric pressure cold plasma jets: a review. Plasma Process. Polym. 4, 777-788.

Macleod, S.M., Stickler, D.J., 2007. Species interactions in mixed-community crystalline biofilms on urinary catheters. J. Med Microbiol. 56, 1549-1557.

Man, N. K., et al., 1998. Evidence of bacterial biofilm in tubing from hydraulic pathway of hemodialysis system. J. artificial organs. 22, 596-600.

Marion-Ferey, et al., 2003. Biofilm removal from silicone tubing: an assessment of the efficacy of dialysis machine decontamination procedures using an in vitro model. J. Hosp. Infection. 53, 64-71.

Moisan, M., et al., 2001. Low-tempererature sterilization using gas plasmas: a review of the experiments and an analysis of the inactivation mechanisms. International J. Pharmaceutics. 226, 1-21.

Pajkos, A., et al., 2004. Is biofilm accumulation on endoscope tubing a contributor to the failure of cleaning and decontamination? J. Hosp. Infection. 58, 224-229.

Pollak, J., et al., 2005. Process for the plasma sterilization of dielectric objects comprising a hollow part. Patent application US2005/0269199, (PCT) WO2004/050128.

Pollak, J., et al., 2007. Long and uniform plasma columns generated by linear field-applicators based on stripline technology. Plasma Sources Sci. Technol. 16, 310-323.

Pollak, J., et al., 2008a. Plasma sterilization within long and narrow-bore dielectric tubes contaminated with stacked bacterial spores. Plasma processes and polymers. 4, 14-25.

Pollak, J., et al., 2008b. Low-temperature low-damage sterilization based on UV radiation through plasma immersion. To appear in J. Phys. D: Appl. Phys. 41, 135212.

Rickard, A. H., et al., 2003. *Bacterial coaggregation: an integral process in the development of multi-species biofilms.* Trends in Microbiol. 11, 94-100.

Roth, V.R., Jarvis, W.R., 2000. Outbreaks of infection and/or pyrogenic reactions in dialysis patients. Seminars In Dialysis. 13, 92-96.

Sladek, R.E.J., et al., 2007. Treatment of Streptococcus mutans biofilms with a nonthermal atmospheric plasma. Letters in Applied Microbiol. 45, 318–323.

Sutherland, I.W., 2001. Biofilm exopolysaccharides: a strong and sticky framework. Microbiol. 147, 3-9.

Vleugels, M., et al., 2007. Atmospheric plasma inactivation of biofilm-forming bacteria for food safety control. IEEE Trans Plasma Sci. 33, 824–828.

2.6 Discussion et problématique de la stérilisation des endoscopes souples par plasma

En somme, nous avons mis au point et caractérisé une nouvelle source de plasma pour créer un plasma uniforme et de faible température du gaz à l'intérieur de tubes diélectriques. Avec un unique applicateur de champ électromagnétique, ce résultat a été obtenu dans des tubes diélectriques d'un diamètre interne compris entre 1.5 et 8 mm. Par la suite, nous avons successivement utilisé cette source de plasma pour stériliser l'intérieur de tubes de Téflon de 4 mm de diamètre interne contaminés par des spores bactériennes ou des biofilms. À ce stade, on pourrait être amené à penser qu'il ne reste que peu d'étapes à franchir avant de pouvoir stériliser des endoscopes souples. Cette perspective étant un sujet d'actualité focalisant un fort engouement industriel, nous avons jugé pertinent de discuter dans cette section les raisons pour lesquels, selon nous, les techniques de stérilisation par plasma, incluant celles présentées dans cette thèse, ne sont actuellement pas capables de stériliser ce type d'instruments.

2.6.1 Complexité des dispositifs à stériliser et présence de longs canaux de faible diamètre

Le désir d'observer les cavités situées à l'intérieur du corps humain n'est pas nouveau: les premières descriptions d'endoscopie ont été effectuées par Hippocrate (460-375 avant notre ère). Les origines de l'endoscopie et les étapes historiques qui ont marqué le développement de cette technique ont été rapportées par Shah [50]. De nos jours, cette méthode est très utilisée à visée diagnostique. De plus, l'endoscopie a grandement amélioré certaines techniques chirurgicales au cours des 50 dernières années [51, 52]. En effet, il est aujourd'hui possible d'effectuer de nombreuses interventions chirurgicales par endoscopie de manière performante et peu invasive, réduisant du même coup les séquelles et le temps d'hospitalisation des patients ou des animaux. Jusqu'à présent, les endoscopes ne sont toujours pas stérilisés, mais hautement désinfectés, du fait de leur complexité et de leur fragilité. Leur coût (5,000-20,000 $ US) ne permet pas un usage unique et des contaminations pathogènes par endoscopie sont donc enregistrées [53]. Celles-ci sont de trois types [54]:

- contamination croisée de patient à patient,

- micro-organismes diffusés pendant l'endoscopie d'une région à l'autre du corps du patient,
- contamination du patient infligée au personnel médical et vice-versa.

Ce constat a donc motivé la communauté scientifique à développer de nouveaux appareils et procédés permettant de stériliser les endoscopes souples. L'objectif de cette section est de montrer les obstacles rencontrés en stérilisation par plasma pour traiter spécifiquement ces instruments médicaux. Préalablement, il est nécessaire de connaître la structure des endoscopes souples et les problèmes actuellement présents lors des procédures de désinfection: la première section dévoile les caractéristiques essentielles de ces appareils médicaux, tandis que la deuxième est consacrée à une revue des techniques traditionnelles de désinfection des endoscopes souples. La problématique de la stérilisation par plasma des endoscopes souples occupe la troisième section.

La conception d'une source de plasma adaptée à la stérilisation d'un endoscope souple requiert nécessairement la connaissance de la structure et du fonctionnement de cet appareil. Il faut donc déterminer:

- le diamètre, la longueur et la configuration des longs tubes diélectriques de faibles diamètres qu'il faut stériliser,
- les emplacements des parties conductrices (métalliques). Dans le cas où l'endoscope serait stérilisé directement en décharge, ces parties conductrices pourraient affecterl'uniformité du traitement, car elles perturberaient la configuration des lignes de champ électrique entretenant la décharge,
- les emplacements des parties électroniques (e.g. caméra CCD) qui pourraient être endommagées par la présence d'un champ électrique servant à créer le plasma,
- la nature des parties diélectriques (polymères Téflon et polyuréthane) constituant majoritairement l'endoscope.

Dans un premier temps, nous allons décrire la configuration d'un endoscope. La figure 2.6 montre la structure d'un gastroscope servant à visualiser l'œsophage, l'estomac et le duodénum [55].

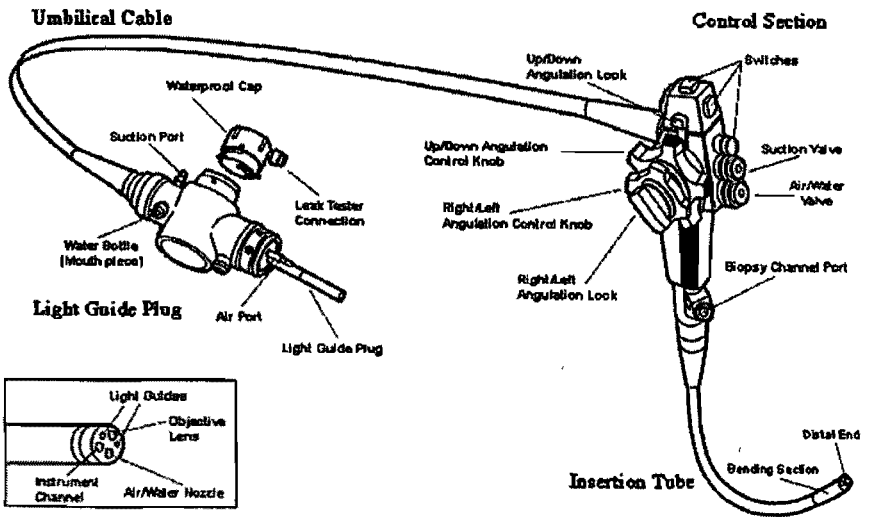

Figure 2.6 Structure d'un endoscope souple (gastroscope), d'après [55].

Tous les endoscopes souples sont composés de quatre parties [56]:

1. La connexion avec la source de lumière: portion de l'endoscope qui est liée à la source de lumière servant à éclairer l'intérieur du corps du patient.

2. Le cordon ombilical: tube qui relie la source de lumière à la section de contrôle.

3. La section de contrôle: partie manipulée par l'opérateur pour manœuvrer de haut en bas ou de gauche à droite la partie distale (c'est-à-dire la plus éloignée) du tube d'insertion. La section de contrôle permet également de commander les valves (air-eau et succion) de l'endoscope. L'entrée du canal de biopsie servant à l'insertion d'instruments (e.g. pour effectuer un prélèvement dans le corps du patient) est située à l'extrémité de la section de contrôle, du côté du tube d'insertion.

4. Le tube d'insertion: c'est la partie qui pénètre à l'intérieur du corps du patient et qui est la plus contaminée durant la procédure.

2.6.2 Revue des techniques traditionnelles de désinfection des endoscopes souples

La procédure de désinfection d'un endoscope est toujours effectuée après un lavage de ce dernier. Nous allons brièvement exposer quelques aspects essentiels de cette procédure qui est cruciale, car cette phase va de pair avec la procédure de désinfection: plus le lavage de l'endoscope est poussé, plus la désinfection sera efficace {American society for gastrointestinal endoscopie, 1998 #165}.

Lavage des endoscopes souples

La phase de lavage, utilisant des détergents enzymatiques, a pour but de retirer la majorité des matériaux organiques présents sur l'endoscope immédiatement après la fin de l'endoscopie [56]. Il est important de respecter un délai le plus court possible entre l'endoscopie et ce lavage. Dans le cas contraire, des micro-organismes pourraient adhérer et éventuellement croître sur les parois de l'endoscope (de là notre étude sur l'inactivation de biofilms présentée à la section 2.5), en particulier à l'intérieur des tubes creux étroits (< 4 mm de diamètre). Intéressés par cette question, nous avons laissé sécher une suspension de 10^6 spores bactériennes de *B. atrophaeus* dans 50 µl d'eau à l'intérieur d'une tubulure de Téflon (1 cm de longueur et 4/6 mm de diamètre interne/externe). Par la suite, nous avons coupé cette tubulure en deux suivant sa longueur et avons photographié (au microscope électronique à balayage) les spores séchées sur la partie inférieure de chaque tubulure où la configuration du dépôt présente de nombreux empilements (p. 76). Ceci démontre la nécessité d'un intervalle de temps très bref entre la fin de l'endoscopie et la phase de lavage, car de tels empilements sont très difficiles à stériliser, quelle que soit la méthode utilisée, alors que les micro-organismes auraient été facilement entraînés à l'extérieur par le lavage tandis qu'elles étaient encore en suspension humide.

Nous allons maintenant décrire brièvement les procédures de lavages des endoscopes souples. La figure 2.7 montre la procédure standard de lavage de l'extérieur du tube d'insertion [57].

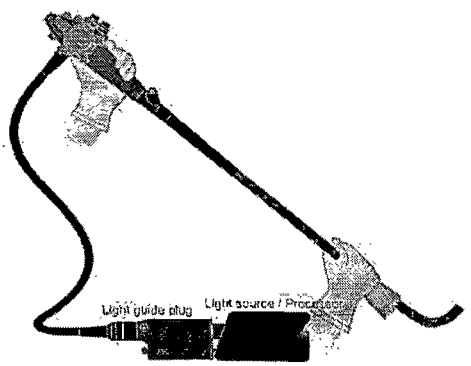

Figure 2.7 Illustration de la procédure standard de lavage de l'extérieur du tube d'insertion avec un linge stérile préalablement trempé dans une solution enzymatique [57]. Le linge est à usage unique.

Quant aux canaux air/eau (figure 2.8.a) et succion/biopsie (figure 2.8.b), ils sont lavés tout d'abord en les purgeant avec une solution enzymatique, puis avec des brosses (écouvillons) de diamètre adapté à celui de chaque canal [57]. Finalement, l'intérieur de chaque canal est rincé à l'eau, puis séché avec de l'air sous haute pression. Il a été montré très récemment que cette phase de séchage est cruciale [58] pour éliminer les résidus organiques et inorganiques.

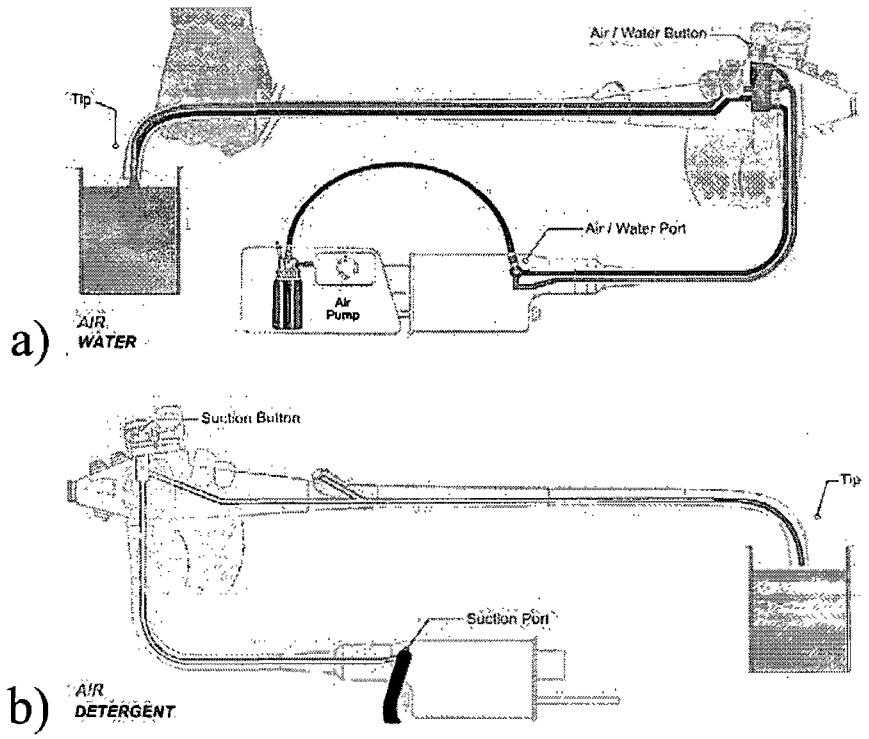

Figure 2.8 Illustration de la procédure standard de lavage successivement a) des canaux air-eau et b) des canaux succion/biopsie [57] en les purgeant avec une solution enzymatique.

Cette phase de lavage prévient donc le séchage de débris sur les surfaces des canaux, tout en permettant l'évacuation d'un grand nombre de micro-organismes. Durant cette phase, l'étanchéité de l'endoscope est également testée [57].

Techniques traditionnelles de désinfection des endoscopes souples

Du fait de leur complexité et de leur fragilité, nous le répétons, les endoscopes souples ne sont toujours pas stérilisés, mais désinfectés. Trois niveaux de désinfection sont définis: haut, intermédiaire et faible, en fonction du type et du nombre de microorganismes éliminés {American society for gastrointestinal endoscopie, 1998 #165}. Les techniques traditionnelles de désinfection des endoscopes souples impliquent un agent chimique ayant des propriétés bactéricides. Nous allons maintenant présenter une brève revue des désinfectants utilisés pour traiter les endoscopes souples (tirée essentiellement de [56]).

Le glutaraldéhyde : un bain de 20 minutes dans une solution contenant 2% de ce produit permet d'obtenir un haut niveau de désinfection. Ce produit est non corrosif pour les métaux, les plastiques et les caoutchoucs, mais est dangereux pour les humains et les animaux. Il peut notamment causer une irritation des yeux, de la gorge et des poumons.

Le peroxyde d'hydrogène : un bain de 30 minutes dans une solution contenant 7.5% de ce produit permet un haut niveau de désinfection. Ce produit est corrosif et peut endommager les plastiques.

L'acide peracétique : un système automatisé de 30 minutes (commercialisé par la marque Steris®) et contenant ce produit permet un haut niveau de désinfection. En fait, le temps d'exposition de l'endoscope à ce désinfectant est de 12 minutes. Ce produit est irritant pour les yeux, la peau et les voies respiratoires.

D'autres désinfectants sont également utilisés pour traiter les endoscopes souples: l'ortho-phthalaldéhyde et le mélange acide peracétique/peroxyde d'hydrogène [56]. Quel que soit le désinfectant utilisé, l'endoscope est plongé entièrement dans un bassin de désinfection, et le désinfectant est introduit à l'intérieur des conduits creux au moyen d'une seringue dans un procédé manuel ou de pieuvres dans un procédé automatique.

2.6.3 Principaux facteurs à considérer pour la stérilisation des endoscopes souples par plasma

La stérilisation par plasma est une alternative possible aux méthodes de stérilisation conventionnelles, car elle offre de nombreux avantages. Ce type de stérilisation est efficace, non toxique et dégrade peu les objets à stériliser. Toutefois, la complexité des endoscopes souples soulève de nombreuses interrogations techniques. Il existe deux types de surfaces à stériliser:

- surfaces externes: il s'agit essentiellement de la portion de l'endoscope qui pénètre à l'intérieur du corps du patient (tube d'insertion, figure 2.6).
- surfaces internes: il s'agit des canaux air/eau et succion/biopsie, c'est-à-dire de longs tubes diélectriques de quelques millimètres de diamètre sur une distance supérieure à un mètre de longueur.

La surface externe de l'endoscope pourrait être stérilisée en moins d'une heure par un système de post-décharge d'ondes de surface. En revanche, stériliser l'intérieur des longs tubes creux, quel que soit le système utilisé (décharge ou post-décharge), demeure une tâche particulièrement ardue. Nous allons en énumérer les raisons:

Systèmes de post-décharge : bien qu'efficaces sur des objets de forme simple, ces procédés sont mal adaptés à la stérilisation de la surface interne de tubes de petit diamètre (< 10 mm) [59]. En effet, il est nécessaire en post-décharge d'utiliser les espèces actives (émetteurs d'UV, radicaux) créées en décharge, espèces qui ont une durée de vie limitée (< 500 ms). Les tubes de petit diamètre possédant une faible conductance hydrodynamique, conne nous l'avons dit plus haut, il est, en effet, impossible d'y faire circuler un gaz à grande vitesse sans engendrer une importante élévation de pression, ce qui conduit à la destruction de ces espèces actives avant qu'elles aient pu jouer leur rôle sur toute la longueur du tube.

Systèmes de décharge : la température du gaz à l'intérieur du plasma est généralement trop élevée par rapport à la température que peuvent supporter les polymères thermosensibles de l'endoscope[1]. De plus, la présence des pièces conductrices de l'endoscope dans le champ de

[1] Il s'agit du Téflon et du polyuréthane.

rayonnement d'un applicateur HF entretenant le plasma à l'intérieur des tubes creux, soulève deux problèmes à considérer. Ces pièces conductrices pourraient:

- affecter la propagation du champ EM ce qui provoquera
    - une diminution de l'uniformité du plasma et donc du traitement,
    - une modification de l'impédance du système, ce qui se manifestera par un retour de puissance vers le générateur, ce qui rend quasiment impossible l'utilisation de notre source de plasma pour traiter ces dispositifs[2]
    - une réduction de l'intensité des lignes de champ électrique à l'intérieur des tubes creux, ce qui pourra éventuellement empêcher la création du plasma dans les tubes, si les pièces conductrices font ombrage au tube diélectrique;
- chauffer, ce qui pourra altérer les constituants thermosensibles de l'endoscope qui sont en contact avec elles.

Étant donné ces obstacles (à la fois en décharge et en post-décharge), aucune publication ne mentionne, à notre connaissance, la moindre tentative de simple désinfection par plasma d'un endoscope souple. En fait, nos recherches actuelles portent sur la stérilisation de l'intérieur d'un long tube diélectrique de faible diamètre, sans nous préoccuper, pour l'instant, des dispositifs auxiliaires contenant certaines parties conductrices et/ou électroniques. Bien qu'il s'agisse d'une réduction de la complexité de la problématique, la réalisation de cet objectif constitue un pas crucial dans l'avancement des technologies de stérilisation par plasma et ouvre le marché du retraitement des cathéters.

2.7 Résumé et conclusion

Nous avons inventé [60], caractérisé [61] et évalué les performances d'un stérilisateur plasma sur des tubes diélectriques contenant des empilements particulièrement conséquents de spores bactériennes de *B. atrophaeus* [62] ou des biofilms de *Staphylococcus aureus* [63], ceux-ci de

[2] En pratique, nous avons inséré le tube d'insertion d'un endoscope (gastroscope de marque Olympus) à l'intérieur de notre applicateur de champ électromagnétique. Puis, nous avons testé la réponse en transmission d'ondes HF le long de l'applicateur à l'aide d'un analyseur de réseaux. Nous avons alors obtenu une détérioration majeure de la propagation des ondes HF due à la présence de l'endoscope (20 dB soit 1 % de puissance transmise) comparée à plus de 90 % de puissance transmise en présence d'un tube purement diélectrique. Ceci résulte de la modification de l'impédance du système en présence des pièces conductrices.

croissance contrôlée par une technique que nous avons mise au point. Notre méthode de stérilisation présente de nombreux avantages incluant son efficacité, sa non-toxicité (pas de phase de ventilation nécessaire) et sa capacité à s'adapter et à obtenir l'uniformité axiale du plasma dans des tubes de différents diamètres internes (de 2 à 8 mm testés). Toutefois, de nombreux points nécessitent de plus amples études afin d'évaluer les capacités de ce système à traiter des tubes médicaux. Par exemple, l'ensemble du travail présenté dans ce chapitre a concerné des tubes formés de Téflon possédant une paroi d'un mm d'épaisseur. Or la plupart des cathéters cardiaques possèdent une paroi de tube beaucoup plus mince, en général de l'ordre de 0.3 mm et sont parfois formés d'autres polymères moins résistants que le Téflon (e.g. le silicone). De plus, notre traitement a montré son efficacité sur seulement 70 cm de longueur (et sur 4 mm de diamètre interne), une longueur inférieure à celle de nombreux cathéters. Il faudra donc désormais évaluer l'efficacité de notre procédé et les dommages induits sur des tubes médicaux possédant les matériaux, les épaisseurs et les longueurs réelles.

Chapitre 3

Stérilisation d'objets par leur immersion dans le plasma

Comme nous l'avons vu au deuxième chapitre, un applicateur de champ électromagnétique de type linéaire offre de nombreux avantages pour réaliser la stérilisation d'objets médicaux, notamment une faible température du gaz de sa décharge (< 50 °C) et l'uniformité axiale de celle-ci. Cependant, la source que nous avons développée et décrite au chapitre précédent présente une forte limitation pratique quant aux types de surfaces qu'elle peut traiter, s'agissant exclusivement de la paroi interne de tubes diélectriques. À la vue des résultats probants que cette source de plasma permettait d'obtenir, nous avons alors pensé à exploiter le même concept d'applicateur linéaire, mais cette fois-ci en utilisant une enceinte parallélépipédique dans laquelle se forme la décharge. La finalité de ce stérilisateur est d'y réaliser la stérilisation de la surface externe d'objets médicaux par immersion de ces derniers dans le plasma. Dans ce troisième chapitre, nous allons présenter le concept de cette source de plasma, ses performances électrodynamiques et la détermination de ses agents biocides. Ce chapitre comporte également, comme le précédent, une section de discussion où nous examinons plus particulièrement une défaillance structurale, que nous avons mise en évidence peut-être pour la première fois, et qui est liée à l'inactivation des spores bactériennes par plasma. Finalement, une brève conclusion clôt ce chapitre.

3.1 Introduction

Les procédés de post-décharge, malgré leurs nombreux avantages, présentent néanmoins quelques limitations qui font obstacle à une réduction importante du temps de stérilisation. Considérons le cas où la source de plasma alimentant la post-décharge est entretenue par une onde électromagnétique (EM) de surface excitée par un lanceur d'ondes de surface, tel le Surfatron [3]. Le plasma est créé dans un volume de gaz très réduit (moins de 1 cm^3 à 2450 MHz) et, parce qu'il résulte d'une forte puissance EM injectée par unité de volume, le plasma ainsi formé est relativement chaud. Pour les besoins de la stérilisation en post-décharge, ce plasma, produit localement, est transporté par un flux de gaz dans une région distante et voit alors

certaines de ses propriétés initiales se modifier (recombinaison des particules chargées, excitation/désexcitation, etc.) tout au long de cette région transitoire. Il aboutit ensuite dans la chambre dite de post-décharge, d'un volume considérablement plus élevé, disons 50 L, que celui du plasma initial: il est maintenant plus froid, avec peu de particules chargées et pratiquement sans champ électrique, un ensemble d'avantages assurant de préserver l'intégrité des objets à stériliser, mais les espèces de la décharge s'en trouvent diluées dans le rapport des volumes décharge/post-décharge. En somme, une telle source de plasma présente les inconvénients suivants en stérilisation:

1) Une énergie importante est perdue dans la région de la décharge et dans la zone de transition pour alimenter les processus cinétiques de production d'espèces qui ne seront pas utilisées pour la stérilisation ; par ailleurs, les espèces actives se trouvant dans l'enceinte de post-décharge subissent une forte dilution en volume par rapport au volume de leur création dans la décharge (p. ex. N et O engendrant NO excité).
2) Le plasma d'onde de surface ne permet pas une exposition aisée d'objets tridimensionnels dans la décharge même, du fait de sa géométrie cylindrique et de son volume limité.

Tirant profit de l'expérience de notre Groupe et de celle acquise au cours du développement du stérilisateur décrit au deuxième chapitre, nous avons conçu, mis au point et caractérisé une source de plasma basé sur un applicateur de champ électromagnétique (EM) s'étendant le long d'une enceinte de stérilisation parallélépipédique et entièrement solidaire de celle-ci. La prochaine section décrit les caractéristiques électrodynamiques de ce stérilisateur par immersion ainsi que l'identification de ses agents biocides.

3.2 Caractéristiques électrodynamiques du stérilisateur par immersion et détermination de ses agents biocides

Comme nous allons le voir dans l'article contenu dans cette section, ce nouveau dispositif permet notamment:

- de distribuer la puissance EM sans point chaud le long de l'enceinte de stérilisation (une faible quantité du flux de puissance est prélevée par unité de longueur).

- de créer, du fait même d'un faible transfert de puissance HF par unité de longueur à la décharge, un plasma de faible température de gaz, ce qui permet de traiter des objets de nature thermosensible placés à l'intérieur même du plasma.

Avec ce dispositif d'immersion des objets à traiter dans le plasma, les espèces actives sont utilisées directement (localement) sans avoir besoin de les transporter, contrairement au procédé de post-décharge. Le rendement énergétique du système est donc meilleur, car l'énergie incidente est utilisée principalement à des fins bactéricides et non pour chauffer le gaz. Dans l'article qui suit, nous allons à la fois présenter ses caractéristiques électrodynamiques (e.g. pourcentage de puissance réfléchie), déterminer ses agents biocides lorsque l'argon est le gaz plasmagène et évaluer les dommages causés par ce plasma à certains polymères. Le lecteur intéressé par le concept de cette source de plasma pourra trouver des informations supplémentaires dans la demande de brevet reproduite à l'annexe 3.

Low-temperature low-damage sterilization based on UV radiation through plasma immersion

(article publié dans Journal of physics D: Applied physics 2008 **41** 135212, 14 pp)

J. Pollak, M Moisan, D Kéroack and M K Boudam

Abstract

This paper introduces a new type of high-frequency (HF) sustained discharge where the HF field applicator is a planar transmission line that allows us to fill with plasma a long chamber of rectangular cross-section (typically 1m × 15 cm × 5 cm). Peculiar interesting features of this plasma source are a low gas temperature (typically below 40 °C in the 1 Torr range in argon), broadband impedance matching with no need for retuning, stability and reproducibility of the discharge (non-resonant behaviour). This type of plasma source could be useful for web processing; nonetheless, it is applied here to plasma sterilization, taking advantage of its low gas temperature to inactivate microorganisms on polymer-made medical devices to avoid damaging them. The predominant biocide species are the UV photons emitted by the discharge whereas most plasma sterilization techniques call for reactive species such as O atoms and OH molecules, which induce significant erosion damage on polymers. Polystyrene microspheres are actually observed to be erosion-free under the current plasma sterilization conditions (scanning electron micrographs have been examined). Moreover, inactivation is quite fast: 10^6 *B. atrophaeus* spores deposited on a Petri dish are inactivated in less than 1 min. Correlation of the UV radiation with the spore inactivation rate is examined by (i) considering the emitted light intensity integrated over the 112–180 nm vacuum UV (VUV) range with a photomultiplier; (ii) looking with an optical spectrometer at the emission spectrum over the 200–400 nm UV range; (iii) using absorption spectroscopy to determine the role of the VUV argon resonant lines (105 and 107 nm) on spore inactivation. It is found that the test-reference spores are mainly inactivated by VUV photons (112–180 nm) that are primarily emitted by impurities present in the argon plasma.

3.2.1 Introduction

Plasma sterilization is emerging as a novel alternative to conventional sterilization techniques, which are essentially based on thermal treatments (dry or moist heat) or chemical treatments (e.g. EtO, H_2O_2). Plasma sterilization offers promising features in terms of efficiency and reliability for inactivating microorganisms. In addition, this technique can be made to operate at low temperatures (<50 °C), does not require venting time and is safe for the operators, patients and materials. The understanding of plasma sterilization is advancing rapidly, raising high scientific and commercial interests in the development of various types of plasma sterilizers. Nevertheless, no sterilizer making use of the plasma biocide species has yet been brought to the market place. Various reasons can be put forward to explain such a delay:

(i)The level of damage induced on the various types of surfaces exposed to a plasma treatment is an essential issue that has not yet been thoroughly assessed. In particular, as many medical devices (MDs) comprise polymers, the etching of polymers by such a process must be very small, allowing for many re-sterilization cycles. In our opinion, this is a paradoxical mission for those choosing to inactivate microorganisms through etching of their membranes rather than relying on lethal lesions to their DNA by UV photons, as we do. Moreover, variations in the hydrophobicity and biocompatibility of the processed surfaces (intended for limited or extended time of contact with tissues or body fluids) must be scrutinized.

(ii) Plasma sterilization of MDs must meet the requirements of hospital standards. In that respect, it is customary to sterilize MDs already enclosed in wrapping materials that protect them afterwards from external contamination during transportation and through storage conditions. However, the various wrapping materials presently used for that purpose are not a priori compatible with a plasma-afterglow sterilization process. This is because they strongly absorb UV radiation and also reduce the diffusion towards the MDs of the various plasma particles, namely, atoms (e.g. oxygen radicals) and molecules (already present or newly formed), species that are eventually excited (becoming potential UV photon emitters) or ionized. Nonetheless, it is possible, under certain conditions, to achieve a plasma, as we do, within the packaging material containing the MD when this material is of the dielectric type. For a plasma-afterglow process, post-wrapping (within the sterilizer) could be envisaged.

(iii) Although the MDs to be sterilized are beforehand washed and disinfected, there is still some possibility that the remaining microbial load be too thick (more than tens of

micrometres) to be successfully inactivated by the plasma species (UV photons in our case): this is eventually the case, for example, with stacked bacteria, thick biofilms (bacteria embedded in an exopolysaccharide matrix, strongly adhering to the MD surface) and soil (e.g. blood products). Such eventualities need to be thoroughly investigated and adequate solutions found.

(iv) All parts of a MD should be exposed to the same density or flux of the plasma species, which requires uniformity of the plasma biocide species everywhere in the sterilizer. As an example, consider the case of a plasma sterilizer filled with a large number of MDs: shadowing effects caused by an MD on a nearby other MD are possible, as well as local depletion of the active species (loading effect resulting, for instance, from surface recombination of the plasma species).

(v) An ideal sterilizer should be able to deal with a wide range of MDs. However, as it is the case with conventional sterilizers, the nature and configuration of the processed MD have a strong impact on the efficiency of plasma sterilization. For instance, MDs comprising tubes with a small inner diameter (typically 2–6 mm) and a comparatively long length (0.5–2 m) are harder to sterilize than planar surfaces, because of a reduced access of the biocide species to all parts of the MDs, unless these are provided by achieving a discharge within the tube itself.

It therefore appears that a given plasma sterilizer cannot process all types of MDs: we actually do not believe in such a thing as a universal plasma sterilizer (there is no such thing as a conventional sterilizer). As a result, our strategy is to try to come up with plasma sterilizers for specific applications. For instance, in order to design a plasma sterilizer dealing with the inner part of polymeric (dielectric) catheters, we worked out a new kind of HF field applicator that allows the plasma to be sustained within such tubes [1]. The electrodynamical properties of this field applicator were analysed in detail [2] and the corresponding system subsequently employed to sterilize the inner part of long narrow-bore dielectric tubes that mimic catheters was reported in [3].

We recently filed a patent application for a planar plasma source that can be used for the sterilization of thermosensitive tri-dimensional objects and also for web processing of dielectric or conducting plates or films [4]. The purpose of this paper is to describe this plasma source and provide some sterilization results concerning surfaces of planar geometry. The plasma biocide species encountered when working with argon as the carrier gas at reduced pressure (typically 1 Torr) are also identified.

The plasma source described in this paper allows sustaining large planar-area non-magnetized microwave plasmas. There are already well-known ways of achieving such types of plasma. For instance, Ghanashev *et al* [5] proposed a plasma source in which the discharge is sustained by a standing electromagnetic (EM) surface-wave propagating along the interface between the plasma and a dielectric plate located on the top wall of a large-diameter cylindrical metal chamber. An alternative to surface-wave discharge for obtaining long and uniform planar discharges is to use field applicators that extend along a straight line and accompanying the discharge tube over distances much larger than the free-space wavelength (these elongated structures are termed linear field applicators) [6]. The scientific literature reports various kinds of such structures that are used as transmission-line field applicators for plasma generation, namely, a circular or rectangular waveguide [7], a slow-wave structure [8, 9], and a troughguide [10]. Surprisingly, field applicators using transverse electromagnetic (TEM) or quasi-TEM transmission lines have not been considered so far for web processing of large planar surfaces. The field applicator described in this paper and used for sterilization purposes is a linear quasi-TEM field applicator.

The paper is organized as follows. Section 3.2.2 presents the concept and the electrodynamic characteristics of this new plasma source and examines its axial uniformity when working with argon as the carrier gas at reduced pressure (typically 1 Torr). The determination of the biocide species provided by the argon plasma and the analysis of survival curves obtained with bacterial spores deposited on Petri dishes make up section 3.2.3. Section 3.2.4 is devoted to determining the level of damage induced by the argon plasma to various polymers. Finally, section 3.2.5 is a brief conclusion.

3.2.2 Description of the plasma source

Our novel plasma source belongs to the category of high-frequency (HF)[1] sustained discharges where the HF field applicator is a planar transmission line. Two main types of such planar transmission lines can be found in the literature: the microstrip line and the stripline. These are briefly described in the following section. An exhaustive review and a possible classification of such existing field applicators [11–17] were recently published by Pollak *et al* [2].

---

[1] The term HF designates here jointly radio and microwave frequencies.

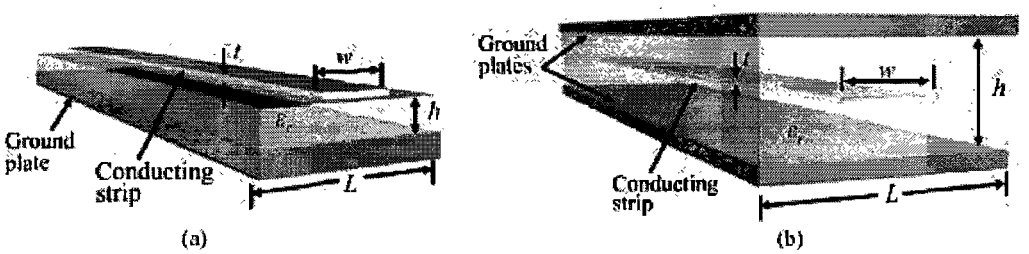

Figure 1 Configuration and characteristic dimensions of the two main types of planar transmission lines used as linear field applicators to sustain plasma: (a) the microstrip line (unsymmetrical line); (b) the stripline (symmetrical line).

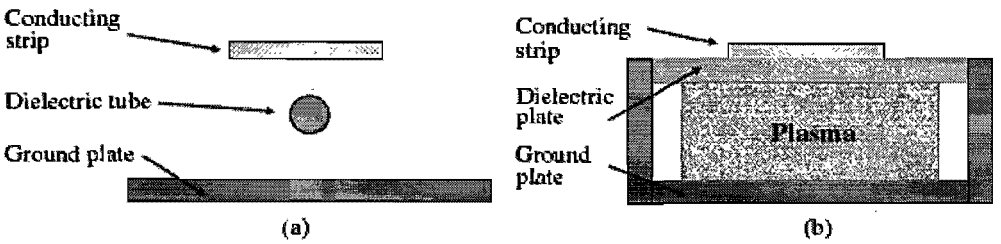

Figure 2 Cross-sectional view of two plasma sources developed in our laboratories using planar transmission lines: (a) tubular discharge [1–3]; (b) planar discharge [4], which is used in this paper.

3.2.2.1 The microstrip line and the stripline

Figure 1(a) shows the configuration and the characteristic dimensions of a microstrip line. A conducting strip of width w and thickness t is located at a constant distance h above a conducting ground plate of width L. A homogeneous dielectric medium (air in our case) of thickness h and relative permittivity ε_r fills the entire region comprised between the ground plate and the conducting strip. Note that a microstrip line is not necessarily a microstructure as implied by its name; it is sometimes also called an 'unsymmetrical line' or a 'singleground-plane line' [18]. Figure 1(b) shows the configuration and characteristic dimensions of a stripline. A conducting strip of width w and thickness t is centred between two parallel conducting ground plates of width L and separated by a distance h. A homogeneous dielectric medium of relative permittivity ε_r fills the entire region comprised between the parallel ground plates and the conducting strip. Striplines are also called 'sandwich lines', 'triplate lines', 'symmetrical lines' or 'double-ground-plane lines' [18].

Using planar transmission line to design HF-sustained plasma sources provides some useful peculiar features: these transmission lines can be operated over a broad range of HF frequencies without the need for impedance retuning and, as shown by Broekaert [13], can be made compact for miniaturization purposes. Due to their intrinsic properties, microwave-field applicators using planar transmission lines can also be arranged in arrays (eventually fed from a unique HF source [19]) to provide large plasma volumes. We have been working initially on the stripline field applicator as a plasma source [1, 2] but we recently turned to the microstrip technology, looking at two different plasma vessel configurations for our plasma sterilization studies. Figure 2(a) shows schematically how to accommodate a tubular discharge in a microstrip configuration: the dielectric tube is positioned centrally between the strip conductor and the ground plate of the planar transmission line in an air–dielectric environment. This configuration has been utilized in its stripline counterpart for sterilizing the inner wall of long narrow-bore thermosensitive tubes [3]. In this paper, we rather focus on filling with plasma a chamber of rectangular crosssection: three of the chamber walls act as ground plates while the fourth one is closed by a dielectric plate on which the conducting strip is resting (figure 2(b)).

3.2.2.2 The design of the microstrip-type planar discharge

Figure 3 shows photographs of an actual prototype of the plasma source schematized in figure 2(b). The role of the dielectric plate is twofold: to provide vacuum isolation of the plasma chamber and to let pass microwaves into it with little attenuation[2]. Plasma is sustained by the electric field of the propagating EM wave guided by the planar transmission line. A Faraday cage fully encloses the plasma source because the microstrip line is not radiation-free at microwave frequencies, in contrast to the stripline [2]. HF power is supplied to the discharge through a coaxial cable (with an N-type connector). A matched load, located past the applicator on the chamber side opposite to the HF power input, dissipates the residual power

---

[2] In our first versions of the planar discharge arrangement, the conducting strip (which is the electrically 'hot' conductor) was fully immersed in the discharge itself. This configuration has been abandoned because it was producing strong plasma non-uniformities and hot spots at the two extremities of the conducting strip (where the N-connectors are attached to the strip). Besides, when the conducting strip is located above the dielectric plate as in figure 2(b), it can mechanically hold the conducting strip and avoid its bending along the length of the applicator.

not absorbed in the discharge. A movable light collimator, 30 mm long and 1 mm inner diameter, is directed perpendicularly to the chamber in front of a fused silica window with its tip located 50 mm away from it and connected to an optical fibre. It provides spatial resolution within the chamber for emitted light intensity measurements.

The characteristic dimensions of this plasma source are labelled in figure 4 and provided in its caption. Figure 4 corresponds to a sketched cross-sectional view of the system shown in figure 3. The gas flow inlet is located on the HF power side, the pumping orifice being on the opposite side. Since $h_1 < h_3$ (figure 4), the electric field lines are mainly confined between the bottom ground plate of the conducting frame and the conducting strip. Because of this and because there is air at atmospheric pressure above the dielectric plate, there is no discharge there. An important feature of this system is that its input-power reflection coefficient is very little affected by the presence of plasma, as shown in the next section. Operating conditions were generally as follows: applied field frequency 200 MHz, argon gas at reduced pressure (10–1500 mTorr) with flow rates in the 5–100 sccm (standard cubic centimetre/min) range.

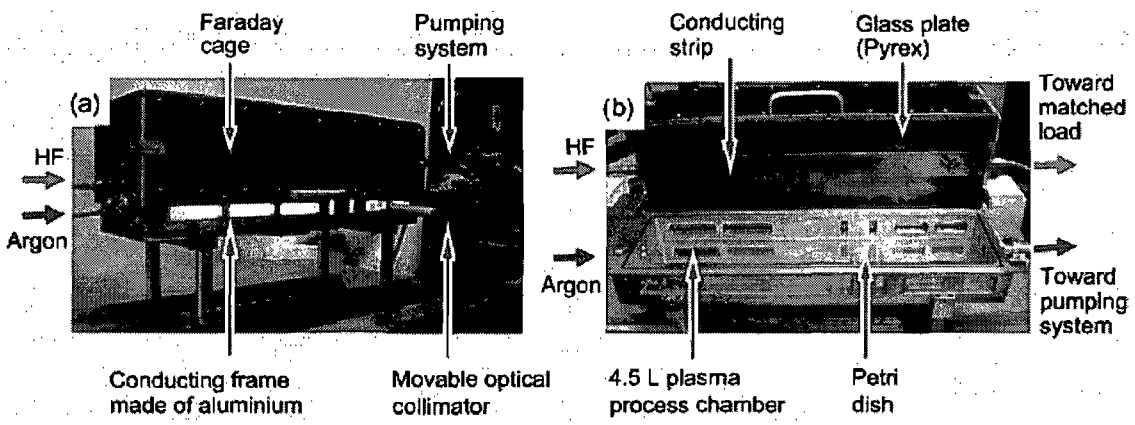

Figure 3 Photographs of the 57 cm long microstrip-type linear field applicator used in this paper to generate plasma in a 4.5 L sterilization chamber: (a) the sterilizer in operation with an argon discharge; (b) the plasma chamber when open for insertion or removal of MDs and Petri dishes.

3.2.2.3. HF power characteristics of the planar plasma source

The power absorbed by the discharge P_A as a function of the incident power P_I when assuming a lossless field applicator is simply given here by [2]

$$P_A = P_I - P_R - P_T. \quad (1)$$

where P_T is the power exiting from the applicator and going into the transmission-line terminating matched load. Power measurements were achieved with the argon gas flow set at 100 sccm at a pressure of 750 mTorr (100 Pa) and with a field frequency of 200 MHz. Figure 5(a) displays the corresponding reflected and transmitted powers as functions of the incident power. The percentage of reflected power at the applicator input remains close to zero over the whole range of incident HF power tested (0–210 W). As the HF power is raised from 0 to 20 W, the plasma length increases as shown in figure 5(b); at 20 W, the full applicator length (57 cm) is filled with plasma; at higher incident HF powers, part of the incoming power flows along the field applicator without being absorbed by the discharge and is, in fact, lost in the terminating matched load that prevents reflection at the applicator end. Because of this, above 20 W, there is a continuous decrease in the percentage of power absorbed by the plasma, as shown in figure 5(a). Since absorbed power in the discharge remains low (with 50 W of incident power, the density of absorbed power by the plasma is below 10 WL^{-1}), gas heating is also low: in fact, the chamber wall and Petri dishes remain, after a few minutes of plasma exposure, at temperatures typically below 40 °C as measured with a thermocouple.

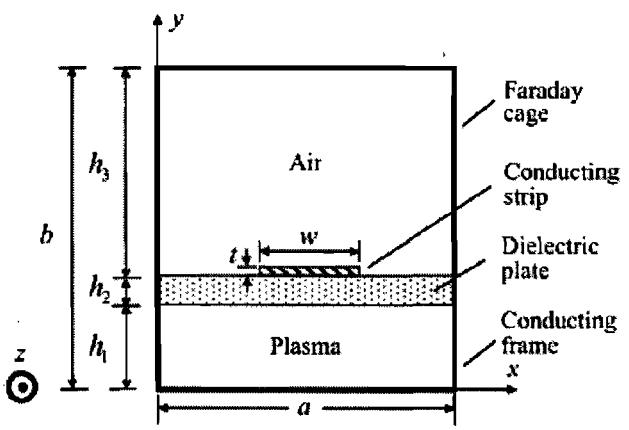

Figure 4 Schematic representation in a cross-sectional view of the sterilization system shown in figure 3. The discharge is confined within the lower part of the system, there being no discharge in the upper part of it filled with air at atmospheric pressure. The field applicator characteristic dimensions are: w = 50.8 mm, t = 3.2 mm, a = 146.1 mm, b = 200.5 mm, h_1 = 50.8 mm, h_2 = 12.7 mm and h_3 = 137.0 mm.

3.2.2.4. Axial distribution of emitted light intensity along the plasma chamber

The light intensity emitted by the discharge as a function of axial position, z, along it was recorded with a photodiode over the 330–800 nm range. The light collimator was set at mid-height of the plasma chamber, i.e. at $y = h_1/2 = 25.4$ mm (see figure 4). The plasma chamber extent ($z = 0$ and $z = 62$ cm) is delimited in the following figures by arrows. Figure 6 shows typical axial distributions of emitted light intensity as observed along the lateral fused silica windows (see figure 3) of the plasma source. In figure 6(a), the applied field frequency is set at 200MHz and the incident power is raised to increase the power absorbed by the plasma and, consequently, its emitted light intensity. Whatever the value of P_A, there is a decrease in the emitted light intensity when going from the power input side to the matched load side. We also observe that the applied field frequency has a significant impact over the density of absorbed power by the plasma, since 74 W at 433 MHz are required to fill the full length of the chamber with plasma in contrast to 17 W at 200 MHz. The overall decrease in the emitted light intensity is more pronounced at 433MHz than at 200 MHz. This is because the wave power absorbed by the discharge per unit length, dP_A/dz, is higher at 433 MHz since there is a higher electron density in the discharge [20]. At any rate, in both cases, the electron density (assumed to a first approximation proportional to light intensity) tends to decrease with increasing z, as can be seen in figure 6(b), since the HF power flow is expended in sustaining the discharge as the wave propagates.

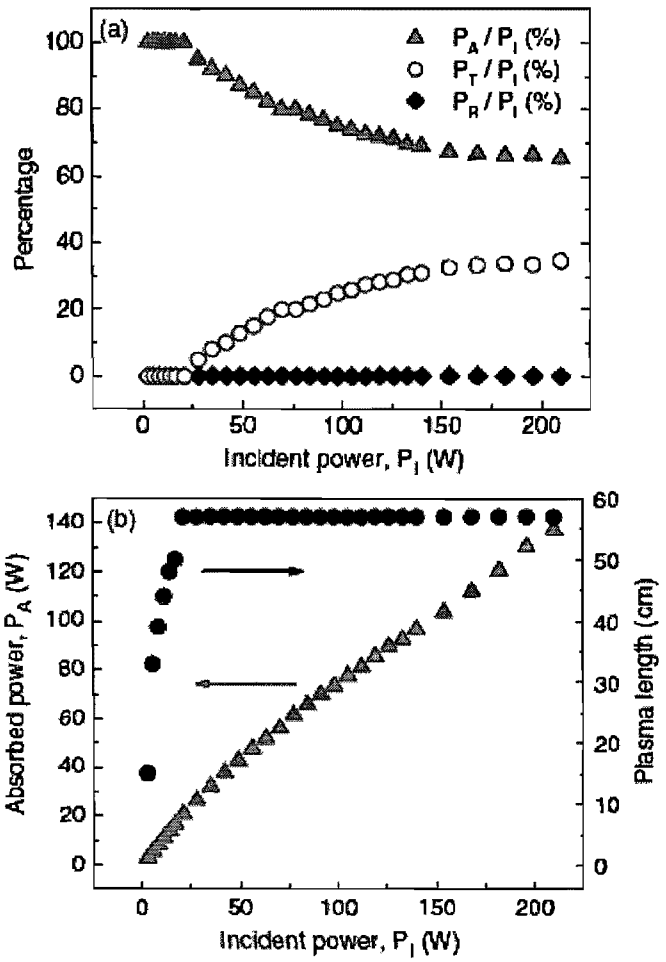

Figure 5 (*a*) Percentage of reflected power, P_R, transmitted power, P_T, and absorbed power, P_A, normalized to incident power, P_I, as functions of P_I , at 200 MHz. Argon gas flow is set at 100 sccm and gas pressure is 100mTorr; (*b*) Power absorbed by the plasma and length of the discharge in the chamber as functions of incident power.

Plasma axial non-uniformity was barely noticeable when using the present linear field applicators to generate plasma within narrow-bore tubes [2, 3]: the plasma volume per unit length was then typically 100 times lower. In more general terms, the decrease in electron density along a linear field applicator is more pronounced the longer the applicator, the larger its cross-sectional dimensions or the higher the field frequency. Axial non-uniformity of the plasma could have undesirable effects for some applications. As far as batch processing is concerned, for instance, a possible solution to compensate for the electron density decrease would be to switch the HF power feeding port with that of the matched load at half process time. A second solution would be to gradually reduce the cross-sectional dimensions of the applicator structure when going from the power input side to the matched load side, as already

proposed by Zakrzewski and Moisan [6] in the general case of a long linear field applicator and by Slinko et al [7] in the specific case of a plasma column lying longitudinally within a rectangular waveguide, the height of which is gradually decreased in the power flow direction. A third possibility is to remove the matched load and utilize its port to actually feed the field applicator from both sides relying on a second microwave generator to avoid phase relation between the propagating waves, which would lead to standing waves along the structure. As far as web processing is concerned, a fourth solution is to position parallel to each other two similar linear field applicator (eventually fed by the same HF generator through a 3 dB divider), but with the HF power feeding side of the first applicator being that of the matched load on the second applicator.

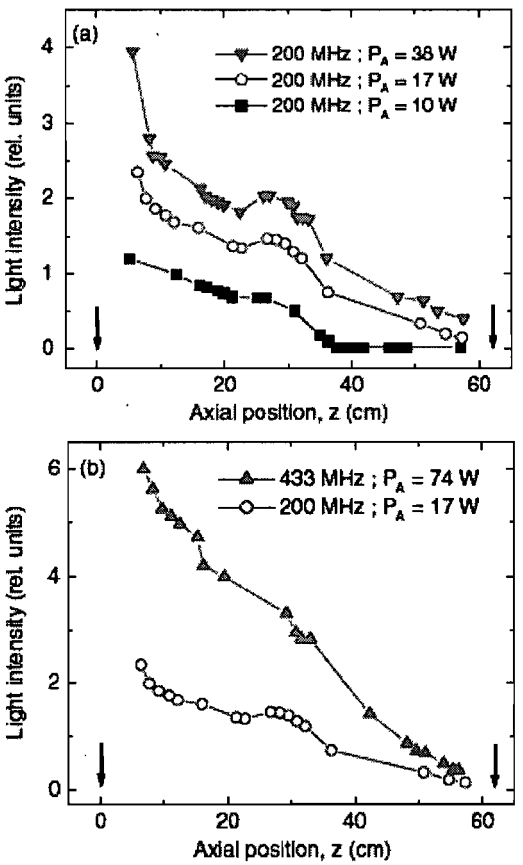

Figure 6 Recorded axial distribution of emitted light intensity along the lateral fused silica windows of the plasma source shown in figure 3. The argon pressure is fixed at 750 mTorr (100 Pa), with a gas flow at 100 sccm. The axial distribution of emitted light intensity is recorded at: (a) a field frequency of 200 MHz and for three values of absorbed power in plasma; (b) field frequencies of 200 MHz and 433 MHz at the absorbed power required to fill the full chamber length with plasma. The plasma chamber extent (z = 0 and z = 62 cm) is delimited in the figures by arrows.

The measurements of the emitted light intensity distribution within this plasma source are far from being completed. For instance, the emitted light intensity distribution needs to be mapped in the direction transverse to the applicator (x and y, see figure 4). Improved uniformity can be achieved by adjusting the key design parameters of this plasma source, namely, the width w and depth h1 of the plasma chamber, for given operating conditions (e.g. field frequency, incident HF power, gas pressure). Such experiments are not within the scope of this paper. Although this field applicator can be employed in various applications [4] (e.g. web coating deposition onto dielectric plates), this paper is dedicated to its use for sterilization purposes, as elaborated in the next section.

3.2.3 Using the reduced-pressure argon planar discharge for microorganism inactivation through plasma immersion: determination of the biocide species nature and characteristics

The plasma source described in section 3.2.2 is used in what follows to inactivate microorganisms. We seek to identify the biocide species acting on them when they are immersed in the argon planar discharge operated at reduced pressure. We show that these are essentially UV photons and, more specifically, vacuum UV (VUV) photons. Various methods were used to come to such a conclusion, including: (i) evaluation of the spore inactivation rate as a function of the UV wavelength range; (ii) close examination of scanning electron microscope (SEM) micrographs for structural damage to the spores before and after plasma treatment; (iii) recording of the plasma optical emission intensity with photomultipliers covering solely the 112–180 nm range; (iv) optical emission spectroscopy (OES) in the 200–400 nm range; (v) optical absorption spectroscopy for determining the (relative) density population of the argon atoms emitting the 105 and 107 nm resonant lines.

The photomultiplier recordings and inactivation tests were carried out at approximately half-length of the field applicator (figure 7). This position is intermediate between the HF power input side and the pumping-system orifice. Spore deposition is achieved on a Petri dish. The suspension (Bacillus atrophaeus ATCC® 9372) is prepared in a classical way (see, e.g. [3]). A given number of spores from this suspension is diluted in 100µl of sterile water and then deposited at the centre of the Petri dish and allowed to dry out over 48 h, under sterile conditions and in the dark, at ambient temperature.

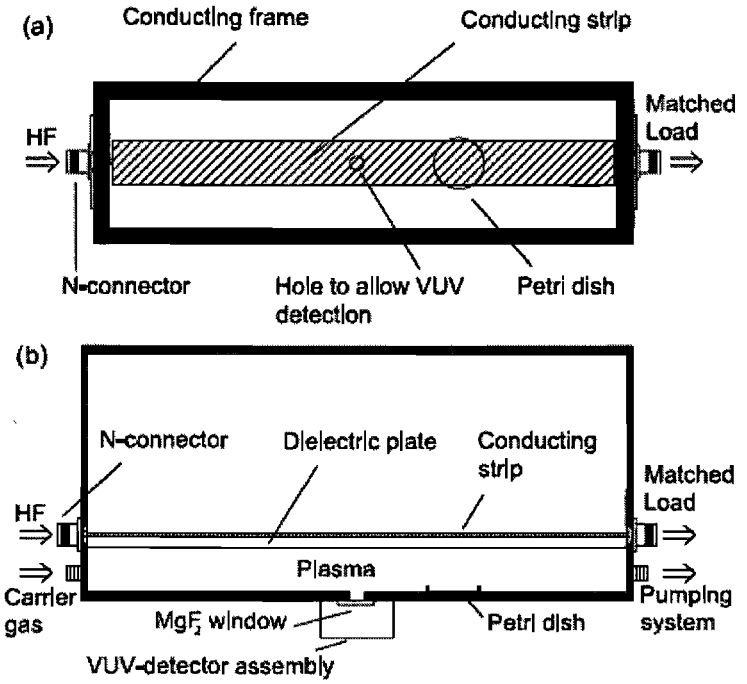

Figure 7. Schematic representation in top and side views of the plasma sterilizer with the locations of the Petri dish and VUV-detector assembly. The hole pierced in the bottom conducting plate to allow for VUV emission recording is off-scale with respect to the rest of the figure: it is only 1mm in diameter, which is large enough to obtain a high signal-to-noise (S/N) ratio (>100) for VUV measurements and, at the same time, low enough not to affect the propagation of the EM wave along the field applicator (hole diameter 1000 times smaller than the guided wavelength). The VUV detector is located in an adjacent box isolated from the discharge chamber by an MgF_2 window and pumped independently for residual air at pressures below 100mTorr.

3.2.3.1 VUV/UV photons: the sole biocide species under the present operating conditions

3.2.3.1.1 Spectral range of action of the VUV/UV photons

Inactivation of bacterial spores immersed in a reduced-pressure plasma can result from at least three different mechanisms and, eventually, a combination of them: these are: (i) UV/VUV irradiation, which alters their genetic material; (ii) etching of the spore membranes by reactive species; (iii) diffusion in the inner core of oxidative species and subsequent damage. To demonstrate that the VUV/UV photons are solely responsible for spore inactivation and, at the same time, to determine the respective contribution of the VUV and UV photons on the

inactivation rate, we have used optical filters (high-pass, in terms of wavelength, flat windows) that were successively placed atop the Petri dish, as shown in the inset in figure 8 [21–24]. Note that these plates prevent the charged and excited particles from reaching the microorganisms (no plasma is produced within the Petri dish), therefore reducing the spore exposure to potential biocide species: at any rate, such a phenomenon is independent of the wavelength of the filter plate! We used three different high-pass filters under cut-off for wavelengths up to 112 nm (MgF_2), 190 nm (fused silica) and 330 nm (Pyrex)[3]. Figure 8 shows the number of surviving spores after 180 s of exposure to plasma when placing successively these three high-pass optical filters over the Petri dish. In all these experiments, the initial number of viable spores is 10^6 (see the dashed line in figure 8). We note the following: (i) when it is the Pyrex filter that is inserted between the plasma and the spores, the full initial number of viable spores is recovered after plasma exposure. This result clearly indicates that photons from this argon plasma with wavelengths above 330 nm have no biocidal action[4]; (ii) the MgF_2 window, among the three filters tested, is the one providing the highest mortality; (iii) the SiO_2 window (>190 nm) obviously leads to a reduced mortality compared with the MgF_2 one. We therefore conclude that the wavelength domain between 112 and 190 nm is, under our specific operating conditions, the most biocide one, since approximately 4 log of inactivation are then observed, in contrast to roughly 1 log in the 190–330 nm range. Employing also *B. atrophaeus* spores, Munakata *et al* [26] have shown that there are two wavelength domains on which the inactivation rate is the highest over the range extending from 115 to 300 nm, namely, 125–170 nm and 220–270 nm. The higher inactivation rate recorded in the VUV range in our case suggests that the corresponding number of photons is larger in the present argon discharge. This statement needs further validation.

The fact that sterility is reached in 3 min with no filter on the Petri dish while some 30 spores are still living when the MgF_2 filter is on could be explained in the following ways: (i) the filtering out by the MgF2 window of the resonant lines located at 105 and 107 nm emitted by the argon plasma, a possibility to be excluded as shown in section 3.2.3.2; (ii) in the absence of windows on top of the Petri dish, some plasma is created in the immediate vicinity of the

---

[3] The optical filters have a thickness of 5mm and their transparency above their cut-off wavelength is higher than 90%.

[4] As shown, for instance, by Cabaj et al [25], UV photons with wavelength higher than 300 nm seem to have no sporicidal effects on *B. atrophaeus*.

spores that participates in the inactivation process; (iii) also in the of windows, some of the atoms and molecules that have diffused between stacked spores (section 3.2.3.4) could eventually then emit VUV/UV photons.

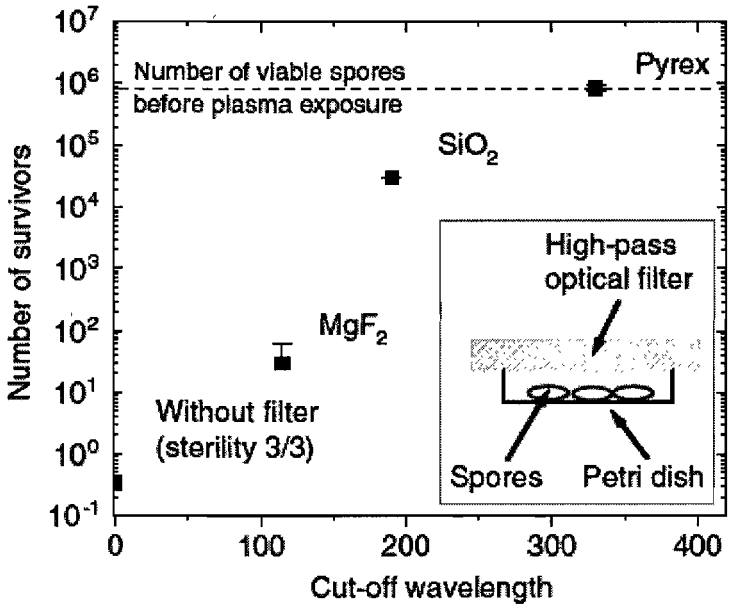

Figure 8 Number of survivors after 180 s of plasma exposure with no window on the Petri dish and with successively 3 high-pass optical filters located on top of it. Almost full optical transmission of these filters can be assumed above their cut-off wavelength. Operating conditions: 100 sccm, 750 mTorr, P_A = 30 W, 200 MHz.

3.2.3.1.2 Searching for apparent structural damage to exposed spores

To look for etching (erosion) damage on the *B. atrophaeus* spores subjected to the inactivation process, we used an SEM. It turns out that no alteration of the spore outer membrane could be observed after the exposure time (3 min) required for reaching sterility (micrographs not shown). To evidence eventual long-run damage, we subjected the spores for 60 min to the action of the argon plasma, that is, to say to more than 20 times the VUV/UV dose required to inactivate a 10^6 spore deposit (see figure 8). Figure 9 shows the corresponding SEM micrographs of unexposed spores compared with those subjected for 60 min to the usual inactivation conditions. No erosion of the exposed spore structure is apparent on these SEM micrographs (see next paragraph), although these spores are all inactivated.

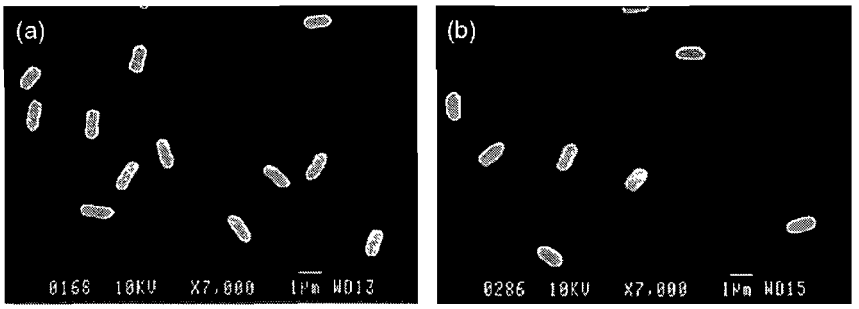

Figure 9 SEM micrographs of B. atrophaeus spores deposited on a Petri dish showing: (a) unexposed spores; (b) spores subjected for 60 min to the argon plasma (more than 20 times the VUV/UV dose required to inactivate a 10^6 spore deposit, see figure 8).

To confirm the absence of erosion concluded from mere visual inspection, we performed a statistical analysis of the spore length and width before and after plasma exposure. This statistical analysis was based on a 100 spores population. Accurate measurements of the spore dimensions were obtained utilizing micrographs with typically the same magnification as in figure 9 and analysing them with a technical-drawing software. Figure 10 shows the obtained spore average width and length, denoted μ, and their corresponding standard deviation, denoted σ, after a 60 min plasma exposure compared with no plasma exposure. The μ and σ values of the exposed spores are not significantly different from that of the non-exposed spores. We can therefore be sure that, under our specific operating conditions, etching is not involved in the inactivation process. In the previous section, using optical filters, we showed that spore inactivation is driven by the VUV/UV photons. The absence of apparent structural damage to the spores is consistent with the assumption that these bacteria are inactivated by VUV/UV photons through lethal lesions to their genetic material (DNA).

Sections 3.2.3.2 and 3.2.3.3 are devoted to optical emission characterization of the argon plasma, namely, the experimental arrangement used and the spectra observed, respectively.

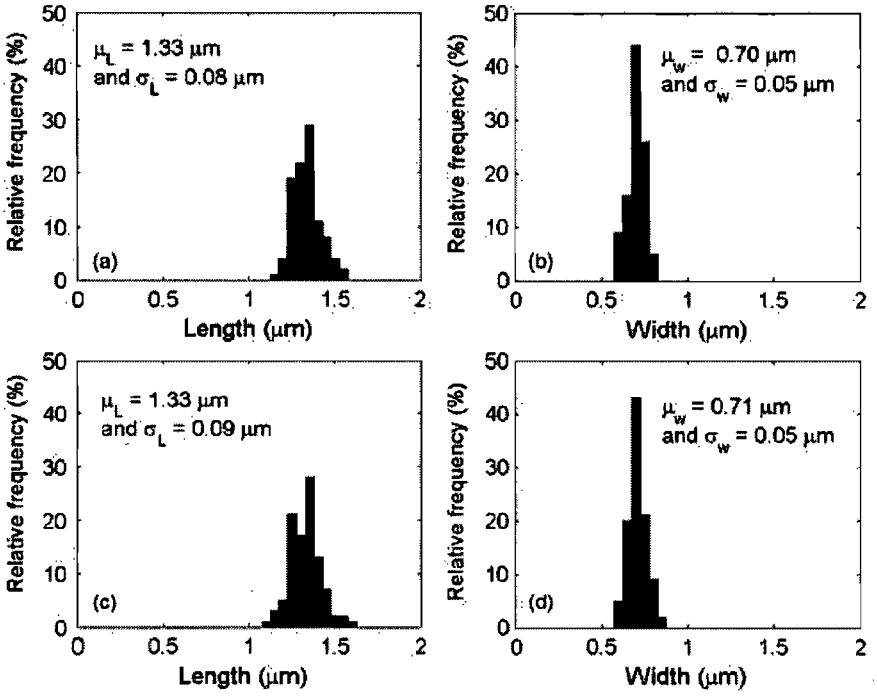

Figure 10 Statistical histograms of the length and width of *B. atrophaeus* spores deposited on Petri dishes. Figures (a) and (b) are related to non-exposed spores while figures (c) and (d) correspond to their plasma exposure for 60 min.

3.2.3.2 Optical emission and absorption spectroscopy arrangements

3.2.3.2.1 OES in the 200–400 nm range

OES measurements were performed, at mid-axial position along the discharge, through a fused silica lateral window of the chamber (see figure 3), collecting light with an optical fibre directed perpendicularly to this window. An échelle monochromator equipped with a UV-sensitive charge-coupled device (CCD) was used to scan the 200–400 nm wavelength range.

3.2.3.2.2 Integrated emission intensity recorded over the 112–180 nm range

Since UV photons are absorbed by air (actually oxygen) at wavelength below 180 nm, our échelle monochromator could not be used to characterize the VUV spectrum. A partial solution to this problem was to use, under vacuum conditions, a VUV photomultiplier (Hamamatsu R7511, see figure 7 for its location with respect to the discharge chamber) and

thus obtain the emission intensity integrated over the wavelength response range of this photomultiplier (112–180 nm).

3.2.3.2.3 Experimental arrangement for optical absorption spectroscopy

Given that the VUV photomultiplier comes with a MgF_2 window (under cut-off for wavelengths below 112 nm), we were not able to record directly the emission intensity of the 105 and 107 nm argon 'resonant' lines. The upper levels of these transitions belong to the $3p^5 4s$ orbital configuration and their lower level is the ground state. The energy difference of these two upper levels with the two metastable-atom levels of the same configuration being small (figure 11(a)), there is a strong pooling interaction between these four levels [27]. As a result, their respective population density is of the same order and it varies similarly as functions of the operating conditions [27]. For convenience and comparison with previous works, we have actually probed the upper level population density of the $^3P_2$ metastable level instead of that of a resonant level. As a matter of fact, we only needed to know the relative variation with operating conditions of this population density, not its absolute value.

The experimental arrangement used to record the relative population density of the $^3P_2$ level, based on a line-absorption method, is illustrated in figure 11(b) [27]. Measurements are carried out transversally to the discharge chamber, at mid-axial position along it, through the fused silica window already mentioned. An argon spectral lamp, located on one side of the chamber, illuminates the plasma through lens L_1 and a diaphragm perpendicularly to the plasma chamber. The light coming out on the other side of the discharge chamber through lens L_2 is sent to a spectrometer (HR-320, Instruments SA) via an optical fibre and it is detected with a photomultiplier (R955, Hamamatsu). A lock-in amplifier is utilized in conjunction with a light chopper to make sure that the intensity of the selected line (Ar I 763.5 nm) collected past the discharge tube, the transmitted intensity, I_t, originates solely from the spectral lamp; the incident line intensity, I_0, is simply obtained by turning the plasma off. The full line-width absorption coefficient is given by

$$A_L(\%) = \left(1 - \frac{I_t}{I_0}\right) \times 100 . \qquad (2)$$

The experimental results related to the three techniques that we just described are presented in the next section and correlated with our spore inactivation data.

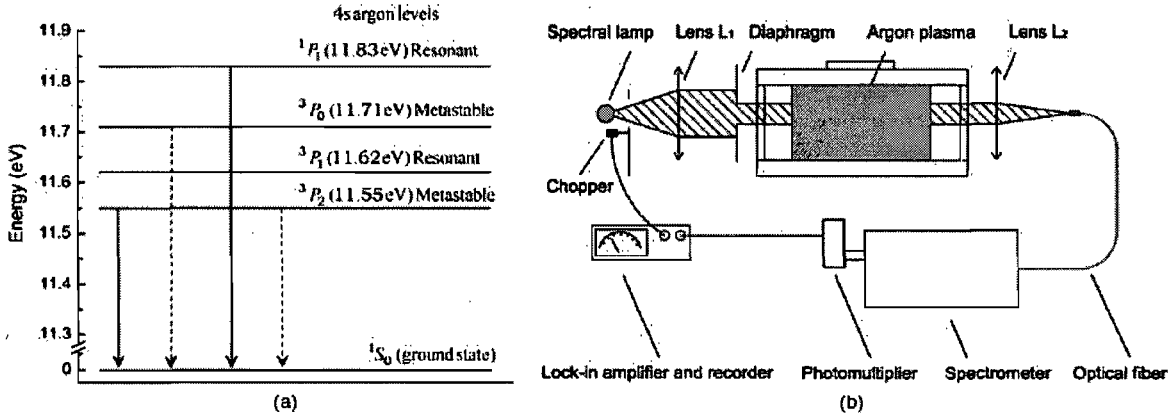

Figure 11 (a) Energy levels of the $3p^5 4s$ argon configuration [28]; (b) experimental arrangement showing the optical system for determining the full line-width absorption coefficient of the argon plasma.

3.2.3.3 Respective biocide roles of the 105 and 107 nm lines and of the VUV (112–180 nm) and UV (200–400 nm) spectral ranges

Figure 12 shows the emission spectrum recorded between 200 and 400 nm, using the échelle spectrometer, from the argon discharge sustained at 200 MHz, at a pressure of 750 mTorr and a flow rate of 100 sccm. The spectrum displayed is not corrected for the detector (CCD) and spectrometer intensity response with wavelength. No argon emission is observed in this spectrum, which is actually dominated by the NOγ system, the 306.4 nm OH system and the 2nd N_2 positive system, all these emissions being indicative of the presence of impurities (residual air and water vapour) in the argon gas. From the inactivation data resulting from figure 8, we know that photons above 330 nm have no sporicidal effect, although their presence in the 330–400 nm spectral range of figure 12 is significant.

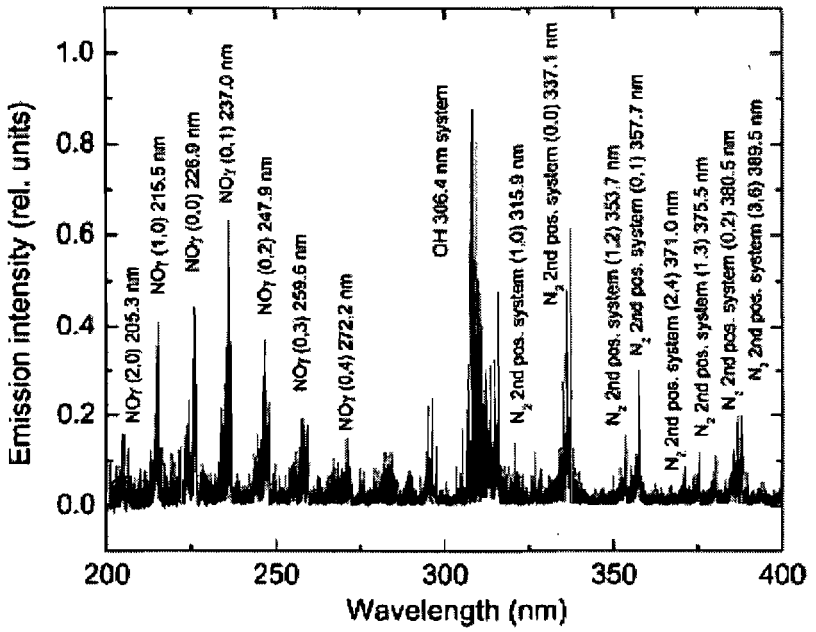

Figure 12 Recorded UV emission spectrum (200–400 nm) from the argon plasma at 750mTorr, with identification of the main molecular systems.

Figures 13(a) and (b) show, as functions of the argon gas pressure, respectively: (a) the number of surviving spores after 15 s of plasma exposure and the VUV intensity recorded with the photomultiplier over the 112–180 nm range; (b) the number of surviving spores after 15 s of plasma exposure and the full line-width absorption coefficient related to the population density of the $^3P_2$ upper level. Each Petri dish initially contains a 2×10^7 spore deposit of *viable B. atrophaeus* spores. The argon flow is set at 14 sccm and incident power at 30 W. Under these operating conditions, the whole length of the discharge vessel is filled with plasma. The fact that the higher the pressure, the higher the VUV emission is interpreted as resulting from a higher excitation rate of the impurities present in the argon plasma as pressure is raised. In contrast, we observe that the optical absorption coefficient of the $^3P_2$ argon metastable atoms (linked to the 105 and 107 nm line emission) strongly decreases as the argon pressure is increased above 30 mTorr to finally reach zero at 1000mTorr. This is because, as pressure is raised above 30 mTorr, the metastable state atoms are no longer lost only by diffusion to the walls, but also by collisional quenching. While there is clearly an increasing spore mortality with the increasing global VUV emission intensity (figure 13(a)), spore mortality is actually the highest when the absorption coefficient has reached zero; that is to say, the VUV transmissions at 105 and 107 nm do not contribute to spore inactivation.

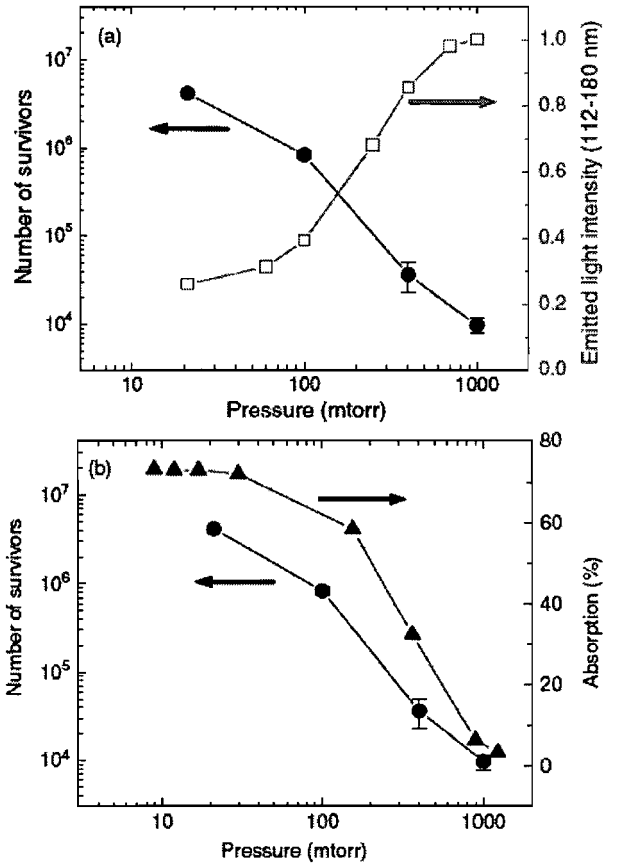

Figure 13 As functions of the argon gas pressure, respectively: (a) the number of surviving spores after 15 s of plasma exposure and the VUV intensity recorded over the 112–180 nm range; (b) the number of surviving spores after 15 s of plasma exposure and the full line-width optical absorption coefficient, which decreases with the decrease in the population density of the $^3P_2$ upper level. The argon flow is set at 14 sccm and incident power at 30W. Each Petri dish initially contains a 2×10^7 spore deposit of viable *B. atrophaeus* spores.

The fact that the VUV/UV photons are the dominant biocide species of the plasma, as demonstrated with figure 8, can be further supported by observing that the decrease in the number of survivors obeys a fluence law, i.e. to say that a given number of survivors is left whatever the VUV/UV intensity Φ, provided Φ times t, the exposure time, makes up a constant value: it corresponds to a given VUV/UV photon number or dose. On practical grounds, the VUV intensity is increased by raising the pressure (see figure 13(a)). Figure 14 shows the number of survivors, on a log scale, as a function of the VUV fluence (112–180 nm). The observed linear decrease in the number of survivors shows that the inactivation process, which is of the exponential type (for details, see section 3.2.3.4), actually obeys a fluence (or dose) law. A similar behaviour is obtained (not shown) with the UV photons

(200–330 nm). This result does not completely rule out the action of other biocide agents, but then these would necessarily be created or stimulated by the VUV/UV photons.

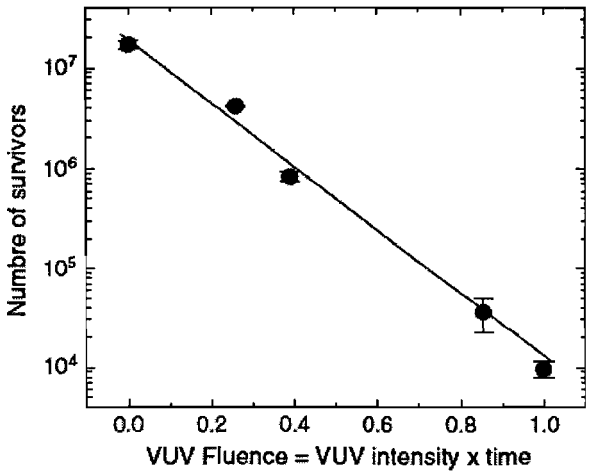

Figure 14 Number of survivors after 15 s of plasma exposure as a function of the VUV (112–180 nm) fluence (dose).

3.2.3.4 Analysis of survival curves obtained under stacked spore conditions

The decrease in the number of surviving microorganisms exposed to a given inactivating stress is most generally exponential and, as such, is adequately reported by their survival curve [29], namely, a plot of the logarithm of the number of still living microorganisms as a function of exposure time to the inactivating agent. Figure 15 shows that the survival curve of *B. atrophaeus* spores exposed to the argon discharge is actually composed of two linear segments. The first segment is related to the inactivation of isolated spores while the second one has to do with aggregated and stacked spores[5] (as initially suggested by Hury *et al* [30]). In that respect, for a given deposit area, the higher the initial population, the higher the number of living spores that should be found at the beginning of the second segment (also designated as the second phase) since the occurrence of stacking is then higher (see next paragraph). For both curves, the argon flowis fixed at 100 sccm at a pressure of 750 mTorr; the discharge is sustained at a field frequency of 200 MHz and the incident power is 42 W (power absorbed by the plasma is 39 W, see figure 5(b)).

[5] Clearly, the top spore on a stack could be considered as an 'isolated' spore from the viewpoint of UV radiation access.

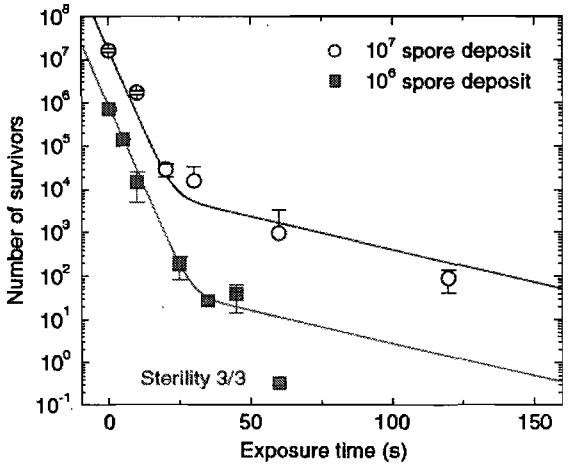

Figure 15 Survival curves of *B. atrophaeus* spores, deposited on a polystyrene Petri dish (see its location in figure 7) and subjected to the planar discharge sustained in argon with a flow rate of 100 sccm and a pressure of 750 mTorr at a field frequency of 200 MHz. The deposit initially contains 10^6 or 10^7 viable spores. Each data point is the averaged result of three independent experiments.

The deposits yielding the survival curves in figure 15 were obtained, in one case, from a dried suspension of 10^6 spores (actually 8.3×10^5) diluted in 100µl of water and, in the other, from a dried suspension of 10^7 spores (1.6×10^7) diluted in 200 µl of water. The area covered by the 10^7 spore deposit is approximately 2 times larger than that from the 10^6 spore deposit, implying that the number of spores per unit area is, in the end, greater for the 10^7 spores deposit, hence a higher probability of spore stacking. The SEM micrographs of these two deposits shown in figure 15 confirm this. The 10^6 spore deposit (figure 16(a)) essentially comprises isolated spores whereas the 10^7 spore deposit (figure 16(b)) includes more aggregated and stacked spores[6]. This reflects in the second phase of the survival curves in figure 15: compare the starting value of the second phase (survivor number extrapolated linearly at t = 0) for a 10^6 and a 10^7 spore deposit, actually here 90 and 13 000 spores, respectively.

[6] Nonetheless, one should not conclude from figure 15 to the absence of stacking in the 10^6 spore deposit. The probability of finding stacked spores is the highest at the periphery of the spore deposit [31].

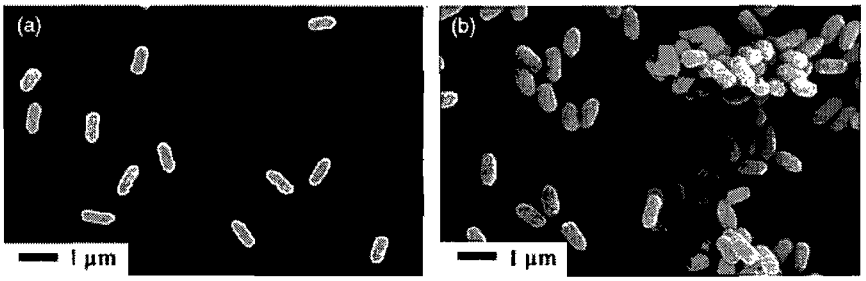

Figure 16 SEM micrographs of unexposed *B. atrophaeus* spores as taken approximately at the centre of their deposition area in the cases of: (a) a dried 100 µl water suspension containing 10^6 spores; (b) a dried 200 µl water suspension containing 10^7 spores. Spore stacking is clearly observed on the 10^7 spore deposit.

Having shown in section 3.2.3.3 that the VUV/UV photons are the only biocide agents of the plasma source used and that the spore inactivation rate obeys a fluence law, we sought to model the inactivation kinetics observed in figure 15. Various mathematical representations of the bacterial inactivation kinetics are available [32]. Since our survival curves are made up of two phases with no shoulder (lag time), we turned to the inactivation model proposed by Cerf [33]:

$$N(t) = N_{0-1} \times 10^{-k_1 It} + N_{0-2} \times 10^{-k_2 It}, \quad (3)$$

where N(t) is the number of still living spores at time t , I is the VUV/UV flux intensity, $k_1 I$ and $k_2 I$ are the slopes of phases 1 and 2, respectively. In this model, N0, the total number of living microorganisms at time t = 0, can be considered to result from the sum of the initial population densities of the first and second phase, respectively:

$$N_0 = N_{0-1} + N_{0-2}, \quad (4)$$

as extrapolated from the experimental survival data at time t = 0: N_{0-1} comprises not only isolated spores, but also top ones in the case of stacked spores, while N_{0-2} relates to the inactivation of spores shielded from UV radiation by other spores (or eventual debris), namely, aggregated and stacked spores. In the present case, the extrapolated value of N_{0-2} is estimated from figure 14 to be approximately 90 for the 10^6 spore deposit and 13 000 for the 10^7 spore deposit. For both deposits, we find $N_0 \approx N_{0-1}$. The set of values required by the model, extracted from the survival data point in figure 14, are listed in table 1 while the solid curves in figure 15 has be drawn from expression (3) using the parameters listed in table 1.

Table 1 Values of the model parameters needed in relation (3), as extracted from the experimental data in figure 14. The data points for both spore deposit numbers have been obtained under the same operating conditions (same UV flux intensity). Using the same kiI values for both deposits amounts to considering that fluence (dose) controls lethality.

	10^6 spores	10^7 spores
N_{0-1}	8.3×10^5	1.6×10^7
$k_1 I$	0.15	0.15
N_{0-2}	90	1.3×10^4
$k_2 I$	0.015	0.015

The agreement between our experimental data and the analytical curve provided by the model is fairly good, except for the second phase of the 10^6 spore deposit: the model curve predicts that sterility should be achieved in approximately 130 s, while experimentally, it is obtained in 60 s. This discrepancy could be related to experimental variations in the number of stacked spores of our deposits, which affects the parameter N_{0-2} of the model. It is indeed difficult to control in a reproducible way the number of stacked spores. Fluctuations in its number value are related to the drying process of the spore suspension, including the temperature and degree of humidity in the drying closet, as well as by the wettability of the substrate material.

An interesting practical aspect that can be inferred from this modelling by looking at table 1 is that the dose required to inactivate those spores shielded from direct UV radiation by other spores is approximately 10 times higher[7] than for isolated spores or top ones in the case of stacked spores. An obvious conclusion is then that the overall time required to reach sterility is definitely controlled by the number of stacked spores.

To further reduce the sterilization time for a given number of stacked spores or to inactivate a thicker stacks of spores, one has to increase the UV intensity and efficiency. At least two ways are open in that direction, which are: (i) to increase the density of power absorbed by the plasma (therefore the electron density, hence atom and molecule excitation rates), which can be done by increasing either the input power or/and the EM field frequency), as stressed in [3]; (ii) to optimize the gas composition with slight admixtures of, for example, N_2, O_2, CO_2 in order to enrich the VUV/UV spectrum, both by increasing its intensity and

[7] This ratio of 10 is relatively close to that obtained by other authors (e.g. Rossi et al [34] found a ratio of 13.3).

favouring the most biocidal wavelength range (<300 nm), having in mind that the argon gas emission by itself is relatively inefficient in that respect (figure 13).

3.2.4 Damage to polymer exposed to the reduced-pressure argon planar discharge

As underlined in the introduction, the plasma sterilization process must not only efficiently inactivate microorganisms but also it should not induce damage to the exposed surfaces. In particular, as many MDs comprise polymers, the etching of polymers should be as limited as possible. In order to evaluate the level of damage induced by the present argon plasma to polymers, we used polystyrene microspheres (PS, approximately one micrometer in diameter). Such PS microspheres have already been employed to compare damage caused by the early and the late N_2–O_2 discharge afterglows (Boudam et al [35]). These microspheres were then found to be quite responsive to various plasma species: the observed off-axis[8] erosion rate correlated with the increase in the O atom density in the afterglow as the O_2 percentage is increased, while the on-axis erosion observed at 0% O_2 appeared related to the action of both the N_2 metastable molecules and the N_2^+ ions. Similar PS microspheres were also employed by Lerouge et al [36] to demonstrate that the high sporicidal efficacy provided by their O_2/CF_4 plasma was related to its high etch rate of polymers. Brétagnol et al [37] also reported that PS microspheres can strongly be etched by an O_2 plasma.

Figure 17 shows SEM micrographs of PS microspheres deposited on Petri dishes: (a) unexposed and (b) located in the planar discharge as shown in figure 7, and subjected for 1 min to the argon plasma; the gas flow is 100 sccm at a gas pressure of 750 mTorr: under these operating conditions, all the spores of a 10^6 deposit are inactivated, see figure 15. As we can see, the exposed microspheres are not disrupted or eroded, a result that could be expected from a pure argon plasma. However in the present case, as we have shown in section 3.2.3.3, the argon plasma is contaminated by air and water vapour but only slightly, containing only a very little amount of oxygen radicals. The absence of etching damage here contrasts with plasma sterilization techniques based on the action of radicals.

---

[8] In Boudam et al [35], the discharge tube feeds the parallepipedic afterglow chamber perpendicularly to its entrance plane and at the centre of it.

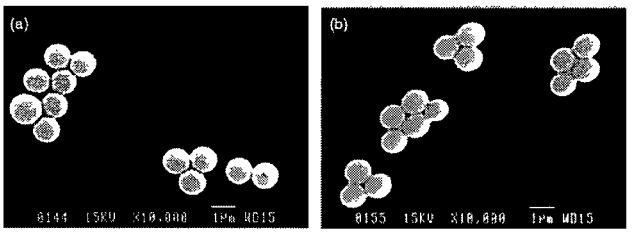

Figure 17 SEM micrographs of microspheres, deposited on Petri dishes: (a) unexposed and (b) located in the planar discharge as shown in figure 7, and subjected for 1 min to the argon plasma. Gas pressure is 750mTorr with an argon gas flow of 100 sccm (under these operating conditions all deposited spores are inactivated, see figure 15).

The surface wettability of polymers currently utilized in the biomedical field was characterized as a function of exposure time to our argon discharge, using the drop shape method (goniometer: VCA Optima®). The three polymers investigated were: Teflon, polyurethane (PU) and silicone. These polymers were located successively at the same position in the discharge chamber as the Petri dishes (see figure 7). Once plasma processing was over, distilled water was dropped onto three different sites on each sample and the measured values of the contact angle were averaged. Figure 18 shows that, for all three polymers, the water contact angle strongly decreased during the first 20 s of plasma exposure time. Beyond this exposure time, the water contact angle tends to stabilize.

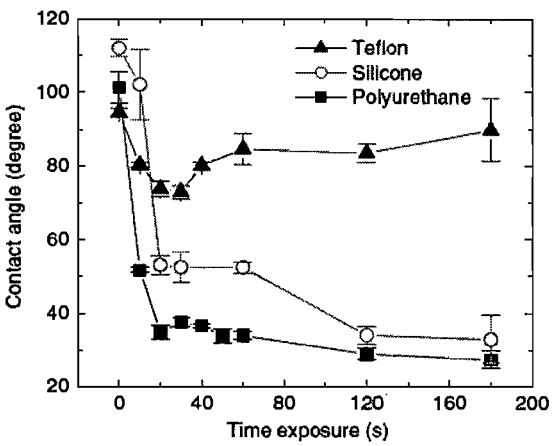

Figure 18 Influence of time exposure to plasma sterilizing conditions on the water contact angle. Operating conditions and location of the polymer samples within the plasma chamber were the same as those used for the sterilization of Petri dishes (see figure 7). The contact angle measurements were carried out between 1 and 2 h after plasma exposure.

In conclusion, even though no erosion is observed as checked using SEM micrographs, there are some modifications of the surface energy of polymers, as attested by the contact angle variations with exposure time. Such changes in the wettability of the polymers could be detrimental when these polymers are in the form of narrow-bore tube, such as catheters. However, we note that Teflon is comparatively little affected in that respect, which is of interest since many MDs are made from that material. Further investigations in that direction are required, for example to check for surface relaxation (aging) and to identify changes in the surface composition of the exposed polymers, for instance using x-ray photoelectron spectroscopy (XPS).

3.2.5 Conclusion

From the beginning of our studies on plasma sterilization, our team has been relying on UV photons as opposed to reactive species to inactivate bacteria, having in mind that UV photons should induce less damage to MDs. In that context, we have worked out operating conditions such that sterility, starting with a 10^6 spore deposit, was reached in less than 40 min, calling for the UV photons emitted by the excited NO molecule formed in the flowing afterglow of an N_2–O_2 discharge. The approach followed in this paper, in some aspects, leads to improvements over the N_2–O_2 flowing afterglow treatment: (i) the time required to reach sterility is considerably lowered (1 min compared with 40 min) by subjecting the MDs to the UV photons from the discharge itself as opposed to those produced in an afterglow; (ii) damage to materials are reduced by using argon rather than a mixture containing O_2 that yields O atoms, a chemically reactive species. Actually, we found out that there was always some air contamination in the 'argon' discharge, implying that O atoms are also present, but fortunately at a much lower level, namely, approximately 0.01% instead of 0.1–0.3% in the optimum N_2–O_2 afterglow: this is confirmed by the absence of erosion on the treated polystyrene microspheres as opposed to their slight erosion observed in the N_2–O_2 afterglow.

A main concern when subjecting MDs to a discharge is that its gas temperature must be low, typically below 55 °C, not to damage MDs made from polymers. We were able to solve this problem by turning to microstrip line field applicators where the HF power delivered per unit volume is very low as opposed to many currently used microwave-sustained plasmas. Such a plasma source is presented in this paper: it is perfectly reproducible, requires no impedance retuning and the argon gas temperature remains below 40 °C.

As far as damage to materials is concerned, we have shown that with the present system there was no erosion on polystyrene microspheres for the exposure time required to achieve sterility. In contrast, we have observed a slow erosion of these microspheres in the N_2–O_2 afterglow. In fact, to see such an erosion effect with the present argon discharge, we have to add 0.1 to 0.2% O_2 to argon.

Nonetheless, there might be limitations to the present planar plasma source as far as sterilization is concerned. (i) We have checked that metallic (conducting) objects were not heated up by the electric field, which is a positive point. However, in the event of crevices in such devices, no plasma can be formed therein and then only diffusion could bring the excited species (potential UV emitters) inside it. This needs to be examined. (ii) For objects located one below the other (referring here to an electric field directed vertically), shadowing effect could result in a reduced field intensity above the object closer to the ground plate, hence a weaker discharge or no discharge at all. The same with a conducting object: we might have to tumble it over at mid-process to make sure that both sides are sterilized. This needs to be investigated. (iii) We have to bear in mind that the UV biocide approach is limited by the thickness of stacked microorganisms or of biofilms (where the microorganisms are embedded in extracellular components) that need to be inactivated. This topic is presently under investigation in our laboratories.

3.2.6 Acknowledgments

The authors are grateful to Mrs J S'eguin for valuable microbiological work and Mr J S Mayer for priceless technical assistance. Thanks are also due to Mrs S Polizu from Ecole olytechnique for highly pertinent comments on contact angle measurements. Financial support for this work was provided by the Fonds Québécois pour la Recherche sur la Nature et la Technologie (FQRNT) and the Conseil de Recherches en Sciences Naturelles et Génie du Canada (CRSNG).

3.2.7 References

[1] Pollak J, Moisan M, Saoudi B and Zakrzewski Z 2005 Process for the plasma sterilization of dielectric objects comprising a hollow part Patent Application US 0269199 Pollak J, Moisan M, Saoudi B and Zakrzewski Z 2004 Patent Application WO 050128

[2] Pollak J, Moisan M and Zakrzewski Z 2007 Long and uniform plasma columns generated by linear field-applicators based on stripline technology Plasma Sources Sci. Technol. 16 310–23

[3] Pollak J, Moisan M, K´eroack D, S´eguin J and Barbeau J 2008 Plasma sterilization within long and narrow-bore dielectric tubes contaminated with stacked bacterial spores Plasma Process. Polym. 5 14–25

[4] Pollak J and Moisan M 2007 Device and method for inactivation and/or sterilization using plasma Patent Provisional Application US 60/884,344 Pollak J and Moisan M 2008 Patent Provisional Application PCT/CA 000032

[5] Ganashev I P and Sugai H 2002 Production and control of planar microwave plasmas for materials processing Plasma Sources Sci. Technol. 11 178–90

[6] Zakrzewski Z and Moisan M 1995 Plasma sources using long linear microwave field applicators: main features, classification and modelling Plasma Sources Sci. Technol. 4 379–97

[7] Slinko V N, Sulakshin S S and Sulakshina L V 1988 On producing an extended microwave discharge at high pressure Sov. Phys.—Tech. Phys. 33 363–5

[8] Bosisio R G, Weissfloch C F and Wertheimer M R 1972 The large volume microwave plasma generator (LMPTM): a new tool for research and industrial processing J. Microw Power 7 325–46

[9] Bosisio R G, Wertheimer M R and Weissfloch C F 1973 Generation of large volume microwave plasmas J. Phys. E: Sci. Instrum. 6 628–30

[10] Sauv´e G, Moisan M, Zakrzewski Z and Bishop C A 1995 Sustaining long linear uniform plasmas with microwaves using a leaky-wave (throughguide) field applicator IEEE Trans. Antennas Propag. 43 248–56

[11] Bilgic A M, Engel U, Voges E, K¨uckelheim M and Broekaert J A C 2000A new low-power microwave plasma source using microstrip technology for atomic emission spectrometry Plasma Sources Sci. Technol. 9 1–4

[12] Bass A, Chevalier C and Blades M W 2001A capacitively coupled microplasma formed in a quartz wafer J. Anal. At. Spectrom. 16 919–21

[13] Broekaert J A C 2002 The development of microplasmas for spectrochimical analysis Anal. Bioanal. Chem. 374 182–7

[14] Iza F and Hopwood J A 2003 Low-power microwave plasma source based on a microstrip split resonator IEEE Trans. Plasma Sci. 31 782–7

[15] Iza F and Hopwood J A 2005 Split-ring resonator microplasma: microwave model, plasma impedance and power efficiency Plasma Sources Sci. Technol. 14 397–406

[16] Schermer S, Bings N H, Bilgic A M, Stonies R, Voges E and Broekaert J A C 2003 An improved microstrip plasma for optical emission spectrometry of gaseous species Spectrochim. Acta A Part B 58 1585–96

[17] Stonies R, Schermer S, Voges E and Broekaert J A C 2004 A new small microwave plasma torch Plasma Sources Sci. Technol. 13 604–11

[18] Harvey A F 1963 Microwave Engineering (New York: Academic)

[19] Pollak J, Moisan M, Zakrzewski Z, Pelletier J, Arnal Y A, Lacoste A and Lagarde T 2007 Compact waveguide-based power divider feeding independently any number of coaxial lines IEEE Trans. Microw. Theory Tech. 55 951–7

[20] Moisan M and Pelletier J 2006 Physique des Plasmas Collisionnels (Grenoble: EDP Sciences)

[21] Feichtinger J, Schulz A, Walker M and Schumacher U 2003 Sterilisation with low-pressure microwave plasmas Surf. Coat. Technol. 174 564–9

[22] Soloshenko I A, Tsiolko V V, Khomich V A, Shchedrin A I, Ryabtsev A V, Bazhenov V Y and Mikhno I L 2000 Sterilization of medical products in low-pressure glow discharges Plasma Phys. Rep. 26 792–800

[23] Xu L, Nonaka H, Zhou H Y, Ogino A, Nagata T, Koide Y, Nanko S, Kurawaki L and Nagatsu M 2007 Characteristics of surface-wave plasma with air-simulated N_2–O_2 gas mixture for low-temperature sterilization J. Phys. D: Appl. Phys. 40 803–8

[24] Sato T, Miyahara T, Doib A, Ochiai S, Urayama T and Nakatani T 2006 Sterilization mechanism for Escherichia coli by plasma flow at atmospheric pressure Appl. Phys. Lett. 89 073902

[25] Cabaj A, Sommer R, Pribil W and Haider T 2002 The spectral UV sensitivity of microorganisms used in biodosimetry Water Sci. Technol.: Water Supply 2 175–81

[26] Munakata M, Saito M and Hieda K 1991 Inactivation action spectra of Bacillus subtilis spores in extended ultraviolet wavelengths (50–300 nm) obtained with synchrotron radiation Phocochem. Photobiol. 54 761–78

[27] Moisan M and Ricard A 1977 Density of metastable atoms in an argon plasma produced by an RF surface wave Can. J. Phys. 55 1010–12

[28] Santiago I and Calzada M D 2007 Population measurement of the $3p^5 4s$ configuration levels in an argon microwave plasma at atmospheric pressure Appl. Spectrosc. 61 725–33

[29] Moisan M, Barbeau J, Moreau S, Pelletier J, Tabrizian M and Yahia L H 2001 Low-temperature sterilization using gas plasmas: a review of the experiments and an analysis of the inactivation mechanisms Int. J. Pharmaceutics 226 1–21

[30] Hury S, Vidal D R, Desor F, Pelletier J and Lagarde T 1998A parametric study of the destruction efficiency of Bacillus spores in low pressure oxygen-based plasmas Lett. Appl. Microbiol. 26 417–21

[31] Philip N, Saoudi B, Crevier M C, Moisan M, Barbeau J and Pelletier J 2002 The respective roles of UV photons and oxygen atoms in plasma sterilization at reduced gas pressure: the case of N2–O2 IEEE Trans. Plasma Sci. 30 1429–36

[32] Xiong R, Xie G, Edmondson A E and Sheard M A 1999 A mathematical model for bacterial inactivation Int. J. Food Microbiol. 46 45–55

[33] Cerf O 1977 Tailing of survival curves of bacterial spores J. Appl. Bacteriol. 42 1–19

[34] Rossi F, Kyli'an O and Hasiwa M 2008 Mechanisms of Sterilization and decontamination of surfaces by low pressure plasma Advanced Plasma Technology ed d'Agostino R et al (Weinheim: Wiley)

[35] Boudam M K, Saoudi B, Moisan M and Ricard A 2007 Characterization of the flowing afterglows of an N_2–O_2 reduced-pressure discharge: setting the operating conditions to achieve a dominant late-afterglow and correlating the NO_β UV intensity variation with the N and O atom densities J. Phys. D: Appl. Phys. 40 1694–711

[36] Lerouge S, Wertheimer M R, Marchand R, Tabrizian M and Yahia L H 2000 Effect of gas composition on spore mortality and etching during low-pressure plasma sterilization J. Biomed. Mater. Res. 51 128–35

[37] Brétagnol F, Valsesia A, Ceccone G, Colpo P, Gilliland D, Ceriotti L, Hasiwa M and Rossi F 2006 Surface functionalization and patterning techniques to design interfaces for biomedical and biosensor applications Plasma Process. Polym. 3 443–5

3.3 Discussion et problématique de l'endommagement de la membrane externe des spores par plasma

Nous avons montré que la source de plasma décrite dans l'article précédent offre un intérêt pratique dans le domaine de la stérilisation. Toutefois, un sujet de science fondamentale touchant à notre compréhension des mécanismes d'inactivation par plasma mériterait un traitement plus approfondi: nous allons apporter un éclairage nouveau sur l'inactivation de spores de *B. atrophaeus* par les VUV/UV d'un plasma.

Il est généralement admis que les rayons VUV et UV inactivent les spores bactériennes par altération de leur matériel génétique. En toute rigueur, on peut affirmer que ce sont les VUV/UV qui sont les agents biocides (tel que démontré avec l'utilisation de filtres optiques dans l'article précédent), mais on ne peut pas assurer avec certitude que ce sont des lésions à l'ADN qui sont responsables de l'inactivation des spores. Il existe deux arguments généralement avancés pour soutenir la thèse de l'endommagement de l'ADN par les VUV/UV: (i) le fait que les spores inactivées par VUV/UV uniquement ne présentent pas de rupture membranaire ou de signe d'érosion de leur membrane externe, même lorsqu'elles sont observées au MEB après exposition au plasma, bien qu'elles soient inactivées (voir e.g. la figure 1.2), (ii) par comparaison, les mécanismes d'inactivation par les photons d'un plasma devraient être similaire avec ceux d'une lampe UV où les dommages aux spores ont fait l'objet de nombreuses études (e.g. [40]). Par exemple, il a été démontré que les UV peuvent être directement absorbés par l'ADN des cellules et y induire des réactions de dégradation impliquant les bases pyrimidiques, thymine et cytosine. Toutefois, il est à noter qu'il existe au moins deux différences majeures sur ce sujet entre un plasma et une lampe germicide: la nature polychromatique de l'émission d'un plasma et la présence de VUV (la plupart des lampes germicides, généralement de mercure, inactivent les spores par l'intermédiaire principalement d'une unique raie située à 254 nm). De ce fait, les mécanismes d'inactivation pourraient être différents et dans cette section, nous allons proposer un autre mécanisme d'inactivation que les dommages à l'ADN, qui devra dans le futur être confirmé ou infirmé par une étude plus poussée.

Nous avons tout d'abord voulu vérifier à nouveau, mais encore plus précisément, qu'il n'y avait pas d'érosion de la membrane externe des spores en observant des micrographies obtenues au microscope électronique à transmission (MET). La figure 3.1 présente des micrographies en

mode balayage (S-MET) et conventionnel (C-MET) de deux spores différentes: l'une exposée 1 minute au plasma d'argon et inactivée et l'autre non exposée au plasma. On peut observer sur la figure 3.1 que les spores de *B. atrophaeus* ne sont pas assez érodées pour qu'une différence soit visible au MET. Ce résultat confirme à nouveau, qu'il y a très peu d'érosion de la surface des spores, du moins en deux dimensions[3] et, au vu de ce résultat, on pourrait à nouveau être amené à conclure que les dommages aux spores affectent uniquement à l'ADN.

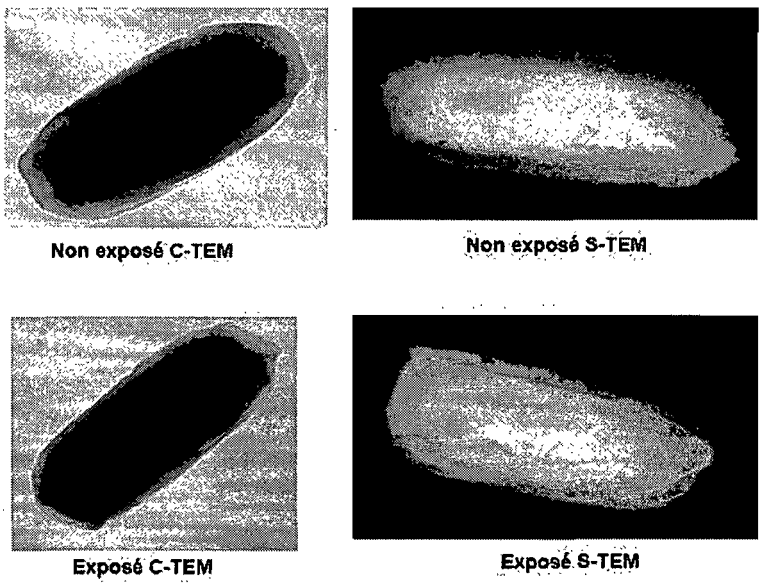

Figure 3.1 Micrographies obtenues au microscope électronique à transmission en mode S-TEM et C-TEM de spores de *B. atropheus* après exposition au plasma d'argon. Il est à noter qu'il ne s'agit pas de la même spore exposée et non-exposée. Par comparaison avec la spore de contrôle, la membrane externe de la spore exposée au plasma n'apparait pas endommagée.

Voici l'idée que nous avons eue: s'il y avait des dommages structuraux internes, même infimes, aux tuniques de protection des spores, ces dernières devraient être moins résistantes à des tensions mécaniques. Or on sait que les spores contiennent de l'eau et qu'elles peuvent, par conséquent, s'hydrater et se déshydrater, ce qui modifie leur volume et pourrait ainsi révéler une faiblesse mécanique structurale non détectable par microscopie. Nous avons testé cette hypothèse

[3] En toute rigueur, il faudrait pousser le diagnostic encore un peu plus loin en observant la troisième dimension (i.e. l'épaisseur des spores) par microscope à force atomique (MFA).

en ajoutant une gouttelette d'eau sur des spores exposées et inactivées (et sur des spores de contrôle non exposées). Nous avons ensuite laissé cette gouttelette d'eau hydrater les spores puis sécher (24 h) avant d'observer les spores au MEB. La figure 3.2 montre des micrographies de spores de *B. atrophaeus* ainsi obtenues: (a) spores non exposées puis hydratées; spores soumises pendant une minute à un plasma d'argon (inactivées) puis hydratées et observées à fort (b) et bas (c) grossissement.

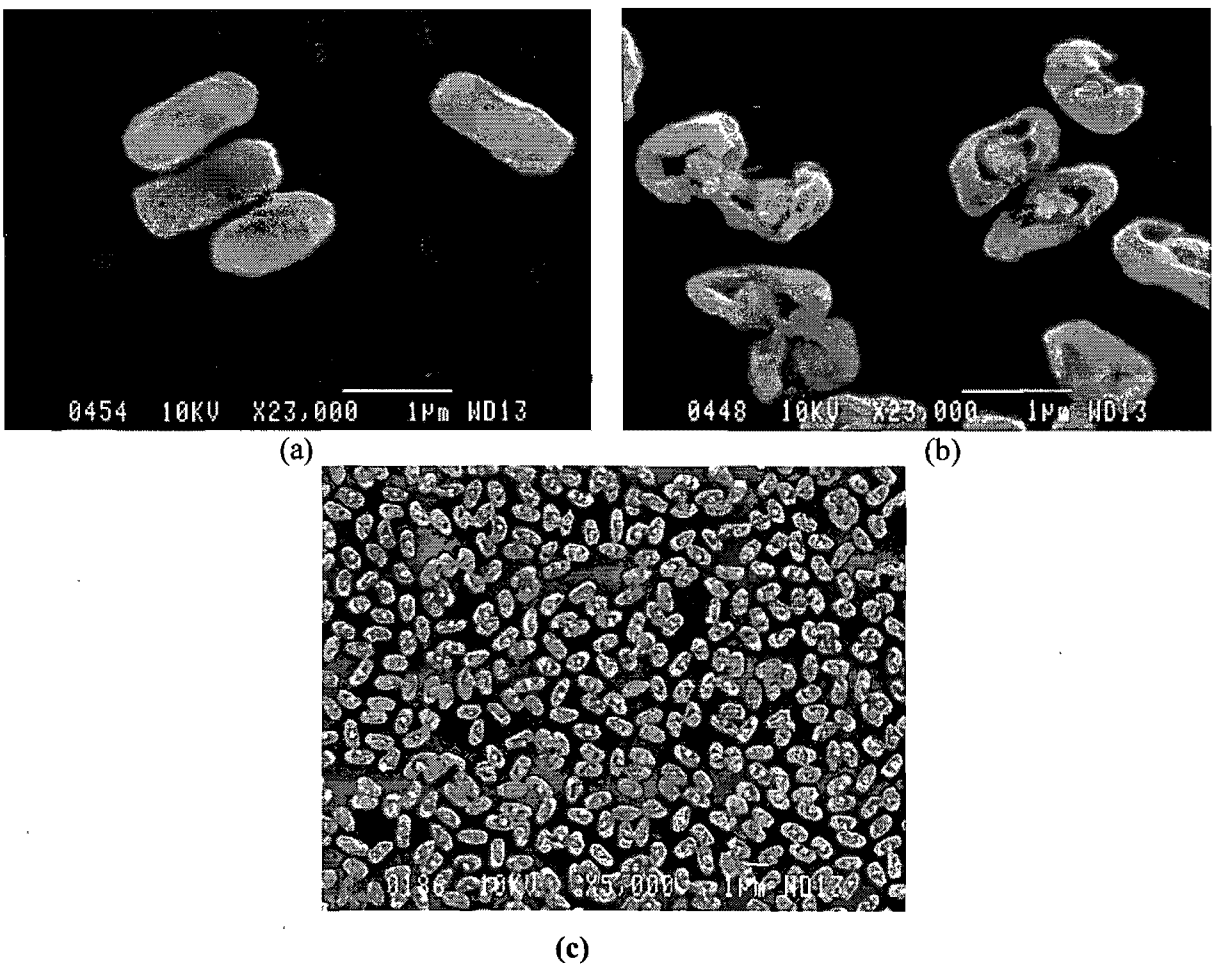

Figure 3.2 Micrographies obtenues au MEB de spores de *B. atrophaeus*: (a) spores non exposées puis hydratées; (b) spores soumises pendant une minute à un plasma d'argon (inactivées) puis hydratées et observées à fort (b) et faible grossissement. Le noyau des spores lysées de la figure (b) a été coloré par J. Barbeau par ordinateur.

Au vu de ces observations expérimentales, nous proposons une nouvelle hypothèse quant aux mécanismes d'inactivation de spores de *B. atrophaeus* par les VUV/UV d'un plasma: l'inactivation de ces spores pourrait être obtenue par affaiblissement de leurs tuniques de protection, qui n'offrent plus de résistance mécanique suffisante pour leur permettre de résister à des stress tel l'hydratation et/ou la déshydratation. Il est à noter, pour finir, que la force de tension résultante à la mise sous vide des spores dans le stérilisateur (avant l'injection de l'argon et lors de leur observation au MEB) pourrait également participer à ce processus de rupture membranaire.

3.4 Résumé et conclusion

En somme, nous avons présenté un stérilisateur par immersion-plasma de configuration parallélépipédique, d'un nouveau type (voir la demande de brevet située à l'annexe 3). Celui-ci apparaît particulièrement adapté pour stériliser des DM de surfaces planes dans le cas de conducteurs ou de formes plus complexes dans le cas de diélectriques. De plus, une première identification des agents biocides de ce plasma a été effectuée: en corrélant une étude spectroscopique en émission et des courbes de survie, nous avons montré que les photons UV sont les agents biocides principaux de ce plasma, plus spécifiquement, ceux du domaine spectral situé entre 112 et 190 nm. Nous avons également démontré que des impuretés (e.g. N_2) présentes à des niveaux très faibles dans l'argon sont nécessaires pour réaliser un système de stérilisation performant dans nos conditions opératoires.

Le plasma créé par ce nouveau dispositif endommage peu la surface des spores bactériennes de *B. atropaheus* : en effet, aucune érosion des spores n'est constatée, ce qui résulte de la faible densité d'espèces oxydantes dans l'enceinte de stérilisation. En ce qui a trait aux polymères non organiques, nous avons vérifié, par microscopie électronique à balayage (MEB), que les dommages produits par ce système sur du polystyrène sont relativement faibles. Le fait que ce système occasionne peu d'érosion peut s'expliquer par:

- le régime relativement bas de pression utilisé ($\leq$ 1 torr, évitant la filamentation de la décharge);
- l'absence de points chauds (poches d'énergie) du à la configuration géométrique de la source de plasma et au mode d'onde progressive utilisé
- les mécanismes d'inactivation: les espèces bactéricides sont essentiellement les photons VUV et UV et non des espèces plus agressives pour les surfaces tels les radicaux.

Finalement, ce nouveau système est à la fois performant et relativement peu agressif pour les polymères thermosensibles. Il pourrait donc être mis à profit pour stériliser des DM, par exemple. Toutefois, nous n'avons que peu de recul sur ce nouveau dispositif et nombre de questions doivent être encore traitées. Ces dernières concernent, d'une part, les mécanismes de stérilisation (l'action biocide des UV sur les spores bactériennes) et, d'autres part, l'usage potentiel d'adjuvants gazeux (e. g. CO_2) dans l'argon afin d'enrichir le domaine spectral des photons UV particulièrement efficaces du point de vue biocide.

Conclusion générale

Nous avons montré qu'il est possible de stériliser au contact direct de la décharge, dans un temps raisonnable et sans érosion apparente, des surfaces de polymère. Nous avons atteint des objectifs précis en ce qui a trait à la géométrie des objets que nous pouvons avantageusement stériliser (e.g. l'intérieur de tubes) et l'amélioration de l'efficacité du procédé (e.g. un temps de stérilisation de quelques minutes).

Nous avons exposé comment ces objectifs ont été réalisés au cours des deuxième et troisième chapitre. Ainsi, nous avons développé, testé et optimisé essentiellement deux types de stérilisateur en contact direct avec la décharge reposant sur des lignes de transmission planes. L'impédance d'entrée de ces dispositifs est quasi indépendante de la présence du plasma dans une large gamme de conditions opératoires (nature et pression du gaz, fréquence du champ HF). Cette particularité permet tout d'abord de nous affranchir de l'utilisation d'isolateurs haute-fréquence protégeant le générateur HF et offre en outre une grande souplesse d'utilisation en termes de conditions opératoires suivant les besoins rencontrés. Dans le même temps, nous avons pu optimiser différents paramètres (notamment la fréquence d'opération) pour obtenir des systèmes de stérilisation efficaces tout en cherchant un compromis entre l'activité biocide des stérilisateurs et les dommages infligés aux matériaux traités. Par ailleurs, nous avons mis au point deux protocoles microbiologiques d'insertion et de récupération de micro-organismes dans des tubes, l'un destiné à l'obtention de spores bactériennes sédimentées sous forme d'empilements, et l'autre permettant la croissance de biofilms directement sur la paroi interne de tubes de polymère (section 2.5). Ces protocoles sont reproductibles et ont représenté une phase cruciale dans nos recherches, car ce sont eux qui ont permis de contrôler les performances de nos prototypes.

Dès que l'on s'engage fortement dans un sujet de recherche, on est tenté d'en grossir l'importance. Ici, le risque est grand de surestimer la place de la stérilisation par plasma parmi l'ensemble des méthodes de stérilisation d'objets médicaux et le rôle des photons UV parmi l'ensemble des agents biocides des plasmas. Les photons UV ont été identifiés comme les espèces biocides prépondérantes de nos dispositifs, car les plasmas que nous créons contiennent, par choix, très peu d'espèces chimiquement réactives comme l'oxygène. En fait, nous avons utilisé principalement de l'argon tout au long de nos recherches, car c'est un gaz rare, donc non

réactif, mais qui est à même d'exciter efficacement les impuretés (e.g. N_2) présentes dans le gaz de décharge afin que celles-ci émettent du rayonnement UV.

Par ailleurs, nous devons réaliser qu'il demeure un important fossé à franchir entre la stérilisation d'une boîte de Petri ou de l'intérieur d'un tube diélectrique et celle d'un instrument médical de nature mixte diélectrique-conducteur et de forme complexe. En effet, il existe, par exemple, une multitude de dispositifs médicaux comportant plusieurs lumières (canaux de faible diamètre sur une comparativement grande longueur). La plupart d'entre eux en contiennent au moins deux et les sources de plasmas développées au cours de ce travail devront être adaptées pour prendre en compte ces spécificités.

En ce qui concerne le stérilisateur par immersion, plusieurs questions devront trouver réponse dans le futur avant d'en faire un système d'usage courant. Pour ne citer que deux exemples, si des crevasses sont présentes dans des objets conducteurs, aucun plasma ne pourra être créé à l'intérieur et il n'y aura que la diffusion pour y amener les espèces excitées (émetteurs potentiels d'UV), d'où l'intérêt a priori de travailler à pression réduite par opposition à la pression atmosphérique.

Par ailleurs, nous devons garder en mémoire que la stérilisation par plasma, qu'elle soit obtenue par érosion ou par pénétration de photons UV, est un traitement de surface finalement limité par l'épaisseur des micro-organismes à traiter si l'on s'en tient à un temps d'inactivation fonctionnellement acceptable. Dans ce sens, il sera donc nécessaire de pousser plus avant l'évaluation des limites de cette technique quant à son efficacité à inactiver des micro-organismes recouverts de différents biomatériaux, tel par exemple des résidus sanguins.

En fait, la stérilisation par plasma est un domaine de recherche qui, selon nous, est à un tournant de son évolution en ce moment: les principaux mécanismes permettant d'obtenir la stérilité ont été analysés et compris, mais aucun dispositif de stérilisation par plasma n'est encore commercialisé[4] ou a prouvé son efficacité à stériliser des dispositifs médicaux, même simples, tels des scalpels (en fait, à notre connaissance, aucune tentative dans ce sens n'a même été rapportée dans la littérature scientifique). En ce qui concerne les systèmes de stérilisation présentés au cours de ce travail de doctorat, au moins trois des sujets traités mériteraient d'être approfondis pour se rapprocher de systèmes de stérilisation viables et commercialisables:

[4] Dans le système Sterrad de stérilisation dit par plasma de Johnson and Johnson, le plasma sert uniquement à décomposer le peroxyde d'hydrogène, chimiquement agressif, en fin de procédé et n'a aucun effet bactéricide [9].

1) Étude de l'inactivation de micro-organismes déposés sur des objets médicaux présentant, dans un premier temps, une forme simple. On pourrait par exemple tester le stérilisateur pour tubes diélectriques sur de véritables cathéters cardiaques ne comportant qu'une seule lumière. On pourrait aussi procéder à une étude paramétrique de son efficacité biocide en fonction du diamètre interne et de la nature polymérique des tubes afin de délimiter le type de cathéter commercialisé pouvant être traité par notre stérilisateur. Quant au stérilisateur fonctionnant par immersion au plasma, il faudrait le mettre à l'épreuve sur des scalpels ou des forceps.
2) Approfondissement des dommages infligés aux matériaux pendant le traitement: nous avons déjà montré que la mouillabilité des polymères est affectée par le plasma, tandis qu'aucune érosion n'est observée par microscopie électronique à balayage. Ce travail pourrait être prolongé en étudiant (i) plus précisément, par microscopie à force atomique, la topographie des polymères traités, (ii) les modifications chimiques des surfaces par spectroscopie photo-électronique par rayon X (XPS) et (iii) l'effet, sur la mouillabilité des polymères, du temps de vieillissement (relaxation des liaisons).
3) Recours à des adjuvants gazeux: des conséquences pratiques importantes surviennent lorsque l'inactivation par plasma repose sur des photons UV provenant de la désexcitation d'impuretés et non de celle du gaz porteur. Par exemple, étant donné que la quantité d'impuretés présentes dans l'enceinte n'est pas toujours la même au départ du procédé de stérilisation, il est difficile de comparer les propriétés biocides de différentes sources de plasmas utilisant de l'argon « pur » sans compter que cela pourrait mener à la non-reproductibilité des traitements. Ces impuretés proviennent en différentes proportions de la bouteille de gaz, de fuites aux transitions d'admission de gaz, de la désorption des parois de l'enceinte et de celles des objets médicaux. Ainsi, il serait avantageux d'injecter un haut flux d'argon (e.g. 1 l/min) avec des adjuvants gazeux dont la nature et la quantité sont contrôlées par l'opérateur. Ceci permettrait de réguler les impuretés gazeuses présentes dans le stérilisateur pour maximiser l'émission UV.

En somme, nous avons mis au point des stérilisateurs par contact avec le plasma qui, de ce fait, offrent des possibilités complémentaires par rapport à celles de la post-décharge en flux. Bien qu'ayant peu de recul sur ces nouveaux dispositifs, par comparaison avec la post-décharge qui a été davantage étudiée et dont les limites sont mieux définies, notre travail apparaît comme

une contribution partielle, mais qui nous semble essentielle, au développement d'un éventuel stérilisateur cette fois en décharge.

Bibliographie (hors publications)

1. Krebs M C Bécasse P Verjat D et Darbord J C 1998 *Gas-plasma sterilization: relative efficacy of the hydrogen peroxyde phase compared with that of the plasma phase* Int. J. Pharm. **160** 75-81
2. Moisan M 2001 *La stérilisation à basse température et en milieu sec au moyen d'un plasma froid* Article non soumis à publication
3. Moisan M Barbeau J Moreau S Pelletier J Tabrizian M et Yahia L H 2001 *Low-tempererature sterilization using gas plasmas: a review of the experiments and an analysis of the inactivation mechanisms* Int. J. Pharm. **226** 1-21
4. Moreau M Orange N et Feuilloley M G J 2008 *Non-thermal plasma technologies: New tools for bio-decontamination* Biotechnology Advances **26** 610-617
5. Nordhauser F M et Olson W P 1998 *Sterilization of drugs and devices* CRC Press, p. 170.
6. Pelletier J 2007 *De la stérilisation conventionnelle à la stérilisation plasma*, in *Atelier "Biomatériaux" du Réseau Plasmas Froids du CNRS - Le Mans (19 -21 mars 2007).*
7. Menashi W P 1968 *Treatment of surfaces* Brevet américain 3 383 163
8. Peeples R E et Anderson N R 1985 *Microwave coupled plasma sterilization and depyrogenation I. System characteristics* J. Parenteral Sci. Technol. **39** 2-8
9. Jacobs P T et Lin S M 1987 *Hydrogen peroxide plasma sterilization system* Brevet américain 4 643 876
10. Laroussi M 2005 *Low temperature plasma-based sterilization: overview and state-of-the-art* Plasma Processes and Polymers **2** 391-400
11. Laroussi M 1996 *Sterilization of contaminated matter with an atmospheric pressure plasma* IEEE Trans. Plasma Sci. **24** 1188-1191
12. Lerouge S Wertheimer M R et Yahia L H 2001 *Plasma sterilization: a review of parameters, mechanisms, and limitations* Plasmas and Polymers **6** 175-188
13. Kylian O Hasiwa M Gilliland D et Rossi F 2008 *Experimental study of the influence of Ar/H_2 microwave discharges on lipid A* Plasma Process. Polym. **5** 26–32
14. Kylian O Hasiwa M et Rossi F 2006 *Plasma-Based De-Pyrogenization* Plasma Process. Polym. **3** 272–275

15. Halfmann H Denis B Bibinov N Wunderlich J et Awakowicz P 2007 *Identification of the most efficient VUV/UV radiation for plasma based inactivation of Bacillus atrophaeus spores* J. Phys. D: Appl. Phys. **40** 5907–5911

16. Laroussi M Mendis D A et Rosenberg M 2003 *Plasma interaction with microbes* New J Physics **5** 1-10

17. Fridman G Brooks A D Balasubramanian M Fridman A Gutsol A Vasilets V N Ayan H et Friedman G 2007 *Comparison of direct and indirect effects of non-thermal atmospheric-pressure plasma on bacteria* Plasma Process. Polym. **4** 370-375

18. Stoffels E Kieft E et Sladek R E J 2003 *Superficial treatment of mammalian cells using plasma needle* J. Phys. D: Appl. Phys. **36** 2908–2913

19. Deng X T Shi J J Chen H L et Kong M G 2007 *Protein destruction by atmospheric pressure glow discharges* Applied physics letters **90** 1-3

20. Moisan M Barbeau J Pelletier J et Saoudi B 2002 *La stérilisation à plasma froid à pression très inférieure à la pression atmosphérique* Le vide **303** 71-84

21. Philip N 2003 *Stérilisation à basse température et à pression réduite en post-décharge de plasma: étude et analyse du rôle des UV dans l'inactivation des spores.* Mémoire de maîtrise, Université de Montréal, Québec

22. Moisan M Barbeau J Crevier M C Pelletier J Philip N et Saoudi B 2002 *Plasma sterilization. Methods and mechanisms* Pure Appl. Chem. **74** 349-358

23. Boudam M K Moisan M Saoudi B Popovici C Gherardi N et Massines F 2006 *Bacterial spore inactivation by atmospheric-pressure plasmas in the presence or absence of UV photons as obtained with the same gas mixture* J. Phys. D: Appl. Phys. **39** 3494-3507

24. Cabaj A Sommer R Pribil W et Haider T 2002 *The spectral UV sensitivity of microorganisms used in biodosimetry* Water science and technology: water supply **12** 175-181

25. Crevier M C 2003 *Effets de la stérilisation par plasma N_2-O_2 en post-décharge sur des spores de B. subtilis et surfaces de biopolymères* Mémoire de maîtrise, Université de Montréal

26. Mendis D A Rosenberg M et Azam F 2000 *A note on the possible electrostatic disruption of bacteria* IEEE Transactions on plasma science **28** 1304-1306

27. Vandencasteele N 2008 *Étude du rôle des espèces constitutives d'un plasma pour la fonctionnalisation de surfaces polymériques.* Thèse de doctorat, Université libre de Bruxelles, Belgique

28. Rabek J F 1996 *Photodegradation of polymers, physical characteristics and applications* Springer

29. Schnabel W 2007 *Polymers and light* Wiley-VCH Verlag GmbH & Co.

30. Truica-Marasescu F E et Wertheimer M R 2005 *Vacuum ultraviolet photolysis of hydrocarbon polymers* Macromol. Chem. Phys. **206** 744-757

31. Lerouge S Fozza A C Wertheimer M R Marchand R et Yahia L H 2000 *Effect of gas composition on spore mortality and etching during low-pressure plasma sterilization* J Biomed Mater Res. **51** 128-135

32. Pelletier J 1992 *La stérilisation par procédé plasma* Agressologie **33** 105-110

33. Boudam M K 2007 *Contribution à l'étude de l'inactivation de micro-organismes par plasma* Thèse de doctorat, Université de Montréal, Québec

34. Pollak J Moisan M Kéroack D et Boudam M K 2008 *Low-temperature low-damage sterilization based on UV radiation through plasma immersion* Journal of physics D: Appl. Phys. **41** 1-14

35. Kuo S P Tarasenko O Nourkbash S Bakhtina A et Levon K 2006 *Plasma effects on bacterial spores in a wet environment* New J Physics **8** 41 1-11

36. Madigan M T et Martinko J M 2005 *Biology of Microorganisms 11ème édition* Pearson Prentice Hall

37. Nicholson W L Munakata N Horneck G Melosh H J et Setlow P 2000 *Resistance of bacillus endospores to extreme terrestrial and extraterrestrial environments* Microbiology and molecular biology reviews **64** 548–572

38. Dricks A 1999 *Bacillus Subtilis Spore Coat* Microbiology and molecular biology reviews **63** 1-20

39. Fritze D et Pukall R 2001 *Reclassification of bioindicator strains Bacillus subtilis DSM 2277 as Bacillus atrophaeus* International journal of systematic and evolutionary microbiology **51** 35-37

40. Setlow P 2005 *Spores of Bacillus subtilis: their resistance to and killing by radiation, heat and chemicals* J. Applied Microbiology **101** 514-525

41. Wikipedia, *Bacteria*. Page consultée le 29/11/2008

42. Costerton G W 2007 *The biofilm primer* Springer-Verlag

43. Barbeau J 2007 *Un monde merveilleux* Journal de l'Ordre des Dentistes du Québec (JODQ) **44** 517-524

44. Hury S Vidal D R Desor F Pelletier J et Lagarde T 1998 *A parametric study of the destruction efficiency of Bacillus spores in low pressure oxygen-based plasmas* Letters in applied microbiology **26** 417–421

45. Zakrzewski Z et Moisan M 1995 *Plasma sources using long linear microwave field applicators: main features, classification and modelling* Plasma Sources Sci. Technol. **4** 379-397

46. Pelletier J Lacoste A Lagarde T Moisan M Arnal Y A et Zakrzewski Z 2004 *Power splitter for plasma device* Brevet américain 6 727 656

47. Costerton W Veeh R Shirtliff M Pasmore M Post C et Ehrlich G 2003 *The application of biofilm science to the study and control of chronic bacterial infections* J. Clin. Invest. **112** 1466-1477

48. Pajkos A Vickery K et Cossart Y 2004 *Is biofilm accumulation on endoscope tubing a contributor to the failure of cleaning and decontamination?* J. Hosp infection **58** 224-229

49. Man N K Degremont A Darbord J C Collet M et Vaillant P 1998 *Evidence of bacterial biofilm in tubing from hydraulic pathway of hemodialysis system* J. artificial organs **22** 596-600

50. Shah J 2002 *Endoscopy through the ages* British J urology **89** 645-652

51. Fuchs G J 2006 *Milestones in endoscope design for minimally invasive urologic surgery: the sentinel role of pioneer* Surg. Endosc. **20** 493-499

52. Linder T E Simmen D et Stool S E 1997 *Revolutionary inventions in the 20th century. The history of endoscopy* Arch Otolaryngol Surg **123** 1161-1163

53. Nelson B D Jarvis W R Rutala A W Foxx-Orenstein A E Isenberg G Dash G P Alavarado C J Ball M Griffin-Sobel J Petersen C Ball K A Henderson J et Stricof R L 2003 *Multi-society guideline for reprocessing flexible gastrointestinal endoscopes* Infection control and hospital epidemiology **24** 532-536

54. American society for gastrointestinal endoscopy 1998 *Infection control during gastrointestinal endoscopy* Gastrointestinal endoscopy **49** 836-841

55. Olympus America 2003 *Product information Melville, NY*

56. Shumway R et Broussard J D 2003 *Maintenance of gastrointestinal endoscopes* Clinical techniques in small animal practices **18** 254-261

57. Quensland Health 2006 *Endoscope reprocessing* Disponible sur: http://www.health.qld.gov.au/endoscopereprocessing, page consultée le 28 décembre 2006

58. Muscarella L F 2006 *Inconsistencies in endoscope-reprocessing and infection-control guidelines: the importance of endoscope drying* American journal of gastroenterology **101** 2147-2154

59. Pollak J 2005 *Applicateurs linéaires de champs EM utilisant la technologie triplaque pour l'entretien de décharges HF (50-2450 MHz)* Mémoire de maîtrise, Université de Montréal, Québec

60. Pollak J Moisan M Saoudi B et Zakrzewski Z 2005 *Process for the plasma sterilization of dielectric objects comprising a hollow part.* Demande de brevet américain 0269199, (PCT) WO2004/050128.

61. Pollak J Moisan M et Zakrzewski Z 2007 *Long and uniform plasma columns generated by linear field-applicators based on stripline technology* Plasma Sources Sci. Technol. **16** 310-323

62. Pollak J Moisan M Kéroack D Séguin J et Barbeau J 2008 *Plasma sterilization within long and narrow-bore dielectric tubes contaminated with stacked bacterial spores* Plasma processes and polymers **5** 14-25

63. Pollak J Séguin J Barbeau J Moisan M 2008 *Biofilm sterilization within polymer tubings by a low temperature gaseous plasma (ionized gas)* Article soumis à la revue International journal of pharmaceutics

ANNEXE 1 Étude d'un diviseur de puissance pour sources de plasma distribuées

Compact waveguide-based power divider feeding independently any number of coaxial lines

(article publié dans IEEE Transactions on microwave theory and techniques 2007 **55** 915-957)

Jérôme Pollak, Michel Moisan, Zenon Zakrzewski, Jacques Pelletier,
Y. A.1. Arnal, Ana Lacoste, and T. Lagarde

Abstract

The device described in this paper has been designed to enable the feeding of many individual plasma sources from a single microwave generator, providing a noninterfering and constant supply of power to each coaxial line driving these plasma sources. The power coming from the generator flows through a waveguide under standing-wave conditions provided by the presence of a conducting plane located at the waveguide end opposite that linked to the generator. Power is extracted from the waveguide, at the maximum of intensity of the -field standing wave, by a waveguide-to-coaxial-line transition designated as a probe. One or two probes can be set at each such maximum of field intensity (and this on both sides of the waveguide wide wall), yielding a compact power divider. Each coaxial line feeds a microwave field applicator, sustaining plasma, through a matching circuit comprising a tuning means and a ferrite isolator (circulator with a matched load), the latter ensuring that whatever happensto the plasma source, the other feeding lines are not affected. The conditions required for a perfect match of the microwave generator to the power divider are elaborated and examples of actual designs are presented.

Index Terms—Equivalent-circuit representation, plasma sources, power divider, waveguide-to-coaxial-line transition.

A.1.1 Introduction

It is often interesting to supply microwave power to many plasma sources (usually through coaxial lines) from a single generator. Such a situation arises, for instance, when trying to achieve large dimension and uniform plasmas by assembling elementary (individual) plasma sources. Another example is the necessity of feeding different plasma sources for sequential plasma processing. The power divider that we are going to describe is usually made to share power evenly, but it is not restricted to that specific condition. An important and distinguishing feature of our device is that the number of coaxial outputs can be any number, even or odd. With the current power divider, each coaxial line feeds a microwave field applicator sustaining plasma through a ferrite isolator (circulator with a matched load) and eventually a tuning means, the isolator ensuring that, whatever happens to a particular plasma source, the other feeding lines are not affected by the power reflected from that plasma source. Finally, this power divider can be made compact and can handle the total power required to provide typically up to 200–250 W per coaxial output lines.

There are already well-known ways of dividing microwave power [1], the most straightforward one being to use a 3-dB coupler, which, in principle, splits power evenly. A cascade of such power dividers can be utilized to provide 2^k outputs, where k is the number of cascaded 3-dB couplers. Another widely used technique is to draw power from a cavity or a ring resonator at its maximums of standing waves. However, microwave cavities, e.g., at 2.45 GHz, cannot provide a large number of coaxial outputs because of their intrinsically limited dimensions since, for the current purpose, they need to be operated in their fundamental modes. As already mentioned, the technique about to be presented can yield any number, odd or even and eventually large, of coaxial outputs; e.g., a 24-coaxial-port divider has been built, which at the same time is compact. Another negative aspect of most existing power dividers is that their output lines are not independent, i.e., a variation in the absorbed power in one branch (e.g., due to changes in plasma operating conditions or during the process of impedance matching) can modify the power flowing through the surrounding coaxial lines, a situation that is avoided in our design because of the presence of an isolator in the matching circuit of each of these output lines.

Our power divider has already been patented [2]. The purpose of this paper is to elaborate upon the analytical expressions yielding the input admittance of the system and also to give

construction details with actual examples of such power dividers. Although our initial aim in designing such a device was to supply plasma sources, it is clear that this power divider can be used in the more general case of loads of any kind, eventually varying with time.

This paper is organized as follows. In Sections A.1.2 and A.1.3, respectively, the geometrical configuration and equivalent circuit for single and multiple probe transitions from rectangular waveguide to coaxial line are presented. Section A.1.4 describes the experimental arrangements and procedures for measuring the divider characteristics, while results from such measurements are given in Section A.1.5. Finally, Sections A.1.6-A.1.7 are devoted to the designing and practical realization of the power divider, while Section A.1.9 contains a brief summary and conclusion.

A.1.2 Single-probe transition: probe configuration and equivalent circuit

A classical configuration of a rectangular-waveguide to coaxial-line transition is shown schematically in Fig. 1. The factors affecting the properties of such a type of transition, when the probe is located on the centerline of the waveguide wide wall, are discussed in details in the literature, e.g., in [3]–[5]. These are the dimensions of the coaxial line and waveguide, the probe penetration depth h into the waveguide and its distance l_s to the waveguide short circuit (end plane), as shown in Fig. 1. There is also an additional possibility of affecting the transition characteristics besides those indicated in [3]–[5]: it is to move the probe to a specific distance d away from the wall centerline [6], [7].

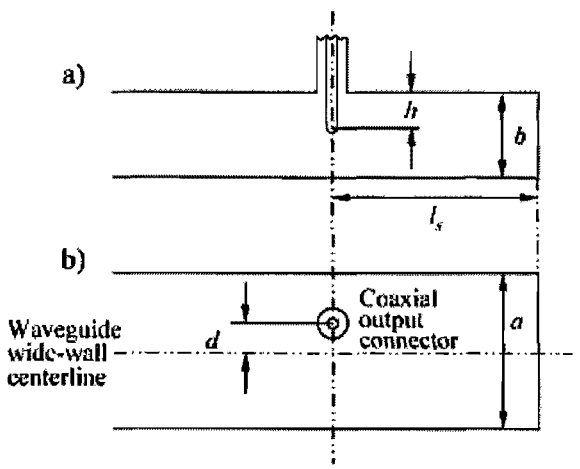

Fig. 1. Schematic representation of a classical transition from a coaxial line to a rectangular waveguide by means of a probe protruding in the waveguide. (a) Side view. (b) Top view. The inner width of the waveguide wide wall is a, while that of the narrow wall is b.

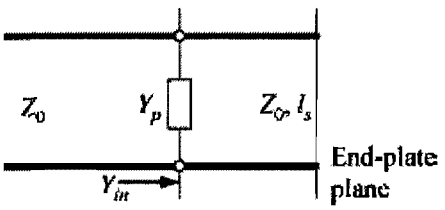

Fig. 2. Equivalent-circuit representation of a probe implemented in a short-circuited waveguide of characteristic impedance Z_0.

The probe microwave properties can be represented by a single admittance referred to the probe axis plane, as shown in Fig. 2. There, $Y_p = G_p + jB_p$ is the probe admittance when the coaxial line is terminated with a matched load. With the end-plate in position at a distance l_s from the probe, the input admittance of the transition, again referred to the probe axis plane, is then[1]

$$Y_{in} = Y_p - \mathrm{j}Z_0^{-1}\mathrm{ctg}\beta l_s \tag{1}$$

where $\beta = 2\pi/\lambda_g$ (λ_g is the wavelength in the waveguide and Z_0, the characteristic impedance of the waveguide). When normalized with respect to the characteristic impedance of the waveguide, Y_{in} becomes:

$$Y_{in}Z_o \equiv y_{in} = g_p + \mathrm{j}b_p - \mathrm{j}\mathrm{ctg}\,\beta l_s \tag{2}$$

with $g_p \equiv G_p Z_0$ and $b_p \equiv B_p Z_0$.

The admittance of an on-centerline probe, Y_{p0}, has been investigated as early as the 1940's [3]. Analytical-graphical methods for determining its value, solely from the geometry of the transition, can be found in the literature (for example [8]). In the present work, we choose to determine Y_{p0} experimentally, as it enables us to take into account factors affecting the probe admittance that cannot be taken into consideration by the analytical-graphical method mentioned.

---

[1] In a circuit, admittances in parallel add in contrast to impedances that add when in series. The admittances at different planes transverse to the waveguide main axis can be considered to be distributed in parallel and when all of them are "seen" (or expressed) in a given reference plane, they simply add.

The admittance of an off-centerline probe, Y_p, of particular interest in the present case, can be obtained following the arguments presented in [7]. The electric field of the fundamental mode in a rectangular waveguide is parallel to the probe axis and its intensity is uniform along that direction. Its distribution across the waveguide axis is $E_0 \cos(\pi d/a)$ where E_0 is the field intensity at the waveguide centerline ($d = 0$). The power absorbed by a probe displaced from the centreline by d, because of the E-field dependence on transverse position, is thus:

$$P_p = P_{p0} \cos^2(\pi d/a), \tag{3}$$

where P_{p0} is the power absorbed by a probe when located on the centerline of the waveguide wide-wall. A similar reasoning applies to the energy stored in the probe region, which is related to its susceptance. Therefore, the normalized admittance of an off-centerline probe as seen in its plane at the axis can be written in the form:

$$y_p \equiv g_p + \mathrm{j}b_p = (g_{p0} + \mathrm{j}b_{p0})\cos^2(\pi d/a) \tag{4}$$

where g_{p0} and b_{p0} are the conductance and admittance of the corresponding on-centerline probe.

A.1.3 Transition implying multiple probe transitions and corresponding input admittance expression

We consider arrays of waveguide-to-coaxial-line probe transitions that provide equal sharing of the waveguide power to numerous coaxial ports. The rectangular (x, z) coordinates used are defined in Fig. 3: the x-axis coincides with the wide wall centerline and the the $x = 0$ origin is chosen to be at the divider input plane.

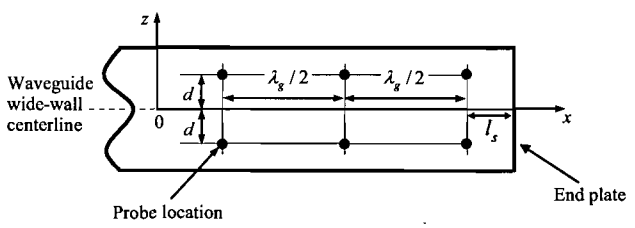

Fig 3. Example of an array of probe transitions, showing the probe locations when gathered by pairs at each anti-node of the E-field standing wave to provide an equal share of power to each of them (same h value). The x-axis coincides with the waveguide wide-wall centerline and $x = 0$ is the divider input plane.

From the general principles of impedance transformation along a lossless transmission line, it follows that the admittance y_p of a probe located at $x = x_p$ is seen in the reference plane (x = 0) as [3]

$$y = \frac{y_p + j\tan\beta x_p}{1 + jy_p \tan\beta x_p}. \tag{5}$$

It directly comes out from (5) and (4) that similar probes located at positions

$$x = x_p + k\frac{\lambda_g}{2};\ z = \pm d, \tag{6}$$

with k an integer number, exhibit the same admittance seen in any chosen reference plane. The same reasoning and resulting formulas apply to the probe transitions located at the same (x, z) positions on the opposite waveguide wide-wall[2]. The total admittance seen in the reference plane is the sum of admittances of all probes, transformed to that plane.

The power divider structure can actually be considered lossless. Therefore, the only possible mechanism of power loss is the power eventually reflected back toward the generator into the circulator matched load. This lowering of the power transmitted to the coaxial outputs can be eliminated by assuring a perfect admittance match at the divider input plane, which requires that $y_{in} = 1$ and thus:

$$g_{in} = 1; \quad b_{in} = 0. \tag{7}$$

The input susceptance b_{in} can be cancelled out by locating the reflecting end-plate in the appropriate position. Further on, we shall consider arrays of probes in which the location of each probe meets condition (6). A convenient choice for the input (reference) plane is the plane in which the first probes of the array are located. The input admittance is then

---

[2] The electric field intensities at the output ports located in the same x-plane or in different x-planes defined by $(x + n\lambda_g)$ are in phase, n being an integer number. In contrast, at output ports located in consecutive x-planes or in different x-planes defined by $(x + (2n+1)\frac{\lambda_g}{2})$, the electric field intensities are π out of phase.

$$y_{in} = Ng_p + \mathrm{j}Nb_p - \mathrm{j}\,\mathrm{ctg}\, 2\pi l_s / \lambda_g \tag{8}$$

where N is the total number of probes in the array and $-\mathrm{j}\,\mathrm{ctg}\, 2\pi l_s / \lambda_g \equiv b_s$ is the admittance seen at the input plane due to the short-circuited section of waveguide of length l_s, located past the last probe(s) in the array. Then, provided the end plate meets condition (7) as to $b_{in} = Nb_p + b_s = 0$, relation (8) leads to:

$$g_p = N^{-1};\ Nb_p = \mathrm{ctg} 2\pi l_s / \lambda_g, \tag{9}$$

which concretely set the values of g_p and b_p required for a perfect admittance match at the divider input plane. The N probes can be distributed along the waveguide in various ways, but still meeting condition (9), thus providing equal power sharing between the various outputs and, at the same time, an admittance match at the waveguide input. However, the minimum length of the divider and, therefore, its compactness, are obtained when, at each x-plane defined in accordance with condition (6), there are four probes (two on each wide wall).

A.1.4 Experimental arrangements and measurement procedures for determining the characteristics of the power divider

The tested transitions, single- and multiple-probe arrays, were implemented on a standard WR-340 rectangular waveguide (internal dimensions approximately 86 mm × 43 mm) for operation at 2.45 GHz. Fig. 4 shows an actual design of such a probe. The probes used are fitted on the external side of the waveguide to *N*-type coaxial connectors that serve as the power divider outputs. Within the waveguide, the probe is terminated by a round-head screw, this screw allowing to adjust the protruding length h of the probe. Two experimental arrangements were employed in the course of the current series of measurements. The first one (Fig. 5), destined to the direct measurement of the admittance of a single probe, calls for a network analyzer (HP 8750C). An auxiliary section of waveguide (see Fig. 5) was used for the analyzer calibration. In this way, the analyzer could directly yield the admittance value of the transition referred to the probe axis plane. In a second set of experiments (Fig. 6), we then measured, on the one hand, the power reflected, at the probe axis plane, by a single on-centerline transition terminated with a matched load and, on the other hand, the power transmitted to the coaxial output of a given probe

of the array. In the case of the transmission measurements, a power-meter bolometric head (matched to 50 Ω) was attached to the output actually under test, all other coaxial outputs being terminated with a matched load. The reflection measurements, as shown in Section V, can be related to the value of the admittance y_{in}.

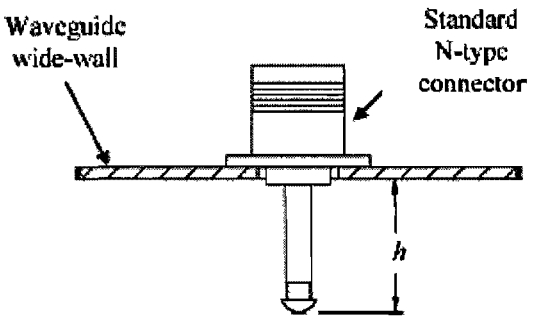

Fig. 4. Probe of adjustable length h, fitted to an N-type (female) coaxial connector.

A.1.5 Measured power divider characteristics

A.1.5.1. Input Admittance of a Transition at the Probe Axis Plane

Fig. 7 shows the results of the admittance measurements made with the network analyzer in the case of a single-probe transition located on the wide wall centerline of a WR-340 rectangular waveguide. The obtained values of the input admittance $y_{in} = g_{in} + jb_{in}$ are represented in the (g_{in}, b_{in}) plane for various probe lengths h and positions l_s of the end plate. As expected, the input conductance increases with the probe length while the position of the end plate affects practically only the susceptance value.

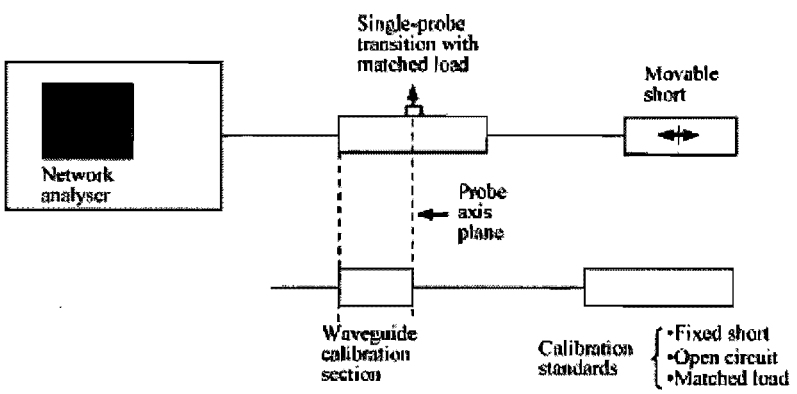

Fig. 5. Experimental arrangement for the direct measurement, at the probe axis plane, of the admittance of a single-probe transition (Fig. 4). The network analyzer yields the admittance values directly at the probe axis plane once it has been calibrated with standard terminations on an auxiliary waveguide section, the length of which ends at the probe axis plane.

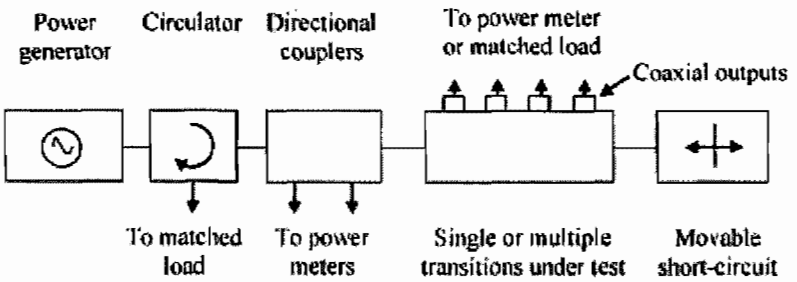

Fig. 6. Experimental arrangement for measuring the power reflected from a probe and the power transmitted to the output of a single on-centerline transition or to a given transition in an array.

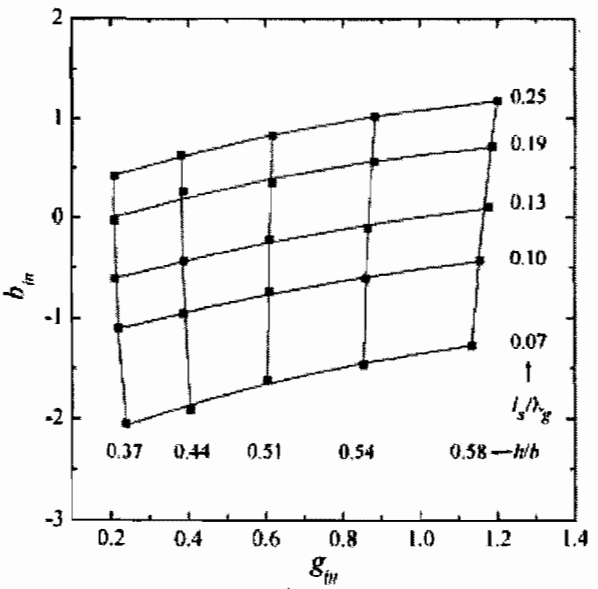

Fig. 7. Measured input admittance components of an on-centerline probe transition as seen at the probe axis plane, as measured with the network analyzer (Fig. 5).

A.1.5.2 Power reflection coefficient in the waveguide due to a single probe

Using the setup shown in Fig. 6, we measured the power reflection coefficient $R = P_R/P_I$ at the single-probe input plane with the probe located at the wide-wall centerline. For any given probe length h, we looked for the minimum value of the reflection coefficient, R_m, by adjusting l_s (which actually corresponds to cancelling out the susceptance b_{in}). The probe conductance can then be readily inferred since under such conditions:

$$g_{p0} = \frac{1 \mp \sqrt{R_m}}{1 \pm R_m}. \tag{10}$$

The ambiguity related to the ± sign in equation (10) can, in practice, be readily removed as we know that g_{p0} increases monotonously with h (Fig. 8). Fig. 8 compares the functional dependence $g_{p0}(h)$, obtained from direct measurements (network analyser) and that inferred from the reflection measurements (power meter). An analytical approximation for this dependence is also plotted in the figure. Transmission measurements (not shown) were also carried out with the network analyser that confirms the present datA.1. These measurements can be considered to be highly reproducible since the power measurements were done in Grenoble, France, while the analyser measurements were made in Montréal, Qc, CanadA.1.

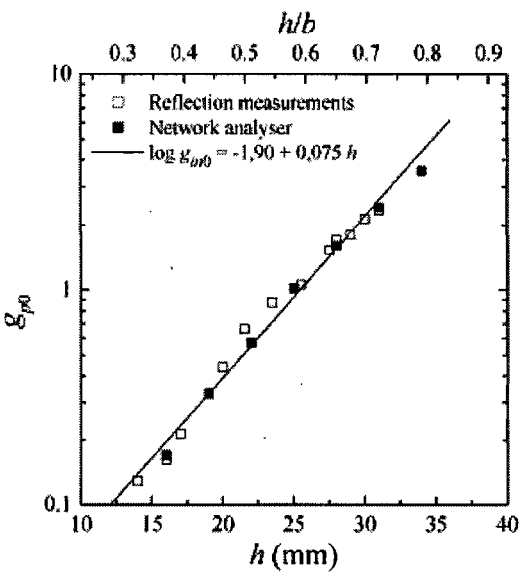

Fig. 8. On-centerline probe conductance value measured directly with the network analyzer and that inferred from power reflection using (10). An analytical approximation to those results is plotted.

A.1.5.3 Power divider frequency bandwidth

Considering a voltage standing-wave ratio (VSWR) of 1.5 (P_R/P_I = 0.04), the frequency bandwidth observed with the network analyzer center frequency set at 2.45 GHz and for a fixed short-circuit position amounts to 40 MHz and it depends, however slightly, on the number N of probes. A little retuning of the movable short circuit can still reduce the VSWR at a given frequency within this bandwidth interval.

A.1.6 Designing a power divider

A.1.6.1 Schematic representation of a compact power divider

Fig. 9 shows a schematized 3-D view of a power divider designed according to the principles developed in this paper. As suggested in Fig. 3, the probes are arranged in groups of four (two on each wide wall), located in planes that are separated axially by multiple of $\lambda_g/2$, thereby minimizing the actual length of the power divider for a given number of probes.

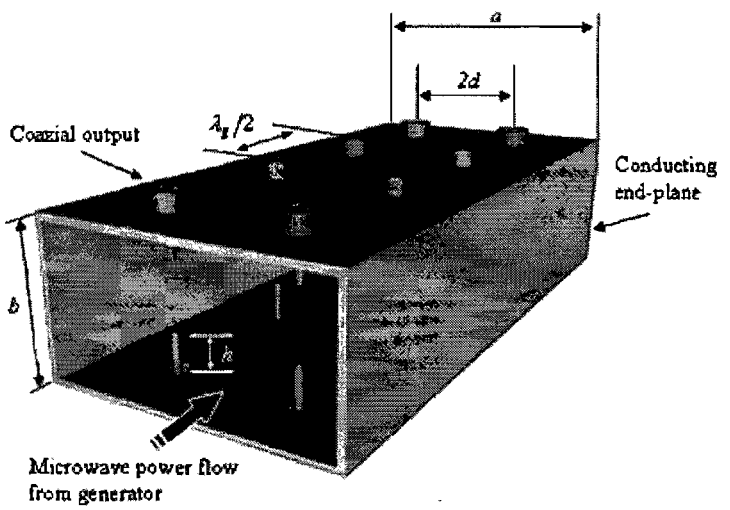

Fig. 9. Simplified 3-D representation of a power divider using the multiprobe waveguide to coaxial-line transition technique. The probes are set by groups of four, each separated by $\lambda_g/2$, yielding a compact power divider.

A.1.6.2 Design Procedure

We start by imposing the characteristics of the rectangular waveguide (i.e., its inner widths *a* and *b*), as well as those of the probe (except its length *h*) and of its coaxial output connector. Choosing the waveguide dimensions sets $\lambda_g/2$, the axial distance between the probes in the array: the wavelength λ_g in a rectangular waveguide depends on the free-space wavelength λ_g, and the waveguide wide wall width, *a*, as

$$\lambda_g = \lambda\left[1-\left(\frac{\lambda}{2a}\right)^2\right]^{-\frac{1}{2}}. \tag{11}$$

Then, assuming that the $g_{p0}(h)$ plot (as the one in Fig. 8) for the particular configuration that we just defined is available, the aim of the design procedure is finally to find *h* and *d*, the probe displacement from the centerline.

Recalling that the individual probe conductance required for a perfect match at the divider input when there are *N* coaxial power outputs imposes:

$$g_p = N^{-1}, \tag{9}$$

the required value of g_p is then obtained by adjusting both *h* and *d*. Indeed, we have from equation (4):

$$\frac{g_p}{g_{p0}} = \cos^2(\pi d/a), \tag{12}$$

where the value of g_{p0} can be taken from the $g_{p0}(h)$ plot. Clearly, the choice of the value of one of the elements of the pair (*h, d*) uniquely determines the value of the other one.

As concerns the minimum length of the power divider, as already mentioned, it is obtained by arranging the outputs by four in consecutive x-planes defined by condition (6). An estimation of this length can be calculated by assuming that l_s is approximately equal to $\lambda_g/4$ and that the distance from the input flange to the location of the first four probes is also approximately equal to $\lambda_g/4$. Then, the divider total length *L* can be expressed as:

$$L \cong \frac{\lambda_g}{2}\left[\text{Int}\left(\frac{N-1}{4}\right)+1\right] \tag{13}$$

where Int (z) denotes the integer part of the fraction z.

A.1.7 Practical realization

Any mismatch (permanent or temporary) in the load of one (or more) output line of the divider causes a reflection of power back into the waveguide that tends to unbalance the power distribution in other output lines. As a result, the distribution of power between outputs is eventually no more even and, furthermore, reflected power appears at the divider input. The essence of this effect is illustrated approximately in Fig. 10. Such a perturbation can be avoided by putting a circulator with a matched load at each coaxial output. Fig. 11 shows in situ a WR-340 power divider with 12 outputs, each equipped with a circulator. Other research groups using the current power dividers are listed in [9]–[15].

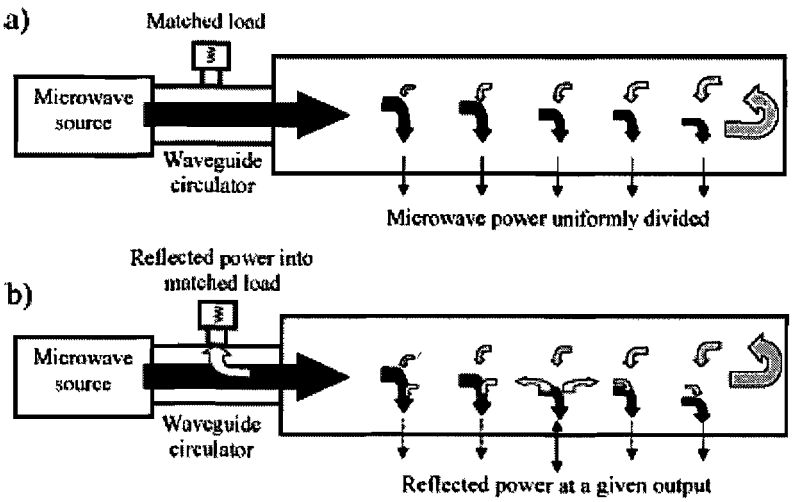

Fig. 10. Approximate representation of the power flow in the waveguide part of the divider. (a) In the case where all transitions are matched (no reflected power from any of the probes). (b) In the case where power is reflected at a given output. The diagram suggests that the nearest neighbor probes on both sides of the mismatched one pick up more power than if matching was perfect.

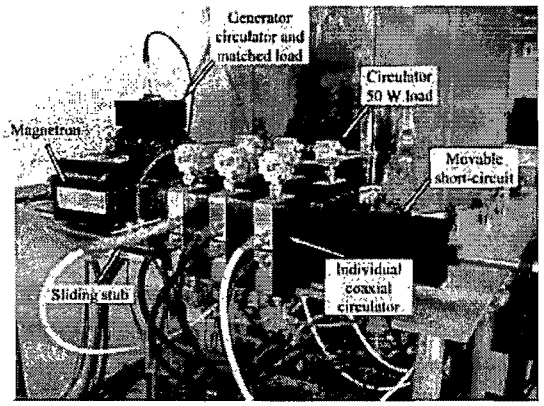

Fig. 11. Power divider (WR-340 standard waveguide) with 12 coaxial outputs, each equipped with an isolator (circulator and matched load). There is a plasma processing chamber in the background. (The power divider shown in this photograph was purchased from Metal Process, Le Pont de Claix, France, equipped with isolators manufactured by Sodhy, Saint-Ouen l'Aumône, France.)

A.1.8 Discrepancies between the calculated and measured input admittance values due to the mutual interaction between probes when given in a plane perpendicular to the waveguide axis

The equivalent-circuit representation used to determine the input admittance of our power divider (formula 8) does not take into account the eventual mutual interaction between neighboring probes. This section estimates the influence of the probe mutual interactions on the input conductance g_{in}.

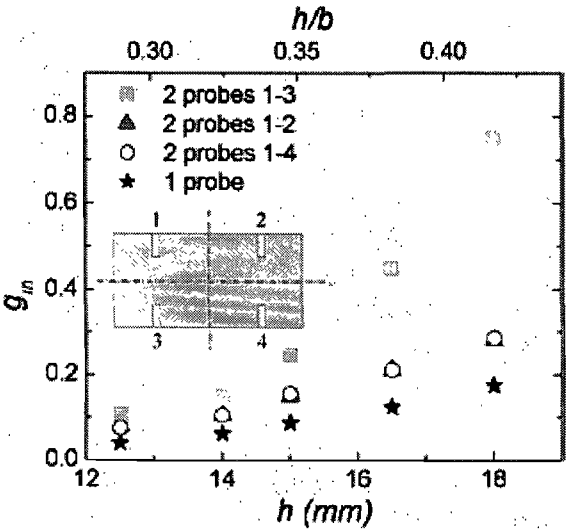

Fig. 12. Input conductance of two probes located in the same x-plane (see Fig. 3) and, as a reference, that of a single probe, as functions of the probe length h. The set of two probes are at the same distance $d = 26.0$ mm ($d/a = 0.30$) from the centerline, but at alternate possible positions with respect to the "top" and "bottom" wide walls. The input conductance g_{in} is measured directly with the network analyzer (see setup in Fig. 5).

In a first step, we consider the mutual interaction between only two probes located in the same x-plane (see Fig. 3). The inset in Fig. 12 shows that two such probes can be positioned in three different ways: probes 1–2 are located on the same wide wall of the waveguide, probes 1–3 are facing each other on opposite wide walls, and probes 1–4 are also on opposite wide walls, but they are separated symmetrically with respect to the waveguide centerline. In the following series of experiments, the probe displacement from the wide wall centerline is constant and set to $d = 26.0$ mm ($d/a = 0.30$). Fig. 12 displays the measured input conductance of the power divider (using the setup described in Fig. 5) for a group of two probes and, as a reference, for a single probe, as functions of the probe length h. Fig. 12 shows that these three different possibilities can be reduced, on practical ground, to only two distinct cases. This is because configurations 1–2 and 1–4 can be considered as being approximately similar. In contrast, when the two probes face each other (position 1–3), their mutual interaction leads to an increase of the conductance of each of them, and then g_{in} is larger than twice g_p [recall that neglecting the mutual interaction between probes leads to $g_{in} = N\, g_p$ (relation 8)]; actually, as could be expected, the mutual interaction

between two antennas facing each other increases when raising h, as the distance between their tips tends toward zero ($h/b = 0.5$).

In a second step, we consider the power divider with up to four probes located in the same x-plane and measure its input conductance. Fig. 13 shows, this time, the difference between the measured value of g_{in} and the calculated or ideal value ($g_{in} = N\, g_p$) when neglecting mutual interaction, as functions of the number of probes located in the same x-plane. The two-probe case is, in fact, that of configuration 1–2 already examined in Fig. 12; as for the three-probe case, there are two possibilities for their positioning, but because of symmetry, it turns out to be the same configuration. Fig. 13 shows that the difference g_{in} - $N\, g_p$, which reflects the discrepancies introduced by neglecting the mutual interaction between probes, is negligible for small enough h/b values. In contrast, for large h/b values, mutual interference effects come into play, which nonetheless can be compensated to provide a perfect admittance match at the divider input. This can be achieved by using, for example, the mechanical solution shown in Fig. 4, reducing by screwing in each probe (recall that $\lambda_g/2$ and d are two possible adjustment parameters, but they are already set by construction). Finally, it is worth mentioning that when N is large, say, 16 or more, since in principle $g_p = g_{in}/N$, the conductance of each probe needs to be small for a perfect admittance match at the divider input, requiring the length h to be reduced, thereby eliminating the problem of mutual interference.

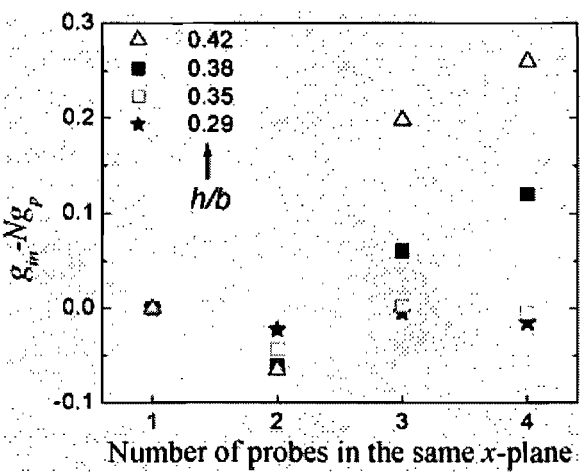

Fig. 13. Difference between the measured g_{in} value and its calculated value when neglecting mutual interaction ($g_{in} = N\, g_p$) as a function of the number of probes located in the same x-plane and for different values of the normalized probe length h/b. Each probe is displaced by $d = 26.0$ mm ($d/b = 0.30$) from the wall centerline.

A.1.9 Conclusion

We have presented a novel device that can distribute microwave power from a rectangular waveguide supplied by a single power generator to any number of output coaxial lines using probe transitions. Each coaxial line is equipped with tuning means (e.g., a sliding stub) and an isolator. The isolator ensures that the various output lines do not interfere, even when their load (e.g., a plasma source) is not well matched to the coaxial line or that their impedance varies with time. Using the equivalent-circuit method, we have elaborated the analytical expressions yielding the input admittance of such a system for the case of even power sharing between the various lines and under conditions that yield a perfect match at the waveguide input. We have also given design indications, in particular as how to make the device compact.

A.1.10 References

[1] K. J. Russell, "Microwave power combining techniques," *IEEE Trans. Microw. Theory Tech.*, vol. MTT-27, no. 5, pp. 472–478, May 1979.

[2] J. Pelletier, A.1. Lacoste, T. L. Lagarde, M. Moisan, Y. Arnal, and Z. Zakrzewski, "PCT WO01/20710," U.S. Patent 6 727 656, Apr. 27, 2004.

[3] G. L. Ragan, *Microwave Transmission Circuits*. NewYork: McGraw-Hill, 1948.

[4] R. B. Keam and A.1. G.Williamson, "Broadband design of coaxial line/rectangular waveguide probe transition," *Proc. Inst. Elect. Eng.—Microw. Antennas Propag.*, vol. 141, pp. 53–58, 1994.

[5] M. E. Bialkowski and P. J. Khan, "Determination of the admittance of a general waveguide-coaxial line junction," *IEEE Trans. Microw. Theory Tech.*, vol. MTT-32, no. 4, pp. 465–467, Apr. 1984.

[6] J. M. Jarem, "A method of moments analysis and a finite-difference time-domain analysis of a probe-sleeve fed rectangular waveguide cavity," *IEEE Trans. Microw. Theory Tech.*, vol. 39, no. 3, pp. 444–451, Mar. 1991.

[7] M. Moisan, Z. Zakrzewski, R. Etemadi, and J. C. Rostaing, "Multitube surface-wave discharges for increased gas throughput at atmospheric pressure," *J. Appl. Phys.*, vol. 83, pp. 5691–5701, 1998.

[8] H. Meinke and F. W. Gundlach, Eds., *Radioengineering Handbook* (in Russian). Moscow, Russia: Gos. Energ. Izd., 1960.

[9] A.1. Lacoste, T. Lagarde, S. Bechu, Y. Arnal, and J. Pelletier, "Multidipolar plasmas for uniform processing: Physics, design and performance," *Plasma Sources Sci. Technol.*, vol. 11, pp. 407–412, 2002.

[10] S. Bechu, O. Maulat, Y. Arnal, D. Vempaire, A.1. Lacoste, and J. Pelletier, "Multi-dipolar plasmas for plasma-based ion implantation and plasma-based ion implantation and deposition," *Surface & Coatings Technol.* , vol. 186, pp. 170–176, 2004.

[11] M. Bernard, A.1. Deneuville, T. Lagarde, E. Treboux, J. Pelletier, P. Muret, N. Casanova, and E. Gheeraert, "Etching of p- and n-type doped monocrystalline diamond using an ECR xygen plasma source," *Diamond and Relat. Mater.*, vol. 11, pp. 828–832, 2002.

[12] D.Vempaire, S. Miraglia, A.1. Sulpice, L. Ortega, E.K. Hlil, D. Fruchart, and J. Pelletier, "Plasma-based ion implantation: A valuable industrial route for the elaboration of innovative materials," *Surface & Coatings Technol.*, vol. 186, pp. 245–247, 2004.

[13] D. Vempaire, J. Pelletier, A.1. Lacoste, S. Bechu, J. Sirou, S. Miraglia, and D. Fruchart, "Plasma-based ion implantation: A valuable technology for the elaboration of innovative materials and nanostructured thin films," *Plasma Phys. and Controlled Fusion*, vol. 47, pp. A153–A166, 2005. [14] A.1. A.1. Ivanov, C. Rouille, M. Bacal, Y. Arnal, S. Bechu, and J. Pelletier, "H-ion production in electron cyclotron resonance driven multicusp volume source," *Rev. Sci. Instrum.*, vol. 75, pp. 1750–1753, 2004.

[15] P. Svarnas, M. Bacal, P. Auvray, S. Béchu, and J. Pelletier, "H-extraction from ECR-driven multi-cusp volume source operated in the pulsed mode," *Rev. Sci. Instrum.*, vol. 77, 2006, 03A512.

ANNEXE 2 Développement d'une source de plasma linéaire pour stériliser l'intérieur de tubes diélectriques médicaux

Process for the plasma sterilization of dielectric objects comprising a hollow part

(United States Patent Application Publication, US 2005 0269199 A1)

Inventors: Jerome Pollak, Michel Moisan, Bachir Saoudi, Zenon Zakrzewski

Abstract

There is provided a process for sterilizing a dielectric contaminated object having at least one hollow part. The process comprises (a) producing a plasma by submitting a gas or a mixture of gases to an electromagnetic field; (b) treating the exterior of the object by means of an after-glow of the plasma; and (c) treating the at least one hollow part of the object by means of a discharge of the plasma, the discharge being produced inside the at least one hollow part. Step (c) is carried out before or after step (b). This process is particularly useful for sterilizing various medical or dental instruments. There is also provided a device for carrying such a process.

A.2.1 Cross-reference to related applications

[0001] The present application is a continuation-in-part of PCT international patent application No. PCT/CA2003/001867 filed on Dec. 1, 2003, which claims priority on Canadian patent application No. 2,412,997 filed on Dec. 2, 2002. These applications are incorporated herein by reference in their entirety.

A.2.2 Field of the invention

[0002] The present invention relates to a process for the sterilization of dielectric objects. More particularly, the invention relates to the plasma sterilization of dielectric objects containing

hollow parts. Such objects can be contaminated, as example, with microorganisms and also with non conventional contagious agents such as pathogenic prions.

A.2.3 Background of the invention

[0003] Traditionally, in hospital quarters, sterilization of surgical instruments is carried out by impregnating them with fluids having anti-bacterial and/or antiviral effects, such as glutaraldehyde or hydrogen peroxide.

[0004] Other methods commonly used for the sterilization of contaminated objects are based on a high temperature thermal treatment of the objects. These processes however are disadvantageous in that they significantly cause damage to a large number of polymers that constitute, in whole or in part, medical and dental instruments.

[0005] Finally, sterilization methods which combine a thermal treatment with a treatment using a disinfecting liquid have been proposed. However, in addition to constituting more complex operations, these methods have the disadvantage of being associated with operations that are long lasting.

[0006] Recently, new techniques of plasma sterilization have been proposed. Patent Applications EP-00.930.937.8 and CA-A-2,395,659 describe these processes as well as devices permitting the sterilization of medical objects by resorting to plasma after-glow, for example containing argon or a mixture of N_2-O_2. These process and devices have shown themselves to be particularly adapted to the sterilization of objects for medical use, such as scalpels or surgical forceps, which are deprived of cavities of a diameter smaller than a few millimeters and a length exceeding one meter.

[0007] These processes are indeed of limited application with respect to the disinfection of objects having deep cavities such as ducts. The reason is that such objects have low hydrodynamic conductance, which makes it difficult to circulate a gas therein, at high speed, a condition that is nevertheless required for using active species (emitters of UV and radicals), with limited life span, which are produced in a plasma source outside the duct (so-called after-glow process), in order that the latter manage to inactivate microorganisms on the entire internal surface of such duct. On the other hand, a particular limitation with plasma sterilization (whether by exposure in the discharge itself or in its afterglow) resides in the treatment of pre-wrapped

objects, which is a common way of dealing with all presently known sterilization techniques. As a matter of fact, the passage of the active species of a plasma or of its after-glow through the wrapping importantly reduces the flux that reaches the surfaces of the object to be sterilized.

[0008] U.S. Pat. No. 5,393,490 describes a process for the sterilization of the surface of contaminated objects by exposing same to the electrically neutral species of an electrical discharge, while maintaining the volume without luminescence and substantially free of field by interposing a barrier between the contaminated objects and the discharge. The barrier (a metallic grid) is transparent to the neutral species and opaque with respect to the charged species that emanate from the discharge. In this case, the flux that reaches the contaminated objects is not a plasma but rather an afterglow. The temperature is kept low therein by operating cooling systems and selecting the gas(es) used to produce the after-glow. The nature of these gases, particularly that of fluorinated gases, is often such that an accelerated degradation of the treated objects if to be foreseen.

[0009] U.S. Pat. No. 5,302,343 describes a similar method of sterilization for the decontamination of the surface of contaminated objects by exposing them to neutral sterilizing species.

[0010] U.S. Pat. No. 6,589,481 describes the use of a pump system for the sterilization of lumen in the presence of peroxide.

[0011] U.S. Pat. No. 3,948,601 describes an entirely afterglow treatment of the inside and the outside of a contaminated object.

[0012] International Application W002070025 describes a process of plasma sterilization in which the contaminated objects are placed in a chamber under atmospheric pressure.

[0013] A need therefore existed for a sterilization method that is devoid of at least one of the limitations of the methods of the prior art while allowing, for example, a safe, rapid, economical and/or highly performing sterilization with respect to its purpose.

A.2.4 Summary of the invention

[0014] According to one aspect of the present invention, there is provided a process for sterilizing a dielectric contaminated object having at least one hollow part. The process comprises:

[0015] **a)** producing a plasma by submitting a gas or a mixture of gases to an electromagnetic field;

[0016] b) treating the exterior of the object by means of an after-glow of the plasma; and

[0017] c) treating the at least one hollow part of the object by means of a discharge of the plasma, the discharge being produced inside the at least one hollow part,

[0018] step (c) can be carried out before or after step (b).

[0019] According to another aspect of the present invention there is provided a process for sterilizing a dielectric contaminated object having at least one hollow part. The process comprises:

[0020] a) producing a first plasma by submitting a gas or a mixture of gases to an electromagnetic field;

[0021] b) treating the exterior of the object by means of an after-glow of the first plasma;

[0022] c) producing a second plasma by submitting a gas or a mixture of gases to an electromagnetic field; and

[0023] d) treating the at least one hollow part of the object by means of a discharge of the second plasma, the discharge being produced inside the at least one hollow part.

[0024] Step (c) can be carried out before or after step (a) and/or step (b), and step (d) is carried out after step (c).

[0025] It has been found that the processes of the present invention permit to sterilize contaminated objects having at least one hollow part with very high performance and without degradation of the sterilized objects.

[0026] According to another aspect of the invention, there is provided a device for sterilizing a dielectric contaminated object and having at least one hollow part. The device comprises:

[0027] a sterilization chamber adapted to receive the object;

[0028] a first plasma source in communication with the chamber, and adapted to produce a plasma to be used for treating the exterior of the object through an after-glow;

[0029] a second plasma source in communication with the chamber, and adapted to produce a plasma to be used for treating the at least one hollow part of the object by means of a discharge, the second source comprising a mouthpiece dimensioned so that when the latter is coupled with the hollow part of the object, the discharge is produced inside the hollow part; and

[0030] an outlet in communication with the chamber and allowing to exhaust gases produced in the chamber.

[0031] The present invention also provides another process for the sterilization of contaminated objects comprising hollow parts. This process includes at least one step in which the presence of an electromagnetic field, whether intrinsically generated by surface wave propagation, or applied from the outside, generates a plasma in the hollow parts of the contaminated object. This treatment may be combined with the sterilizing treatment of a plasma after-glow. Sterilization of the thus treated contaminated objects has the advantage for example of being carried out with very high performance and without degradation of the treated objects.

[0032] Another aspect of the present invention relates to a process that allows sterilization of a contaminated dielectric object, the latter including at least one hollow part. This process includes at least one step in which at least one electromagnetic field, having a sufficient intensity to produce a plasma inside a gas or a mixture of gases introduced into the hollow part(s) of the contaminated object, is directly applied from outside the contaminated object to the hollow part(s) or is intrinsically produced inside the hollow part(s) 00.930.937.8, more particularly in the corresponding claims as well as in International Application WO 20041011039, more particularly in the corresponding claims. These documents are incorporated by reference in the present application. The content of Applications CA-A-2,395,659 and CAA-2,273,432 is also incorporated by reference.

[0056] This type of discharge advantageously corresponds to a plasma comprising sterilizing species generated in situ by subjecting a gas flow comprising between 0.5 and 20% atomic oxygen, to an electrical field that is sufficiently intense to generate a plasma. The sterilizing species cause destruction of the micro-organisms. It should be noted that the gas has no biocidal property before its passage into the electrical field, and that the percentage of atomic oxygen in the gas flow is adjusted in a manner to obtain an UV radiation of maximum intensity. Preferably, exposure takes place in the after-glow zone or in the excitation zone of the plasma.

[0057] The electrical field of the discharge is then advantageously generated by a micro-wave discharge and the sterilizing species comprise for example photons, radicals, atoms and/or molecules.

[0058] Advantageously, in addition to atomic oxygen, the gas flow used comprises nitrogen, neon, argon, krypton, xenon, helium, oxygen, carbon monoxide, carbon dioxide, nitrogen oxides, air, and mixtures thereof.

[0059] According to another variant, in addition to atomic oxygen, the gas flow comprises nitrogen, argon and mixtures thereof, preferably the proportion of oxygen in the gas flow varies between 2% and 5%.

[0060] Temperature in the after-glow is preferably lower than or equal to 500 Celsius. This after-glow treatment is indifferently carried out in isolated fashion or repetitively in a multi-step sequential process.

[0061] The after-glow steps that can be considered comprise for example a pulsed gas in a direct electrical or electromagnetic field, a pulsed field in a gas in continuous flow, a pulsed gas in a synchronously pulsed field, a gas change, or a mixture of these steps.

[0062] A sterilization device that can be used to carry out such sterilization by after-glow is also described in Patent Application EP-A-0.0930.937.8 as comprising a plasma source associated with a sterilization chamber through a discharge tube in which there is injected a gas or a mixture of gases possibly giving the plasma, the chamber comprising an object to be sterilized, and a vacuum pump to bring in the gases into the chamber to keep it under reduced pressure. The plasma source comprises an EM field applicator such as a surfatron or a surfaguide. The sterilization chamber is entirely or partially made of Pyrex^{TM} or of aluminum, for example.

[0063] A process for sterilizing contaminated objects by after-glow is described in Application WO 20041011039 mentioned above.

[0064] This process is carried out in a sterilization chamber that is provided with at least one discharge duct. The discharge duct(s) open(s) into the sterilization chamber and is (are) supplied with a liquid or gas supply flow. The contaminated objects are treated in the sterilization chamber with sterilizing species that are present in a zone of after-glow or in a zone of excitation of a plasma that is produced, at the level of the discharge duct(s), by subjecting the gas supply flow to an electrical field and in which the ratio R=(SCD)/(SCS), in which (SCD) represents the cross-section of the discharge duct in contact with the sterilization chamber or the sum of the cross-sections of the discharge duct(s) and (SCS) is the cross-section of the sterilization chamber (SCS), agrees with the relation $0.05<R<0.70$.

[0065] Preferably, the structural characteristics of the sterilization chamber are selected so that R agrees with the relation $0.09 \leq R \leq 0.60$, still more preferably $0.15 \leq R \leq 0.5$. According to a particularly interesting embodiment $0.2 \leq R \leq 0.40$, preferably R is about 0.25.

[0066] The electrical field that generates the plasma is advantageously a high frequency field whose frequency is normally between 10 Megahertz and 3 Gigahertz, and which varies from 100 to 2450 MHz. According to a still more advantageous embodiment the frequency is between 200 and 915 MHz.

[0067] The gas supply flow may be adjusted by controlling the flow and/or the gas pressure in the chamber, so as to obtain an Ultra Violet (UV) radiation of maximum intensity. It is advantageously selected so that it flow is between 50 and 3000 cm^3 per minute.

[0068] The pressure that is generated inside the sterilization chamber is between 0.1 and 10 Torrs.

[0069] The gas flow supply advantageously comprises argon and the pressure that is generated inside the sterilization chamber is between 0.1 and 4 Torrs.

[0070] According to another variant, the gas flow comprises nitrogen and molecular oxygen and the pressure that is obtained inside the sterilization chamber is between 1 and 8 Torrs.

[0071] The gas flow supply includes at least one component selected from the group consisting of molecular oxygen, nitrogen, neon, argon, krypton, xenon, helium, oxygen, carbon monoxide, carbon dioxide, gases of formula NO_x, in which x represents a whole number selected from the group consisting of 1, 2 or 3, air, and mixtures of at least two or more of these gases.

[0072] According to an advantageous embodiment, the gas flow supply includes molecular oxygen. Preferably, the gas flow includes at least 0.10% molecular oxygen, still more advantageously at least 0.04% molecular oxygen.

[0073] According to another interesting embodiment, in addition to molecular oxygen, the gas flow supply includes at least two other gases.

[0074] Thus, in addition to molecular oxygen, at least three other gases that may for example include nitrogen, argon and helium or nitrogen, argon and nitrogen dioxide, or still molecular oxygen, xenon or krypton may be present in the gas flow supply.

[0075] The gas flow supply can be between 10 and 5000 cm^3 standard per minute, preferably this flow is between 50 and 3000 cm^3 per minute.

[0076] When the gas flow consists of NO_x, nitrogen, or an oxygen-nitrogen mixture, the pressure inside the sterilization chamber can be between 2 and 8 Torrs.

[0077] By way of illustration, the gas flow can have the following composition:

[0078] from 0.04 to 30% O_2,

[0079] from 0.05 to 99.91% nitrogen; and

[0080] from 0.05 to 99.91% argon.

[0081] Or, the gas flow can have the following composition:

[0082] from 0.04 to 30% O_2;

[0083] from 0.05 to 99.91% nitrogen; and

[0084] from 0.05 to 99.91% krypton.

[0085] Or still, the gas flow can have the following composition:

[0086] from 0.04 to 30% O_2;

[0087] from 0.05 to 99.91% nitrogen; and

[0088] from 0.05 to 99.91% xenon; or

[0089] from 0.05 to 99.91% neon.

[0090] According to another advantageous embodiment, the gas flow can have the following composition:

[0091] from 0.04 to 98.5% O_2;

[0092] from 0.05 to 99.6% nitrogen;

[0093] from 0.05 to 99.6% xenon; and

[0094] from 0.05 to 99.6% neon.

[0095] Preferably, the gas flow includes from 0.1 to 10% O_2, still more preferably it includes from 0.2 to 5% O_2.

[0096] Among the sterilizing species thus produced in the after-glow, photons, radicals, atoms and/or molecules may be mentioned. The photon and/or radical population are important, and may even constitute the most important part.

[0097] According to another interesting variant of sterilization step by after-glow, the contaminated objects are exposed, in a sterilization chamber, to a plasma that is generated in at least one discharge duct that opens in the chamber, from a N_2 gas flow, the plasma comprising sterilizing species produced when subjecting the gas flow to an electrical field that is sufficiently intense to produce the plasma. This process comprises exposing contaminated objects to the

sterilizing species, this exposure taking place in a zone of after-glow or in a zone of plasma excitation and it is characterized in that:

[0098] the percentage of molecular oxygen in the flow of gas N, is adjusted to a content x, of molecular oxygen, such that $0 < x < 0.5$ (x preferably varying from 0.1 to 0.4%), preferably by controlling the flow and/or by controlling gas pressure in the chamber, so as to obtain an UV radiation of maximum intensity;

[0099] molecular oxygen is at least partly converted into atomic oxygen; and

[0100] the cross-section of the discharge duct at its inlet into the sterilization chamber (SCD) and that of the sterilization chamber (SCS) agree with the relation $0.05 < (SCD)/(SCS) < 0.7$,

[0101] cross-section (SCD) again representing the cross-section of the discharge duct in contact with the sterilization chamber and which is perpendicular to the direction of the gas flow that feeds the discharge duct and cross-section (SCS) representing the cross-section of the chamber in contact with the discharge duct and that is perpendicular to the plasma flow.

[0102] As a variant for the production of an after-glow that is suitable for the implementation of the sterilization processes according to the invention, one may mention the exposure of the contaminated objects to a plasma that is generated in at least one discharge duct that opens into a sterilization chamber, and this from a gas flow including at least one of the gases of the group consisting of oxygen and rare gases such as helium, neon, argon, krypton and xenon, the plasma comprising sterilizing species generated when subjecting the gas flow to an electrical field that is sufficiently intense to generate the plasma, the process is characterized in that:

[0103] the gas flow is adjusted, preferably by controlling the flow and/or by controlling the gas pressure inside the chamber, so as to obtain an UV radiation of maximum intensity; and

[0104] the cross-section of the discharge duct at its inlet into the sterilization chamber (SCD) and that of the sterilization chamber (SCS) agree with the relation $0.05 < (SCD)/(SCS) < 0.70$.

[0105] The temperature inside the sterilization chamber is advantageously 60° Celsius or less, and preferably this temperature is about 30 ° Celsius. Exposure to after-glow lasts between 10 minutes and 4 hours.

[0106] This treatment step by after-glow may be carried out in isolated fashion or in a repeated manner in a multi-step sequential process, for example by using a pulsed gas in an electrical or electromagnetic field that is applied in a continuous manner, a pulsed electrical field in a gas in

continuous flow, or in a pulsed gas in a synchronously pulsed electrical field, a gas change; or a combination of these steps.

[0107] Within the framework of the present invention, a mixture of N_2-O_2, is preferably used to produce the afterglow, which makes it possible to obtain an excellent uniformity of distribution of the active species in the sterilization chamber.

[0108] Advantageously, in the step where the contaminated object is treated with an after-glow, the object is of the hollow duct type including at least two free ends, each end being provided with a mouthpiece and being placed in the sterilization chamber so that the first mouthpiece is in contact with a surface wave exciter and the second mouthpiece is connected to a pump system that exhausts the discharge effluents and, possibly, micro-organism parts, that are expelled in gas form outside the sterilization chamber.

[0109] The processes of the invention give particularly interesting results when decontaminating endoscopes, catheters and generally hollow ducts with parallel axes disposed in a cylindrical or oblong wrapping.

[0110] The parameters of the useful cycle of electromagnetic power (hereinafter called EM) produced during sterilization, for example when it operates and when it is stopped, are advantageously adjusted to prevent any damage to the wall of the channel duct, resulting from heating.

[0111] The useful power cycle EM (of the surface wave) for its part is adjusted to a value between 1 and 100%.

[0112] Treatment of the hollow part(s) with the electromagnetic surface wave preferably lasts between 45 and 120 minutes, preferably about 60 minutes and/or the temperature in the hollow tube is between 30 and 60 degrees Celsius, preferably between 30 and 45 degrees Celsius.

[0113] The excitation frequency of the plasma produced in the hollow part(s) of the contaminated object is between 10 kHertz and 10 GigaHertz, preferably this frequency is between 1 MHertz and 2500 MHertz.

[0114] The wrapping, disposed in the chamber as well as the duct, is kept opened at one end and is subject to sterilization through the after-glow or the surface wave. The opened side of the wrapping is then preferably oriented to face the source of plasma that produces the after-glow.

[0115] Once sterilization of the contaminated object is over, the object is transferred, while keeping it in a sterile environment, in the wrapping that is present in the chamber.

[0116] It is then advantageous to proceed to the sealing of the wrapping containing the object inside the sterilization chamber, for example by thermo-welding.

[0117] The contaminated object and/or the wrapping are preferably placed on removable supports independently provided in the sterilization chamber. During the process, these supports are possibly moved upwardly and laterally, depending on the needs of the sterilization steps and as a function of the size and shape of the objects to be decontaminated.

[0118] By way of illustration, a surface wave generator of the type SURFAGUIDE such as the one sold by Liquid Air, under the reference UPAS, may be used. [O1191 Under these circumstances, the operations of moving objects and/or the support inside the sterilization chamber are carried out in a sterile environment, by means of an articulated arm that is controlled from the outside.

[0119] Under these circumstances, the operations of moving objects and/or the support inside the sterilization chamber are carried out in a sterile environment, by means of an articulated arm that is controlled from the outside.

[0120] The electromagnetic surface wave exciter is disposed at one end of the duct(s) to be sterilized or, coaxially with respect to the duct, at any point along this object.

[0121] The electromagnetic field applicator may be an applicator of the capacitive type.

[0122] The EM field applicator of the capacitive type may then consist of conductive plates disposed in parallel. The parallel plates may be coated with a dielectric material and are disposed on either part of the object to be decontaminated. These plates are advantageously supplied with an EM power generator.

[0123] The electromagnetic field applicator advantageously consists of turns that produce an electromagnetic field in the dielectric duct, and this field leads to the formation of a plasma in the hollow parts of the object to be sterilized.

[0124] The external faces of the hollow duct(s) to which hollow mouthpieces have been fixed (which prevent sterilization) are subject to sterilization while in the absence of the mouthpieces, during the same step as the one used to sterilize the outer part of the contaminated object andlor its wrapping.

[0125] Another aspect of the present application consists of a sterilizing device including a sterilization chamber, the chamber being provided with a source of after-glow and a generator of

surface waves and/or a linear shaped EM field applicator, the latter two being capable of producing a plasma in the hollow part of a dielectric object.

[0126] The sterilizing chamber of this device is supplied with a plasma after-glow and is provided with a surface wave generator. The sterilizing chamber may also include means adapted to handle the objects disposed therein in a sterile manner.

[0127] The device is provided with a device for exhausting the gases from the plasma that is formed in the sterilization chamber, outside the chamber.

[0128] Another aspect of the present invention consists of a process for sterilizing contaminated dielectric objects, including at least one hollow part, the objects being disposed inside a sealed or non sealed wrapping. This process includes at least one step in which at least one electromagnetic field is produced inside the hollow part(s) of the contaminated objects andlor inside the wrapping.

[0129] Many objects may also be present simultaneously in the same sterilizing chamber and by implementing the process of the invention.

[0130] There is a definite advantage to proceed in two steps to sterilize contaminated objects, especially because it is difficult and even impossible with certain gases, to efficiently produce a discharge, simultaneously, inside a tube and on its outside, when the two media are in the same gas at the same pressure.

[0131] The process as described in U.S. Pat. No. 5,302,343 and U.S. Pat. No. 6,589,489 issued to Jacob requires the use of a barrier that filters the charged particles and only allows neutral particles to pass therethrough. Under these operating conditions, the neutral species will not easily penetrate inside the hollow tube rapidly enough to remain active. Indeed, a gas cannot circulate at high speed (essential condition for the species to remain active) inside a tube of very small diameter without producing a large pressure gradient, i.e. very high pressure at the gas admission side and low pressure at the pump side. Thus, the conditions for UV optimization are met only along a small linear section of the interior of the hollow tube.

[0132] Under these circumstances, the process according to the invention is faster and therefore more efficient.

[0133] The process according to the present invention solves this problem by using a gas stream which is nearly stationary (static) and by producing a plasma therein that will be the same all along the discharge tube, thereby ensuring the same sterilization efficiency along a hollow tube, such as an endoscope.

[0134] The surface wave that is used is of the EM wave category: see in this respect the publication of Margot and M. Moisan, Characteristics of surface-wave propagation in dissipative cylindrical plasma columns, J. Plasma Physics, vol. 49, pp 357-374 (1993).

[0135] A linear applicator such as described in Sauvé et al. (1995) IEEE Transactions on Plasma Science, vol. 43, pp. 248-256 can also be used to impose an EM field inside the hollow parts, the EM field not being produced by a surface wave, but rather with a leaky wave.

[0136] Another advantage of the present plasma sterilization process resides in the fact that the temperature of the discharge gas (T_g) remains in sufficiently weak operation either (case of the surface wave) because the EM wave operates in batch (notion of impulsion), or also because the frequency of this wave is decreased, or still (case of the linear applicator) by operating in such a way that the EM power output that is produced by the field applicator is weak (for example, by making sufficiently small holes in the wave guide in which the EM wave, that is produced by the micro-wave generator, circulates).

[0137] While the methods described in U.S. Pat. No. 5,302,342 and in U.S. Pat. No. 5,393,490 advocate either to cool the outer wrapping of the system to reach this goal, or to modify the nature of the gas mixture. Within the framework of the present application, to reach an optimization of the intensity of UV emission, one plays around with the composition of the mixture or its pressure. Generally, it is not possible to simultaneously reach a UV optimization and a reduction of the T_g.

A.2.5 Brief description of the drawings

[0138] In the following drawings which represent by way of examples only particular embodiments of the invention:

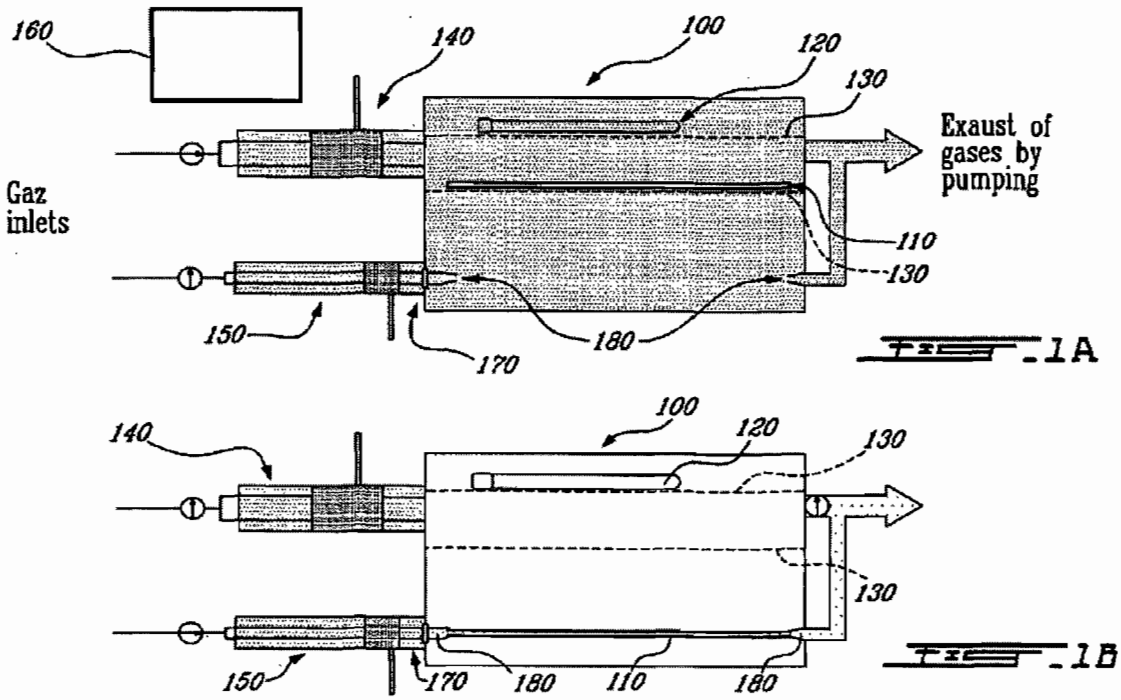

FIG. 1A

FIG. 1B

[0139] FIGS. 1A and 1B schematically represents a device for plasma sterilization according to a particular embodiment of the present invention. Such a device is used for carrying out a process according to a particular embodiment of the invention. Sterilization is carried out in two steps in which the order may Vary i.e. the step shown in FIG. 1A can be carried out before or after the step shown in FIG. 1B. FIG. 1A corresponds to the sterilization of the outside of a hollow tube and its wrapping while FIG. 2A corresponds to the sterilization of the inside of the hollow tube in which a gas circulates; in this case, a chamber containing the hollow tube is under reduced pressure: no gas circulates therein. The parts that are colored in gray are filled with a gas capable of producing a plasma and the parts that are not colored are under vacuum. The flow of gases used is controlled by means of flow-meters.

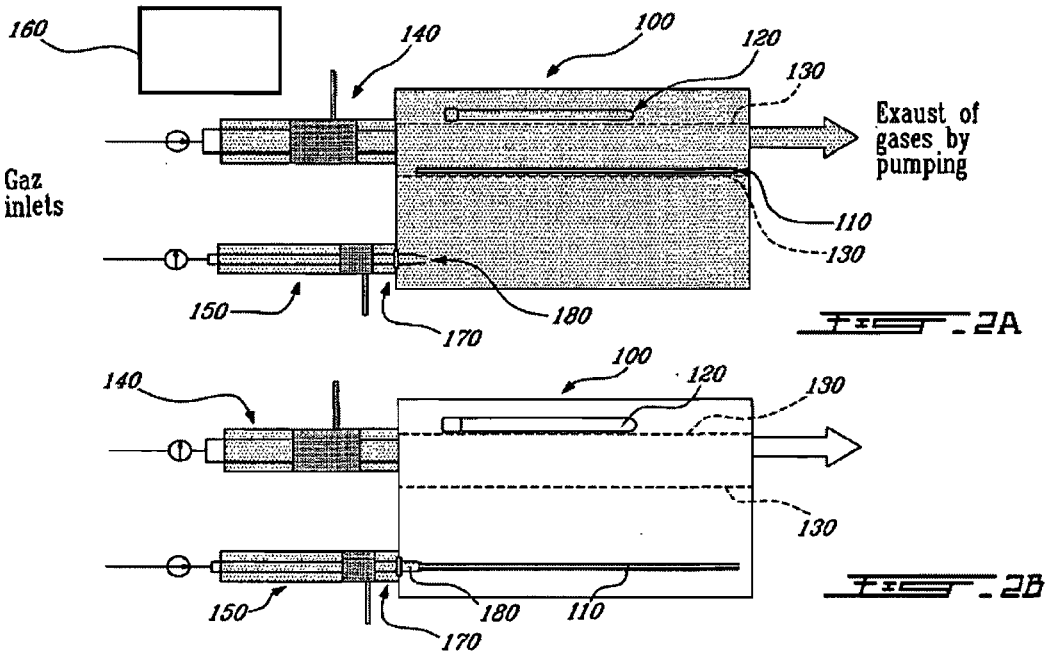

[0140] FIGS. 2A and 2B schematically represent another device for plasma sterilization according to a particular embodiment of the present invention. FIGS. 2A and 2B each represents a step carried out during a process according to a particular embodiment of the invention. As indicated for FIGS. 1A and lB, the step of FIG. 2A can be carried out after or before the step of FIG. 2B. In FIG. 2A, sterilization of the outside of a tube and its wrapping is shown, while in FIG. 2B, sterilization of the inside of the tube is shown.

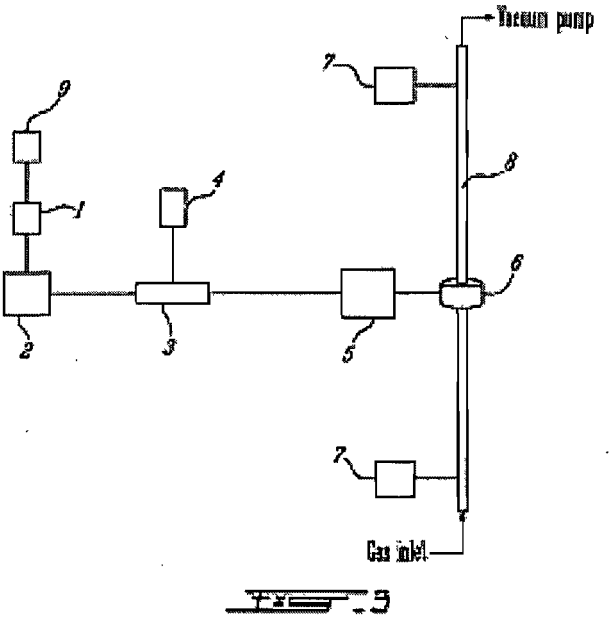

FIG. 3

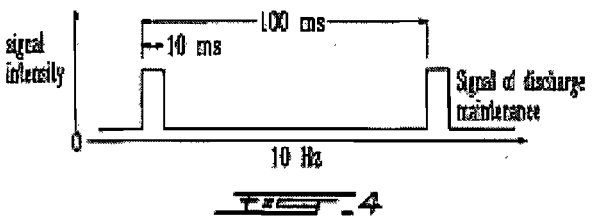

FIG. 4

[0141] FIG. 3 represents an assembly, according to a particular embodiment of the invention, for using wave surface propagation to produce a plasma inside a hollow tube made of a dielectric material without damaging the latter by heat; this is made possible by controlling gas temperature and adjusting the time during which the electromagnetic wave is produced in the gas discharge.

[0142] FIG. 4 represents the serrated pulse that guides the oscillator which feeds the amplifier that produces the electromagnetic power that is required to give the electrical discharge in a device according to another embodiment of the present invention.

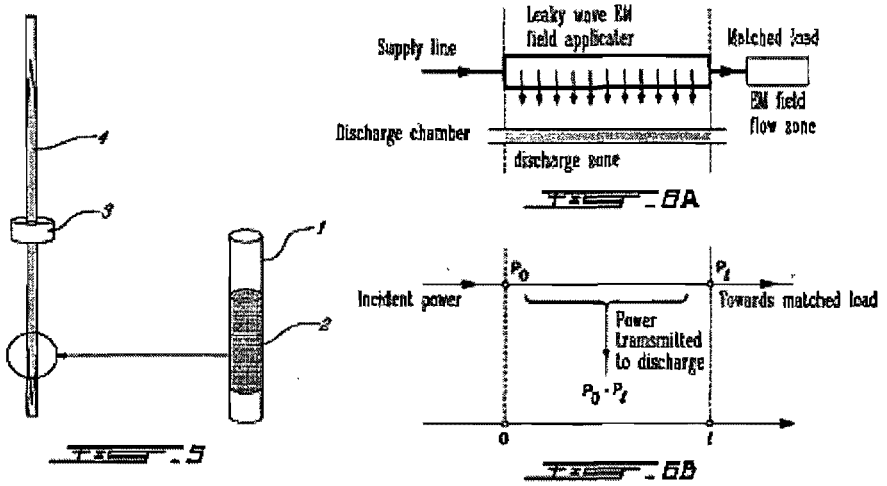

[0143] FIG. 5 shows a way to easily verify the sterilizing activity of a device according to another embodiment the invention by inserting a thin Teflon™ tube section inside the discharge tube. This section was previously contaminated with 50 µliter of a suspension containing 10^6 spores of *B. subtilis*.

[0144] FIG. 6A is a schematic representation of the principle of using an applicator of linear geometry to feed a discharge tube, that, in itself, is co-linear, and such as described in the publication of G. Sauvé, M. Moisan, Z. Zakrzewski, C. B. Bishop. IEEE Transactions on Antennas and Propagation, 43, 248-256 (1995).

[0145] FIG. 6B represents a power distribution associated with using the applicator of FIG. 6A.

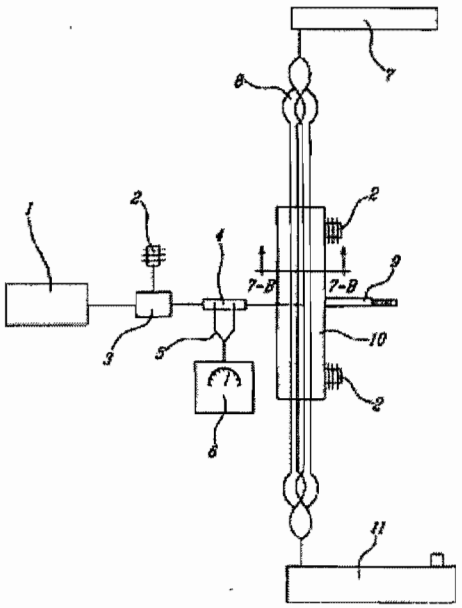

FIG. 7A

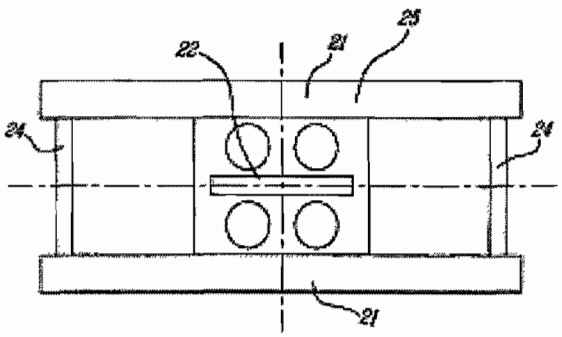

FIG. 7B

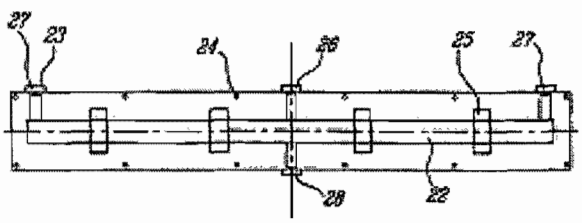

FIG. 7C

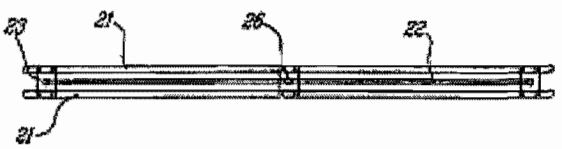

FIG. 7D

[0146] FIG. 7A shows a particular type of linear applicator, according to another embodiment of the invention, so-called tri-plate system, in conformity with the schematic diagram of FIG. 6A but particularly adapted to the simultaneous sterilization of a plurality of hollow tubes. This device operates, in this example, at the frequency of 915 MHz. The figure represents an experimental device according to the invention that makes use of a tri-plate applicator. Element (1) represents an HF generator, (2) an adapted charge, (3) a circulator, (4) a bi-directional line, (5) a trigger-circuit (switch), (6) a bolometer, (7) a bottle of gas, (8) a gas flux dividing system, (9) a short-circuit piston for impedance tuning, (10) a tri-plate applicator and (11) a pumping system.

[0147] FIG. 7B represents a cross-section view taken along the lines 7B-7B of FIG. 7A.

[0148] FIG. 7C represents a top view of the device of FIG. 7B, wherein parts have been omitted for illustration purposes.

[0149] FIG. 7D represents a side view of the FIG. 7B, wherein parts have been omitted for illustration purposes.

A.2.6 Detailed description of preferred embodiments of the invention

[0150] The preferred embodiments described hereinafter are given by way of example only and should not be interpreted as constituting any kind of limitation to the scope of the present invention.

[0151] It has been shown that the processes of the invention can achieve with success sterilization of hollow cylinders with small diameters (preferably with a diameter between 0.5-4 mm) and which are very long (preferably between 1.0-2.5 m). Such cylinders are reputed to be interiorly very difficult to sterilize with an after-glow flux.

[0152] The propagation of a surface wave inside the duct generates a plasma (discharge) in the hollow part of the dielectric duct to be decontaminated. The operating conditions are optimized in such a manner that sterilization takes place without causing damages to the internal wall of the duct.

[0153] On the other hand, the outer part of this duct may be sterilized with a plasma after-glow, using techniques that are the object of European Application number EP-A-00.930.937.8 and International Application WO 20041011039.

[0154] According to an advantageous embodiment of the present invention, it is proposed to sterilize objects outside any wrapping thereof and to proceed to their wrapping only when the sterilization cycle is over.

[0155] After having initially placed the required wrapping in the same chamber as the product to be sterilized, it is first sterilized by after-glow and this preferably takes place at the same time as the object to be wrapped. The object is then transferred, under the sterile environment of the chamber, into the wrapping, for example, by means of articulated pliers. The wrapping is then closed and sealed, for example, by thermo-welding.

[0156] A new sterilizer that is adapted for the implementation of the process according to the invention calls for two sterilization modes, namely plasma after-glow and surface wave plasma which are sequentially operated in the same chamber. This device therefore comprises two plasma sources (supplied for example by means of micro-waves) with their electrical field applicator (a wave launcher in the case of surface wave plasma). This system, which consists of a single sterilization chamber, is kept under reduced gas pressure, in the presence of a gas flow.

[0157] The processes of the invention can advantageously be carried out in a device as illustrated in FIGS. 1 to 13 of International Application No WO 2004/011039. It includes a plasma source coupled to one of the walls of the sterilization chamber by means of at least one discharge tube in which there is injected a gas or a mixture of gases possibly generating the plasma, the chamber comprising the objects to be sterilized, and a vacuum pump to bring in the gases into the chamber and keep it under reduced pressure. The plasma source comprises an electrical field applicator and the ratio R agrees with the relation $0.05 < R < 0.7$. By way of example, the electrical field applicator is of the surfatron or surfaguide type.

[0158] Use of a Surface Wave Plasma

[0159] When the material of the duct is based on polymers, therefore generally a good dielectric, it is possible to use the dielectric nature of its structure to make it a propagation medium for an electromagnetic (EM) surface wave which, at the same time, will produce and maintain a plasma inside the duct. There is thus produce a plasma inside the channel without having to introduce a conductor therein (an electrode), as this would be required if a direct current discharge would be intended (electrical field of constant intensity), for example.

[0160] Maintenance of a plasma column, inside a dielectric (glass, molten silica, for example) duct (tube), with an EM surface wave guided by this tube is described in the publication of M.

Moisan and Z. Zakrzewski, entitled "Plasma Sources Based on the Propagation of Electromagnetic Surface Waves", J. Phys. D: Appl. Phys. 24,1025-1048 (1991).

[0161] Other types of plasma may be used for the same purposes. Thus, those produced by a capacitive type discharge could be used. In this case, the hollow duct is placed between the two plane electrodes disposed in parallel relationship and supplied with an EM field. It is also possible to use a plasma that is produced by an inductive type of excitation, such as one which is advantageously produced inside the hollow tube when the latter is placed inside turns, that extend coaxially to the tube, and are supplied with an EM field.

[0162] Implementation

[0163] In order not to overly heat the duct, which could damage it, a wave excitation frequency that is preferably equal to or lower than 200 MHz is used.

[0164] Thus, the density of the plasma produced is limited. The temperature of the gas (heated by electronic collisions) is therefore reduced.

[0165] A lower temperature may be obtained or a higher frequency may however be used while the temperature of the gas is not too high, provided however that there is used a type of supply, by impulsion, of the EM output applied, that is characterized by sufficiently long idle periods.

[0166] This result is obtained by resorting, for example, to a modulation in gaps (FIG. 4) or still, to a sinusoidal modulation, of the output of the generator. The length of the idle period of the gap is selected so as to avoid exceeding a maximum temperature. A decrease of the EM wave frequency and the duration of the operation and idle periods of the EM output impulsion may also be combined so as not to exceed a desired optimum temperature.

[0167] In the examples that are presented herein, the process for sterilizing the duct is carried out following a plurality of steps, in a device such as illustrated in FIGS. 1A and 1B. A hollow tube (110), for example an endoscope and its wrapping (120), are placed on dielectric supports (130) in a sterilization chamber (100). A source of plasma (140) for producing an after-glow is connected to the upper part of the sterilization chamber (100) and the surface wave exciter (150) is connected to the lower part of the sterilization chamber (100). A microwave generator (160) is connected to the source of plasma (140) and a dielectric channel(170) is connected to the exciter (150). Arrow orientations indicate if the valve that controls gas circulation is opened (tube direction) or closed (orientation perpendicular to tube axis). In the first step of the process illustrated in FIG. 1A (note that the order of the steps shown in FIGS. 1A and 1B may be

reversed), the inside as well as the outside of the wrapping (120) as well as the hollow tube (110) are sterilized.

[0168] The outside of the tube (110) is carefully sterilized in an efficient manner. However, in view of the difficulty to rapidly circulate a gas flow inside a hollow tube (110) of small diameter, the inside of the tube is imperfectly sterilized. In the second step shown in FIG. lB, the inside of the endoscope is directly sterilized by propagating a surface wave that produces a plasma inside the hollow tube (110). When sterilizing the inside of the hollow tube (110) as shown in FIG. lB, the tube (110) is connected at each end to a mouthpiece (180).

[0169] The processes schematically represented in FIGS. (1A and 1B) and (2A and 2B) are similar. They differ only in the way the inside of the tube (110) is sterilized (see FIGS. 1B and 2B). In fact, the device used in FIG. 1B is slightly different than the one used in FIG. 2B. In FIG. 2B, as opposed to FIG. lB, one of the end of the hollow tube (110) to be sterilized is free i.e. no mouthpiece (180). Exhaust of gases from the plasma is carried out through the same orifice as the one used when operating in after-glow. Parts colored in gray are filled with a gas that is capable of producing a plasma and the parts that are not colored are under vacuum. The flow of gases used is controlled by means of a mass flow-meter. The main steps for implementing the processes are commented hereinafter.

[0170] In a first step, as shown in FIGS. 1A and 2A, the exterior of the tube (110) as well as its wrapping (120) are subject to sterilization by after-glow, preferably according to one of the processes already described in the publication of M. Moisan, S. Moreau, M. Tabrizian, J. Pelletier, J. Barbeau and L'H. Yahia entitled "Process for Sterilizing Objects with Plasma" or in the Canadian Patent Application filed on May 28, 1999 and identified under number CA-A-2,273,432, in the name of Université de Montreal. To do this, the active species are from a source of plasma with a diameter typically of 25-30 mm. During this step, the mouthpieces that are intended to be inserted on the outer faces of the duct ends, are also sterilized.

[0171] In a second step (FIGS. 1B and lA), it is the interior of the duct (110) that is subject to sterilization, this time by means of a surface wave plasma that extends along its entire length. To do this, first, an articulated arm provided with pliers (not illustrated in FIG. 1) is preferably used in order to insert the end of the duct on the (dielectric) mouthpiece (180) of the tube (110) (dielectric) that carries the surface wave exciter (150); the mouthpiece (180) of this tube connects up to the outer face of the duct (110); another mouthpiece (180) of the same type connects the

duct outlet to the pump group. Once the "interior" sterilization is terminated, the articulated arm (not shown) (always under sterile condition) is used to remove the two mouthpieces (180) from the duct (110).

[0172] In a third step, the articulated arm is used to insert the duct in a wrapping bag that is sealed, for example, under heat (thermo-welding).

[0173] In a fourth step, the sterilization chamber (100) may then be opened and the wrapped duct is recovered and transferred into the room where it may either be used immediately, or stored.

[0174] The process described above is given by way of example, and other variants that use a surface wave plasma, may be used to sterilize the interior of the tube.

[0175] Thus, among the many possible variants, in the second step already described, the end of the duct opposed to the gas inlet, may remain free. Pumping and exhausting of the effluents is then carried out as in the first step (FIG. 2B).

[0176] According to another variant, the wave launcher is positioned inside the chamber and is placed half way in the duct, thereby providing a better axial uniformity of the plasma in the duct.

[0177] Finally, according to another embodiment, it is possible to reverse the order of the two previously described steps, and this as long as it appears to be easier, even faster, to slide the duct in the launcher as well as to insert the mouthpieces on the duct even before starting the sterilizing operations, while the sterilization chamber is opened to free air.

[0178] Sterilization Gas

[0179] A sterilization gas is used for the production of the plasma after-glow and for the production of the surface wave inside the essentially dielectric object to be decontaminated.

[0180] The two Patent Applications EP-A-00.930.937.8 and PCT/CA03/01116 describe particularly advantageous embodiments of sterilization by plasma after-glow, with a N_2O_2 mixture (see also M. Moisan, S. Marceau, M. Tabrizian, J. Pelletier, J. Barbeau. L'H. Yahia, "Process for Sterilizing Objects with Plasma" and Canadian Patent Application, filed under serial number (May 28, 1999), 2,273,432 in the name of the Université de Montreal), or with pure argon, or other rare gases or gas mixtures as described in the publication of M. Moisan, N. Philip, B. Saoudi entitled "High Performing Process for Low Temperature Plasma Gas Sterilization" and Canadian Application number 2,395,659 filed on Jul. 26, 2002, in the two cases thanks to UV photons.

[0181] A good uniformity of the active sterilizing species is obtained in the after-glow chamber preferably with a mixture of N_2-O_2. It should be noted however that the N_2-O_2 mixture is more abrading on materials than argon, and this, because of the presence of atomic oxygen that is provided with a high chemical reactivity. Thus, argon may be used for sterilizing the interior of the hollow tube. The problem of spatial non uniformity of the active species does not exist, while the exterior of the duct may advantageously be sterilized by after-glow with a suitable mixture of N_2-O_2. Thus, abrasion of the duct, which is the most delicate part of this device, is minimized.

[0182] In the step of sterilizing the interior of the duct with a surface wave, the gas flow of the discharge is adjusted to a level:

[0183] that is sufficiently low not to produce an important pressure gradient in the duct; and

[0184] that is sufficiently high to ensure a good renewal of the gas and exhaust of the sterilization effluents.

[0185] Indeed, sterilization conditions for rare gases such as argon depend in a critical manner on the local pressure of the gas, because the latter acts on the intensity of emission of the UV photons as described in the publication of M. Moisan and of A. Ricard published in Can. J. Physics 55, 1010-1012 (1977). It should be noted that when there is an important pressure gradient, the pressure or the gas flow must be adjusted again during sterilization so that each duct section is successively at an optimal pressure and receives a maximum flow of photons.

[0186] Surface Wave Launcher

[0187] There are an important number of surface wave launchers that can be used for the purposed indicated. In the device described, an exciter called Ro-box, mentioned in U.S. Pat. No. 4,810,933, was preferably adopted.

[0188] Examples of Hollow Ducts

[0189] In a particularly advantageous manner, endoscopes for example those described in the U.S. Pat. No. 6,471,639 whose content is incorporated by reference into the present Application, catheters or hollow ducts assemblies with parallel axes disposed in a cylindrical or oblong wrapping, were sterilized.

[0190] Other Device

[0191] The FIGS. 7A, 7B, 7C and 7D represent an experimental device according to the invention that makes use of a tri-plate applicator. Element (1) represents an HF generator, (2) an adapted charge, (3) a circulator, (4) a bi-directional line, (5) a trigger-circuit (switch), (6) a

bolometer, (7) a bottle of gas, (8) a gas flux dividing system, (9) a short-circuit piston for impedance tuning, (10) a tri-plate applicator and (11) a pumping system. FIG. 7B represents a transverse cross-section of the tri-plate applicator illustrated by reference 10 in FIG. 7A with Teflon™ spacers holding tubes not illustrated. With (21) that represents a metallic plate, (22) a central conductive band, (23) a connector N, (24) a metal spacer, (25) a Teflon™ spacer, (26) a power input, (27) a possible service line for matched charges and (28) a possible service line of a short-circuit piston for impedance tuning. FIG. 7C represents a view from above of the device of FIG. 7A and FIG. 7B, with the upper plate removed from the tri-plate system. FIG. 7D represents a side view without tubes and spacers.

A.2.7 Examples

[0192] The following examples reported hereinafter are given purely by way of illustration and should not be interpreted as constituting any kind of limitation to the claimed object.

Example 1
Experimental Assembling and Corresponding
Results Concerning the Use of Surface Wave
Discharge for the Inactivation of *B. subtilis* Spores
Introduced into a Hollow Tube-FIG. 3.

[0193] This assembling shows how to use the propagation of a surface wave to produce a plasma inside a hollow tube of dielectric material without damaging the latter with heat and how to control the value of the gas temperature of the gas discharge to obtain this result. The temperature of the exterior of the hollow tube is advantageously measured with a thermocouple.

[0194] This embodiment of the process of the invention makes it possible to sterilize the interior of a hollow tube. In FIG. 5, element (1) represents the discharge tube, (2) the cross-section of tube 1 cm long and made of Teflon™, whose interior is contaminated, (3) a robox surface wave exciter and (4) the plasma.

[0195] The high frequency (HF) power input consists of an amplifier controlled by an oscillator, whose frequency is fixed at 100 MHz in the example. Emission of the oscillator is interrupted at a

given fixed interval as determined by a computer. One of the selected modes of operations is a gap impulse lasting 10 milliseconds followed by an idle period of 90 milliseconds, giving rise to a rhythmical pace for the impulsion, of 10 Hz (FIG. 4).

[0196] The fact of not continuously feeding the discharge permits to adjust the temperature of the gas that is in the hollow tube of which the interior is intended to be sterilized without damaging the material of which it is made. The longer the duration of the idle period, the cooler is the discharge in the hollow tube. On FIG. 4, it will be noted that the control signal of the oscillator does not go exactly to zero during the so-called idle period, which makes it possible to maintain a minimum discharge (very short length), thus avoiding to have to restart the setting up of a minimum discharge by means of an outside impulse.

[0197] The frequency of operation was lowered to the lowest value that is compatible with the impedance coupler used (circuits L (inductance) and C (capacitance) in air), such as 100 MHz, was also used for decreasing gas heating.

[0198] It appeared of interest to modify the assembling in order to be able to operate at a still lower frequency, for example a few hundreds of kHz, however in this case a coupler impedance system of a different, heavier type, must be used.

[0199] The main part of endoscopes is made of Teflon™, which is an excellent dielectric material but which does not put up with temperatures that are too high. It is considered that the maximum temperature to be used to make sure that the integrity of Teflon™ is maintained, is in theory 260 degrees Celsius. However, in practice, to prevent any deformation of Teflon™ as well as of the polymer that coats Teflon™ (often polyurethane), the temperature must be kept below 60 degrees Celsius.

Example 2

Use of Two Different Gases to Carry Out Sterilization

[0200] A) In a first case, pure argon was used to produce, inside the hollow tube, a gas discharge with a power HF of 100 MHz, by propagating a surface wave. The discharge takes place in a quartz tube (molten silica) with 3 mm internal diameter (tube in which sections 1 cm long of a Teflon™ tube, contaminated with *B. subtilis*, see FIG. 5, were slid). To make sure that the discharge is uniform along the hollow tube, a very small discharge of gas ($\leq$ 0.3 cm^3/min.) was

used. Pressure was fixed at 0.3 Torr, a value that was determined from results obtained in 26 mm tubes described in the publication of M. Moisan, N. Philip, B. Saoudi, entitled "High Performing System and Process for Sterilizing with Gas Plasma at Low Temperature" and in Canadian Application number 2,395,659 filed on Jul. 26, 2002, supposing that the intensity of UV emission directly depends on electronic temperature, which depends on a law of similars in pR (product of pressure P times radius R of the tube). Heating of the tube is then low, less than 40 to 50 degrees Celsius for operating conditions with impulse in uniform gap (active time=dead time) of 10 Hz of rhythmical pace.

[0201] In corresponding FIG. 3, element (1) represents the oscillator, (2) the amplifier, (3) the bidirectional line of power measurement, (4) the bolometer, (5) the impedance coupling box, (6) the robox surface wave exciter, (7) the gas pressure gauge, (8) the discharge tube, (9) the function generator (computer).

[0202] It was also noted that it was possible to sterilize the contaminated Teflon™ section in about 15 minutes. The maximum level of UV intensity at the pressure that was used could be optimally adjusted by proceeding to a measurement of the absorption that gives the density of population of the state of higher energy of the transition that emits UV photons.

[0203] B) A mixture of N2-O, was used in which the percentage was fixed, by means of an optical spectrometer, so as to maximize the UV intensity that is emitted at 305 nm by direct observation of the discharge light by means of an optical spectrometer. The discharge took place at 100 MHz in a tube with a diameter of 3 mm and the pressure was fixed at about 0.3 Torr, the flow being very weak as in the case of argon. Under continuous operation of HF supply, the discharge was too hot, and it is therefore necessary to use a system of operation with idle period as described in example 1 (FIG. 4). This system of operation gives rise to a temperature that does not exceed 40 Celsius.

Example 3

Linear Shaped Applicator of Micro-Wave Field Disposed Along the Hollow Tube to be Sterilized and on the Exterior Side Thereof

[0204] First, there is described the block diagram of the principle based on resorting to a linear sterilizing applicator. With reference to FIG. 6, the micro-wave power flux that is transmitted by the generator to the feeding line flows through openings in the structure of the applicator giving rise to an electrical field that allows to provide a discharge in the tube facing it, in parallel fashion. Power that is not used at the end of the applicator is dissipated in a so-called matched charge (in order to avoid a reflection of the EM wave at the end of the applicator). It is possible to imagine such a system wherein the density of the plasma produced is uniform along the tube to be sterilized. The advantage of this system is that it produces a plasma of much lower density than that of the surface wave. Thus, we can use a HF supply operating at 915 MHz and in continuous manner (no dead time) without unduly heating the discharge tube. The main disadvantage seems to be a loss of power in final instance (price to pay to ensure uniformity of discharge along the tube). The use described here of a linear applicator concerns only the sterilization of the interior of the hollow tube. To sterilize its exterior, this system must be implanted in the after-glow chamber described in FIGS. 1 and 2.

[0205] Bibliographical References

[0206] M. Moisan and A. Ricard, Can. J. Physics 55, 1010-1012 (1977).

[0207] M. Moisan, S. Moreau, M. Tabrizian, J. Pelletier, J. Barbeau, L'H. Yahia, "Process for Sterilization of Objects with Plasma" (Canadian Patent Application, serial number of filing (May 28, 1999), 2,273,432 in the name of Université de Montreal.

[0208] M. Moisan, S. Moreau, M. Tabrizian, J. Pelletier, J. Barbeau, L'H. Yahia, "System and Process of Sterilization by Gas Plasma at Low Temperature", International Patent Application (Patent Cooperation Treaty (PCT)), number PCT/CA00100623 (May 26,2000) in the name of Université de Montreal. Publication of this Application under number WO 00172889 dated Dec. 7, 2000.

[0209] M. Moisan, N. Philip, B. Saoudi, "High Performing System and Process for Low Temperature Plasma Gas Sterilization", Canadian Patent Application Number 2,395, 659 filed Jul. 26, 2002.

[0210] M. Moisan. Z. Zakrzewski, U.S. Pat. No. 4,810,933 (Mar. 7, 1989).

[0211] M. Moisan, Z. Zakrezewski, "Plasma Sources Based on the Propagation of Electromagnetic Surface Waves". J. Phys. D: Appl. Phys. 24, 1025-1048 (1991).

[0212] Although the present invention has been described by means of specific implementations, it is understood that many variations and modifications may be grafted to the implementations, and the present invention aims at covering such modifications, uses or adaptations of the present invention following in general, the principles of the invention and including any variation of the present description which will become known or conventional in the field of activity in which the present invention is found, and that may apply to the essential elements mentioned above, in accordance with the scope of the following claims.

A.2.8 Claims

What is claimed is:

1. A process for sterilizing a dielectric contaminated object having at least one hollow part, said process comprising:

a) producing a plasma by submitting a gas or a mixture of gases to an electromagnetic field;

b) treating the exterior of said object by means of an after-glow of said plasma; and

c) treating said at least one hollow part of said object by means of a discharge of said plasma, said discharge being produced inside said at least one hollow part, wherein step (c) is carried out before or after step (b).

2. The process of claim 1, wherein said gas comprises molecular oxygen, nitrogen, neon, argon, krypton, xenon, helium, oxygen, carbon monoxide, carbon dioxide, gases of formula NO_x, in which x represents a whole number selected from the group consisting of 1, 2 or 3, or air.

3. The process of claim 1, wherein said mixture of gases comprises at least two gases selected from the group consisting of molecular oxygen, nitrogen, neon, argon, krypton, xenon, helium, oxygen, carbon monoxide, carbon dioxide, gases of formula $NO_{,,}$ in which x represents a whole number selected from the group consisting of 1, 2 or 3, and air.

4. The process of claim 1, wherein said mixture of gases is a mixture of N, and O_x.

5. The process of claim 1, wherein the electromagnetic field is one produced by a surface wave.

6. The process of claim 1, wherein the contaminated object is a cylindrical hollow duct.

7. The process of claim 6, wherein the ratio obtained by dividing the length of the cylinder that constitutes the contaminated object by the diameter of the cylinder is between 5.10^3 and $0.3.10^3$.

8. The process of claim 6, wherein said hollow duct includes at least two free ends, each end being provided with a dielectric mouthpiece and positioned in a sterilization chamber so that a first mouthpiece is in contact with a surface wave exciter and that a second mouthpiece is connected to a pump system that exhausts effluents from the discharge.

9. The process of claim 1, wherein the contaminated object is a hollow tube.

10. The process of claim 1, wherein treatment of the hollow part(s) with the electromagnetic surface wave lasts between 45 and 120 minutes andlor the temperature in the hollow tube, during the treatment, is between 30 and 60 degrees Celsius.

11. The process of claim 1, wherein the frequency of excitation of the plasma during the discharge is between 10 kHz and 10 GHz.

12. The process of claim 1, wherein the frequency of excitation of the plasma during the discharge is between 1 MHz and 2500 MHz.

13. The process of claim 1, wherein a wrapping adapted to receive said object is treated during said after-glow.

14. The process of claim 13, wherein the interior part of the wrapping is oriented to face a source where said afterglow plasma is produced.

15. The process of claim 13, wherein, once sterilization is over, the sterilized object is transferred, while keeping a sterile environment, into said wrapping that is present in a chamber where said process is carried out.

16. The process of claim 15, further comprising the step of sealing said wrapping containing the sterilized object by a thermo-welding process.

17. The process of claim 1, wherein said object is selected from the group consisting of endoscopes, catheters and hollow ducts assemblies with parallel axes disposed in a cylindrical or oblong envelope.

18. The process of claim 1, wherein the hollow part of said object is first treated, and the exterior of said object is thereafter treated.

19. A process for sterilizing a dielectric contaminated object having at least one hollow part, said process comprising:

a) producing a first plasma by submitting a gas or a mixture of gases to an electromagnetic field;

b) treating the exterior of said object by means of an

after-glow of said first plasma;

c) producing a second plasma by submitting a gas or a mixture of gases to an electromagnetic field; and

d) treating said at least one hollow part of said object by means of a discharge of said second plasma, said discharge being produced inside said at least one hollow part, wherein step (c) is carried out before or after step (a) and/or step (b), and step (d) is carried out after step (c).

20. The process of claim 19, wherein said gas in step (a) comprises molecular oxygen, nitrogen, neon, argon, krypton, xenon, helium, oxygen, carbon monoxide, carbon dioxide, gases of formula NO_x, where x represents a whole number selected from the group consisting of 1,2 or 3, or air.

21. The process of claim 19, wherein said mixture in step (a) comprises at least two gases selected from the group consisting of molecular oxygen, nitrogen, neon, argon, krypton, xenon, helium, oxygen, carbon monoxide, carbon dioxide, gases of formula NO_x, where x represents a whole number selected from the group consisting of 1, 2 or 3, and air.

22. The process of claim 19, wherein said gas in step (c) comprises molecular oxygen, nitrogen, neon, argon, krypton, xenon, helium, oxygen, carbon monoxide, carbon dioxide, gases of formula NO_x, where x represents a whole number selected from the group consisting of 1, 2 or 3, or air.

23. The process of claim 19, wherein said mixture in step (c) comprises at least two gases selected from the group consisting of molecular oxygen, nitrogen, neon, argon, krypton, xenon, helium, oxygen, carbon monoxide, carbon dioxide, gases of formula NO_x, where x represents a whole number selected from the group consisting of 1, 2 or 3, and air.

24. The process of claim 19, wherein the first plasma is produced from a mixture of N, and O,.

25. The process of claim 19, wherein the second plasma is produced from argon.

26. A device for sterilizing a dielectric contaminated object and having at least one hollow part, said device comprising:

a sterilization chamber adapted to receive said object;

a first plasma source in communication with said chamber, and adapted to produce a plasma to be used for treating the exterior of said object through an afterglow;

a second plasma source in communication with said chamber, and adapted to produce a

plasma to be used for treating said at least one hollow part of said object by means of a discharge, said second source comprising a mouthpiece dimensioned so that when the latter is coupled with the hollow part of said object, said discharge is produced inside the hollow part; and an outlet in communication with said chamber and allowing to exhaust gases produced in said chamber.

27. The device of claim 26, further comprising another outlet in communication with said chamber, said another outlet comprising a mouthpiece dimensioned so that when the latter is coupled with the hollow part of said object, gases produced inside the hollow part, during the discharge, are exhausted through the latter so as to avoid contact of the gases with said object.

28. The device of claim 26, characterized in that said object is a hollow tube, and in that one of the ends of the tube is adapted to be coupled with the mouthpiece of the second plasma source, and that the other end of the hollow tube is adapted to be coupled with the mouthpiece of the other outlet, so that the discharge is carried out inside the tube thereby avoiding contact between the exterior of the tube and the second plasma, its discharge and the gases produced during the latter.

29. The device of claim 28, wherein the sterilization chamber includes one or more supports.

30. The device of claim 29, wherein the support(s) are adjustable with respect to their position in said chamber.

31. The device of claim 26, wherein said sterilization chamber includes means for handling said object placed therein in a sterile manner.

ANNEXE 3 Développement d'une source de plasma linéaire pour stériliser des objets médicaux par immersion

Device and method for inactivation and/or sterilisation using plasma

(US patent application 60/884,344)

Inventors: J. Pollak and M. Moisan

Abstract

The invention concerns a method of sterilization and/or inactivation of at least one surface of at least one contaminated object. The method being characterized in that one subjects the surface to the discharge plasma generated from an applicator of electromagnetic field of linear type, the plasma having a temperature and an absorbed power per unit of volume predetermined by the operating conditions, so as to sterilize the surface without significantly degrading it. The invention also concerns a device enabling the sterilization and/or inactivation of at least one surface of at least one contaminated object by means of a plasma. This method and this device can be used to sterilize or inactivate several types of objects, such as packages, films, metal plates, dielectric plates, prosthesis used in the medical field, etc.

A.3.1 Field of the invention

The present invention concerns the sterilization and/or inactivation by plasma of contaminated objects, such as those contaminated with micro- organisms. In particular, the invention concerns a method of plasma sterilization of various objects, such as three-dimensional objects.

A.3.2 Background of the invention

The field of sterilization of heat-sensitive three-dimensional objects continues to be the subject of much research. Traditionally, this sterilization is done by impregnating the objects being

treated with fluids such as peracetic acid, glutaraldehyde, or hydrogen peroxide or by thermal treatments (dry or moist heat).

Plasma sterilization is emerging as a novel alternative to conventional sterilization techniques. Plasma sterilization offers promising features in terms of efficiency and reliability for inactivating micro-organisms. In addition, this technique can be made to operate at low temperatures (< 50 °C), does not require venting time and is safe for the operators, patients and materials. The understanding of plasma sterilization is advancing rapidly, raising high scientific and commercial interests in the development of various types of plasma sterilizers. Nevertheless, no sterilizer making use of the plasma biocide species has yet been brought to the market place. Various reasons can be put forward to explain such a delay: 1) The level of damage induced on the various types of surfaces exposed to such a plasma treatment is an essential issue that has not yet been thoroughly assessed. In particular, as many medical devices (MDs) comprise polymers, the etching of polymers by such a process must be very small, allowing for many re-sterilization cycles. An alternative solution which would permit to avoid substantially degrading or damaging the MDs would be highly desirable. Moreover, variations in the hydrophobicity and biocompatibility of the processed surfaces (intended for limited or extended time of contact with tissues or body fluids) must be scrutinized. 2) Plasma sterilization of MDs must meet the requirements of hospital standards. In that respect, it is customary to sterilize MDs already enclosed in wrapping materials that protect them afterwards from external contamination during transportation and through storage time. However, the various wrapping materials presently used for that purpose are not compatible with a plasma afterglow sterilization process. This is because they strongly absorb UV radiation and also reduce the diffusion toward the MDs of the various plasma particles, namely atoms (e.g. oxygen radicals) and molecules (already present or newly formed), species that are eventually excited (becoming potential UV photon emitters) or ionised. An alternative solution which would permit the inactivation or sterilization of an object located inside a dielectric package would be highly desirable. 3) All parts of a MD should be exposed to substantially the same density or flux of the plasma species, which requires uniformity of the plasma biocide species everywhere in the sterilizer. As an example, consider the case of a plasma sterilizer filled with a large number of MDs: shadowing effects caused by an MD on a nearby other MD are possible, as well as local depletion of the active species (loading effect resulting, for instance, from surface recombination of the plasma species).

Several systems making use of the post-discharge of a plasma have recently been proposed. International application W02004/050128 describes a method of plasma sterilization of objects

of basically dielectric nature and containing a hollow part. In this document, the contaminated objects, and possibly also their packaging, are subjected alternately to the post-discharge of a plasma and to an electromagnetic field of sufficient intensity to create a plasma inside the hollow parts.

A.3.3 Summary of the invention

One aspect of the present invention relates to a method of sterilization and/or inactivation of at least one surface of at least one contaminated object. The method comprises submitting the at least one surface to a plasma discharge generated from an applicator of electromagnetic field of linear type. The plasma can have a temperature below 80 °C, and an absorbed power per unit of volume of plasma of less than 20 W / LI so as to sterilize and/or inactivate the at least one surface without substantially degrading it.

Another aspect of the present invention concerns a device enabling the sterilization and/or inactivation of at least one surface of at least one contaminated object using a plasma. The device comprises:

- a chamber adapted to receive the object to be treated and a discharge of the plasma; and
- an applicator of electromagnetic field of linear type, adapted to generate the plasma discharge in the chamber so as to sterilize the at least one surface without damaging it in substantial manner.

It has been shown that this method and this device for sterilization and/or inactivation of objects can handle various objects, such as three- dimensional objects including but not limited to packaging films, dielectric or metallic plates, medical prosthesis and/or their packaging, etc. These objects are immersed in a plasma containing, for example, species (UV, radicals, ions) having bactericidal properties. The sterilization of these contaminated objects, such as objects contaminated by 10^6 reference spores, is done quickly (for example, in less than 10 minutes or less than 1 minute) and at low temperature (e.g., temperature below 40 °C). Moreover, this method and device do not substantially degrade the objects being sterilized, it is nontoxic, and does not require any venting step after exposure to the plasma.

It was also observed that peculiar interesting features of the device and method of the present invention comprise a low gas temperature and a broadband impedance matching of the plasma source with no need for retuning, as well as stability and reproducibility of the discharge (non resonant behavior).

One or more three-dimensional object can be subjected directly to the bactericidal species of a plasma created in a chamber. This plasma can be engendered by an EM wave, propagating along the linear applicator. The plasma can occupy nearly ail of the volume of the chamber, except for that taken up by the objects being sterilized. This plasma can be cold (e.g., a temperature below 40 OC) and thus it only slightly heats the objects being sterilized. This is a result of the low power absorbed per unit of volume of the plasma created (for example, less than 20 W/L).

When using the method and device of the present invention inactivation and/or sterilization can be carried out, for example, by subjecting the contaminated object to the discharge of the plasma for a period of less than 60 minutes, less than 30 minutes, less than 15 minutes, less than 10 minutes, less than 5 minutes, or less than 1 minute. The temperature of the plasma can be, for example, less than 70 °C, less than 60 °C, less than 50 °C, less than 40 °C, less than 35 °C, less than 30 °C, or less than 20 °C. For example, the power absorbed per unit of volume of plasma can be less than 15 W/L, less than 10 W/L, or less than 5 W/L. The at least one object can be subjected to at least two treatments by the action of the discharge of the plasma: the object can be repositioned inside the chamber of the applicator of electromagnetic field of linear type between each treatment so as to treat all the surfaces of the object.

After a predetermined period of time, the power input and output of the applicator of electromagnetic field of linear type can be reversed so as to achieve a uniform treatment. The at least one surface can be treated in succession as it is introduced into the applicator. In such a case the object is in movement into the device and a portion is treated and when the portion is sterilized and/or inactivated, this portion exits the device and the successive portion is then treated.

The plasma can be generated by means of at least one high-frequency generator able to operate at a frequency of about 13.56 MHz to about 2.45 GHz or about 200 MHz to about 5.8 GHz. The plasma can comprise at least one rare gas for example argon. The plasma can also comprise N_2, CO_2, and/or O_2.

At least two objects can also be treated simultaneously by the plasma in the method and device of the invention. For example, the at least two objects can be treated simultaneously by the applicator, each of the objects being arranged, in the applicator, in a different chamber. The chambers can be insulated from each other. The same or different conditions of plasma generation can be applied in the chambers.

The at least one object being sterilized can be arranged in the sterilization chamber of the applicator so as to simultaneously sterilize all the outer surfaces of the object. Such an object

can be, for example, a medical device, a dielectric film, such as agri-food industry packaging film or medical packaging film. For example, a film can be sterilized as it is rolled off. The film can be entering the chamber of the applicator at a predetermined height of the chamber, then leaving the chamber without interrupting the sterilization process or the electromagnetic power serving to maintain the plasma, the two surfaces of the dielectric film being then inactivated or sterilized simultaneously under the action of the bactericidal species of the plasma. For example, two dielectric films can be simultaneously inactivated or sterilized, then sealed in succession by thermal welding at certain spots.

The lower or upper surface of a dielectric plate, in contact with the plasma, can be disinfected or sterilized in succession. For example, a dielectric plate, such as one made of glass or fused silica, can move past inside the applicator, so that the lower surface and the upper surface of this dielectric plate can be inactivated or sterilized at the same time. The object to be treated can be a metal plate, moving past inside the applicator, so that the lower surface and the upper surface of this plate are inactivated or sterilized at the same time.

The at least one object can be sterilized directly inside its package (for example a film). The plasma can be created outside the object, as well as in a sufficient volume included between the package and the object.

Sterilization and/or inactivation of the at least one surface of the at least one object can be done without causing erosion to the surface. Determination of such an erosion-free treatment can be made by observing and comparing polystyrene micro-spheres by means of Scanning Electron Microscopy before and after sterilization and/or inactivation.

Sterilization and/or inactivation can be carried out in a chamber, and wherein at least one wall defining the chamber comprises at least one aperture so as to simultaneously permit treatment of at least one other object disposed outside of the chamber by means of a flowing afterglow of the plasma. The at least one wall can comprise a plurality of apertures, the apertures being adapted so as to prevent affecting propagation of an electromagnetic field along a transmission line. For example, the apertures can have a size which is at least three times inferior to the width of a conducting strip.

The applicator of electromagnetic field of linear type can comprise at least one conducting strip such as a metal strip extending from one end of the chamber to its opposite end. Alternatively, the applicator of electromagnetic field of linear type can comprise at least one metal strip having two opposite ends, the ends being in contact with a single one of the ends of the chamber. The strip can have an essentially constant width. Alternatively, the strip can have a width varying between the two ends. For example, the width of the strip can vary in an

essentially increasing manner from an HF input to an output (load). The strip can include at least one curved portion. The applicator can further comprise a power divider. The field applicator can be an applicator of high-frequency field having a planar configuration. A planar transmission line can be used. For example a strip line, such as a three-plate line or a microstrip line can be used.

The geometry of the conducting strip and/or the ground plate of the applicator of electromagnetic field can be linear, circular, or of some other shape.

The sterilization chamber can comprise one or more dielectric supports to hold the objects being sterilized. The chamber can also comprise one conducting strip and at least one dielectric plate so as to insulate the strip from the plasma discharge.

The electromagnetic field applicator can be of distributed type. The latter can be formed by at least two planar transmission lines, each one extending for the entire length of the applicator. For example, there can be a network of linear applicators. The applicators can be compartmentalized so as to prevent risks of cross contamination between the various objects being sterilized and enabling treatments by different plasmas in each compartment.

The method and device of the present invention can comprise means for introducing the at least one object to be treated into the chamber for a predetermined period of time, and for removing it when sterility and/or inactivation is achieved.

The device and method of the present invention can be adapted to treat a moving object in continuous manner. They can comprise means for introducing at least one part of the at least one object to be treated into the chamber for a predetermined period of time, and for removing it when sterility and/or inactivation is achieved for this part. The means thus making it possible to treat the object in succession and in continuous manner.

At least one wall defining the chamber can be provided with at least one aperture adapted to permit a flowing afterglow of the plasma to diffuse outside the chamber. Such a configuration enables treatment of at least another object disposed outside the chamber. The at least one wall can comprise a plurality of apertures. The apertures are adapted so as to prevent affecting propagation of an electromagnetic field along the transmission line.

The apertures can have a size which is at least three times inferior to the width of the conducting strip.

The distance between the conducting strip and an upper end and/or a bottom end of the chamber can be constant.

The distance between the conducting strip and an upper end and/or a bottom end of the chamber can be decreasing from an inlet to an outlet of the chamber.

The distance between the conducting strip and an upper end and/or a bottom end of the chamber can be variable from an inlet to an outlet of the chamber.

Various sterilized and/or inactivated objects can be obtained by implementing the method of the present invention and by using the device of the invention.

The present invention also involves a device comprising:

- a generator or a set of generators of high frequency (HF), able to operate at a frequency between 13.56 MHz and 2.45 GHz or 200 MHz and 5.8 GHz;
- a transmission line (e.g. a coaxial cable) able to transmit the power of the generator to the HF field applicator;
- a HF field applicator, of linear type, able to create a plasma from a gas (or gas mixture) subjected to its action;
- an adapted load, placed at the end of the line and serving to dissipate the power not used to maintain the plasma. In another mode of operation, this adapted load can be replaced by a short circuit or by a second power supply, coming from either the same generator or from another generator; and
- a detector of ultraviolet (UV) radiation.

The term HF can designate jointly radio and microwave frequencies.

The present invention can find application, for example, in the sterilization of heat-sensitive medical prosthesis. However, the invention is not limited to the field of sterilization of medical prosthesis. For example, it can also be applied to the disinfection or sterilization of plane surfaces in a moving process, for example, the surfaces being used in the food industry.

A.3.4 Brief description of the figures

The present invention can be illustrated without being limited to the following examples, in which:

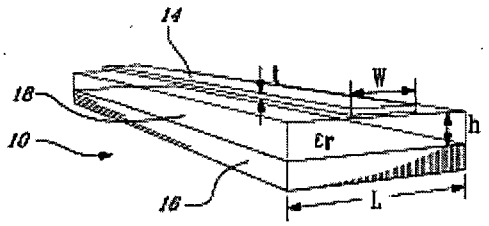

FIG. 1A

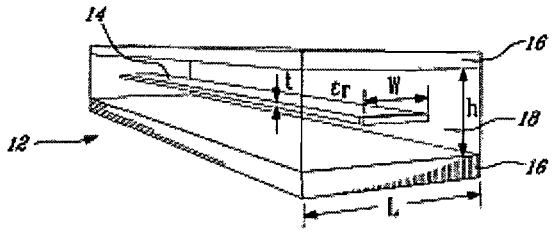

FIG. 1B

Figure 1 shows a perspective view of a schematical representation of two devices according to particular examples of the present invention, in which the device comprises a microstrip line (1a) and a three-plate line (1b);

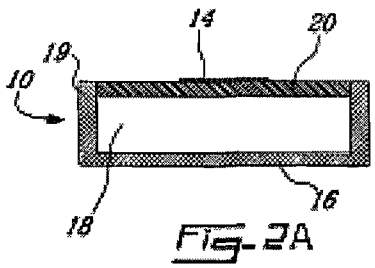

FIG. 2A

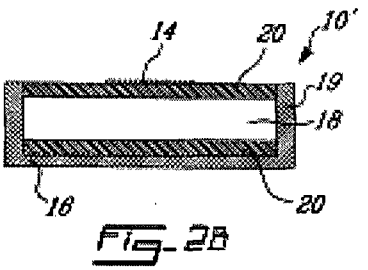

FIG. 2B

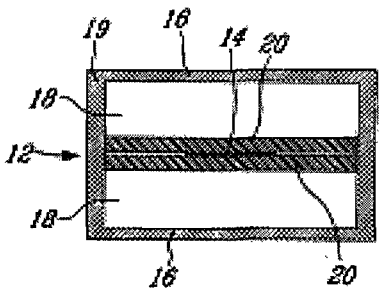

FIG. 2C

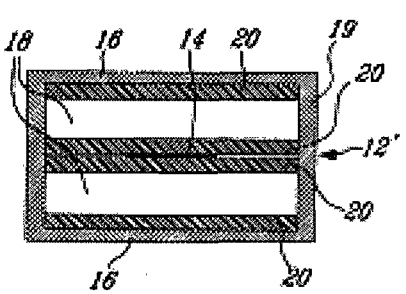

FIG. 2D

Figure 2 shows a schematical cross section view of four different examples of devices of sterilization according to different embodiments of the present invention, the applicators in Figure 2a and Figure 2b having a microstrip line as defined in Figure la, while the applicators in Figure 2c and Figure 2d have a three-plate line as defined in Figure 1b;

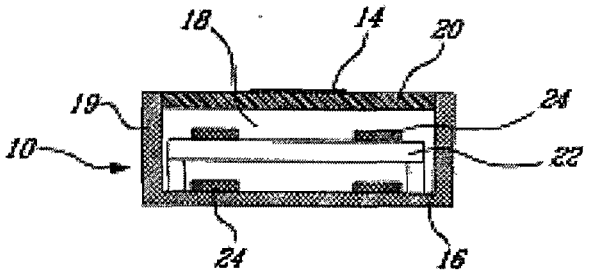

FIG. 3

Figure 3 shows a schematical cross section view of the linear applicator shown in Figure 2a in which a dielectric support meant to hold one or more objects to be sterilized has been inserted in the sterilization chamber;

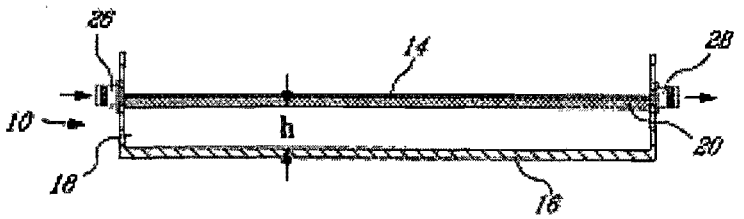

FIG. 4A

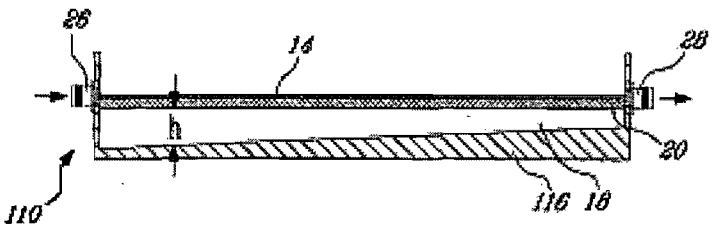

FIG. 4B

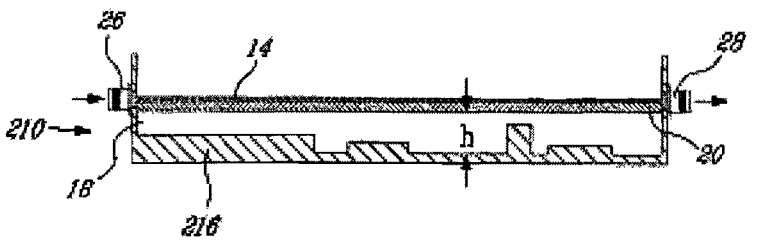

FIG. 4C

Figure 4 shows a schematical cross section view of three sterilization devices according to different examples of the present invention, the three systems having different axial configurations of the ground conductor: 4a "classical" configuration with h constant; 4b "ramp" configuration where h varies as a linear function of the axial position, and 4c configuration where h varies axially in some way;

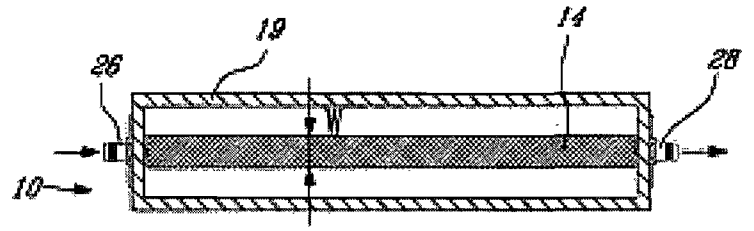

FIG. 5A

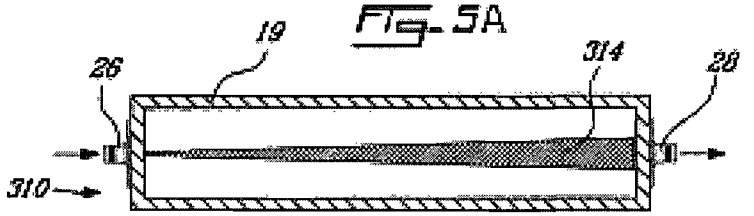

FIG. 5B

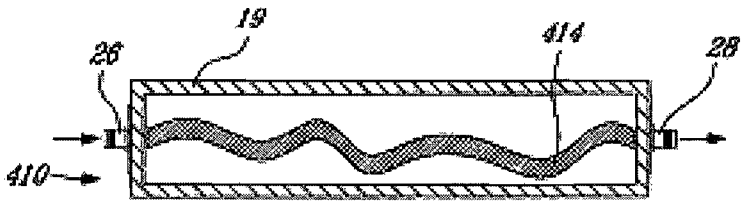

FIG. 5C

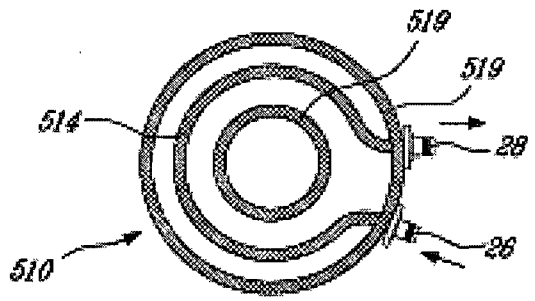

FIG. 5D

Figure 5 shows a schematical top view of four different sterilization systems according to particular examples of the present invention, the systems having four different configurations of the central conducting strip: 5a constant width, 5b variable width, 5c any configuration, of constant width or not, and 5d circular geometry;

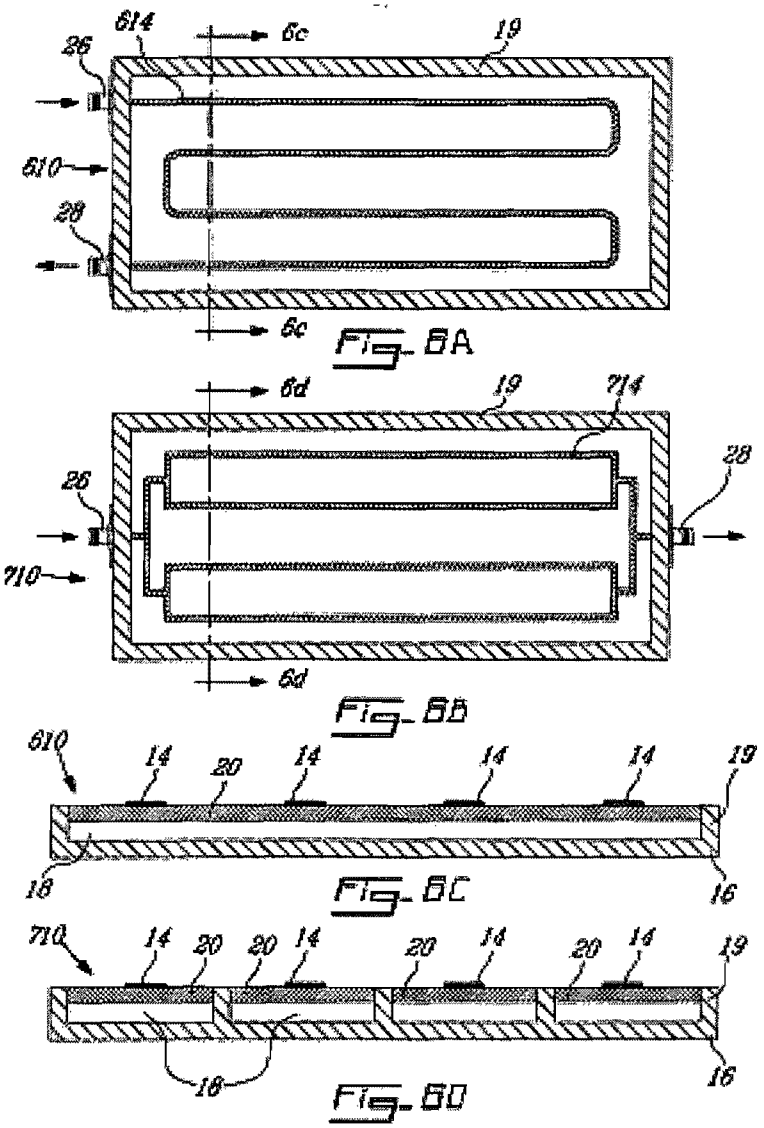

Figures 6a and 6b schematically represent top views of various networks of linear applicators according to particular examples of the present invention, in which Figure 6a represents a structure not containing a power divider system; Figure 6b a structure containing a power divider system located inside the applicator; while Figures 6c and 6d represent, respectively, cross section views of devices of Figures 6a and 6b taken along lines 6c-6c and 6d-6d, wherein Figure 6c shows a device with a single chamber, and Figure 6d a device with partitioned compartments;

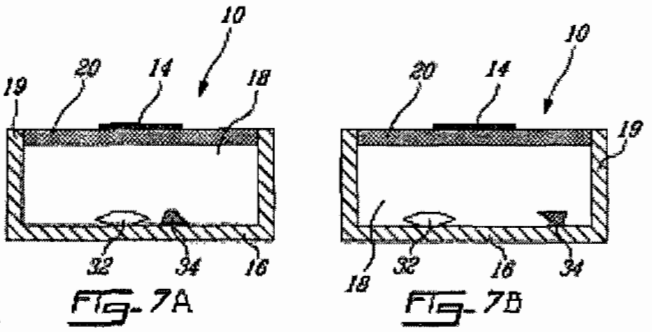

Figure 7a and 7b represent schematical cross section views of a system of sterilization of a three-dimensional object according to a particular example of the present invention, in 7b the object as well as its package have been turned over and shifted laterally and/or axially with respect to 7a;

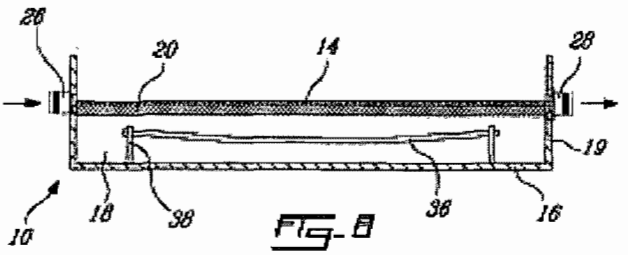

Figure 8 represents a schematical side view of the device allowing for sterilization of the external surfaces of a catheter or flexible endoscope, according to one particular example of the present invention;

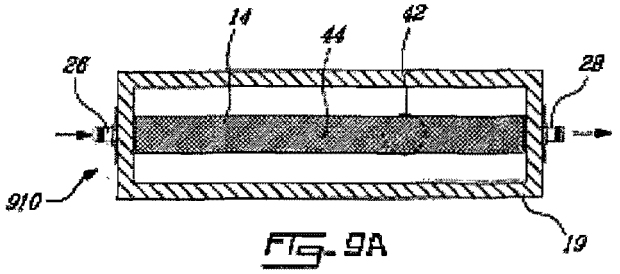

FIG. 9A

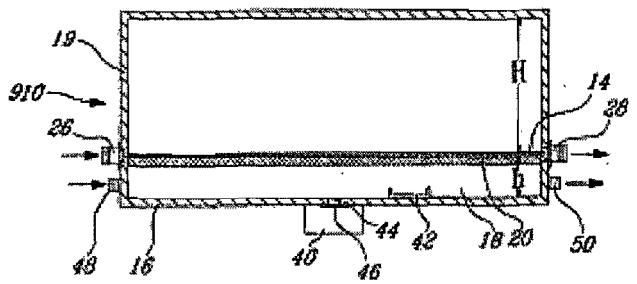

FIG. 9B

Figure 9 is a schematic representation of a system of sterilization according to a particular example of the present invention, in a) a top view is presented, and in b) a cross section is presented;

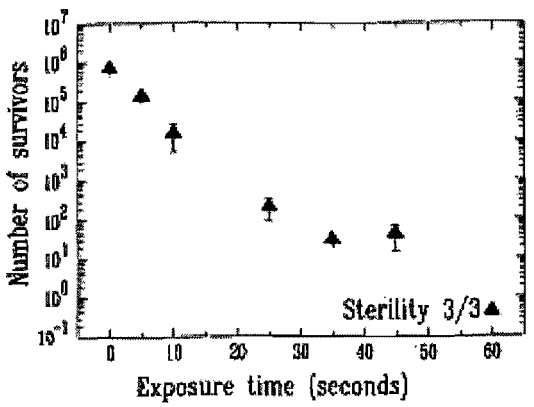

FIG. 10

Figure 10 shows a survival curve of spores of *Bacillus atrophaeus* obtained as a function of treatment time of a Petri dish with a device such as shown in Figures 9a and 9b;

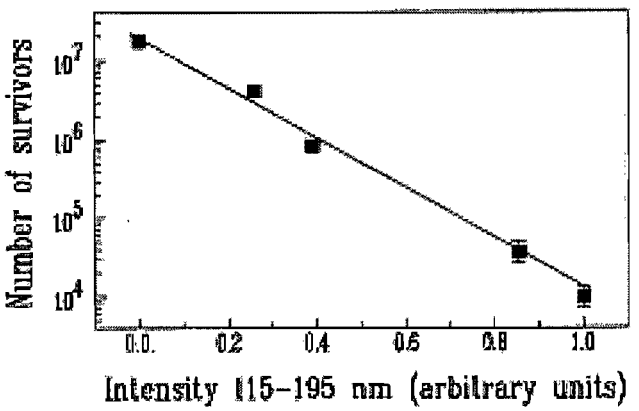

FIG. 11

Figure 11 shows a line expressing the number of surviving spores as a function of the incident UV flux (115-195 nm), after 10 seconds of treatment by a method of a particular example of the present invention, in which a plasma of argon is used, as well as the device shown in Figures 9a and 9b;

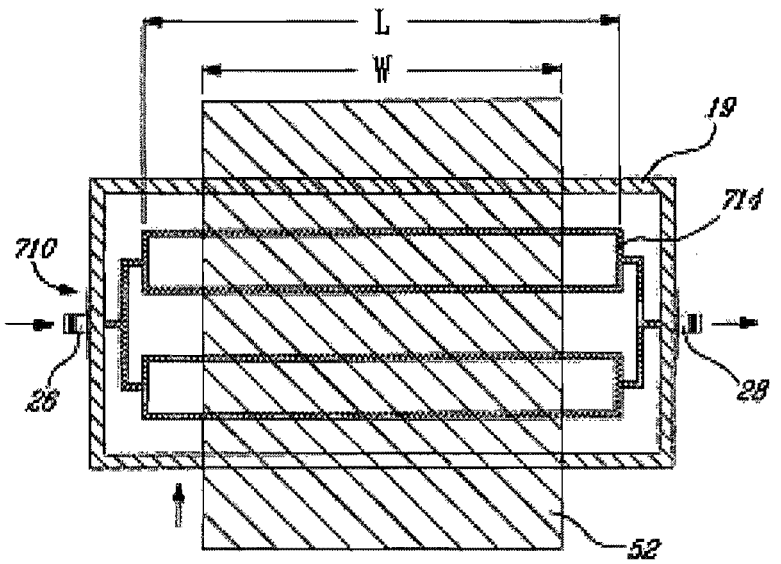

FIG. 12

Figure 12 shows schematically the embodiment of a method of a particular example of the present invention, this figure showing a top view of a linear applicator formed by four conducting strips, energized by a power divider system integrated into the applicator and used to treat a dielectric or conducting plate as it moves past;

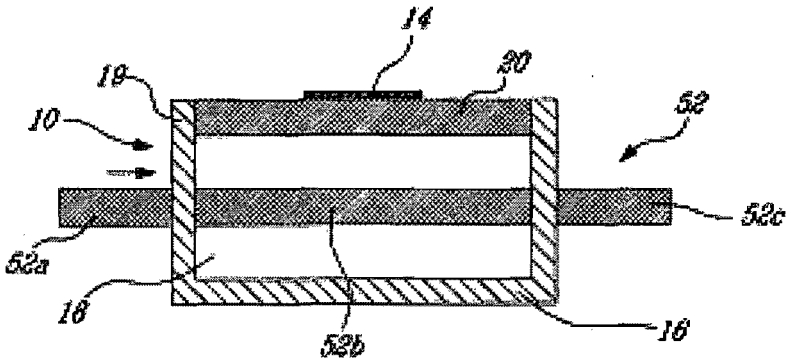

FIG. 13

Figure 13 is a schematical representation of a device for inactivation or sterilization of the two surfaces of a dielectric plate as they move past, according to one particular example of the present invention;

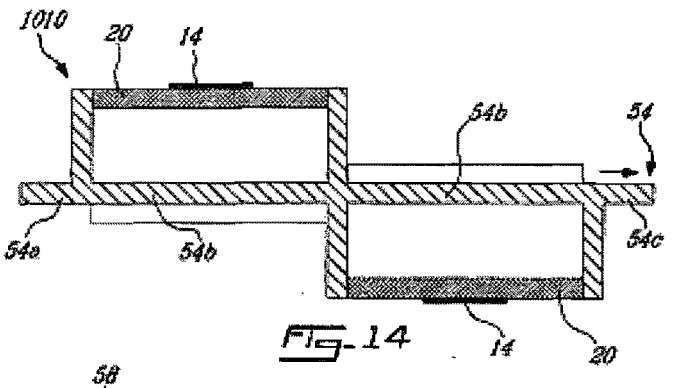

FIG. 14

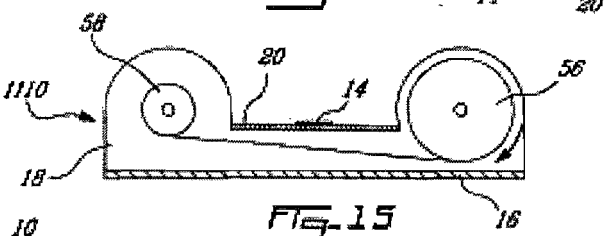

FIG. 15

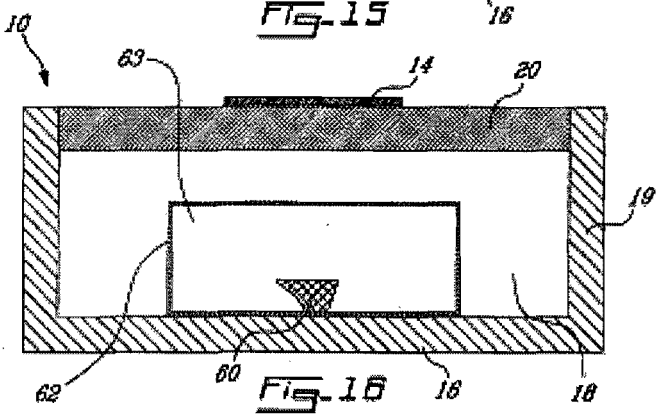

FIG. 16

Figure 14 is a schematical representation of a device for inactivation or sterilization of the two surfaces of a metal plate as they move past, according to one particular example of the present invention;

Figure 15 is a schematical representation of a device for inactivation or sterilization of the two surfaces of a dielectric film for packaging of agri-food products or medical products as they move past, according to one particular example of the present invention;

Figure 16 is a schematical representation of a device for inactivation or sterilization of an object located inside a dielectric package according to one particular example of the present invention;

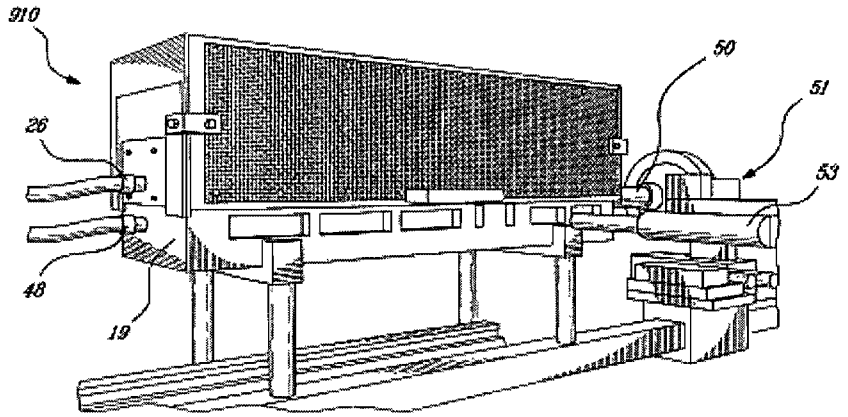

Fig. 17

Figure 17 is a perspective view of a device for inactivation or sterilization according to one particular example of the present invention;

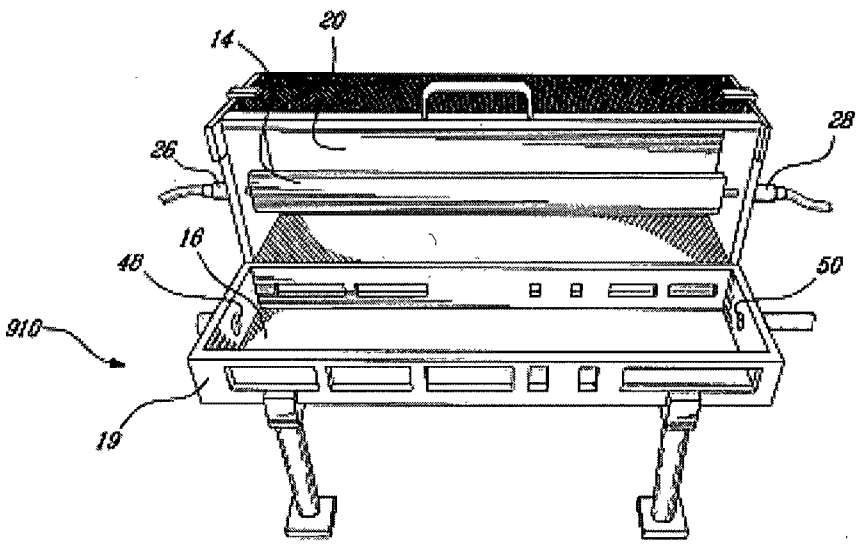

Fig. 18

Figure 18 is another perspective view of the device of Figure 17, in which the upper pivoting part has been deployed;

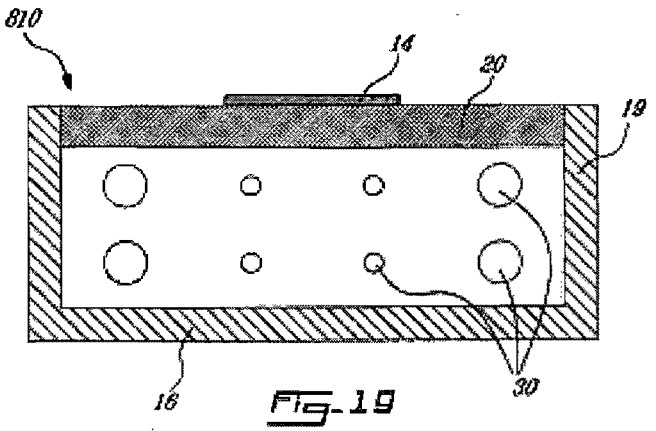

FIG. 19

Figure 19 is a schematical cross section view of the injection and evacuation planes of the plasmagenic gases of a sterilization device according to one particular example of the present invention in which the injection and the evacuation of the plasmagenic gases are realized by means of a network of circular holes situated parallel to the axis of the linear applicator;

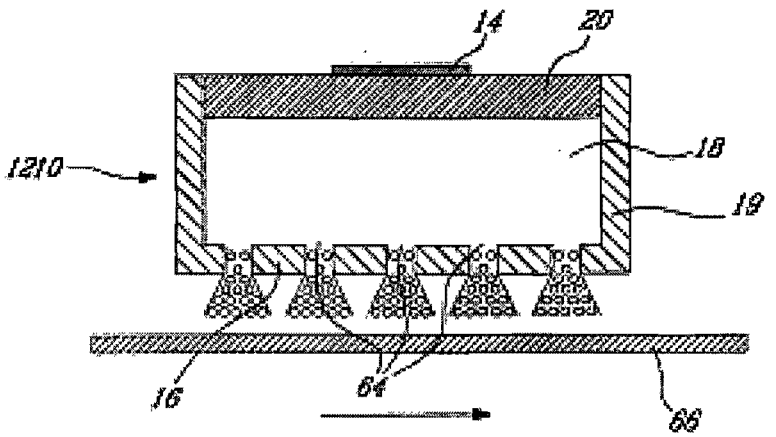

FIG. 20

Figure 20 shows a schematical cross section view of a device according to another example of the present invention, wherein a bottom part of the frame comprises a plurality, of apertures so as to permit treatment of an object disposed outside the chamber by a flowing afterglow plasma passing therethrough;

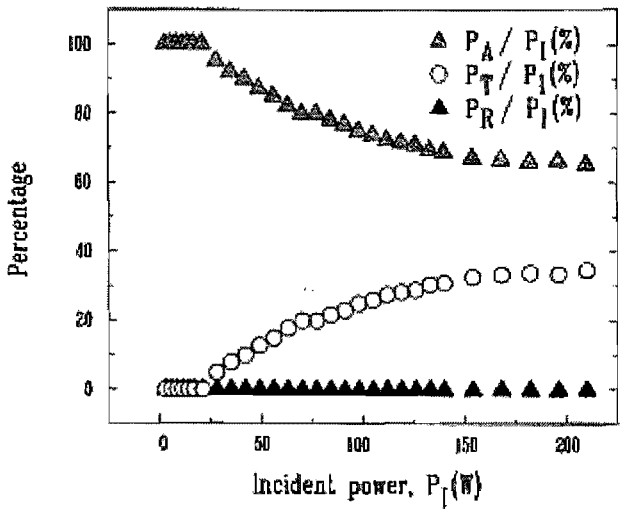

FIG. 21A

Figure 21a is a curve showing the percentage of reflected power, P_R, transmitted power, P_T, and absorbed power, P_A, normalized to the incident power, P_I,, as functions of P_I, at 200 MHz, during an experiment carried out with a device according to an embodiment of the present invention and according to an embodiment of a method of the present invention;

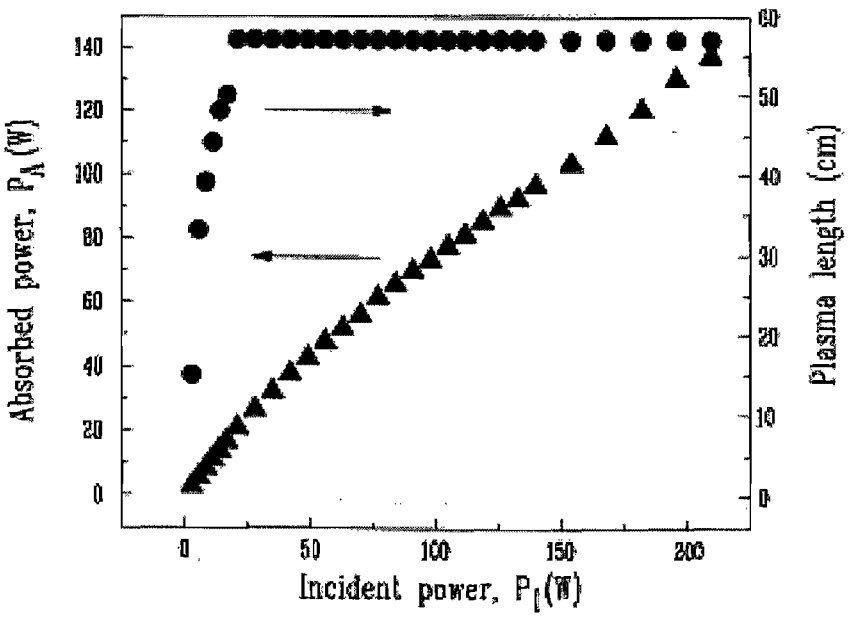

FIG. 21B

Figure 21b is a curve showing the power absorbed by the plasma and length of the discharge in the chamber as functions of incident power during an experiment carried out with a device according to an embodiment of the present invention and according to an embodiment of a method of the present invention; and

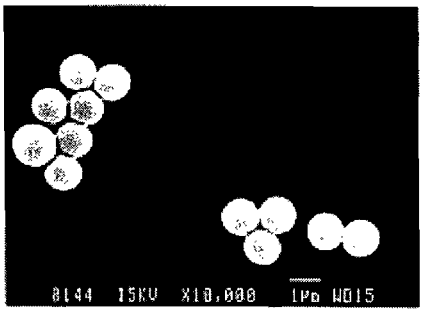

Fig. 22A

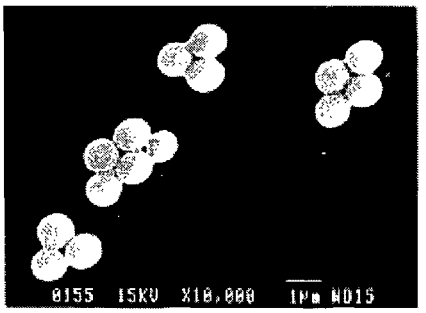

Fig. 22B

Figures 22a and 22b represent Scanned Electron Microscope (SEM) micrographs of polystyrene microspheres treated according to an embodiment of a method of the present invention using a device according to an embodiment of the present invention, wherein Figure 22a shows the microspheres before treatment and Figure 22b show the microspheres after treatment.

A.3.5 Detailed description of the invention

The following examples are given to better define the present invention and should not be interpreted as limiting the present invention.

Planar linear applicators

The term linear applicator designates a particular class of electromagnetic field applicator. These are structures which extend for the entire length of the chamber comprising the plasma, as is described in the publication of Z. Zakrzewski and M. Moisan appearing in Plasma Sources Sci. Technol. 4, 379-397 (1995). There are many different linear applicators, in particular those using waveguide technology, and they make it possible to obtain plasmas having a good axial uniformity. Even so, this type of microwave transmission line only operates in a narrow band of operating frequencies, generally centered about 2.45 GHz or 915 MHz.

To take advantage of the axial uniformity offered by the linear applicators while making it possible to work in an extended band of operating frequencies, linear applicators based on planar transmission lines using the TEM mode (electric field and magnetic field perpendicular to the direction of propagation of the waves) have been developed.

Among the different planar transmission lines, two types of strip lines have been developed. Figure la shows a microstrip line 10 and Figure 1b shows a three-plate line 12. The structures implemented are based on these two types of transmission line, the microstrip line (unsymmetrical line) and the stripline (symmetrical line). Striplines are also called "sandwich lines", "triplate lines", "symmetrical lines" or "double-ground-plane lines" Pollak J, Moisan M, Kéroack D and Boudam article to be published).

Figure 1 a shows the configuration and the characteristic dimensions of a microstrip line. A conducting strip 14 of width W and thickness t is located at a constant distance h above a conducting ground plate 16 of width L. A homogeneous dielectric medium 18 (for example air) of thickness h and relative permittivity ε_r fills the entire region (or chamber) comprised between the ground plate and the conducting strip. Note that a microstrip line is not necessarily a microstructure as implied by its name; it is sometimes also called an "unsymmetrical line" or a "single-ground-plane line". Figure 1b shows the configuration and characteristic dimensions of a stripline. A conducting strip 14 of width W and thickness t is centred between two parallel conducting ground plates 16 of width L and separated by a distance h. A homogeneous dielectric medium of relative permittivity *E,* fills the entire region comprised between the parallel ground plates and the conducting strip.

These new devices are represented in Figures 2a-d. The plasma sources based on the microstrip line (Figures 2a and 2b) are able to create a plasma in a single chamber 18 defined by a conducting frame 19, whereas it is possible to create plasmas in two different chambers with the plasma sources based on the three-plate line (Figures 2c and 2d). In this second configuration, the sterilization chambers are located on either side of the central conducting strip 14. Figures 2b and 2d represent variants of structures 2a and 2c, respectively. They use a second dielectric 20 plate between the plasma and the conducting ground plate or plates 16.

The dielectric plate 20 of Figure 2a, transparent to the electromagnetic field (low loss factor), has the role of isolating the plasma from the surrounding air, which prevents contamination of the plasmagenic gas. lt also makes it possible to avoid contact between the plasma and the central conducting strip. This plate can have a minimum thickness, depending on its length and its width, and letting it withstand exposure to vacuum without breaking. For example, the material used can be borosilicate glass (Pyrex®) due to its low cost price, its relative low loss factor, and its good physical and chemical behavior.

For powers less than about 300 W, the connections between the generator and the applicator and between the applicator and the matched load can make use of standard N connectors and coaxial cables with a low loss factor (for example, RG3931U). For higher powers and at high

frequency (915 MHz or 2450 MHz), waveguide transitions to the linear applicator can be realized.

Figure 3 shows the device 10 in which a dielectric support 22 has been inserted so as to hold objects 24 at a given height while other objects 24 remain on the conducting ground plate 16. It is possible to insert one or more dielectric supports inside the chamber 18.

Geometry and configurations

For example, it is possible to use a linear applicator whose geometry and/or configuration varies along its length (Figures 4 and 5).

Figure 4a shows a cross section view of a linear microstrip applicator of constant height h which has a conducting strip 14, a conducting ground plate 16, a chamber 18, a conducting frame 19, a dielectric plate 20, a HF power input 26, and a power output 28 (toward matched load). Figures 4b-4d have the same components with the exception of the geometry of the plate 16. Figures 4b and 4c are examples of linear applicators of variable height h. In Figure 4b, the height of the conducting ground plate 116 decreases linearly along the length of the applicator, while in Figure 4c the height h of the conducting ground plate 216 is some function of the axial position. It can thus be that the distance (or height h) between the conducting strip and a bottom part of the chamber is constant (Figure 4a), decreasing (Figure 4b), or variable (Figure 4c). The height or distance H in Figure 9b (distance between the conducting strip 14 and an upper part of the device or frame) can also vary similarly to the various embodiments shown in Figures 4a-c. It was observed that by varying h or H it was possible to obtain a better axial uniformity of the plasma. It can also permit to adjust impedance of the plasma source in accordance with the transmission line impedance.

The central conducting strip 14 can also have several different geometries and/or configurations. Figure 5a presents a top view of the applicator 10 whose central conducting strip 14 has a constant width W. The device 310 in Figure 5b has a conducting strip 314 which has an increasing width. The width of conducting strip 414 in device 410 (Figure 5c) varies along the structure. In another variant, a device 510 has a conducting strip 514 of circular geometry, as well as a metal frame 519 of circular geometry (Figure 5d).

In fact, the geometry and configuration of the applicator depend basically on the application in question. In particular, when the three-dimensional object being sterilized has a complex structure, it can be useful to take advantage of the geometrical flexibility of microstrip or

three-plate lines in order to adapt the shape of the applicator to that of the object being sterilized.

Modes of utilization

Several different modes of utilization of the invention can be considered. For example, in the case when the residual power at the exit of the applicator is much lower than the incident power at the entry of the applicator, it is possible to reverse the input and output of power at the end of a particular time, so as to achieve a more uniform treatment along the length of the sterilization chamber. This reversal of the direction of power flow can be achieved with HF flip flops (switches).

In order to avoid any power losses, the matched load located at the end of the microwave line can be replaced by a short circuit (standing wave mode in the chamber). This method can prove useful, e.g., when a very high (or very low) intensity of electromagnetic field and/or concentration of sterilizing species is required at certain coordinates along the chamber.

In another example, the matched load located at the end of the applicator can be replaced by another HF power supply coming from either a second generator (with operating frequency equal to the first one, or not), or from the same generator. In the latter case, the power is previously divided (equally or not) at the output of the single generator.

It is also possible to use the HF power in pulsed mode in ail the previously described modes of utilization, for example, in order to lower the temperature of the plasmagenic gas.

Length of the structures

The length of the applicators can vary, for example, from a dozen centimeters up to several dozen meters. In fact, there is in theory no limit on the length of the plasma created by a linear applicator, except for the length of the linear structure and the power put out by the generator. This is an intrinsic feature of a linear applicator of HF field.

Width of the structures

The width of the device can vary, for example, from several centimeters up to several meters. For example, in a device 710 a sterilization chamber of large width can be filled with a plasma in its entirety by using several metal strips 714 spaced out along the structure (Figure 6b) and

arranged in parallel. For example, a single generator can feed power to all these linear applicators 610 by using a serpentine strip system 614 (Figure 6a) or a power divider located inside or outside the applicator (not shown). When the linear applicator is based on a planar type transmission line, such as a microstrip line (Figure la) or three-plate line (Figure 1b), the power dividing system can be integrated in the linear applicator and be realized by the same transmission line technology (example with a microstrip line, Fig. 6b). Thus, this method makes it possible to optimize the invention in terms of packing density. Thus, several linear applicators based on a planar transmission line can easily be arranged in the form of a network, energized by a power divider system, which makes it possible to fill up a large lateral volume. The power divider system can be placed, for example, right inside the applicator, and it can divide the power by 2k, where k is an integer. Figures 6b and 6d illustrate this possibility with the example of a linear applicator formed by 4 conducting strips (k = 2), which allows one to obtain a plasma source of larger lateral volume than with a linear applicator using a single metal strip. It should be noted that the total incident power needs to increase in proportion to the number of conducting strips used.

The distance between each strip cannot be less than a certain value, in order to avoid any interaction in the propagation of the EM waves between each of the strips. This distance also must not exceed a certain value in order to obtain a good lateral uniformity of the plasma so created. In fact, the optimal distance between each of the conducting strips basically depends on the height h between the conducting strips and the ground plane or planes, the width w of the strips, and the pressure of the gas.

Figure 6d shows the use of a network of linear applicators with a compartmentalized sterilization chamber, that is, one divided into several lateral sections by tight walls extending over the entire length of the structure. The use of such a system can prove beneficial, for example, when one wishes to treat several objects at the same time, yet avoid any risk of a cross contamination between these different objects arranged separately in each compartment. This last configuration can also be of interest when one wishes to perform different treatments in each compartment. In particular, it is thus possible to inject mixtures of different plasmagenic gases in each of the compartments (both for the pressure and flow rate of the gases, and for the configuration of each linear applicator (see Figures 4 and 5)).

Depth of the structures

Unlike for the length and the width of the linear applicators described in the present invention, there is a practical limit on the depth (height) of these structures. This limit results from the existence of modes of higher orders that can be excited above a maximum frequency, resulting in loss of certain of the properties of the applicator that require the presence of a TEM mode. For example, for the three-plate line, this value is given in the publication of I. J. Bahl and R. Garg appearing in Microwaves, pp. 90-96 (January 1978) :

$$f_{max}(GHz)=\frac{15}{h\sqrt{\varepsilon_r}}\frac{1}{\left(\frac{w}{h}+\frac{\pi}{4}\right)} \qquad (5)$$

where w and h are in cm, w being the width of the central strip and h the distance between the conducting ground plates (Figure 1b). It corresponds to the cutoff frequency of the first TE mode of higher order able to be excited.

Injection of gases

The injection and evacuation of the plasmagenic gases in the sterilization chamber can be accomplished, for example, by means of openings located in the axis of the structure, through the lateral plates of the applicator, through the conducting ground plate or plates. It should be noted that once the openings intended for the injection and evacuation of the plasmagenic gases have been determined, it is still possible to reverse the direction of circulation of the plasmagenic gases for a more uniform treatment.

Positions of the openings for injection and evacuation of plasmagenic gases

The injection and evacuation of the plasmagenic gases in the sterilization chamber can be achieved in various ways, by an appropriate modification of the geometry and/or the configuration (respective positions) of the gas inlet and outlet openings.

According to one particular example of the invention, the gas flow is injected and evacuated by a network of openings 30 in the device (Figure 19), in order to get a better lateral homogeneity of the plasma and, thus a more uniform treatment in the entire volume of the sterilization chamber. It can also be profitable to adjust separately the flow rate of plasmagenic gases circulating through each opening by using several flow meters or by modifying the geometry (and thus the hydrodynamic conductance) of the openings. For example, the

evacuation rate of the plasmagenic gases is the lowest through openings of small diameter (Figure 19).

Alternatively, the gas flow is evacuated by openings located beneath the objects being sterilized, so as to direct the flow of bactericidal species preferably ont0 them. This method can be of interest when one wishes to obtain a better inactivation rate or when the object being sterilized is made up of may layers of fibers (such as a mask or a bandage), forming a mesh impermeable to UV and too dense to enable the creation of the plasma between each of its meshes. It should be noted that in the case of a very dense mesh it may be of interest to stretch the object in one or more directions in the course of the sterilization procedure. This temporary modification of the structure of the object being sterilized should be reversible so that it does not lose certain of its intrinsic properties (such as its water- tightness).

Sterilization of different objects by different treatments

As shown in Figure 20, there is provided a device 1210 similar to device 10 shown in Figure 2a, with the exception that the device 1210 is provided with a plurality of apertures 64. In fact, the conducting ground plate 16 is provided with such apertures so as to permit to simultaneously treat at least one other object 66 disposed outside of the chamber 18 by means of a flowing afterglow of the plasma. The apertures being adapted so as to prevent affecting propagation of the electromagnetic field along the transmission line. For example, the apertures can have a size which is at least three times inferior to the width of a conducting strip.

Procedure for the sterilization of three-dimensional objects

There is provided an example of general method that can be used so as to treat objects with the method and device of the present invention. In a first stage, the sterilization chamber does not contain any contaminated object. The chamber is then placed under vacuum, and the plasmagenic gas or gases are injected inside the chamber. Under the action of an EM field, a plasma is then created and all the interior surfaces of the chamber (especially the lower metal plate on which certain objects being sterilized may rest), which are thus in contact with the bactericidal species of the plasma, will be sterilized.

In a second stage, the object 34 to be treated are removed from their packaging 32 inside the chamber in a sterile environment. The object and also its packaging are arranged on the

lower plate 16 of the sterilization device 10 (Figure.7a). All the surfaces of the object 34 and the package 32 are in direct contact with the plasma are then sterilized, except for the surfaces of the objects in contact with the lower plate.

In a third stage (see Figure 7b), the object 34 and its package 32 undergo a rotation, so as to sterilize the surfaces not so treated in the first stage, that is, those being in contact with the lower plate. The manipulation of the objects can be done inside the chamber by an operator provided with sterile gloves or an automated system (e.g., manipulator arms), whose ends designed to be in contact with the objects (to hold them) are sterile. It should be noted that at the end of the second stage certain surfaces of the chamber having been in contact with the object(s) (and/or the package(s)) being sterilized are not necessarily still sterile. This is why, after having been rotated, the objects, and possibly also their package, do not stay during the third stage in the same place in the chamber as during the second stage (compare Figures 7a and 7b): they are shifted axially and/or transversely inside the sterilization chamber. This process can be carried out, for example, by means of a rotary drum (rocker arm), made of a dielectric material (and thus transparent to the EM field) of low loss factor.

Alternatively, as shown in Figure.8, the three-dimensional objects (for example object 36) to be sterilized, and possibly also their packaging (not shown), can be held by their ends at a certain height in the chamber 18 (e.g., at mid height), by means of sterile dielectric hooks 38 (such as Teflon), so as to simultaneously sterilize all the outer surfaces of the objects being treated, except for the surfaces in contact with the hooks. Figure 8 illustrates one such possibility: this is a side view of a linear applicator where a medical prosthesis (such as a catheter or an endoscope) is held by its ends inside the sterilization chamber.

Sterilization gas

The air initially present in the chamber can be evacuated down to a reduced pressure between 1.33 mPa and 133 Pa. A rare gas (e.g. argon) or a gas mixture (e.g. $N_2/0_2$) is then introduced into the sterilization chamber by means of one or more mass flow meters. The gas flow rate can be between 5 and 10,000 standard milliliters per minute (mLsm). At low pressure, for example, (< 133 Pa), the HF power applied is enough to ignite the discharge, while at high pressure it is necessary to use a Tesla coil or a piezoelectric device to initiate it.

At the end of the cycle, after the time necessary to achieve sterility of the surfaces exposed to the bactericidal species of the plasma has expired, the return to atmospheric pressure is done

in a few seconds by opening a valve with filter (sterile) having pores, for example, of about 0.22 μm.

HF power characteristics of the planar plasma source

The power absorbed by the discharge P_A as a function of the incident power P_I when assuming a lossless field applicator is simply given here by: $P_A = P_I - P_R - P_T$.

P_T is the power exiting from the applicator and going into the transmission-line terminating matched load. According to an example, carried out with a device of the present invention, power measurements were achieved with the argon gas flow set at 100 sccm at a pressure of 750 mtorr (100 Pa) and with a field frequency of 200 MHz. Figure 21a displays the corresponding reflected and transmitted powers as functions of the incident power. The percentage of reflected power at the applicator input remained at zero over the whole range of incident HF power tested (0-210 W). As the HF power is raised from O to 20 W, the plasma length increases as shown in Figure 21b; at 20 W, the full applicator length (57 cm) is filled with plasma; at higher incident HF powers, part of the incoming power flows along the field applicator without being absorbed by the discharge and is, in fact, lost in the terminating matched load that prevents reflection at the applicator end. Because of this, above 20 W, there was a continuous decrease of the percentage of power absorbed by the plasma, as shown in Figure 21a.

Since absorbed power in the discharge remained low (with 50 W of incident power, the density of absorbed power by the plasma is below 10 W/L), gas heating is also low: in fact, the chamber wall and Petri dishes remained, after a few minutes of plasma exposure, at temperatures typically below 40 °C as measured with a thermocouple.

Examples

The following examples are given merely as an illustration and should not be interpreted as limiting the present invention.

The linear applicator used in the following experiments is similar to the device schematically represented in Figure 2a. It is a structure of microstrip type, containing a conductive frame of aluminium serving as the ground, a copper or brass strip and a plate of borosilicate glass (Pyrex®). Schematical top and cross section views of this applicator are shown, respectively, in Figures 9a and 9b. An N connector 26, placed at the entry of the

device, receives the electromagnetic power of a HF generator, operating at 200 MHz. Another N connector 28, placed at the exit of the device, allows for transferring the unused HF power to maintain the plasma to a matched load, thus preventing the power from being reflected at the end of the applicator 910. It should be noted that a Faraday cage 19 (Figure 9b) makes it possible to avoid any risk of leakage of EM energy to the outside of the microstrip applicator. Its height H (notation defined in Figure 9b) is much higher than h, so that the electric field which creates and maintains the plasma is almost totally confined to the inside of the chamber where the sterilization takes place. The conducting plate 16 is provided with an aperture 44 for allowing UV measurements by the detector 40 which comprises a window 46 (for example made of MgF_2). The device 910 (see Figures 9a, 9b, 17 and 18) is also provided with a gas inlet 48 connected to a gas tank (not shown) and a gas outlet 50 connected to a pumping system and an optical collimator 53. The dimensions of the device 910 were as follows (see Figures la and 9b for reference letters): width (W) of the conducting strip 14 = 50.8 mm; thickness (t) of the conducting strip 14 = 3.2 mm; width (L) of the frame 19 = 146.1 mm; total height of the frame 19 = 200.5 mm; height h (see Figure 9b) = 50.8 mm; height H (see Figure 9b) = 137.0 mm; thickness of the dielectric plate 20 = 12.7 mm.

The plasmagenic gas used was highly pure argon at a pressure of 93 Pa and a flow rate of 100 mLsm. The HF power was set at 43 W at the entry of the device. Under these operating conditions, the reflected power was equal to 3 W and the power lost at the end of the line is equal to 10 W. Thus, the power absorbed by the plasma is equal to 30 W.

One makes sure that the intensity of the UV radiation is constant between each experiment by making use of the UV detector 40 (Figure 9b) in the form of a photomultiplier tube, for example.

A Petri dish of polystyrene 42 was placed inside the chamber, at the place specified in Figure 9b. This Petri dish contains 1 million spores of *B. subtilis* (recently renamed B. atrophaeus) deposited from a suspension of 100 µl. The corresponding survival curve so obtained is shown in Figure 10. Three independent experiments were repeated, making it possible to obtain a mean and a standard deviation (error bar) for each of the points. As it can be clearly seen, the 3 Petri dishes were sterilized in 1 minute.

It was observed that the overall time required to reach sterility is function of the amount of stacked spores and their degree of stacking.

Mechanisms of sterilization

In order to determine which bactericidal species of the argon plasma are responsible for the sterility (see preceding section), the number of spores of *B. subtilis* surviving after 10 seconds of exposure as a function of the incident UV flux (115-195 nm) was plotted (Figure 10). The UV flux incident on the Petri dish is checked by varying the argon pressure in the chamber between 20 mtorr and 1 torr. In this pressure interval, the UV flux increases as the pressure rises. The other operating conditions (argon flow rate, incident power, location of the Petri dish in the chamber, nature of the deposit of spores) are identical to those described in the preceding section. The UV detector can be placed, for example, beneath the lower metal plate; in this case, the UV rays are collected through an opening 44 (about 1 mm in diameter) pierced through this plate (Figures 9a and 9b).

It was mentioned for Figure 10 that the number of spores surviving (on logarithmic scale) diminishes as a linear function with increasing UV flux (115-195 nm), which shows that the UV rays might be the preponderant bactericidal species when an argon plasma is created in the method of the present invention and under the experimental conditions described in the preceding section. Given that a pure argon plasma at low pressure cannot emit any ray between 115 and 195 nm, it can be envisioned, through without being bound to this hypothesis, that this UV emission results from the presence of impurities (of nitrogen and/or oxygen) inside the sterilization chamber.

Disinfection or sterilization of plates in succession

Due to their planar geometry, the linear applicators described in the present invention naturally lend themselves to the treatment of plane surfaces. As it can be seen in Figure 12, a device such as schematically represented in Figure 6b can be used to perform such a task. The length "L" of the linear applicator 710 is usually larger than the width "W" of the surfaces treated (Figure 12). Granted that a minimal time is needed for the bactericidal species of the plasma to play their role (about 1 minute, see Figure 10), the configuration of the applicator should be adapted to the speed of movement of the surfaces being treated. In particular, the incident HF power, the width of the applicator, and the number of conducting strips forming the network (as described in Figure 12) need to increase when the speed of movement increases, in order to keep a constant time of action for the bactericidal species. More precisely, when the sterilizing agents of the plasma are the UV rays, it is necessary to provide the surfaces being treated with a minimum UV flux to achieve sterility. If the speed of

movement is too fast, sterility of the surfaces will not be achieved, and thus one only gets a degree of inactivation of these surfaces (disinfection of more or less high level).

When the object being treated is a dielectric or metal plate such as the plate 52 in Figure 12, its treatment can be done in the following way.

In the case of a dielectric plate being treated, this will replace the one in Figure 2a. Thus, a single one of its two surfaces (its lower surface in contact with the plasma) is inactivated or sterilized as it moves past. It should be noted that an interlayer of air may exist between the conducting strip and the dielectric plate to allow for a possible variable thickness of the plate being treated.

In the case of a conductive plate being treated, this will then replace the conducting ground plate of Figure 2a. A single one of its surfaces (its upper surface in contact with the plasma) is then sterilized as it moves past. In the case when several dielectric and/or conductive plates need to be inactivated or sterilized at the same time, it is advisable to use one of the configurations 2b, 2c or 2d for the treatment:

configuration 2b : 2 dielectric plates and O conductive plate;

configuration 2c : 2 dielectric plates and 2 conductive plates;

configuration 2d : 4 dielectric plates and 0 conductive plate;

It is also possible to treat simultaneously the lower surface and the upper surface of a single dielectric plate 52 (Figure 13) or conducing plate 54 (Figure 14) such as a metal plate. 52a and 54a represent an untreated portion of the plate, 52b and 54b represent a portion of the plate during treatment, and 52c and 54c represent a portion of the plate after treatment. In Figure 14 a device 1010 permits to treat the upper surface and then lower surface of a conducting plate 54.

Disinfection or sterilization of dielectric films in succession

Figure 15 shows a device 1010 useful for disinfection or sterilization of two surfaces of a dielectric film (such as an agri-food product or a medical packaging film) in succession. The device 11 10 comprises a conducting strip 14, a conducting plate 16, a chamber 18 for receiving the film and treating it with a plasma discharge, a dielectric plate 20, a roll 56 comprising the untreated film, and a roll 58 for receiving the sterile or inactivated film. Furthermore, a linear applicator can also be used for the disinfection or sterilization of two dielectric films in succession, being afterwards joined by thermal welding (not shown).

It should be noted that the treatment of packaging films can also be accompanied by the sterilization of three-dimensional objects. In this operating mode, the objects are sterilized outside of their package (Figures 7-8). Once the sterilization cycle is over, the objects are packaged in a sterile environment, inside the sterilization chamber or not, as already mentioned in the international application W02004/050128 page 21.

Direct sterilization inside a dielectric package

The sterilization of a three-dimensional object by the present invention can also be realized directly inside a dielectric package. As was previously stipulated (Figure 11), the method of sterilization described in the present method might result from the bactericidal action of the UV photons. Now, the majority of packages let only a slight proportion of photons pass through their wall. This section describes a method for sterilizing an object situated inside a package and in a reasonable length of time. The method consists in creating the plasma directly inside the package, the latter being formed of a dielectric material transparent to the applied EM field. To do this, the air initially present in the package should first be evacuated and replaced by the plasmagenic gas or gases. The time for this operation depends directly on the porosity of the package, as well as the quality of its seal: the more hermetic the package, the longer it will take.

Furthermore, to create the plasma inside the package, a minimum distance between the object being sterilized and its package needs to be observed. This is due to the existence of a so-called sheath around any object immersed in a plasma. If the package perfectly adheres to the shape of the object with a distance less than one millimeter between the object and its package, the plasma can only be generated with difficulty inside the package. On the other hand, if the package is designed so that a distance of several millimeters is observed between the object and its package, it is possible to create the plasma inside the package (Figure 16). As shown in Figure 16, an object 60 disposed in its package 62 can be sterilized or inactivated in the device 10. It can be seen that there is a significant volume between 63 the package 62 and the object 60 in order to create a plasma therebetween.

For example, a package made up of two parts: one made of semirigid dielectric material (such as Teflon), possibly recyclable, and the other of a flexible material, such as a disposable packaging paper (e.g. Kimguard®), can be used.

Erosion-free treatment of surfaces

As previously indicated, the plasma sterilization process must not only efficiently inactivate micro-organisms, but also it should not induce damage to the exposed surfaces. In particular, as many medical devices (MDs) comprise polymers, the etching of polymers should be as limited as possible. Polystyrene microspheres (PS, approximately one micrometer in diameter) were used in order to evaluate the level of damage induced by the method and device of the present invention to contaminated objects. Such PS microspheres have already been employed to compare damage caused by the early and the late N2-Oz discharge afterglows (Boudam *et al.* J. *Phys. D: Appl. Phys.* 40 1694-1711). These microspheres were then found to be quite responsive to various plasma species: the observed off-axis erosion rate correlated with the increase of the O atom density in the afterglow as the O2 percentage is increased, while the on-axis erosion observed at O % Oz appeared related to the action of both the N2 metastable molecules and the Pi2-ions. Similar PS microspheres were also employed by Lerouge *et al.* in *Journal of Biomedical and Material Research* 51 128-135 so as to demonstrate that the high sporicidal efficacy provided by their O_2/CF_4 plasma was related to its high etch rate of polymers. Brétagnol *et al.* in *Plasma processes and polymers* 3 443-445 also reported that PS microspheres can strongly be etched by an O_2 plasma.

Figure 22a shows SEM micrographs of PS microspheres before treatment. These microspheres were then deposited on Petri dishes, located in the planar discharge as shown in Figures 9a and 9b, and subjected for 1 minute to an argon plasma. The gas flow was 100 sccm at a gas pressure of 750 mtorr. Under these operating conditions, all the spores of a 10^6 deposit were inactivated, as shown in Figure 10. As it can be seen in Figure 22b, the exposed microspheres were not disrupted or eroded. The absence of etching damage here contrasts with plasma sterilization techniques based on the action of radicals. It was thus demonstrated that the method and device of the present invention permit inactivation and/or sterilization without however substantially damaging or degrading the treated surface(s).

Although the present invention has been described with the help of specific examples, it is understood that many variations and modifications can be grafted onto these examples, and the present invention aims to cover such modifications, usages or adaptations of the present invention generally following the principles of the invention and including every variation of the present specification that will become known or conventional in the field of activity where the present invention lies, in accordance with the scope of the following claims.

A.3.6 Claims

1. A method of sterilization and/or inactivation of at least one surface of at least one contaminated object, said method comprising submitting said at least one surface to a plasma discharge generated from an applicator of electromagnetic field of linear type, the plasma having a temperature below 80 °C, and having an absorbed power per unit of volume of plasma of less than 20 W 1 L, so as to sterilize and/or inactivate said at least one surface without substantially degrading it.

2. The method of claim 1, wherein said surface is sterilized after having been subjected to the discharge of said plasma for a period of less than 60 minutes.

3. The method of claim 1, wherein said surface is sterilized after having been subjected to the discharge of said plasma for a period of less than 10 minutes.

4. The method of claim 1, wherein said surface is sterilized after having been subjected to the discharge of said plasma for a period of less than 5 minutes.

5. The method of claim 1, wherein said surface is sterilized after having been subjected to the discharge of said plasma for a period of less than 1 minute.

6. The method of any one of claims 1 to 5, wherein the temperature of said plasma is less than 40 °C.

7. The method of any one of claims 1 to 5, wherein the temperature of said plasma is less than 35 °C.

8. The method of any one of claims 1 to 5, wherein the temperature of said plasma is less than 30 °C.

9. The method of any one of claims 1 to 8, wherein the power absorbed per unit volume of plasma is less than 15 W / L.

10. The method of any one of claims 1 to 8, wherein the power absorbed per unit volume of plasma is less than 10 W / L.

11. The method of any one of claims 1 to 8, wherein the power absorbed per unit volume of plasma is less than 5 W *I* L.

12. The method of any one of claims 1 to 11, wherein said at least one object is subjected to at least two treatments by the action of the discharge of said plasma, said object being repositioned inside the chamber of the applicator of electromagnetic field of linear type between each treatment so as to treat all the surfaces of the object.

13. The method of any one claims 1 to 11, wherein, after a predetermined period of time, the power input and output of the applicator of electromagnetic field of linear type are reversed so as to achieve a uniform treatment of said surface.

14. The method of any one of claims 1 to 11, wherein said surface is treated in succession as it is introduced into said applicator.

15. The method of any one of claims 1 to 14, wherein said plasma is generated by means of at least one high-frequency generator able to operate at a frequency of about 13.56 MHz to about 2.45 GHz or about 200 MHz to about 5.8 GHz.

16. The method of any one of claims 1 to 15, wherein said plasma comprises at least one rare gas.

17. The method of any one of claims 1 to 15, wherein said plasma comprises argon.

18. The method of any one of claims 1 to 17, wherein said plasma comprises N_2, CO_2 and/or O_2.

19. The method of any one of claims 1 to 18, wherein at least two objects are treated by said plasma simultaneously.

20. The method of any one of claims 1 to 18, wherein at least two objects are treated simultaneously by said applicator, each of said objects being arranged, in the applicator, in a different chamber, said chambers being insulated from each other.

21. The method of claim 20, wherein the same conditions of plasma generation are applied in all the chambers.

22. The method of claim 20, wherein different conditions for plasma generation are appiied in each of the chambers.

23. The method of any one of claims 1 to 22, wherein said at least one object being sterilized is arranged in the sterilization chamber of said applicator so as to simultaneously sterilize and/or inactivate all the outer surfaces of said object.

24. The method of any one of claims 1 to 23, wherein said at least one object being sterilized is a dielectric film, such as agri-food industry packaging film or medical packaging film.

25. The method of claim 24, wherein said film is sterilized as it is rolled off, said film entering the chamber of the applicator at a predetermined height, then leaving said chamber without interrupting the sterilization process or the electromagnetic power serving to maintain said plasma, the two surfaces of said dielectric film being then inactivated or sterilized simultaneously under the action of the bactericidal species of the plasma.

26. The method of claim 25, wherein two dielectric films are simultaneously inactivated or sterilized, then sealed in succession by thermal welding at certain spots.

27. The method of any one of claims 1 to 23, wherein the lower or upper surface of a dielectric plate, in contact with the plasma, is disinfected or sterilized in succession.

28. The method of any one of claims 1 to 23, wherein a dielectric plate, such as one made of glass or fused silica, moves past inside said applicator, so that the lower surface and the upper surface of this dielectric plate are inactivated or sterilized at the same time.

29. The method of any one of claims 1 to 23, wherein the object being treated is a metal plate, moving past inside said applicator, so that the lower surface and the upper surface of this plate are inactivated or sterilized at the same time.

30. The method of any one of claims 1 to 23, wherein said object is sterilized directly inside its package, said plasma being created outside the object, as well as in a sufficient volume included between the package and the object.

31. The method of any one of claims 1 to 30, wherein said method permits sterilization andlor inactivation of said at least one surface of said at least one object without causing erosion to said surface.

32. The method of claim 31, wherein said method permits an erosion-free sterilization andlor inactivation of polystyrene micro-spheres, as determined by observing said sterilized and/or inactivated polystyrene micro-spheres by means of Scanning Electron Microscopy as compared to said polystyrene micro-spheres before sterilization and/or inactivation.

33. The method of any one of claims 1 to 32, wherein said sterilization and/or inactivation is carried out in a chamber, and wherein at least one wall defining said chamber comprises at least one aperture so as to simultaneously permit treatment of at least one other object disposed outside of said chamber by means of a flowing afterglow of said plasma.

34. The method of claim 33, wherein said at least one wall comprises a plurality of apertures, said apertures being adapted so as to prevent affecting propagation of an electromagnetic field along a transmission line.

35. The method of claim 34, wherein said apertures have a size which is at least three times inferior to the width of a conducting strip.

36. A device for enabling sterilization and/or inactivation of at least one surface of at least one contaminated object, using a plasma, said device comprising:

- a chamber adapted to receive said object to be treated and a discharge of said plasma;

and

- an applicator of electromagnetic field of linear type, adapted to generate said plasma discharge in the chamber so as to sterilize said at least one surface without damaging it in substantial manner.

37. The device of claim 36, wherein said applicator of electromagnetic field of linear type comprises at least one conducting strip such as a rnetal strip extending frorn one end of said chamber to its opposite end, said strip having an essentially constant width.

38. The device of claim 36, wherein said applicator of electromagnetic field of linear type comprises at least one metal strip extending from one end of said chamber to its opposite end, said strip having a width varying between the two ends.

39. The device per claim 38, wherein the width of the strip varies in essentially increasing manner from the HF input to the output (load).

40. The device of any one of claims 37 to 39, further including a power divider system intrinsic to the applicator.

41. The device of any one of claims 37 to 39, wherein said strip includes at least one curved portion.

42. The device of claim 36, wherein said applicator of electromagnetic field of linear type comprises at least one metal strip having two opposite ends, said ends being in contact with a single one of the ends of said chamber.

43. The device of claim 42, wherein said strip includes at least one curved portion.

44. The device of any one of claims 36 to 43, wherein the field applicator used is an applicator of high-frequency field having a planar configuration.

45. The device of claim 44, characterized in that a planar transmission line is used, said line being a strip line, such as a three-plate line or a microstrip line.

46. The device of any one of claims 36 to 45, wherein the geometry of the conducting strip and/or the ground plate of the applicator of electromagnetic field is linear, circular, or of some other shape.

47. The device of any one of claims 36 to 46, wherein the sterilization chamber comprises one or more dielectric supports to hold the objects being sterilized.

48. The device of any one of claims 36 to 47, comprising at least one conducting strip and at least one dielectric plate so as to insulate said strip from the discharge plasma.

49. The device of claim 36, wherein the electromagnetic field applicator is of distributed type, the latter being formed by at least two planar transmission lines, each one extending for the entire length of the applicator.

50. The device of claim 36, comprising a network of linear applicators, said applicators being compartmentalized, thus preventing risks of cross contamination between the various objects being sterilized and enabling treatments by different plasmas in each compartment.

51. The device of any one of claims 36 to 50, characterized in that it is adapted to treat a moving object in continuous manner.

52. The device of any one of claims 36 to 50, characterized in that it comprises a means for introducing said at least one object to be treated into the chamber for a predetermined period of time, and for removing it when sterility andlor inactivation is achieved.

53. The device of any one of claims 36 to 50, characterized in that it comprises a means for introducing at least one part of said at least one object to be treated into the chamber for a predetermined period of time, and for removing it when sterility andlor inactivation is achieved for this part, said means thus making it possible to treat said object in succession and in continuous manner.

54. The device of claim 45, wherein said chamber is provided with at least one aperture adapted to permit a flowing afterglow of said plasma to diffuse outside said chamber, thereby enabling treatment of at least another object disposed outside said chamber.

55. The device of claim 54, wherein said chamber comprises a plurality of apertures, said apertures being adapted so as to prevent affecting propagation of an electromagnetic field along said transmission line.

56. The device of claim 55, wherein said apertures have a size which is at ieast three times inferior to the width of said conducting strip.

57. The device of claim 37, wherein the distance between said conducting strip and an upper end of said chamber is constant.

58. The device of claim 37, wherein the distance between said conducting strip and a bottom end of said chamber is constant.

59. The device of claim 37, wherein the distance between said conducting strip and an upper end and/or a bottom end of said chamber is decreasing from an inlet to an outlet of said chamber.

60. The device of claim 37, wherein the distance between said conducting strip and an upper end and/or a bottom end of said chamber is variable from an inlet to an outlet of said chamber.

61. Object sterilized or inactivated, obtained by a method as defined in any one of claims 1 to 32.

Annexe 4

Contribution de l'auteur, localisation des publications insérées dans la thèse de doctorat et acceptation des coauteurs

Tel que mentionné dans l'introduction générale, cette thèse rassemble les brevets et les articles scientifiques pour lesquels notre contribution est majeure, tel qu'attestée par le fait d'en être premier auteur. Il s'agit de 2 demandes de brevets (la version américaine de chacune y est reportée pour l'essentiel) et de 5 articles (dont 4 déjà publiés). La faculté des études supérieures de l'Université de Montréal demande que l'étudiant fasse état explicitement de son apport original, indépendant et spécifique à chacun des articles cosignés et demande de commenter de façon approprié le rôle joué par tous les coauteurs. Ces renseignements sont fournis ci-dessous.

Article 1

J Pollak, M Moisan et Z Zakrzewski 2007 Long and uniform plasma columns generated by linear field-applicators based on stripline technology *Plasma Sources Sci. Technol.* **16** 310-323

Ma contribution se situe principalement au niveau de la conception des expériences et de leur réalisation, de la mise en forme des résultats ainsi que de l'écriture du premier jet du manuscrit. M. Moisan a également participé à la conception des expériences, à l'analyse des résultats en plus de récrire des paragraphes entiers de l'article. Z. Zakrzewski a proposé certaines des solutions techniques qui ont permis le développement de la source de plasma dévoilée dans l'article.

Article 2

J Pollak, M Moisan, Z Zakrzewski, J Pelletier, Y A Arnal, A Lacoste et T Lagarde 2007 Compact waveguide-based power divider feeding independently any number of coaxial lines, IEEE Transactions on microwave theory and techniques **55** 951-957

Ma contribution se situe au niveau de la prise des mesures expérimentales, de la mise en forme des résultats ainsi que de l'écriture d'une partie du manuscrit. Zenon Zakrzrzewski a proposé le concept du diviseur de puissance et a imaginé une grande partie des expériences que j'ai réalisées au laboratoire en plus d'écrire le premier jet de plusieurs sections de l'article. Par ailleurs, M. Moisan a également contribué au développement du diviseur de puissance en proposant d'adjoindre un circulateur sur chaque prise de puissance pour les rendre indépendantes les unes des autres. Il a par ailleurs largement contribué à améliorer la qualité du manuscrit soumis à publication. Les autres co-auteurs ont participé aux expériences réalisées à Grenoble.

Article 3

J Pollak, M Moisan, D Kéroack et M K Boudam 2008 Low-temperature low-damage sterilization based on UV radiation through plasma immersion J. Phys. D: Appl. Phys. **41** 1-14

Ma contribution se situe principalement au niveau de la conception des expériences et de leur réalisation, de la mise en forme des résultats ainsi que de l'écriture du premier jet du manuscrit. M. Moisan a également participé à la conception des expériences, à l'analyse des résultats en plus de récrire des paragraphes entiers de l'article. D. Kéroack a contribué à certaines expériences de spectroscopie d'émission optique et a commenté le manuscrit, tandis que M K Boudam a conçu l'expérience de spectroscopie d'absorption optique et a co-écrit une section de l'article.

Article 4

J Pollak, M Moisan, D Kéroack, J. Séguin et Jean Barbeau 2008 Plasma sterilisation within long and narrow bore dielectric tubes contaminated with stacked bacterial spores Plasma Process. Polym. **5** 14–25.

Ma contribution se situe principalement au niveau de la conception des expériences et de leur réalisation, de la mise en forme des résultats ainsi que de l'écriture du premier jet du manuscrit.

M. Moisan a également participé à la conception des expériences, à l'analyse des résultats en plus de récrire des paragraphes entiers de l'article. D. Kéroack a commenté le manuscrit et a participé à la mise en place des expériences de spectroscopie sous vide. J. Séguin a effectué les travaux microbiologiques et a participé à l'écriture du premier jet de l'article. J. Barbeau a contribué à la conception et à l'analyse des expériences microbiologiques en plus de commenter le manuscrit soumis à publication.

Article 5

J. Pollak, J. Séguin, J. Barbeau, M. Moisan 2008 Biofilm sterilization within polymer tubings by a low temperature gaseous plasma (ionized gas) Article soumis à publication dans la revue International Journal of Pharmaceutics.

Ma contribution se situe principalement au niveau de la conception des expériences et de leur réalisation, de la mise en forme des résultats ainsi que de l'écriture du premier jet du manuscrit. M. Moisan a également participé à la conception des expériences, à l'analyse des résultats en plus de récrire des paragraphes entiers de l'article. J. Séguin a effectué les travaux microbiologiques et à participé à l'écriture du premier jet de l'article. J. Barbeau a contribué à la conception et à l'analyse des résultats microbiologiques en plus de commenter le manuscrit soumis à publication.

Brevet 1

J Pollak, M. Moisan, B. Saoudi et Z Zakrzewski Process for the plasma sterilization of dielectric objects comprising a hollow part 2005 US 0269199

Ma contribution se situe principalement dans la conception et la description des modes de fonctionnement de l'un des stérilisateurs décris dans la demande de brevet. Z. Zakrzewski a également contribué à cette invention. B. Saoudi et M. Moisan ont conçu les étapes du procédé de stérilisation et ont écrit la majeure partie de la demande de brevet.

Brevet 2

J Pollak et M. Moisan 2008 Device and method for inactivation and/or sterilisation using plasma 2007 US 60/884,344

Ma contribution se situe dans l'invention de la source de plasma et du procédé de stérilisation ainsi que dans l'écriture du premier jet de la demande de brevet. M. Moisan a également participé à ces inventions ainsi qu'à la réécriture de la demande de brevet. La localisation de ces 7 documents dans la présente thèse de doctorat est représentée sous forme imagée ci-dessous.

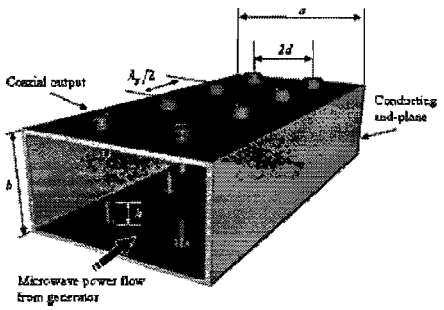

Annexe 1 Pollak *et al* IEEE Trans. Microw. Theory Tech. **55** 2007

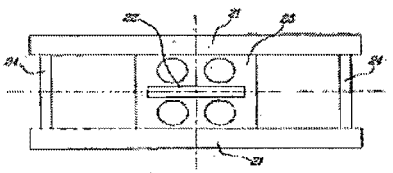

Annexe 2 Pollak *et al* US 0269199 2005

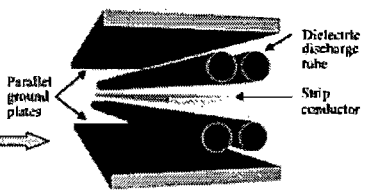

Section 2.3 Pollak *et al* Plasma Sources Sci. Technol. **16** 2007

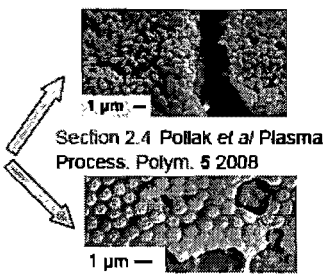

Section 2.4 Pollak *et al* Plasma Process. Polym. **5** 2008

Section 2.5 Pollak *et al* Int. J. Pharm. 2008, soumis

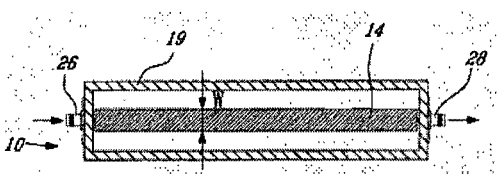

Annexe 3 Pollak *et al* US 60/884,344 2007

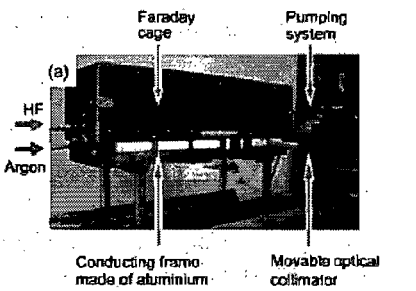

Section 3.2 Pollak *et al* J. Phys. D: Appl. Phys. **41** 2008

Figure A4 Localisation des publications insérées dans la thèse de doctorat.